# MOLECULAR AND ISOTOPIC RECORDS OF COMBUSTION INPUTS TO THE ENVIRONMENT OVER THE LAST 250 YRS

By

ANA LÚCIA CESSEL DE LIMA

M.Sc. Analytical Chemistry, Pontifícia Universidade Católica do Rio de Janeiro, 1998
B.Sc. Oceanography, Universidade do Estado do Rio de Janeiro, 1992

Submitted in partial fulfillment of the requirements for the degree of
Doctor of Philosophy

at the
MASSACHUSETTS IINSTITUTE OF TECHNOLOGY
and the
WOODS HOLE OCEANOGRAPHIC INSTITUTION
June 2004



Author: _____
Joint Program in Oceanography
Massachusetts Institute of Technology and
Woods Hole Oceanographic Institution



Certified by: _____
Timothy I. Eglinton, Thesis Co-Supervisor

Certified by: _____
Christopher M. Reddy, Thesis Co-Supervisor

Accepted by: _____
Philip M. Gschwend
Chair, Joint Committee for Chemical Oceanography
Woods Hole Oceanographic Institution

**MOLECULAR AND ISOTOPIC RECORDS OF COMBUSTION INPUTS TO THE ENVIRONMENT OVER THE LAST 250 YRS**

by

Ana Lúcia Cessel de Lima

Submitted to the MIT/WHOI Joint Program in Oceanography on March 26, 2004,
in partial fulfillment of the requirements for the degree of Doctor of Philosophy
in the field of Chemical Oceanography and Environmental Engineering

## THESIS ABSTRACT

The most ubiquitous source of polycyclic aromatic hydrocarbons (PAHs) to the environment is incomplete combustion. This study generated a high-resolution historical record of pyrogenic PAH emissions since pre-industrial times from anoxic aquatic sediments, allowing for detailed comparison with energy consumption data. We show that an increase in PAH concentrations over the last decade may be due to a rise in emissions from diesel-powered vehicles. Compound-specific radiocarbon measurements demonstrated unequivocally that the proportion of PAHs derived from fossil fuel combustion has increased substantially during the 20$^{th}$ century. $\delta^{13}C$ and $\Delta^{14}C$ measurements were also used to constrain the relative importance of combustion versus *in situ* production as sources of perylene. In addition, a comparison of the down-core concentration and isotopic profiles of black carbon (BC) generated by a combination of chemical and/or thermal oxidation methods highlighted the limitations of these methods when applied to sedimentary matrices. Finally, parallel lead and cesium isotopic records revealed two new potential stratigraphic markers in North American sedimentary records. $^{206}Pb/^{207}Pb$ profiles show a distinct peak in the mid-19$^{th}$ century, while a $^{137}Cs$ peak was found to coincide with the 1986 Chernobyl accident.

## ACKNOWLEDGMENTS

A vast array of people have helped make the past 5 years challenging, fun and memorable. Naming them all would double the size of this thesis, so pardon me if I leave a few out.

First and foremost, I would like to thank my two advisors Tim Eglinton and Chris Reddy. Having two advisors can be tricky business: two sets of corrections to every page you write, two people thinking faster than you at all times. However, it also means double the chance of discussing your project and, in their case, two complimentary advising styles. Tim and Chris's comments and interest in this research was always stimulating and their personal support invaluable.

My committee members John Farrington, Phil Gschwend and Ed Boyle were extremely gracious with their time and gave advise freely. Their breadth of knowledge and meticulous attention to detail greatly enhanced this work.

Thanks to Julia Westwater and Marsha Gomes in the Education Office at WHOI for taking all of the hassle out of administrative tasks and to Ronni Schwartz for guiding me through the initial culture shock of MIT.

A large group of people were directly involved in all aspects of the analyses presented in this thesis. This study would have taken five times longer if it weren't for the laboratory assistance of Sean Sylva, Bob Nelson, Leah Houghton, Carl Johnson, John Andrews, Bridget Bergquist, Matt Reuer, Rick Kayser, Angela Dickens, Barry Grant, and the NOSAMS team. I owe extra-special thanks (and several bags of chocolate) to Daniel Montluçon and Li Xu. Daniel saved me so many times in the lab and Li (the 2D-PCGC master) always worked his miracles to make the machines work properly.

This work also benefited greatly from comments and suggestions from Ann McNichol, Andrew Solow, Andrew Beet, Konrad Hughen, John King, Francis Dudas, Peter Appleby, Ken Buesseler, and John Crusius. Thank you all for reading/helping me through the several iterations of this thesis.

Work is not life's only purpose and I have been fortunate to meet and enjoy the company of some incredible people in the past few years. Bridget Bergquist, Carrie Tuit, Joanna Wilson, Vanja Ceraj, Greg Slater, Anna Cruse, Ann Pearson, Dana Gerlach, Christie Haupert, Gesine Mollenhauer, Helen White, Nick Drenzek, and Tracy Quan are some of the good friends I made at WHOI. But it was with my husband Mike that I shared my best memories from the past 5 years. Since we met in our first year of graduate school, we have laughed, cried, studied, cooked, danced, traveled, written 2 theses and built a home together. Mike is the most supportive, fun and caring person I could have wished for. I'll certainly keep you for the next 125 years!

Funding for this research was provided by the National Science Foundation (OCE-9708478 and CHE-0089172). I also acknowledge the generous support from the Brazilian Council for Research (CNPq) that started me off in this journey.

# TABLE OF CONTENTS

## TABLE OF FIGURES

**CHAPTER 4**



**CHAPTER 5**

**CHAPTER 6**

## TABLE OF TABLES

# CHAPTER 1

## GENERAL INTRODUCTION

Combustion processes are responsible for a great part of the environmental contamination observed nowadays. If combustion reactions involving hydrocarbons and $O_2$ were 100% efficient, $CO_2$ and water vapor would be the only products emitted into the atmosphere. However, burning of modern (wood) and fossil (e.g., oil and coal) organic matter for power generation, manufacturing, domestic heating, land clearing and transportation are usually incomplete and release a vast array of contaminants to the atmosphere, such as the carbon based black carbon particles (BC) and polycyclic aromatic hydrocarbons (PAHs). While most of the initial regulations concerning combustion aimed at reducing inorganic emissions ($CO_x$, $NO_x$ and $SO_x$), a new standard on the permissible amount of particulate matter smaller than 2.5 μm in diameter ($PM_{2.5}$) was adopted by the United States Environmental Protection Agency in 1997 (15 μg $m^{-3}$ and 65 μg $m^{-3}$ for annual and 24-hour standard, respectively) (EPA, 1997). The presence of fine aerosol particles in the atmosphere can have hazardous health effects as they are too small to be stopped in the upper respiratory tract and can penetrate into the lungs (Pedersen et al., 1980; Samet et al., 2000).

The carcinogenic and mutagenic properties linked to $PM_{2.5}$ are mostly related to PAHs associated with them (Prado and Lahaye, 1982; Busby et al., 1988). This group of compounds encompass suspected carcinogens and mutagens such as benzo[*a*]pyrene (Denissenko et al., 1996), which are commonly identified in the exhaust of gasoline and diesel vehicles (Westerholm et al., 1988; Benner Jr. et al., 1989), emissions from coal and oil fired power plants (Masclet et al., 1987), residential heating (Ramdahl et al., 1982), municipal and medical incinerators (Davies et al., 1976; Colmsjö et al., 1986; Lee et al., 2002) and wood burning (Freeman and Cattell, 1990; Jenkins et al., 1996; Fine et al., 2001). Although there are natural sources of PAHs (e.g., natural forest fires, volcanic

eruptions and oil seepage), anthropogenic inputs are predominant and by far the most important to air pollution. Because of their diverse inputs and association with fine particles, combustion-derived PAHs (pyrogenic PAHs) are ubiquitous in the contemporary environment. Atmospheric transport spreads these compounds to remote locations such as Arctic ice (Kawamura and Suzuki, 1994) and snow (Masclet et al., 2000), high altitude lake sediments (Fernández et al., 1999) and deep-sea sediments (Ohkouchi et al., 1999).

Sedimentary records show good correlation between PAH concentration profiles and energy consumption associated with industrialization. Classic studies conducted in the 1970s and 1980s along the east coast of the United States showed that PAH concentrations began to increase gradually around 1880, coincident with the onset of the Industrial Revolution, and reached a maximum in the 1950s (Hites et al., 1980a; Gschwend and Hites, 1981) when coal usage was still high (EIA, 2000). Due to the substitution of coal with cleaner burning fuels in the early 1960s, PAH concentrations in sediments show a steady decrease from then onwards (Gschwend and Hites, 1981). Because most of the historical records of PAH found in the literature were generated before the 1990s, this trend towards lower concentrations was assumed to persist into the present. However, recent studies reveal that PAH inputs are no longer decreasing. In 2000, Van Metre and collaborators reported that PAH emissions were increasing again in certain areas of the United States and suggested that this new rise in PAH paralleled the increase in automobile usage in the watersheds studied. In contrast, results by Schneider and collaborators (2001) from Lake Michigan revealed constant PAH inputs since the 1980s. Most importantly, these studies indicated that the declining trend in PAH inputs that began in the 1970s has at best stabilized. This new rise in PAHs concentration is in contrast to current declining trend of other organic contaminants, such as polychlorinated biphenyls (PCBs).

It is often assumed that the majority of pyrogenic PAHs found in the environment have a fossil fuel origin. However, unregulated combustion of modern biomass such as in incineration of domestic wastes, charbroiling, land clearing, forest and grass fires and

residential home heating (Schauer et al., 1996) are all potential sources of PAHs. Because these activities are not regulated, it is important to establish the proportions of pyrogenic PAHs derived from both fossil and modern sources. The half-life of radiocarbon makes it an ideal tracer to discriminate fossil fuel organic matter ($\Delta^{14}C$= -1000‰) from those containing modern biomass ($\Delta^{14}C > 0$‰). For example, Cooper and collaborators (1981) conducted one of the earlier studies to use bulk radiocarbon measurements to discriminate the contribution of specific sources of particles to urban air. This study showed that a large portion of the atmospheric particles collected in Portland, OR during the winter derived from burning of wood (39-70%) for residential heating. Measurement of the radiocarbon content of individual molecules was impaired by analytical capabilities until the late 1990s, when Eglinton and collaborators (1996) successfully demonstrated the use of a preparative capillary gas chromatograph (PCGC) for isolation of compounds in enough quantity for radiocarbon determination by accelerated mass spectrometry (AMS).

The main goal of this thesis was to construct a historical record of pyrogenic PAH emissions from fossil fuel and biomass sources since pre-industrial times. We aimed at determining the extent to which the proportion of fossil fuel derived pyrogenic PAHs has varied and to evaluate which PAHs represent the most effective tracers of modern and fossil combustion sources. In addition, we evaluated the potential sources of perylene, a PAH of unknown precursor and three methods for isolation of black carbon through comparison with the well defined PAHs. A general outline of this thesis is as follows:

Chapter 2 comprises an extensive literature review of recent findings on the formation, dispersion and fate of combustion derived PAHs to the environment. Because PAHs can be produced during the combustion of any type of organic matter (fossil or otherwise), the biggest challenge in regulating atmospheric emissions of this group of carcinogens relies on estimating the relative contributions of their major sources. Chapter 2 also reviews some of the traditional methods for inferring sources of PAHs to the environment (historical records and diagnostic ratios) and describes two techniques that

have recently been applied to source apportioning (stable carbon isotopic composition and radiocarbon measurement).

In Chapter 3 we construct a high-resolution record of past changes in PAH deposition in the New England area. We revisited the Pettaquamscutt River, Rhode Island - a site of pioneering studies on sedimentary PAH (Hites et al., 1980b) - where we collected several sediment freeze-cores. The results obtained for the PAH fluxes reveals remarkable structure in the profile that allow for detailed comparison with historical records of energy consumption. They also showed that the steady decrease in PAH concentrations that began in the 1950-60s has reverted in this region since the mid-1990s. We show evidence that (a) the major source of PAH to this area has consistently been combustion processes, (b) that the relative abundance of PAHs has varied over time, and (c) use historical information on energy consumption to conclude that the recent increase in PAH concentrations may be due to a rise in emission from diesel-powered vehicles.

Chapter 4 reviews the use of $^{210}Pb$ for calculating sediment accumulation rates and displays the first known record of a Chernobyl $^{137}Cs$ peak in sediments from North America. This chapter evaluates different methods for calculating $^{210}Pb$ chronology and checks them against the independent varve counting. The highly refined depth-age relationship was paramount to understanding historical trends in this work and is used throughout this thesis.

Chapter 5 addresses the use of the anthropogenic lead archaeostratigraphy (ALAS) calibration curve (Hurst, 2000) to estimate the changes in isotopic fingerprint of gasoline additives and separate them from contributions from other sources of Pb. While this approach was not fruitful, we unveiled a large mid-19$^{th}$ century peak in $^{206}Pb/^{207}Pb$ ratio (most likely resultant from intense mining and smelting of lead ores in the Upper Mississippi Valley district) that we believe could be useful as a stratigraphic marker for sedimentary records from the Northeastern United States.

In Chapter 6, we describe the procedure utilized for combining sediment samples from four sediments cores and isolating individual PAHs for subsequent compound-specific radiocarbon and stable carbon analysis. Utilizing the data obtained by these

analysis we construct a molecular $^{14}C$ record of combustion-derived PAH and determine how the proportion of fossil fuel derived PAHs has varied since pre-industrial times. We compare records from a suburban (Pettaquamscutt River) and a remote site (Siskiwit Lake) and evaluate which PAHs serve as the most effective tracers of fossil and modern combustion sources. Chapter 7 examines the down-core record of concentration, radiocarbon and stable isotopic composition of perylene and total organic carbon in the two aquatic systems investigated in Chapter 6. Perylene is a parent PAH found virtually in every sedimentary system investigated. This compound is thought to be produced *in situ* from an unknown precursor, but can also be produced by the incomplete combustion of fossil and modern biomass. By utilizing a combination of $\delta^{13}C$ and $\Delta^{14}C$ measurements on perylene and total organic carbon, we were able to discern the importance of fossil-fuel derived perylene to the sedimentary profile of this PAH.

Chapter 8 compares the concentration and radiocarbon results obtained for PAHs to that of sedimentary black carbon. Because there is still no agreement within the scientific community as to what fraction of the black carbon continuum each published analytical procedure quantifies, we compare down-core profiles of black carbon generated by a combination of chemical and/or thermal oxidation methods. The results obtained illustrate the complexity of BC determinations and highlight the benefits of comparing BC results to that of a better-defined combustion product.

Chapter 9 concludes the thesis by summarizing the results obtained at each step and suggesting future research directions.

Throughout this thesis, the following compounds will be abbreviated as follows: phenanthrene (Phen), anthracene (Anth), fluoranthene (Fla), pyrene (Py), benz[*a*]anthracene (BaA), chrysene (Chry), benzo[*b*]fluoranthene (BbF), benzo[*k*]fluoranthene (BkF), benzo[*a*]pyrene (BaP), benzo[*e*]pyrene (BeP), dibenz[*a,h*]anthracene (DBA), indeno[*1,2,3-c,d*]pyrene (IP), benzo[*g,h,i*]perylene (BghiP) and coronene (Cor). Total PAHs is calculated as the sum of these 14 compounds.

## REFERENCES


Benner Jr. B. A., Gordon G. E., and Wise S. A. (1989) Mobile sources of atmospheric polycyclic aromatic hydrocarbons: A roadway tunnel study. *Environ. Sci. Technol.* **23**(10), 1269-1278.

Busby W., Jr, Stevens E., Kellenbach E., Cornelisse J., and Lugtenburg J. (1988) Dose-response relationships of the tumorigenicity of cyclopenta[cd]pyrene, benzo[a]pyrene and 6-nitrochrysene in a newborn mouse lung adenoma bioassay. *Carcinogenesis* **9**(5), 741-746.

Colmsjö A., Zebühr Y., and Östman C. (1986) Polynuclear aromatic compounds in flue gases and ambient air in the vicinity of a municipal incineration plant. *Atmos. Environ.* **20**(11), 2279-2281.

Cooper J., Currie L., and Klouda G. (1981) Assessment of contemporary carbon combustion source contributions to urban air particulate levels using carbon-14 measurements. *Environ. Sci. Technol.* **15**(9), 1045-1050.

Davies I., Harrison R., Perry R., Ratnayaka D., and Wellings R. (1976) Municipal incinerator as source of polynuclear aromatic hydrocarbons in environment. *Environ. Sci. Technol.* **10**(5), 451-453.

Denissenko M., Pao A., Tang M.-S., and Pfeifer G. (1996) Preferential formation of benzo[*a*]pyrene adducts at lung cancer mutational hotspots in P53. *Science* **274**, 430-432.

Eglinton T. I., Aluwihare L. I., Bauer J. E., Druffel E. R. M., and McNichol A. P. (1996) Gas chromatographic isolation of individual compounds from complex matrices for radiocarbon dating. *Anal. Chem.* **68**(5), 904-912.

EIA. (2000) Annual Energy Review, pp. 414. http://www.eia.doe.gov/emeu/aer/contents.html, Energy Information Administration. US Department of Energy.

EPA. (1997) National air quality status and trends. Six principal pollutants:Particulate matter (PM). http://www.epa.gov/oar/aqtrnd97/brochure/pm10.html, U.S. Environmental Protection Agency.

Fernández P., Vilanova R. M., and Grimalt J. O. (1999) Sediment fluxes of polycyclia aromatic hydrocarbons in European high altitude mountain lakes. *Environ. Sci. Technol.* **33**, 3716-3722.

Fine P., Cass G. R., and Simoneit B. R. T. (2001) Chemical characterization of fine particle emissions from fireplace combustion of woods grown in the Northeastern United States. *Environ. Sci. Technol.* **35**, 2665-2675.

Freeman D. J. and Cattell F. C. R. (1990) Woodburning as a source of atmospheric polycyclic aromatic hydrocarbons. *Environ. Sci. Technol.* **24**, 1581-1585.

Gschwend P. M. and Hites R. A. (1981) Fluxes of polycyclic aromatic hydrocarbons to marine and lacustrine sediments in the northeastern United States. *Geochim. Cosmochim. Acta* **45**, 2359-2367.

Hites R., Laflamme R., and Windsor Jr J. G. (1980a) Polycyclic aromatic hydrocarbons in marine/aquatic sediments: their ubiquity. 289-311.

Hites R. A., Laflamme R. E., Windsor Jr J. G., Farrington J. W., and Deuser W. G. (1980b) Polycyclic aromatic hydrocarbons in an anoxic sediment core from the Pettaquamscutt River (Rhode Island, USA). *Geochim. Cosmochim. Acta* **44**, 873-878.

Hurst R. W. (2000) Applications of anthropogenic lead archeostratigraphy (ALAS Model) to hydrocarbon remediation. *Environ. Forensics* **1**, 11-23.

Jenkins B. M., Jones A. D., Turn S. Q., and Williams R. B. (1996) Particle concentrations, gas-particle partitioning, and species intercorrelations for polycyclic aromatic hydrocarbons (PAH) emitted during biomass burning. *Atmos. Environ.* **30**(22), 3825-3835.

Kawamura K. and Suzuki I. (1994) Ice core record of polycyclic aromatic hydrocarbons over the past 400 years. *Naturwissenschaften* **81**, 502-505.

Lee W.-J., Liow M.-C., Tsai P.-J., and Hsieh L.-T. (2002) Emissions of polycyclic aromatic hydrocarbons from medical waste incinerators. *Environ. Sci. Technol.* **36**, 781-790.

Masclet P., Bresson M., and Mouvier G. (1987) Polycyclic aromatic hydrocarbons emitted by power stations, and influence of combustion conditions. *Fuel* **66**, 556-562.

Masclet P., Hoyau V., Jaffrezo J. L., and Cachier H. (2000) Polycyclic aromatic hydrocarbon deposition on the ice sheet of Greenland. Part I: Superficial snow. *Atmos. Environ.* **34**, 3195-3207.

Ohkouchi N., Kawamura K., and Kawahata H. (1999) Distributions of three- to seven-ring polynuclear aromatic hydrocarbons on the deep sea floor in the Central Pacific. *Environ. Sci. Technol.* **33**, 3086-3090.

Pedersen P., Ingwersen J., Nielsen T., and Larsen E. (1980) Effects of fuel, lubricant, and engine operating parameters on the emission of polycyclic aromatic hydrocarbons. *Environ. Sci. Technol.* **14**(1), 71-79.

Prado G. and Lahaye J. (1982) Mechanisms of PAH formation and destruction in flames - Relation to organic particulate emissions. In *Mobile Source Emissions Including Polycyclic Organic Species* (ed. D. Rondia, M. Cooke, and R. Haroz), pp. 259-275. D. Reidel Publishing Company, Liège, Belgium.

Ramdahl T., Alfheim I., Rustad S., and Olsen T. (1982) Chemical and biological characterization of emissions from small residential stoves burning wood and charcoal. *Chemosphere* **11**(6), 601-611.

Samet J., Dominici F., Curriero F., Coursac I., and Zeger S. (2000) Fine particulate air pollution and mortality in 20 U.S. cities, 1987-1994. *The New England Journal of Medicine* **343**(24), 1742-1749.

Schauer J. J., Rogge W. F., Hildemann L. M., Mazurek M. A., and Cass G. R. (1996) Source apportionment of airborne particulate matter using organic compounds as tracers. *Atmos. Environ.* **30**, 3837-3855.

Schneider A., Stapleton H., Cornwell J., and Baker J. (2001) Recent declines in PAH, PCB, and toxaphene levels in the northern Great Lakes as determined from high resolution sediment cores. *Environ. Sci. Technol.* **35**(19), 3809-3815.

Westerholm R., Alsberg T., Frommelin A., Strandell M., Rannug U., Winquist L., Grigoriadis V., and Egebaeck K.-E. (1988) Effect of fuel polycyclic aromatic hydrocarbon content on the emissions of polycyclic aromatic hydrocarbons and other mutagenic substances from a gasoline-fueled automobile. *Environ. Sci. Technol.* **22**(8), 925 - 930.

# CHAPTER 2

# LITERATURE REVIEW
# COMBUSTION-DERIVED PAHS IN THE ENVIRONMENT

## 1. INTRODUCTION

Polycyclic aromatic hydrocarbons (PAH) are ubiquitous contaminants in the environment. They are found in measurable concentrations even in remote locations such as Arctic ice (Kawamura and Suzuki, 1994) and snow (Masclet et al., 2000), high altitude lake sediments (Fernández et al., 1999) and deep-sea sediments (Ohkouchi et al., 1999). The sources and environmental fate of PAH have been the subject of extensive studies due to the toxic properties of some of their homologues. Compounds such as benzo[*a*]pyrene have been shown to be potent carcinogens and mutagens in various laboratory experiments (IARC, 1983), and their concentrations and sources are consequently closely monitored.

PAH reach the environment by several different pathways. These compounds are present in unburned petroleum (petrogenic PAH) and can be released directly to the environment both by human activities (oil spill) and natural processes (oil seepage). Even though oil spills attract a lot of attention from the media and public in general, due to the visible and acute effects that they produce, they usually do not significantly contribute to the PAH concentration inventory. Diagenetic processes are also suspected to generate certain PAH (e.g. perylene) from biogenic precursors (Laflamme and Hites, 1978; Tan and Heit, 1981), although conclusive evidence for this mechanism is still lacking. In general, biosynthesis is considered a localized source, with little impact on global concentrations. The most prominent and ubiquitous source of PAH to the environment is the incomplete combustion of modern (wood) and fossil (petroleum and coal) biomass.

Several studies published in the 1970s laid the groundwork for apportioning the sources of PAHs to the environment. The historical record approach was used in 1975 to

constrain the sources of heavy metals (Pb, Zn and Cd) and PAHs to Lake Constance, Germany. Both groups of pollutants were shown to be present in low concentrations prior to 1900, at which point their content increased toward the top of the sediment column, reaching a maximum at about 1965. The good agreement among the profiles of different compounds suggested a common input source. The authors concluded that increased consumption of coal in Europe after 1900 could account for the delivery of both groups of pollutants to the study area (Müller et al., 1977). A few years later, Lee and collaborators (1977) analyzed soot produced by the combustion of wood, coal and kerosene and compared the PAH distribution obtained for these samples to that of ambient samples from Boston, MA and Indianapolis, IN. The authors observed that combustion of wood and kerosene typically produced less alkylated PAHs than combustion of coal. By comparing the plot of alkylated PAHs from the source samples to that of particulate matter from Indianapolis and Boston, they concluded that combustion of coal was the most likely source of PAHs to Indianapolis, while burning of wood and kerosene could explain the distribution of PAHs encountered in Boston. The first attempt at characterizing the global distribution of PAHs in sediment and soils was conducted by Laflamme and Hites in 1978. The results obtained for a variety of samples collected worldwide showed similar qualitative pattern of parent PAHs, although absolute concentrations varied markedly. Their study revealed that higher concentrations of PAHs were encountered closer to urban centers versus remote sites, leading them to suggest that combustion processes were responsible for the widespread distribution of similar assemblages of PAHs.

A great deal has been learned about the sources and fate of PAHs since these classic papers were published. This review outlines some of the most recent findings on the formation, dispersion and fate of combustion derived PAHs to the environment. Because one of the challenges in regulating atmospheric emissions of this group of carcinogens relies on estimating the relative contributions of their major sources, the second part of this article will evaluate the traditional methods for inferring sources of PAHs to the environment, namely historical records and diagnostic ratios, and describe

two new techniques that have recently been applied to source apportioning (stable carbon isotopic composition and radiocarbon measurement). Throughout the text, the following abbreviations will be used: phenanthrene (Phen), anthracene (Anth), fluoranthene (Fla), pyrene (Py), benz[*a*]anthracene (BaA), chrysene (Chry), benzo[*b*]fluoranthene (BbF),benzo[*k*]fluoranthene (BkF), benzo[*a*]pyrene (BaP), benzo[*e*]pyrene (BeP), dibenz[*a,h*]anthracene (DBA), indeno[*1,2,3-c,d*]pyrene (IP), benzo[*g,h,i*]perylene (BghiP) and coronene (Cor). The structures of these compounds, as well as that of retene (1-methyl-7-isopropyl-phenanthrene) are displayed in Figure 1.

## 2. FORMATION

Much effort has been placed in understanding the experimental conditions that favor efficient combustion, so as to minimize the formation of products of environmental and health concern (Frenklach et al., 1984; Macadam, 1997; Palotás et al., 1998; Ritchter and Howard, 2000). During combustion, the organic compounds present in the fuel are fragmented into smaller unstable molecules (free radicals) that can react, through a number of different chemical pathways, to produce the first aromatic ring (Ritchter and Howard, 2000). Further reaction of this aromatic ring with small molecules (2-3 carbons; e.g. $C_2H_2$ - acetylene) leads to growth of the aromatic system and formation of larger and more stable multi-ring structures (Figure 2). It is well established that mechanisms of formation of PAHs and of soot are closely intertwined (Macadam, 1997; Wal et al., 1997; Ritchter and Howard, 2000) with high molecular weight PAHs (~500-1000 amu) functioning as molecular precursors of soot particles (Ritchter and Howard, 2000). In general, an inverse correlation is seen between the amount of PAHs and soot in flames, where a decrease in PAHs concentration is linked to the start of soot formation (Prado and Lahaye, 1982). A limit to the amount of PAHs produced and emitted during combustion is imposed by either the incorporation of high molecular weight PAHs into the solid phase (soot) and/or their destruction by direct burnout (Prado and Lahaye, 1982; Macadam, 1997). The later process corresponds to the pyrolytic oxidation of PAHs to CO and $CO_2$. Under fuel-rich conditions $OH^{\bullet}$ radicals are usually the main oxidant

responsible for this convertion, while under fuel-lean conditions $O_2$ dominates (Ritchter and Howard, 2000).

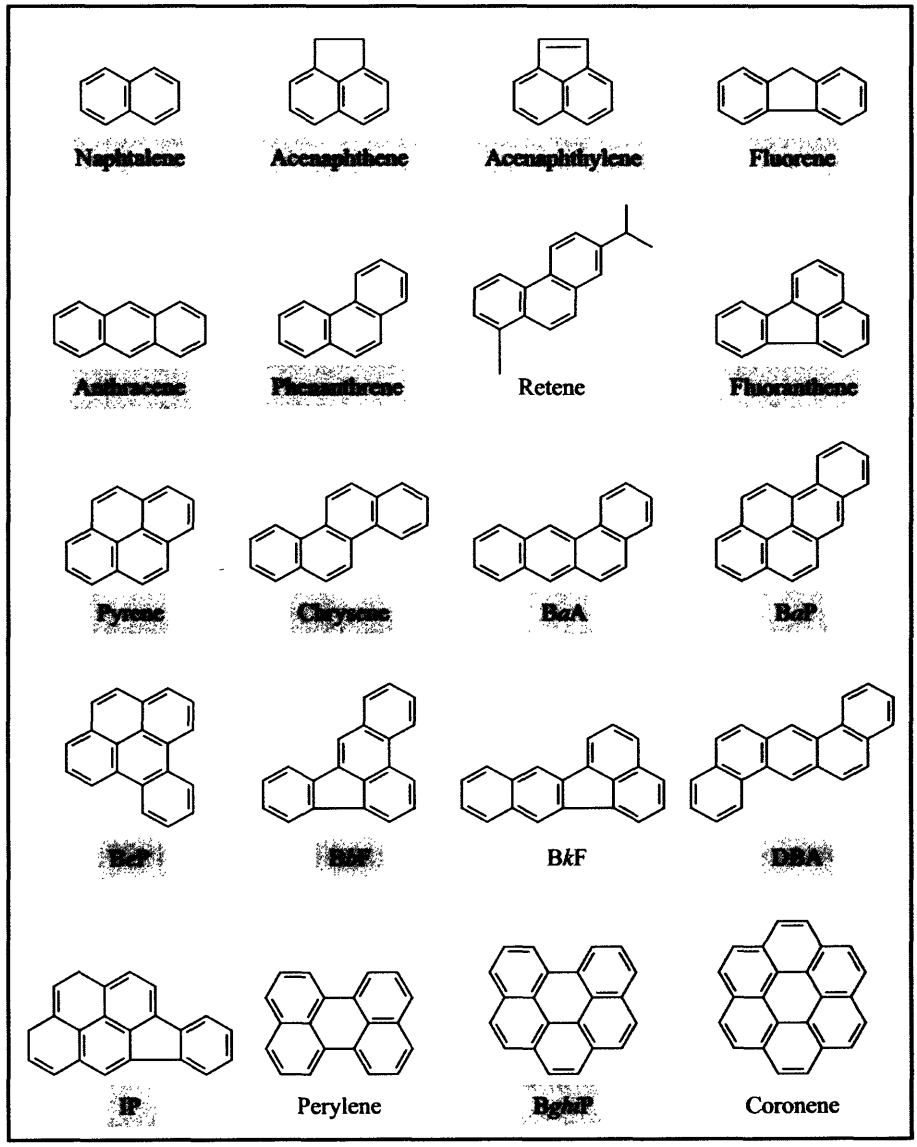


Figure 1. Structure of selected PAHs. Highlighted compounds comprise the Environmental Protection Agency (EPA) list of 16 priority PAHs.

There is general agreement that similar qualitative mixtures of PAHs are produced regardless of the type of fuel used (Ramdahl et al., 1982; Jenkins et al., 1996). Parent PAHs with 3-, 4- and 5-rings dominate emissions from both wood burning and vehicle exhaust (Figure 3), as larger molecules have higher tendency to be incorporated into soot particles (Ritchter and Howard, 2000). But while the assemblage of PAHs emitted by different sources apparently varies only slightly, burning conditions can significantly influence the amount of each PAH produced, so that the relative proportion of PAHs from a single fuel source may vary widely (e.g., combustion of white pine and eucalyptus wood, Figure 3) (Ramdahl et al., 1982; Masclet et al., 1987; Jenkins et al., 1996).

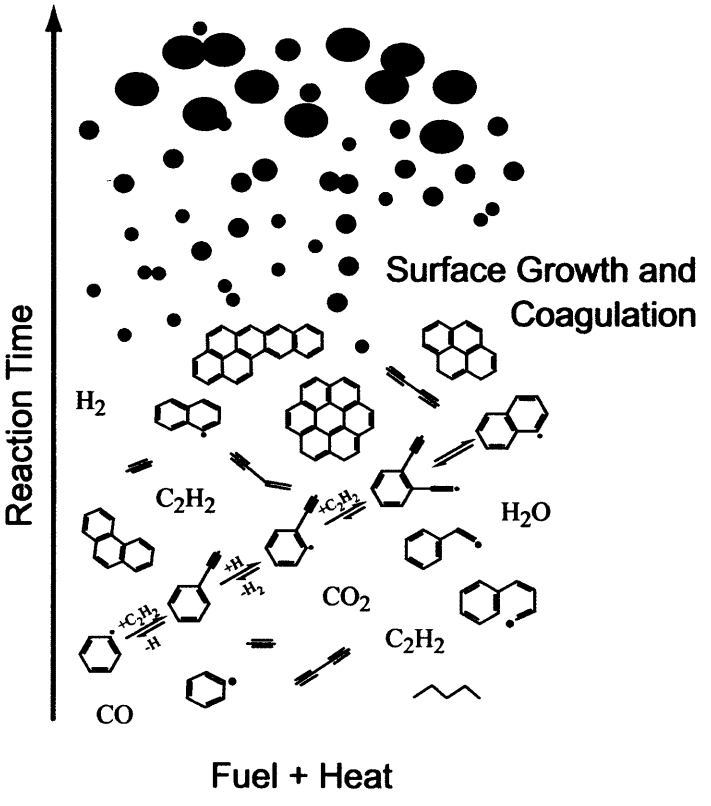


Figure 2. Schematics of formation of PAHs and soot particles during combustion, based on Ritchter and Howard (2000). PAH growth pathway presented was proposed by Frenklach and collaborators (1984).

## 2.1 Type of fuel

The type of fuel burned seems to directly influence the growth mechanism of PAHs and therefore, the amount of these compounds released by the combustion process. Laboratory experiments have shown that benzene flames produce 100 times more polycyclic aromatic compounds than aliphatic fuels (ethylene, methane) for the same carbon to oxygen ratio (C/O) and temperature (Ritchter and Howard, 2000). Results from the combustion of 11 different fuels on a gasoline engine showed that a 10% increase in the aromatic content of the fuel elevated the emissions of BaA, BaP and BghiP by ~20% (Pedersen et al., 1980).

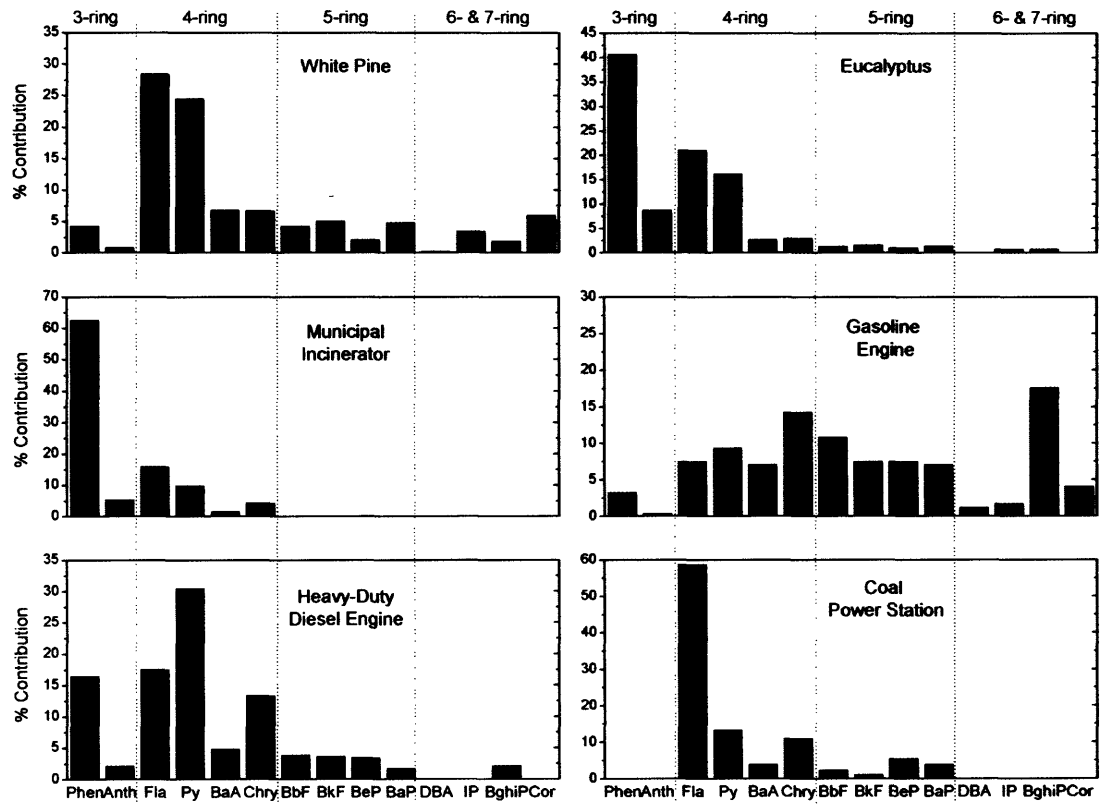


Figure 3. Distribution of PAHs produced by the combustion of 6 different fuels. Data from white pine (Fine et al., 2001), eucalyptus (Schauer et al., 2001), municipal incinerator (Colmsjö et al., 1986), gasoline and heavy-duty diesel engine (Rogge et al., 1993) and coal power station (Masclet et al., 1987).

Other studies have also demonstrated good correlation between the amount of individual PAHs in fuels and their emission by automobiles. Experiments conducted in Sweden using four different fuels in a gasoline engine showed a linear correlation ($r^2$=0.72) between the initial concentration of PAHs in the fuel and the amount of PAHs in the exhaust (Westerholm et al., 1988). The same general trend was observed in California for vehicles running on gasoline (Marr et al., 1999), although the magnitude of the PAH emissions varied greatly between studies. While Marr and collaborators (1999) reported that about 3 μg of an individual PAH was emitted per mg of that compound in the fuel (Figure 4), Westerholm and co-authors found that emission factors varied from compound to compound (approximately 1 μg $mg^{-1}$ for Chry and triphenylene, 7 μg $mg^{-1}$ for Py and 40 μg $mg^{-1}$ for BaP). The non-zero intercept encountered in both studies indicated that PAHs were emitted regardless of their presence in the original fuel, mainly because large PAHs can be fragmented during combustion. Therefore, PAH emissions do not necessarily have to resemble the original fuel. A recent study addressing the partitioning of PAHs between the gas and particulate phases has given a good example of the difference in PAH assemblage between original fuel and emission from a motor vehicle. While the gasoline used on the experiment contained large PAHs, such as BeP and perylene (6.8 and 2.8 mg $g^{-1}$, respectively), the tailpipe emissions by the catalyst-equipped vehicle was virtually devoid of these compounds (Schauer et al., 2002).

Automobile emissions encompass a mixture of PAHs derived from several compartments including: a) PAHs initially present in the fuel; b) PAHs formed during combustion; c) PAHs accumulated in the lubricating oil; and d) PAHs accumulated in the exhaust system (Acres et al., 1982; Pruell and Quinn, 1988; Marr et al., 1999; Schauer et al., 2002). For example, unburned and burnt fuel were shown to accumulate in motor oil, raising the amount of PAHs from undetectable in fresh oil to substantial amounts in used oil (e.g., 190 μg $g^{-1}$ Phen, 650 μg $g^{-1}$ methyl-phenanthrene and 50 μg $g^{-1}$ Chry) (Pruell and Quinn, 1988). The type of engine (spark ignition, diesel), age of the vehicle, presence of a catalytic converter, vehicle speed and cold versus hot starts are factors that affect PAH emissions (Pedersen et al., 1980; Acres et al., 1982; Rogge et al., 1993; Maricq et

al., 1999; Schauer et al., 2002). Some studies suggest that the increase in PAH concentration observed in the air of large cities is directly correlated to the increasing number of diesel vehicles (Rogge et al., 1993; Miguel et al., 1998; Kim et al., 2001). In agreement with that, exhaust emissions from motor vehicles measured in the Caldecott Tunnel in northern California during the summers of 1996 and 1997 demonstrated that PAH concentrations in the truck-influenced tunnel were higher than in the light-duty tunnel, even though the latter had two-times more traffic than the former (Marr et al., 1999). Uncombusted fuel can also contribute significantly to PAH emissions from diesel engines (Williams et al., 1989).

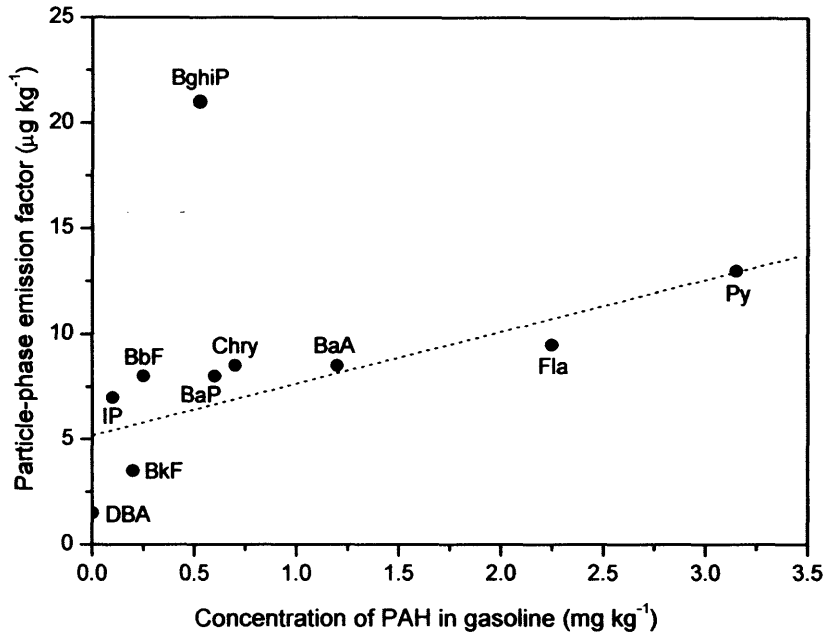


Figure 4. PAH emission factor versus concentration in gasoline. Linear fit does not include BghiP ($r^2$ = 0.67; slope = 2.9 μg PAH emitted per mg in the fuel). Modified from Marr et al. (1999).

Residential heating is also an important source of PAHs to the atmosphere, especially in the winter months. Atmospheric studies conducted in several urban and

rural locations in the state of New Jersey concluded that 98% of BaP present in the winter derived from residential wood burning (Harkov and Greenberg, 1985). In addition, total PAH concentrations of approximately 20 mg per kg of dry wood burnt have been measured for small residential stoves in Norway (Ramdahl et al., 1982). Combustion in residential wood stoves and fireplaces is commonly incomplete because of insufficient access to air and slow, low-temperature burning conditions. In fact, data indicate that BaP emissions from residential wood combustion are 6 times higher per BTU than emissions from residential coal burning, 400-fold greater than gasoline combustion and about 9,000 times greater than emissions from residential oil furnaces (Harkov and Greenberg, 1985). These differences in emission factors are quite significant given that the sources of energy for residential heating have varied significantly over time in the USA. Consumption of natural gas for residential heating increased from 26% of the total in the 1950s to 51% in 2000, while consumption of fuel oil and wood decreased from 22% to 9.8% and from 10% to 1.7%, respectively, in the same period (EIA, 2003). The use of coal for residential heating has not been significant since 1973 when consumption dropped to 1.2% (from 34% in 1950) (EIA, 2003). This suggests that residential heating has probably become a smaller contributor of PAHs to the atmosphere in the last 50 years. However, while consumption of wood for residential heating has decreased in the last 50 years, the elevated PAH emissions generated by this source may be responsible for a significant portion of the current levels of atmospheric PAHs observed during the winter in cold regions.

A number of studies have attempted to characterize the emissions generated by the combustion of different types of biomass. Some of the data available in the literature include pine, oak and eucalyptus (Schauer et al.), red maple, red oak, paper birch, white pine, eastern hemlock, balsam fir (Fine et al., 2001), barley, corn, rice, wheat, almond, walnut, ponderosa pine and douglas fir (Jenkins et al., 1996), among others. It has been observed that PAHs emission factors can vary by 2 orders of magnitude depending only on the type of vegetation burnt (Jenkins et al., 1996). Other parameters such as moisture content, burning conditions, whether or not the fire is stoked, and even the type of

arrangement of the wood in a pile can results in different yields of these compounds (Jenkins et al., 1996; Simoneit, 2002). This large variability underlines the importance of burning conditions on the products generated by combustion (Ramdahl et al., 1982; Jenkins et al., 1996).

### 2.2 Amount of Oxygen

PAHs are produced by the incomplete combustion of organic fuels. Therefore, a rise in the amount of excess oxygen leads to a more efficient combustion process to the point where oxygen is not limiting and combustion is complete. The importance of excess air during combustion is shown repeatedly in laboratory experiments. For example, burning of a coal sample in a fluidized bed at fixed temperature (850°C) and air flow (860 L $h^{-1}$) produced elevated amounts of PAHs when 5% excess air was used, but concentrations dropped an order of magnitude when 20% excess air was applied (Mastral et al., 1998). Similar results have been obtained for vehicle engines, wood fires and residential oil burners. A 7% decrease in excess air in residential oil burners (from 24 to 17%) produced a 10-fold increase in the amount of soot generated. When excess air was lowered from 17% to 13%, soot formation increased by an additional factor of 10 (Prado and Lahaye, 1982). Residential burning of wood also shows greater PAH emissions under oxygen starved conditions. Combustion of spruce in a small residential wood stove was shown to produce an order of magnitude less PAHs when air was not limiting (Figure 5) (Ramdahl et al., 1982). In engines and natural fires the amount of air is measured as a ratio of that to fuel (A/F). Because leaner mixtures (high A/F) supply higher quantities of oxygen, more efficient combustion can occur, resulting in lower emissions of PAHs. In general, PAH emissions by automobile engines decrease with an increase in the amount of air supplied, up to the point of lean misfire (A/F = ~17.5) when PAHs emissions increase sharply (Pedersen et al., 1980; Acres et al., 1982). Interestingly, PAH concentrations were also shown to rise when the percentage of excess air injected during the combustion of coal samples in fluidized bed was elevated from the optimum 20% to 40% (Figure 5) (Mastral et al., 1998). The latter study showed that independent of the

amount of excess oxygen, 3-, 4- and 6-ring PAHs were always produced in higher quantities than 5-ring compounds (Mastral et al., 1998).

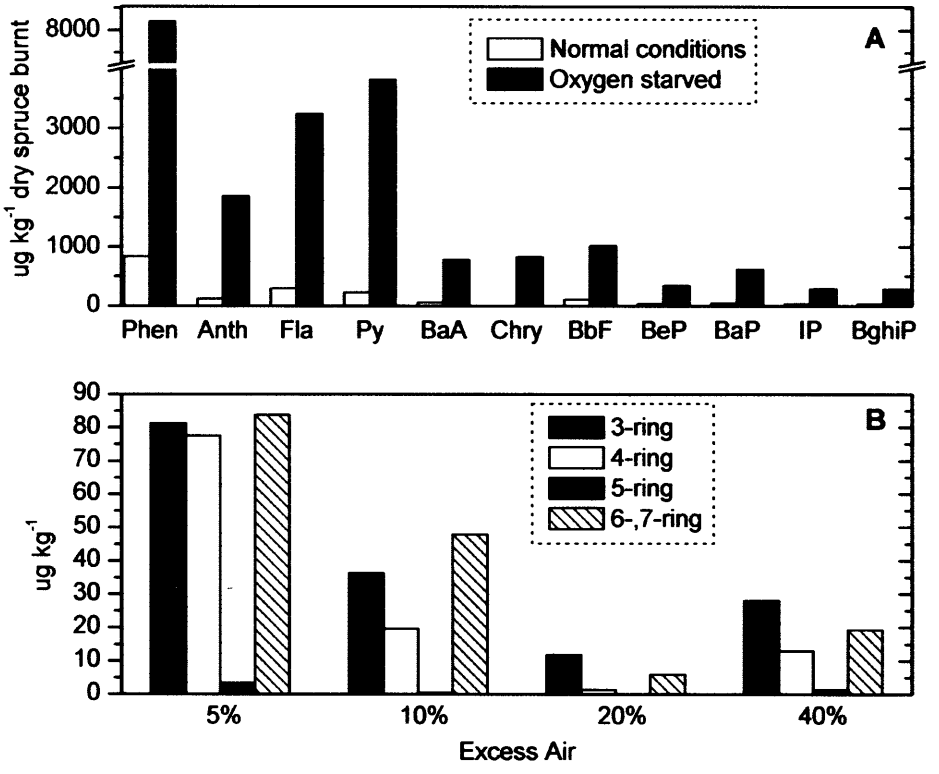


Figure 5. (a) Emission of PAHs during burning of spruce in a residential wood stove under normal (flaming) and air starved conditions. Modified from Ramdahl and collaborators (1982); (b) PAH distribution by number of rings as a function of the percentage of excess air during coal combustion in fluidized-bed. (3-ring = acenaphthene + fluorene + Anth), (4-ring = Py + BaA + Chry), (5-ring = BkF + BaP), (6-7-ring = perylene + DBA + Cor). Modified from Mastral and collaborators (1998).

## 2.3 Temperature

The molecular distribution of PAHs has also been linked to the temperature at which these compounds are formed. Low temperatures, such as in forest fires and cigarettes are thought to generate mixtures enriched in alkyl-substituted PAHs, whereas

higher temperatures may favor production of parent compounds (Figure 6) (Blumer, 1976; Laflamme and Hites, 1978). While studying the effects of engine conditions on the emission of PAHs from diesel combustion, Jensen and Hites (Jensen and Hites, 1983) showed that as the temperature of the engine exhaust decreased the concentration of alkylated PAHs increased relative to parent compounds. However, the proportion of alkyl substituted to parent PAH is not the only property affected by the temperature of combustion. Varying temperature conditions were shown to increase the amount of total PAH emissions by 1000-fold at a municipal incinerator plant in Sweden. During a normal day of operation (Tuesday to Friday) the incineration plant emitted ~ 10 ng $m^{-3}$ of each individual PAH, while on a cold start up day (Monday) concentrations were measured at ~ 10 μg $m^{-3}$ (Colmsjö et al., 1986). Mastral and collaborators (1999) have also shown that during automobile waste tire combustion in a fluidized-bed the quantity of PAHs emitted

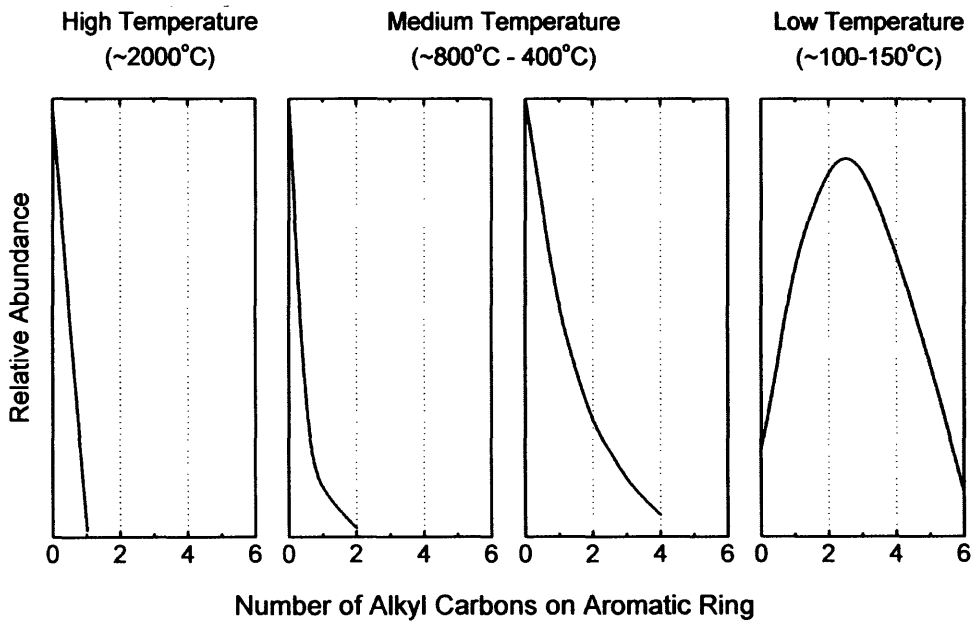


Figure 6. The relative abundance of PAHs as a function of the number of alkyl carbons at different temperatures of formation (Blumer, 1976).

is a direct function of the temperature achieved. For a fixed 20% excess oxygen and 860L $h^{-1}$ air-flow the amount of total PAHs was reported to vary from 4477 μg $kg^{-1}$ (at 650°C) to 390 μg $kg^{-1}$ (at 750°C) and 32198 μg $kg^{-1}$ (at 850°C). Higher temperatures in this system seem to favor more rapid exit velocities of the flue gas from the reactor, leading to shorter time for PAH oxidation reactions to occur.

In summary, the amount and composition of PAH emitted by a single source can vary greatly according to the combustion conditions (temperature, oxygen levels). It is therefore extremely difficult to anticipate the assemblage and quantity of PAHs emitted knowing only the type of fuel (Ramdahl et al., 1982; Colmsjö et al., 1986; Jenkins et al., 1996).

## 3. ENVIRONMENTAL FATE

The environmental fate of PAHs is primarily controlled by their physicochemical properties, although natural processes (e.g. biological degradation), concentration of oxidizing pollutants (e.g., $NO_x$, $O_3$, $OH^{\bullet}$ radicals), temperature and light intensity are also important factors (Kamens et al., 1988; Matsuzawa et al., 2001). For example, Kamens and collaborators have shown that BaP adsorbed to wood soot has longer half-life in a cool (-10°C), dry (2 g $m^{-3}$ $H_2O$) and dark (light = 0.4 cal $cm^{-2}$ $min^{-1}$) environment (half-life = 6 h), such as during winter in high latitudes, than under warm (20°C), humid (10 g $m^{-3}$ $H_2O$) and bright (light = 1 cal $cm^{-2}$ $min^{-1}$) conditions (half-life = 0.5 h), such as in the tropics. Similar trends in persistence were also reported for BaA, Chry, BbF, BkF, IP, BghiP and retene (Kamens et al., 1988).

Pyrogenic PAHs are emitted into the atmosphere either in the gas or particulate phases and their deposition is strongly dependent on the partitioning between these compartments. Some of the factors that can influence partition include (a) vapor pressure of the PAH; (b) amount of fine particles in the atmosphere; (c) ambient temperature; (d) PAH concentration (Yamasaki et al., 1982; Baek et al., 1991a).

Removal of PAHs from the atmosphere can occur by either wet or dry deposition and measurement of both is necessary in order to assess total removal. Wet deposition of

PAHs is relatively simple to evaluate since it is a function of rain and snow precipitation, which can be measured easily (Golomb et al., 2001). Typically, PAHs present in the gas phase dissolve within clouds and into raindrops (Offenberg and Baker, 2002), while PAHs bound to particles are washed out from the atmosphere through this process. Dry deposition results from the direct fallout of PAHs adsorbed to large particles and this mechanism is greatly dependent on the size of these particles (Windsor and Hites, 1979; Baek et al., 1991a). For example, using 1μm and 10μm as the diameters of small and large PAH-bearing particles, it was calculated that the small particles could be transported for ~1300km before settling to the surface, while the larger ones would settle much closer to the source, ~13 km (settling velocity = 6 x $10^{-5}$ m $sec^{-1}$, particle density = 2 g $m^{-3}$, height = 20m and wind = 4 m $sec^{-1}$) (Windsor and Hites, 1979). Measurement of dry deposition rates is complicated by uncertainties related to the velocity of deposition of atmospheric particles, which is a function of the prevailing atmospheric conditions, such as wind speed and humidity (Golomb et al., 2001).

The size of the particles can directly impact the assemblage of PAHs they carry with them. Urban aerosols range in size from a few nanometers (nm) to several micrometers (μm), with particles less than 2.5 μm usually referred to as fine (Seinfeld and Pandis, 1998). Polluted areas tend to have a bimodal distribution of sizes with peaks in the 0.05 to 0.12 μm (mode I) and 0.5 to 1.0 μm (mode II) size ranges (Venkataraman and Friedlander, 1994). Laboratory studies have shown that the size distribution of automobile soot (diesel and gasoline) ranges from a few nm up to 0.3 μm, with mean diameter of about 0.1 μm (Kim et al., 2001). Measurements inside tunnels have also concluded that over 85% of the soot emitted by vehicles is smaller than 0.2 μm (Venkataraman et al., 1994). Measurements of PAHs associated with size-segregated aerosols in Boston, MA showed that 5-ring PAHs (BaP, BeP, benzofluoranthenes and perylene) were predominantly associated to particles in the 0.1-2 μm size range (Allen et al., 1996). These samples demonstrated an inverse correlation between the molecular weight of the PAH and the size of the particles with which they were associated. Lower molecular weight PAHs (3- and 4-ring) were found mostly associated with larger

particles (0.5 to 6 μm), while coronene was present mainly in the 0.01 to 1 μm range (Allen et al., 1996). Similar fractionation of PAHs with particle size was reported for samples collected in Chicago (Offenberg and Baker, 1999). Interestingly, recent measurements in the Caldecott Tunnel (San Francisco, CA) reported that gasoline-derived PAHs existed in the ultrafine size mode (0.05-0.26μm), while diesel-derived compounds were found to vary between 0.26-4 μm (Marr et al., 1999). The size distribution of diesel particles found in this study is noteworthy as it is thought that particles ranging in size from 0.1 to 2.5 μm are less efficiently removed from the atmosphere and tend to have longer atmospheric residence times than finer and coarser particles (Seinfeld and Pandis, 1998).

Total scavenging ratios (gas + particle) can vary among individual PAHs by more than 3 orders of magnitude, but in general they are greater for the less volatile compounds (Offenberg and Baker, 2002), which are more likely to be associated with particles. That is in agreement with dry deposition being the main mechanism of removal of PAH from the atmosphere (Gschwend and Hites, 1981; McVeety and Hites, 1988; Golomb et al., 1997; Offenberg and Baker, 2002) and to the high dry to wet PAH flux ratios (e.g. 9:1) usually observed (McVeety and Hites, 1988). Due to their hydrophobic nature (log $K_{ow}$ = 3 to 8), PAHs deposited onto aquatic systems will tend to associate with settling particles. The strong adsorption of PAHs onto particles (soot in special) can reduce their bioavailability, slowing their biodegradation rates and preserving them in the sediments (McElroy et al., 1989; McGroddy et al., 1996). Some of the factors that can further affect the environmental distribution and fate of PAHs are discussed below.

### 3.1 Physicochemical properties

The structure and physical properties of PAHs can greatly impact their volatility, solubility, sorption and decomposition behaviors (Schwarzenbach et al., 2003). PAHs range from slightly soluble in water (naphthalene) to extremely insoluble (DBA), and from very volatile (naphthalene) to semi-volatile (perylene) (Table 1). Typically, the higher the mass of the compound the lower its vapor pressure and water solubility.

Because of the effect that mass has on these parameters, PAHs also show a decrease in vapor pressure and water solubility with increasing alkyl substitution (Boehm and Quinn, 1973; Garrett et al., 1998).

Table 1. Physical and chemical data for 15 individual PAHs.

| Compound | No. Rings | MW | *S* ($ng\ L^{-1}$)[a] | Log $K_{ow}$[a] | $V_p$ (Pa)[a] | Carcinogenic Activity[b] |
|---|---|---|---|---|---|---|
| Naphthalene | 2 | 128 | 31 | 3.37 | 10.4 | - |
| 2-Methylnaphthalene | 2 | 142 | 25 | 3.86 | 9 | - |
| Phenanthrene | 3 | 178 | 1.10 | 4.57 | 0.02 | - |
| Anthracene | 3 | 178 | 0.045 | 4.54 | 0.001 | - |
| Pyrene | 4 | 202 | 0.132 | 5.18 | 0.0006 | - |
| Fluoranthene | 4 | 202 | 0.26 | 5.22 | 0.00123 | - |
| BaA | 4 | 228 | 0.011 | 5.91 | $2.8x10^{-5}$ | low |
| Chrysene | 4 | 228 | - | 5.86 | $5.7x10^{-7}$ | low |
| BaP | 5 | 252 | 0.0038 | 6.04 | $7.0x10^{-7}$ | strong |
| BeP | 5 | 252 | 0.004 | - | $7.4x10^{-7}$ | - |
| BbF | 5 | 252 | 0.0015 | 5.80 | - | - |
| BkF | 5 | 252 | 0.0008 | 6.00 | $5.2x10^{-8}$ | - |
| Perylene | 5 | 252 | 0.0004 | 6.25 | $1.4x10^{-8}$ | - |
| BghiP | 6 | 276 | 0.00026 | 6.50 | - | - |
| DBA | 6 | 278 | 0.0006 | 6.75 | $3.7x10^{-10}$ | strong |

MW = molecular weight; *S* = water solubility; $K_{ow}$ = octanol-water partition coefficient; $V_p$ = vapor pressure

[a] Mackay, 1992

[b] Budzinski et al., 1997

The distribution of atmospheric PAHs between gas and particulate phase is mostly determined by the vapor pressure of the compound. It is usually reported that PAHs with 3-4 rings are present in the atmosphere mainly in the gas phase (Phen, Fla, and Py), equal concentrations in the vapor and gas phases are found for Chry and BaA, and PAHs with 5- or more rings are mostly evident in the particle phase (Yamasaki et al., 1982; Fraser et al., 1998). These findings are consistent with the measured vapor pressures of these compounds. Nevertheless, variations on the distribution of PAH between the gas and particulate phases are present in the literature. Measurements in a Baltimore tunnel reported 3-ring PAHs mostly in the gas-phase (~90%), while Fla and Py

were evenly distributed between the particle and vapor phases (Benner Jr. et al., 1989). In contrast, analysis of ambient and tunnel air in Los Angeles showed the majority of Fla and Py (99% and 98.8%) and some BaA and Chry (42% and 44%) in the vapor phase, but PAHs larger than Chry were found preferentially adsorbed to particles (Figure 7a) (Fraser et al., 1998). Partitioning between the gas and particle phases is also a function of the number of particles available in the atmosphere. It has been observed that because small quantities of particulate matter are produced during combustion of kerosene (Figure 7b), PAHs emitted by this process tend to partition preferentially to the gas phase (Oanh et al., 2002). In contrast, the abundance of particles generated by the combustion of wood enables even small compounds (Fla) to partition to the particle phase (Schauer et al., 2001).

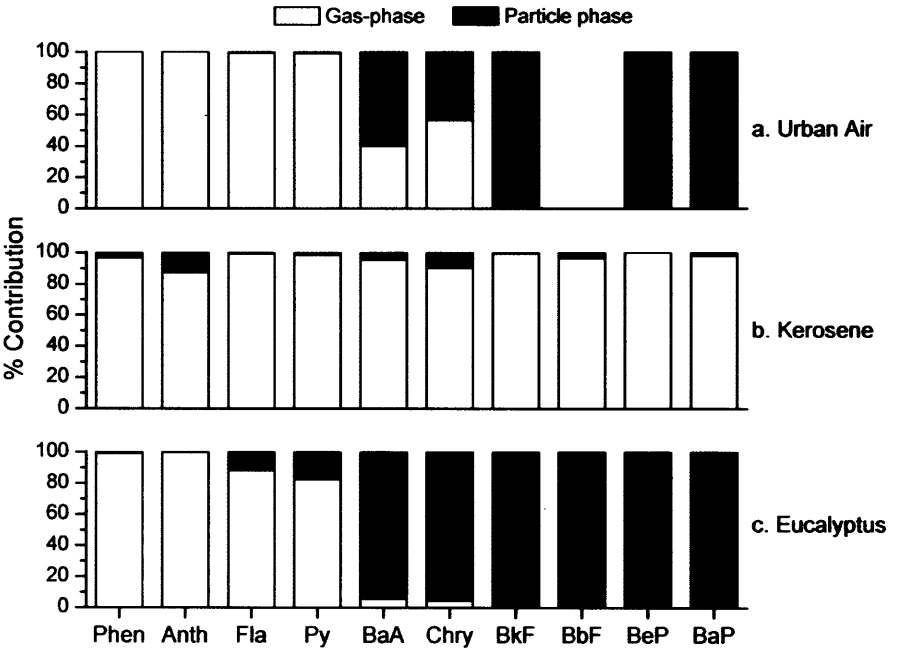


Figure 7. Partitioning of selected PAHs between the gas and particulate phases (a) distribution in atmospheric air in Los Angeles, CA (Fraser et al., 1998); (b) emission during combustion of kerosene in a cookstove (Oanh et al., 2002); and (c) emission by the combustion of eucalyptus in a fireplace (Schauer et al., 2001).

Solubility ($S$) in water is another property that defines the environmental fate of PAHs. PAHs are hydrophobic, meaning they have a higher tendency to associate with particles than to dissolve in water (as measured by the octanol-water partition coefficient, $K_{ow}$, Table 1). Although PAHs tend to have low water solubility, the difference in $S$ among individual PAHs is significant enough to have an impact on their distribution in the environment. For example, sediment trap studies conducted in the Mediterranean Sea showed a decrease in total PAH fluxes from 200 m in the water column to 2000m, and from there to the underlying sediments (Lipiatou et al., 1993) (Figure 8a). While the profile of benzofluoranthenes did not vary significantly with depth, that of Phen showed a marked decrease in flux. The authors suggested that because Phen is more soluble than the benzofluoranthenes, it can partition into the dissolved phase and be susceptible to

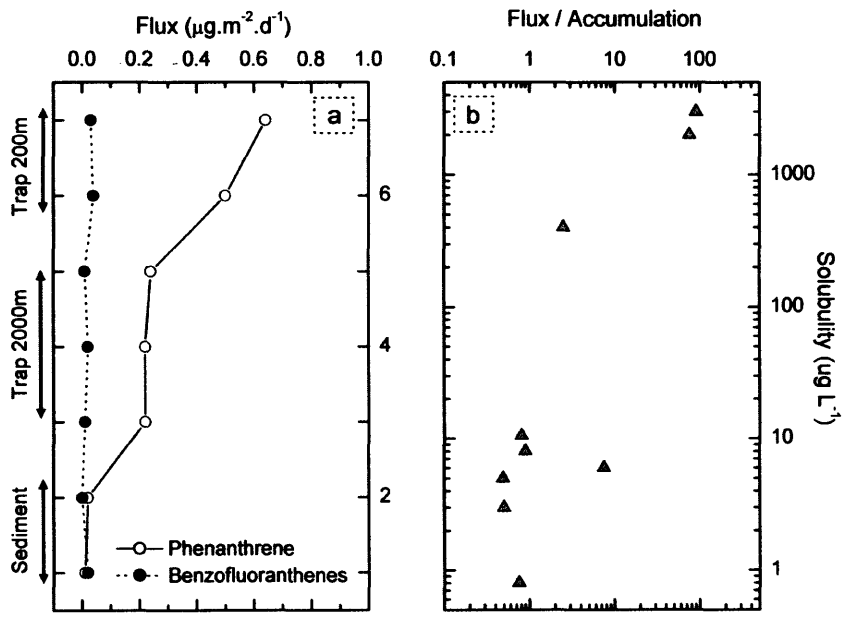


Figure 8. (a) Flux of Phen and benzofluoranthenes in sediment traps and surficial sediment from the Mediterranean sea (Lipiatou et al., 1993); (b) recycling ratios of PAHs in Lake Superior (calculated as the ratio between flux through the water column and accumulation in the sediments) versus their aqueous solubility (Baker et al., 1991).

degradation in the water column. Their results agree with previous study conducted in Lake Superior that showed a positive correlation between solubility and recycling of PAHs in the water column (Figure 8b) (Baker et al., 1991).

### 3.2 Biodegradation

It is well documented that low molecular weight PAHs (such as naphthalene) are more likely to undergo microbial degradation than higher molecular weight compounds (Cerniglia and Heitkamp, 1989; Budzinski et al., 1998). Typically, susceptibility to biodegradation decreases as the number of fused rings in the PAH increases. Microbial degradation experiments have also demonstrated that alkyl substituted PAH degrade more slowly than parent compounds. For example, Heitkamp and collaborators (Heitkamp and Cerniglia, 1987) reported faster degradation rates for Phen than for 2-methylnaphthalene (Figure 9) in sediments from a pristine and an oil-exposed ecosystem. Experiments using crude oils have yield similar results (Garrett et al., 1998). Because sediments are usually the final destination of PAHs in the environment, extensive research has been conducted on the aerobic degradation of sedimentary PAHs (Bauer and Capone, 1988; Cerniglia and Heitkamp, 1989; Yuan et al., 2001) and potential pathways for bacterial oxidation of several compounds have been reported (Cerniglia and Heitkamp, 1989). Interestingly, prior exposure to PAHs seems to enhance the capacity of a microbial population to degrade these compounds (Bauer and Capone, 1988). Apparently, microbial communities can adapt to metabolize a compound after prolonged exposure to it (Cerniglia and Heitkamp, 1989). The faster degradation rates reported for certain PAHs in previously exposed sediments therefore result from the selection and proliferation of microbial communities capable of degrading these compounds (Bauer and Capone, 1988).

Until the late 1980s it was assumed that PAHs deposited in anoxic sediments were not affected by biodegradation (Cerniglia and Heitkamp, 1989; Rothermich et al., 2002). However, microbial mediated transformations of PAHs in anaerobic environments are now known to occur under denitrifying and sulfate reducing conditions. Marine

surface sediments incubated under denitrifying conditions have resulted in degradation of PAH from 3- to 5-rings. As in aerobic degradation, the more soluble, lower molecular weight PAHs (acenaphthene and Phen) degraded faster than less soluble, higher molecular weight compounds (BaA and BaP) (MacRae and Hall, 1998). Moreover, when the biodegradation rate of compounds of the same size is compared, it becomes clear that the microbial community preferentially degrades the most soluble isomer (e.g, Phen was shown to degrade faster than the less soluble Anth). The main reason for the preferential biodegradation of more soluble compounds is presumed to be the preference of microorganisms to assimilate substrates from the water phase (MacRae and Hall, 1998). That implies that particle-bound pyrogenic PAHs, which are less available to dissolution than PAHs derived from petroleum spills (Farrington et al., 1983; McGroddy et al., 1996; Gustafsson and Gschwend, 1997) are also less susceptible to degradation by microorganisms. In fact, treatment of PAH contaminated sediments dredged from Milwaukee Harbor showed that PAH sorbed onto coal-derived particles underwent minimal biodegradation, while those sorbed on clay/silt particles were readily biodegraded (Talley et al., 2002). Another example of the greater susceptibility of unbound hydrocarbons to weathering and degradation was given by Jones and collaborators (1986). Monitoring of two sites in the Humber Estuary (UK) after the spillage of 6000 tones of a Nigerian light crude oil showed that 12 months after the accident most of the oil-derived hydrocarbons had been weathered (biodegraded and water washed). As a result, non-alkylated (combustion-derived) PAHs predominated in the sediments over alkylated PAHs (typical of petrogenic sources). That is noteworthy as, in general, parent PAHs are preferentially biodegraded over alkylated species. The fast disappearance of alkylated petrogenic PAHs over combustion-derived parent PAHs corroborated the idea that particle-bound species are not readily available for partitioning into the dissolved phase, which greatly affects their biodegradability and renders them persistent in the environment (Jones et al., 1986).

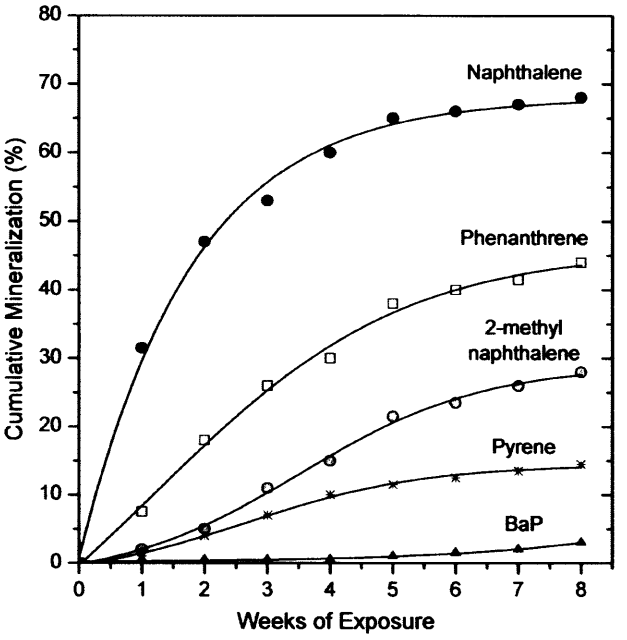


Figure 9. Rate of biodegradation of several PAHs in an estuarine system exposed to oil (Heitkamp and Cerniglia, 1987).

Degradation of petrogenic PAHs under sulfate reducing conditions was demonstrated recently for sediments from San Diego Bay (CA), Boston Harbor (MA) and Tampa Bay (FL) (Coates et al., 1997; Hayes et al., 1999; Rothermich et al., 2002). Lower molecular weight PAHs were shown to degrade faster than larger molecules (4- and 5-ring) during the one year monitoring of the concentration of PAHs in sulfate reducing sediments from the Boston Harbor (Rothermich et al., 2002). On the first 105 days of the experiment there was no apparent degradation of 4- and 5-ring PAHs, but concentrations of these compounds decreased with continued incubation. After 338 days, Py had decreased 13%, BaA 9%, Chry 25% and BaP 24%, compared to fluorene 67% and Phen 58%. Sediments poisoned by molybdate to inhibit sulfate-reducing bacteria showed no significant change in PAH levels during this time (Rothermich et al., 2002). Although laboratory experiments show relatively fast degradation of selected PAHs, their fate is greatly dependent on the environmental conditions at the site of deposition. For example,

samples taken 30 years after the West Falmouth oil spill in Massachusetts still show elevated levels of polycyclic aromatic hydrocarbons in the marsh sediments (Reddy et al., 2002a). Although the microbial community at this site could have adapted to anaerobically degrade the oil, the abundance of organic-rich plant remains may quickly reduce the pool of electron acceptors necessary for anaerobic degradation. It is thought that in this situation PAH composition in the sediments may persist unchanged indefinitely (Reddy et al., 2002a).

### 3.3 Photodegradation and Chemical Oxidation

PAHs present in the atmosphere are susceptible to both chemical oxidation and photochemical alterations (Baek et al., 1991b). PAHs can react with atmospheric ozone ($O_3$), $NO_x$, $SO_x$ and $OH^{\bullet}$ radicals to form products sometimes more toxic than the PAH precursor, as in the case of nitro-PAHs. The half-life of a individual PAH can range widely depending on the ambient conditions. Exposure of soot-bound PAHs to air containing 10 ppm of $NO_x$ showed that individual PAHs exhibit different half-lives that can range from 7 days (BaP) to 30 days (Phen and Cor). However, when these samples were exposed to ambient laboratory air (230 days) or to air containing 5ppm $SO_2$ (99 days) they did not react significantly (Butler and Crossley, 1981). Experiments using wood smoke from a residential stove and gasoline soot from an internal combustion engine also demonstrated rapid degradation of PAHs exposed to sunlight, $O_3$ and $NO_2$ in an outdoor smog chamber (Kamens et al., 1988). PAHs were shown to degrade at a much faster pace during sunlight than at night, suggesting photoinduced decay is a more important factor than chemical oxidation. After 5 hours of sunlight, BaP concentrations in the wood smoke had declined 4-fold, whereas no degradation was observed during the following hours of darkness. PAH decay resumed the next day when sunlight was again available (Figure 10). Similar results were obtained for PAHs bound to gasoline soot. The authors concluded that sunlight had greater influence on the rate of decay of PAH than either $O_3$ or $NO_2$ (Kamens et al., 1988).

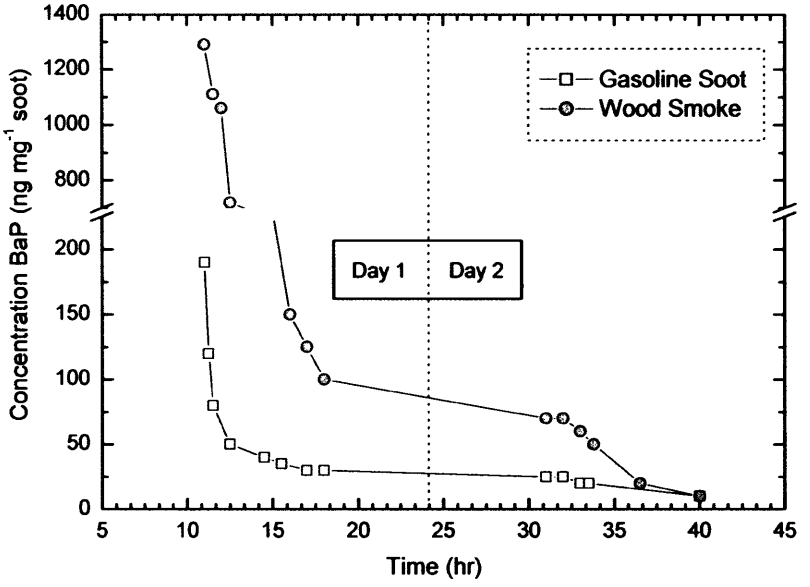


Figure 10. Degradation of BaP present in gasoline and wood soot over a 30-h period of outdoor sunlight and darkness. Modified from Kamens and collaborators (1988).

Photochemical reactions can thus act rapidly and have important effects on the fate of PAHs. Experiments with crude oils have shown that alkyl substituted PAHs photodegrade at a faster rate than parent compounds (Ehrhardt et al., 1992; Garrett et al., 1998). Garrett and collaborators observed a significant increase in the extent of photooxidation of Phen, dibenzothiophene and Chry with increasing alkyl substitution when crude oils were irradiated for 48 h with a 55W UV light. Among the 3 parent compounds studied, Chry showed greater photodegradation than either Phen or dibenzothiophene (Garrett et al., 1998). The degree to which a compound is susceptible to photolytic reactions is dictated, among other things, by its absorption spectrum and by the nature of the particle to which it is absorbed (Schwarzenbach et al., 2003). PAHs absorb light over a wide range of wavelengths ($\lambda$) and, in general, linear PAHs can absorb over a wider range and up to higher wavelengths than their angular isomers. For example, the absorption spectrum of Anth ranges from ~200-390 nm, compared to ~200-350 nm for Phen (Figure 11) (Pretsch et al., 1989; Schwarzenbach et al., 2003) and this

difference in susceptibility to photodegradation can markedly change the relative proportion of these compounds during atmospheric transport (Gschwend and Hites, 1981). Laboratory simulations have shown that BaA, BaP, and alkylated Phen, Fla, Py are photoreactive under UV-visible conditions (290 to 600 nm) so these compounds can be removed from aerosols during atmospheric transport. In contrast, Chry and BeP are more photostable and tend to persist reasonably unchanged during atmospheric transport (Simó et al., 1997).

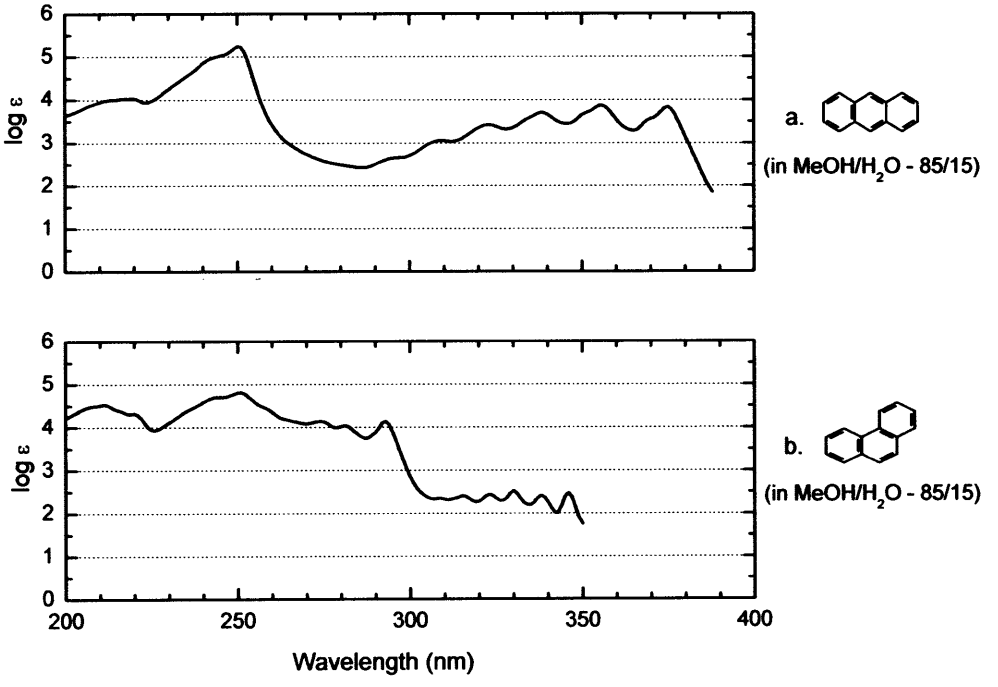


Figure 11. Absorption spectra of (a) anthracene and (b) phenanthrene.

The association of PAHs with soot is thought to protect these compounds from transformations in the atmosphere and in the water column (Lipiatou et al., 1993; Tolosa et al., 1996). Indeed, PAHs adsorbed onto fly ash have shown less susceptibility to photodegradation than pure compounds. For example, approximately 90% of Py present

in a dilute solution degraded after 7.5 h of exposure under a 275-W sunlamp, while only 13% of Py adsorbed to fly ash photodecomposed after 24 h under similar light (Korfmacher et al., 1980). Similar results were obtained for Anth and BaP, but Phen and Fla showed greater resistance to photodegradation. Fla present in solution decomposedonly 10% when exposed to illumination for 9.5 h and no photodegradation was observed when this compound was adsorbed on fly ash (Korfmacher et al., 1980). Laboratory experiments have also found that the characteristics of the particle can influence the fate of atmospheric PAHs. After determining the half-life of 18 individual PAHs in 16 different substrates, Behymer and Hites (1988) concluded that most particle-bound PAHs can undergo some degree of photolysis and that the type of particle can influence greatly the extent of photodegradation suffered by the compound. When Standard Reference Material (SRM) 1650 from the National Institute of Standards and Technology (NIST) was exposed to a 900-W light source, Py remained fairly stable towards photodegradation (half-life = 9.24 ± 0.53 h) compared to BaP (half-life = 1.63 ± 0.48 h) (Matsuzawa et al., 2001). This later study concluded that the propensity of individual PAHs adsorbed to diesel soot to undergo photodegradation was BaP > Phen > Py, Chry, Fla (Matsuzawa et al., 2001). In contrast, experiments with fly ash showed that after approximately 24 hours under a 275-W light source BaP and Py had undergone similar photodecay (10% and 13%, respectively) (Korfmacher et al., 1980), thus further emphasizing the influence of the substrate. It has also been observed that when NIST SRM 1650 is mixed with extracted soil (SRM 1650/soil = 5/95) the rate of photodegradation of BaP and Phen are reduced (Matsuzawa et al., 2001). Under these conditions shielding of light by the soil is apparently the most important factor.

## 4. SOURCE APPORTIONMENT

Several different methods are reported in the literature for apportionment of the sources of PAHs encountered in the environment. Some of these methods include the use of historical records (Heit et al., 1988; Latimer and Quinn, 1996; Gevao et al., 1998; Van Metre et al., 2000; Schneider et al., 2001; Lima et al., 2003), source diagnostic ratios

(Colombo et al., 1989; Yunker et al., 1996), principal component analysis (Yunker et al., 1999; Dickhut et al., 2000), multiple linear regression (Simcik et al., 1999), chemical mass balance (Gordon, 1988; Christensen et al., 1999; Zheng et al., 2002; Li et al., 2003), stable carbon isotopic composition (O'Malley et al., 1994; McRae et al., 1999; Okuda et al., 2002a) and more recently, the radiocarbon content of specific PAHs (Currie et al., 1997; Reddy et al., 2002b; Reddy et al., 2003). Because of the extent of this topic, we will refrain from discussing the 3 statistics based methods.

### 4.1 Source diagnostic ratios

Source diagnostic ratios such as the sum of methyl-phenanthrenes and methyl-anthracenes to phenanthrene (ΣMPhen/Phen), fluoranthene to pyrene (Fla/Py) and 4,5-dimethyl-phenanthrene to the sum of methyl-phenanthrenes and methyl-anthracenes (4,5-MPhen/ΣMPhen) have been extensively applied in differentiating between pyrogenic and petrogenic PAH sources (Gschwend and Hites, 1981; Prahl and Carpenter, 1983; Colombo et al., 1989; Lipiatou et al., 1993; Budzinski et al., 1995; Pereira et al., 1999; Readman et al., 2002; Yunker et al., 2002). Other ratios such as the and 1,7-dimethylphenanthrene to 2,6-dimethylphenanthrene (1,7-DMPhen/2,6-DMPhen) are thought to indicate the relative contribution of pyrogenic PAHs derived from biomass burning (higher 1,7-DMPhen) versus fossil-fuel combustion (higher 2,6-DMPhen) (Benner Jr. et al., 1995). Table 2 shows a brief summary of the ratios commonly applied in source apportioning and their range.

Pioneer work by Youngblood and Blumer (1975) suggested that the distribution of alkylated versus parent PAH in sedimentary environments could be used to distinguish between high temperature versus low temperature sources of these compounds. Laflamme and Hites (1978) applied this concept to samples collected worldwide in an attempt to distinguish between pyrogenic and petrogenic PAHs. The ΣMPhen/Phen ratio has been widely since in apportioning sources of PAHs to the environment (Hites et al., 1980; Gschwend and Hites, 1981; Prahl and Carpenter, 1983; Lipiatou et al., 1993; Ohkouchi et al., 1999; Pereira et al., 1999). Petroleum-derived PAHs are usually heavily

alkylated. However, diesel engines and wood combustion can also emit ΣMPhen in higher proportions than Phen, easily exceeding the ΣMphen/Phen range commonly cited for combustion sources (Prahl and Carpenter, 1983) (Table 2 and Figure 12). Experiments on diesel burning as a spill clean up countermeasure have reported no obvious dominance of parent PAHs over alkylated homologues (Wang et al., 1999). In addition, it has been suggested that an elevated contribution of alkylated PAHs (especially methyl-phenanthrenes) can either be attributed to petrogenic sources or to exhaust emissions from heavy-duty diesel trucks (Rogge et al., 1993).

Table 2. Commonly applied values for selected PAH source diagnostic ratios.

| Ratios | Automobile | Coal | Wood | Crude oil | Combustion | Petroleum |
|---|---|---|---|---|---|---|
| ΣMPhen / Phen | - | 0.25[e] | 0.33[a] | 3.3 – 33[a]<br>2 - 5.9[c]<br>3.1 - 5.6[e] | 0.5 – 1[c] | 2 – 6[c] |
| Phen / Anth | - | 3[a] | 3[a] | 50[a] | < 10[f] | > 10[f] |
| Fla / Py | 0.6[a] | 1.4[a] | 1[a] | 0.6 - 10[a] | >1[f] | - |
| BaA / Chry | 0.28[a]<br>0.52 ± 0.06[b] | 1[a]<br>1.11 ± 0.06[b] | 0.93[a]<br>0.79 ± 0.13[b] | 0.06 - 0.4[a] | - | - |
| BbF / BkF | 1.26 ± 0.19[b] | 3.70 ± 0.17[b] | 0.92 ± 0.16[b] | - | - | - |
| BaP / BeP | 0.07[a]<br>0.88 ± 0.13[b] | 1.19[a]<br>1.48 ± 0.03[b] | 2.27[a]<br>1.52 ± 0.19[b] | 0.3 - 5[a] | - | - |
| IP / BghiP | 0.33 ± 0.06[b] | 1.09 ± 0.03[b] | 0.28 ± 0.05[b] | - | - | - |
| 4,5DMP / ΣMP | - | 0.3[a]<br>38.5[e] | 1[a] | 0.01 - 0.03[d]<br>0[e] | - | - |

[a] (Gschwend and Hites, 1981); [b] (Dickhut et al., 2000); [c] (Prahl and Carpenter, 1983); [d] (Youngblood and Blumer, 1975); [e] (Garrigues et al., 1995); [f] (Budzinski et al., 1997)

The notion that 1,7-DMPhen/2,6-DMPhen can be used as a tool to discern between PAHs derived from biomass burning versus fossil-fuel combustion (Benner Jr. et

al., 1995) has also been recently challenged by studies on the aerobic degradation of crude oils (Budzinski et al., 1998; Mazeas et al., 2002). After incubating a sample of Arabian light crude oil for 7 days under oxic conditions, 2,6-DMPhen was shown to be the most easily degradable dimethylphenanthrene isomer (20% remaining after 7 days), while 1,7-DMPhen was 3-times more resilient (60% remaining after 7 days) (Budzinski et al., 1998; Mazeas et al., 2002). If 2,6-DMPhen is preferentially lost by biodegradation in sediments, then the 1,7-DMPhen/2,6-DMPhen ratio will result in answers that are biased towards a biomass burning signature.

Other source diagnostic ratios are based on the relative stability of individual PAHs. Linear or predominantly linear PAHs (Anth, BaA, BaP, DBA) and those containing a 5-membered ring (Fla, BbF, BkF, IP) are less stable than their clustered isomers of similar molecular mass (Blumer, 1976; Yunker and MacDonald, 1995). It is thought that during the combustion process a greater proportion of the less stable isomer is produced, so the relative abundance of unstable to stable PAHs of similar molecular mass could give an estimate of the origin of these compounds. Budzinki and collaborators (1995; 1997) have demonstrated through thermodynamic calculations that the Phen/Anth ratio is strongly dependent on the temperature of combustion. Phen/Anth was reported to vary from 5.6 at 1000 K to 8.3 at 700 K, up to 49 at 300 K. Because petrogenic PAHs are formed at lower temperatures than combustion derived PAHs, the authors suggested that the Phen/Anth ratio was a robust way of discerning the sources of sedimentary PAHs between petrogenic (Phen/Anth >10) and pyrogenic (Phen/Anth <10) PAHs. However, care should be taken as emissions from diesel engines and municipal incinerators have been shown to produce Phen/Anth signatures that could be mistaken for a petrogenic input of PAHs (Figure 12). Budzinski and collaborators also suggest that the use of various ratios can enhance the capability of discerning between petrogenic and combustion sources and propose that a plot of Phen/Anth versus Fla/Py could help distinguish sources with more accuracy. Plotting of Phen/Anth values against Fla/Py for a number of environmental samples is reported to accurately distinguish between areas contaminated by pyrogenic and petrogenic PAHs. Nevertheless, when literature values of

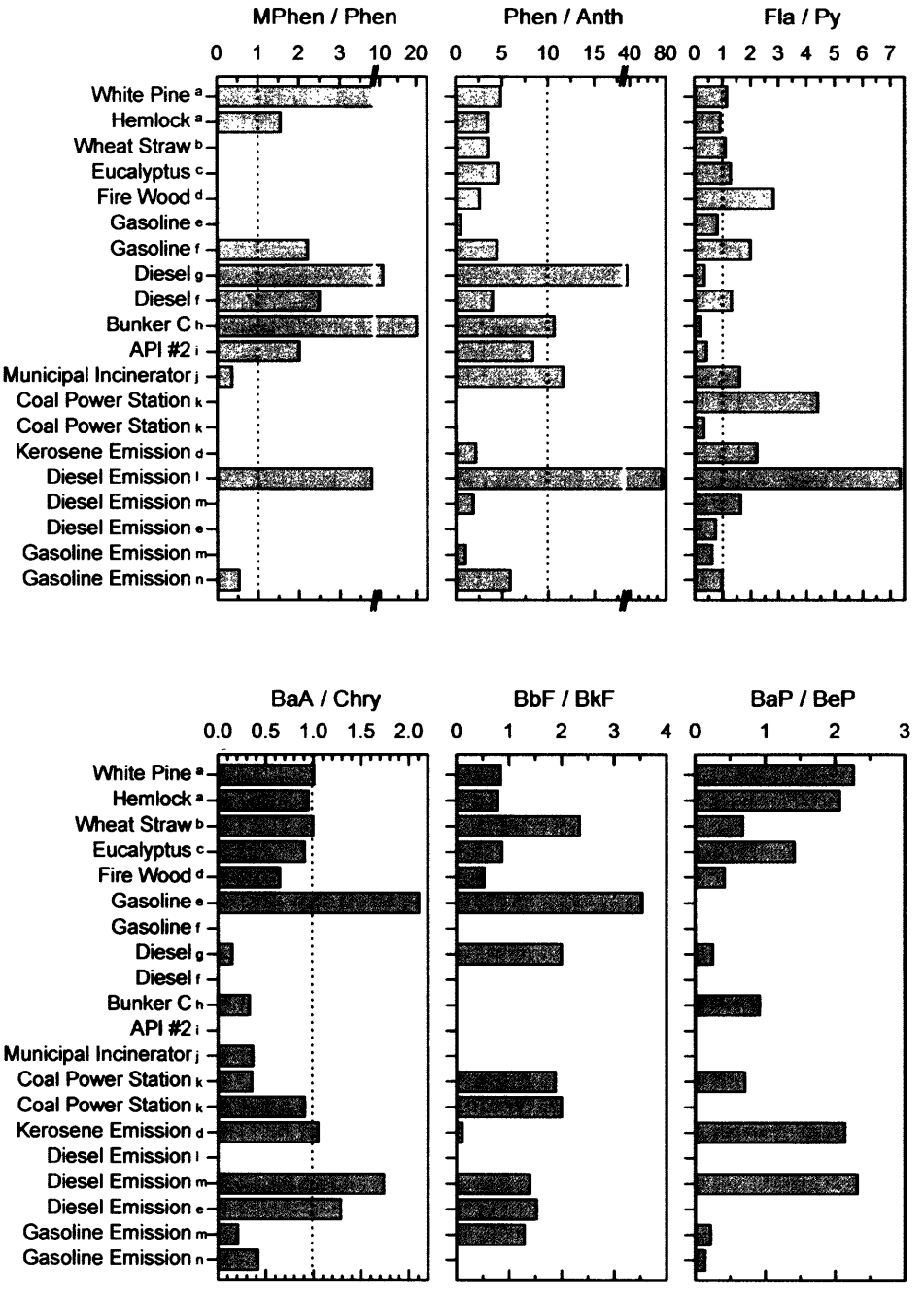


Figure 12. Comparison between commonly cited source diagnostic ratios and primary sources of PAHs. [a] (Fine et al., 2001); [b] (Jenkins et al., 1996); [c] (Schauer et al., 2001); [d] (Oanh et al., 2002); [e] (Marr et al., 1999); [f] (Williams et al., 1986); [g] (Wang et al., 1999); [h] (Wang et al., 1997); [i] (Reddy, 1997); [j] (Colmsjö et al., 1986); [k] (Masclet et al., 1987); [l] (Jensen and Hites, 1983); [m] (Khalili et al., 1995); [n] (Schauer et al., 2002).

Phen/Anth and Fla/Py for primary sources of PAHs are plotted against each other (Figure 13) no obvious trend emerges. Independent of the source, the majority of the Phen/Anth - Fla/Py pairs plot in the region stipulated as pyrogenic.

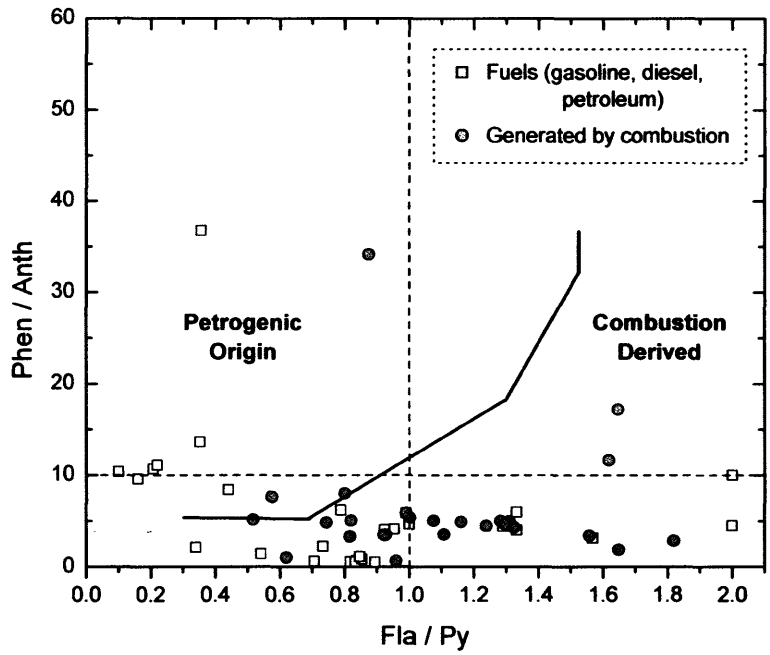


Figure 13. Cross plot of the Phen/Anth and Fla/Py ratios for primary sources of PAHs. Petrogenic sources encompass diesel fuel, gasoline, crankcase and crude oil, while pyrogenic sources include combustion of wood, gasoline, diesel, kerosene and garbage (Colmsjö et al., 1986; Nishioka et al., 1986; Williams et al., 1986; Pruell and Quinn, 1988; Benner et al., 1990; Rogge et al., 1993; Khalili et al., 1995; Jenkins et al., 1996; Wang et al., 1997; Marr et al., 1999; Wang et al., 1999; Fine et al., 2001; Schauer et al., 2001; Oanh et al., 2002; Schauer et al., 2002).

The accurate use of diagnostic ratios depends primarily on the uniqueness of the fingerprint of the sources. While ratios can be somewhat helpful in distinguishing petrogenic from combustion-derived sources, the diversity of fuels and combustion conditions discussed previously are likely to produce variations in ratios from a single source, hindering the identification of biomass versus fossil fuel combustion inputs. Additionally, PAHs can be transformed by atmospheric processes and diagnostic ratios

measured in atmospheric and sediment samples can differ greatly from those reported for the original sources (Schauer et al., 1996). As a rule, source diagnostic ratios should be used with care and in the context of the study area.

### 4.2 Historical records

The use of sedimentary records to apportion the sources of PAH relies on accurate information on the type and quantity of fuels used through time. Historical data shows that wood burning was the main energy source utilized until the late 1800s when it was surpassed by coal combustion (www.eia.doe.gov/emeu/aer) (Figure 14). The consumption of coal peaked in 1910 at 82 % and proceeded to decline as petroleum use ascended. By 1950, petroleum was the main fuel used in the USA, but coal still accounted for approximately 35% of the total. Natural gas replaced coal as the second most important energy source by the end of the 1950s, and in the early 1970s, natural gas utilization was 50% higher than coal burning. However, in the early 1980s consumption of coal and natural gas became nearly identical at 20%. These trends in energy consumption have been widely used as reference for assigning sources to PAHs archived in marine and lacustrine sediments (Grimmer and Böhnke, 1975; McVeety and Hites, 1988; Gevao et al., 1998; Van Metre et al., 2000; Lima et al., 2003; Yunker and Mcdonald, 2003), soils (Jones et al., 1989; Wild et al., 1990) and peat (Sanders et al., 1995).

In general, sedimentary records have shown good correlation between PAH concentration profiles and energy consumption associated with industrialization. A typical profile of total PAHs (e.g., Siskiwit Lake, Figure 15) shows a gradual increase in concentrations beginning around 1880, coincident with the onset of the Industrial Revolution, to a maximum in the 1950s (Gschwend and Hites, 1981) when coal usage was still high. Because of the substitution of coal with cleaner burning fuels, such as oil and natural gas, a steady decrease in PAH concentrations is usually observed from the 1960s onwards (Gschwend and Hites, 1981; EIA, 2003). The stricter emission controls that came into effect in the 1960s, and the use of catalytic converters in the 1970s (Acres

et al., 1982) most likely contributed to the steady decline in sedimentary PAH concentrations usually observed during this period despite the fact that overall energy consumption continued to increase (Figure 14). Since most of the historical records of PAH found in the literature were generated before the 1990s, the assumption that PAH concentrations continued to decline persisted for over 2 decades. However, in 2000, Van Metre (2000) reported that PAH emissions were increasing again in certain areas of the United States. Based on the analysis of sediment cores from locations experiencing diverse population growth since the 1970s, it was shown that all 10 sites studied exhibited a recent increase in pyrogenic PAH concentrations. The rise in PAH paralleled the increase in automobile usage in these watersheds, implying a link between PAH inputs and urban sprawl. Contrary to these findings, relatively constant PAH inputs were

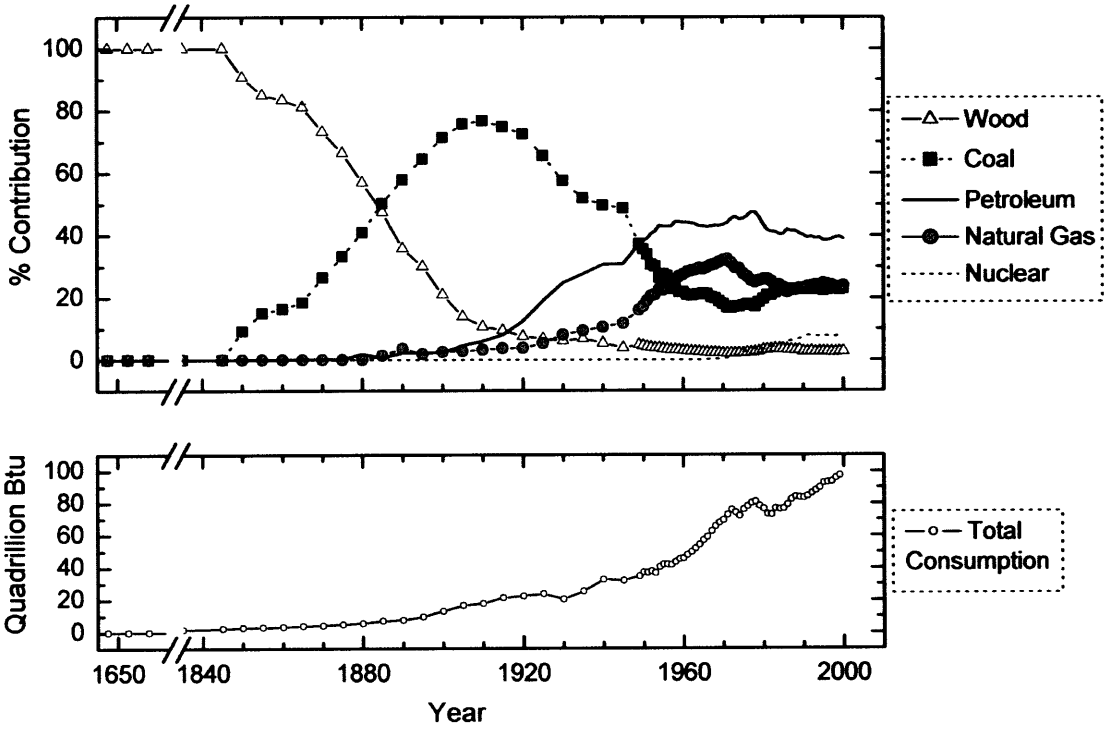


Figure 14. Historical data on the consumption of fuels for energy production in the USA. Modified from www.eia.doe.gov/emeu/aer. Hydroelectric power contributes less than 4 % of the total and is not shown.

observed since the 1980s in cores collected in Lake Michigan (Figure 15) (Schneider et al., 2001). While these studies seem to disagree on the current trend in PAH inputs, neither has reported a continual decrease in PAH concentrations. This indicates that the declining trend that began in the 1970s has, at best, stabilized.

A recent study conducted in the anoxic sediments of the Pettaquamscutt River basin, Rhode Island, reported that PAH concentrations were in the rise again and suggested that diesel consumption was the most probable source of this increase (Lima et al., 2003). This high-resolution historical record showed that between 1983 and 1996 the flux of total PAHs remained relatively constant (210 ±12 ng $cm^{-2}$ $yr^{-1}$), in agreement with

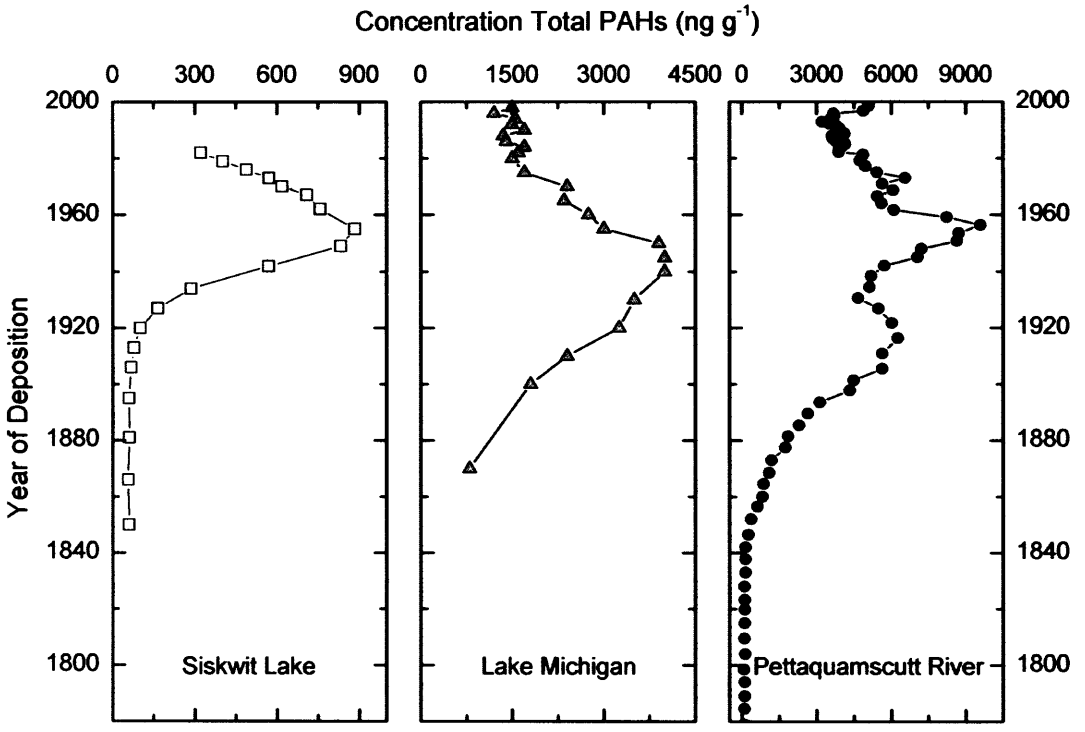


Figure 15. Historical records of total PAH concentrations. Siskiwit Lake sediments exemplifies a typical PAH profile as depicted in the 1980s (McVeety and Hites, 1988). PAH record from Lake Michigan shows constant concentrations from the 1980s into the late 1990s (Schneider et al., 2001), while in the Pettaquamscutt River PAH concentrations show an increase in the second half of the 1990s (Lima et al., 2003).

Lake Michigan sedimentary PAH record (Schneider et al., 2001). However, between 1996 and 1999 the flux of total PAHs to the Pettaquamscutt River sediments rose by 48% (57% from the 1983-1996 mean) (Figure 15). This increase in PAHs flux was said to outpace the growth in population (13.4 %) and in number of vehicles (14 %) in that area during that time interval, but correlated well with an increase in fuel utilization for transportation (gasoline by 7% and diesel by 20%). The authors suggested that traffic of heavier vehicles, which use diesel[1] as fuel, and not passenger automobiles, was most likely responsible for the increased PAH load to southern Rhode Island. This study highlighted the valued utility of high-resolution sampling and detailed historical data on the apportioning of sources of PAHs to the environment.

### 4.3 Stable carbon isotopic composition

O'Malley and collaborators (1994) were the first to measure the carbon isotopic composition of individual PAHs from environmental samples. Compound-specific isotope analysis (CSIA) allows the determination of isotopic signatures of individual compounds and was initially developed to help reconstruct biogeochemical processes (Hayes et al., 1989). This technique has been widely employed for the discrimination of the sources of hydrocarbons encountered in modern and ancient sediments (Freeman et al., 1990; Rieley et al., 1991). Measured $^{13}C/^{12}C$ ratios are reported in the delta ($\delta$) notation, in permil (‰), relative to the Pee Dee Belemnite standard:

$$\delta^{13}C(‰) = \frac{(^{13}C/^{12}C)_{Sample}}{(^{13}C/^{12}C)_{PDB}} - 1) * 1000 \qquad (1)$$

O'Malley and collaborators (1994) have suggested that the isotopic composition of PAHs present in environmental samples is not altered by weathering processes. Evaluation of the effects of evaporation, photodecomposition and microbial degradation of PAH standards under controlled laboratory conditions revealed no significant

[1] Diesel engines produce 1 to 2 orders of magnitude more soot and associated PAH than a comparable gasoline engine.

alteration of the isotopic composition of individual compounds (O'Malley et al., 1994). Similar results were obtained for the aerobic biodegradation of an Arabian crude oil sample (Mazeas et al., 2002). During this experiment, the stable carbon composition of methyl-phenanthrenes remained reasonably constant after 16 days of biodegradation, indicating that bacterial degradation did not induce isotopic fractionation in petrogenic PAHs. Since fractionation due to weathering is also not expected to change the $\delta^{13}C$ of PAHs, the isotopic composition of these compounds have been used to distinguish among sources contribute to PAH burdens in sediments (O'Malley et al., 1996), soils (Lichtfouse et al., 1997; Hammer et al., 1998) and aerosols (Ballentine et al., 1996; Okuda et al., 2002b).

Carbon isotopic measurements of individual PAHs showed different $\delta^{13}C$ values for an automobile exhaust and a wood soot sample (O'Malley et al., 1994). In general, the automobile soot exhibited more $^{13}C$-depleted (i.e., "lighter" or more negative $\delta^{13}C$ values) for 3- and 5-ring compounds (Phen, Anth, benzofluoranthenes and BaP) versus 4-ring PAHs (Fla, Py, BaA and Chry). However, BaA present in the wood soot sample was $^{13}C$-enriched relative to Fla and Py (Figure 16). When assessing the possible PAH contributions to the sediments of Conception Bay, Newfoundland (Figure 16), the authors relied on the similarity of $\delta^{13}C$ values between the environmental sample and that of wood soot to suggest that wood burning was the most likely source of PAHs to that system. On a later contribution, O'Malley and collaborators (1996) combined the isotopic composition and molecular abundance of 4- and 5-ring PAHs to calculate the contribution of crankcase oil, wood and car soot to the sediments of the St. John's Harbour, Newfoundland. The results obtained for that site suggested that 20-50% of the PAHs encountered in the sediments could be derived from crankcase oils versus 50-80% from wood burning and automobile soot. However, the relative importance of the two combustion sources could only be implied by the mixing curves. Recently, a 3-endmember model was used to calculate PAH contributions from wood burning, gasoline and diesel engine vehicle emissions to the Malaysian air (Okuda et al., 2002b). Measurement of haze and non-haze air samples showed comparable PAH $\delta^{13}C$ values,

implying that a single source was responsible for PAHs present in the atmosphere. Results obtained from the 3-endmember model demonstrated that automotive exhaust was the most likely source of the PAHs found in smoke haze events in Malaysia (65 to 75% contribution). This study also showed that even though wood burning contributed 25-35% of the PAHs found in the Malaysian atmosphere, their presence was not correlated to haze events (Okuda et al., 2002b).

The use of compound-specific carbon isotope characterization of PAHs as a source apportioning technique relies on the premise that combustion-derived compounds retain the isotopic signature of their original precursors. It is thought that the range in $\delta^{13}C$ values of PAHs generated during pyrolysis is correlated to the isotopic signature of the source. However, the initial samples analyzed by O'Malley and collaborators (O'Malley et al., 1994) demonstrated that the isotopic composition of PAHs generated by wood burning varied with ring size, with 3- and 5-ring PAHs being more $^{13}C$-depleted than 4-ring compounds (Figure 16). Similar variations were observed for PAHs derived from automobile exhaust, despite inherent differences in combustion conditions between these two processes (Figure 16). The effects of temperature of formation on the $\delta^{13}C$ of PAHs were addressed by McRae and collaborators (1999), who determined the isotopic composition of PAHs derived from coals of different ranks and process conditions. The authors observed that the $\delta^{13}C$ values of individual PAHs became more $^{13}C$-depleted with increasing temperature of formation. For relatively mild conversion processes, such as low temperature carbonization where the major aromatics are alkyl-substituted 2±3 ring PAHs, the isotopic signatures were similar to those of the parent coals. However, the resultant PAHs became more $^{13}C$-depleted in going to high temperature carbonization, gasification and combustion. For example, PAHs produced by high temperature fluidized-bed pyrolysis (900°C) were approximately 4‰ more depleted than PAHs produced by low temperature carbonization. Isotopic composition also seemed to correlate with the molecular size of the PAH, with $\delta^{13}C$ becoming more depleted with increasing number of rings. Because coal is characterized by low molecular weight PAHs (2-3 rings) McRae and collaborators reasoned that at low temperatures these compounds

are not affected by the combustion process and maintain their original $\delta^{13}C$ signatures. However, larger molecular weight PAHs formed during combustion most likely result from condensation reactions, which can select against the formation of $^{13}C$ —$^{12}C$ bonds, generating more $^{13}C$-depleted PAHs. The authors concluded that the $\delta^{13}C$ of coal-derived PAHs was mainly controlled by the specific ring-growth process acting during combustion. At low temperatures of formation PAHs maintain $\delta^{13}C$ signatures similar to their source, but as the temperature increases and more condensation occurs they become more $^{13}C$-depleted. It is possible that the different temperatures achieved during the combustion of coal, wood, gasoline and diesel may allow for a wide enough range in $\delta^{13}C$ that can help further constrain the environmental sources of combustion-derived PAHs, but this has yet not been achieved.

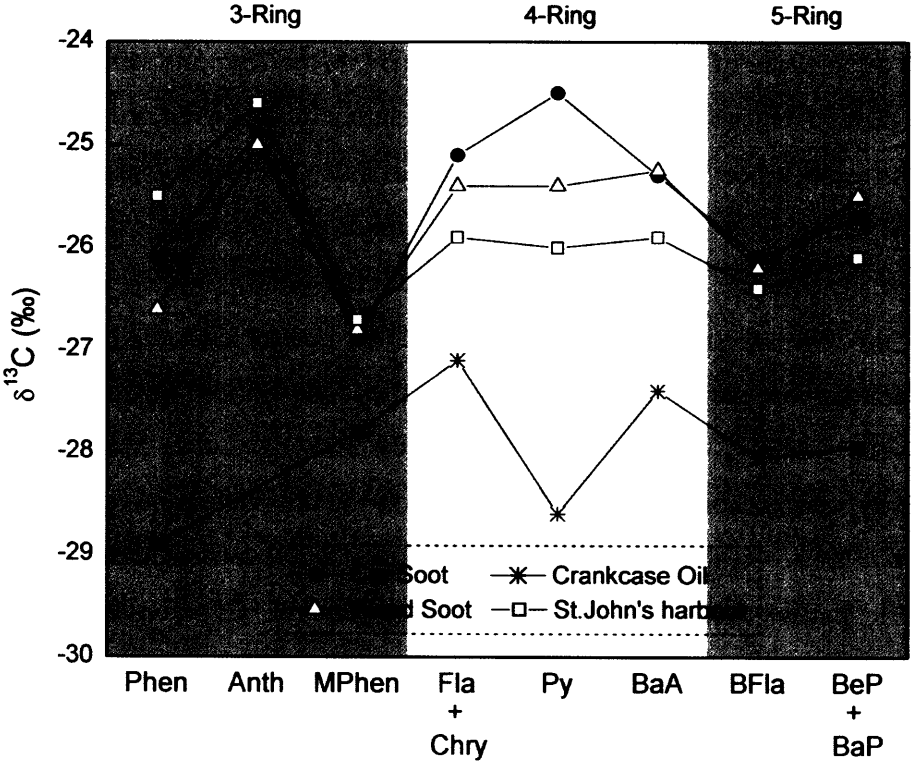


Figure 16. Isotopic composition of individual PAHs in three potential contamination sources and in sediments from the St. John's harbour, Newfoundland (O'Malley et al., 1996). Mphen = methyl-phenanthrene and Bfla = benzofluoranthenes.

## 4.4 Radiocarbon Measurements

Measurement of the radiocarbon ($^{14}C$) content of organic compounds is a powerful tool in assessing contributions of modern and fossil carbon in environmental matrices. Radiocarbon is produced naturally in the atmosphere by collisions between cosmic-ray neutrons and $^{14}N$ ($^{14}N_7 + {}^{1}n_0 \rightarrow {}^{14}C_6 + {}^{1}H_1$). This labeled carbon is readily oxidized to $^{14}CO_2$ in the atmosphere and incorporated into plant biomass by uptake during photosynthesis. While a plant is alive, it is constantly utilizing $^{14}CO_2$ and its biomass is in approximate equilibrium with atmospheric concentrations that reflect contemporary levels of $^{14}C$. When the plant dies, this incorporation process stops and the radiocarbon present in the biomass decays away with a half-life of 5730 years. This long half-life makes $^{14}C$ measurements suitable for discriminating between modern ($^{14}C$-rich) and fossil fuel ($^{14}C$-free) carbon since the latter forms over geologic (i.e. multimillion-year) time scales. This creates two well-defined end members that can be used to apportion the sources of combustion derived PAHs. Moreover, any isotopic fractionation during or post-PAH formation should be small relative to the signal of interest.

The radiocarbon approach has been successfully applied in distinguishing modern from fossil carbon in a number of studies (Cooper et al., 1981; Dasch, 1982; Hawthorne et al., 1992; Lichtfouse and Eglinton, 1995; Eglinton et al., 1997; Reddy et al., 2002c; Reddy et al., 2003). Cooper and collaborators (1981) conducted one of the earlier studies to use radiocarbon measurements to assess the contribution of specific sources of carbonaceous particles in urban air. This study showed that a large portion of the atmospheric particles collected in Portland, OR during the winter derived from burning of wood (39-70%) for residential heating. A similar study reported that 20% of the fine atmospheric particles collected in the winter in Denver, CO derived from fireplaces (Dasch, 1982). The use of radiocarbon to apportion sources of a specific compound class was reported in 1995 (Lichtfouse and Eglinton, 1995). $^{14}C$ measurements were used to assess the origins of *n*-alkanes extracted from a cultivated soil in France. The *n*-alkane fraction was shown to contain 34% modern and 66% fossil carbon, demonstrating the clear fossil fuel contamination of that site (Lichtfouse and Eglinton, 1995).

Analytical constrains prevented the determination of the $^{14}C$ content of individual compounds until the late 1990s. The low natural abundance of $^{14}C$ (~ 1 in $10^{12}$) requires that a large amount of carbon (≥ 50 μg) be isolated for measurement by accelerator mass spectrometry (AMS). In addition, environmental matrices are highly complex and accurate isotopic measurements can be affected by co-eluting peaks and the presence of an underlying unresolved complex mixture (UCM). Isolation of individual compounds became possible with the advent of automated preparative capillary gas chromatography (PCGC), described and tested by Eglinton and collaborators (Eglinton et al., 1996a). This technique allows the isolation of sufficient quantities of a specific compound through repetitive injections of a mixture on a modified capillary gas chromatograph. The purified individual compound can then be submitted to $^{14}C$ determination (after combustion to $CO_2$ and reduction to graphite) by AMS.

The use of compound-specific radiocarbon measurements for discerning sources of PAHs was first demonstrated by Eglinton and collaborators (1996b) and Currie and collaborators (1997). Two recent contributions by Reddy and collaborators (Reddy et al., 2002b; Reddy et al., 2003) highlight the potential of this approach. The first study evaluated the variability of the $^{14}C$ signature of individual PAHs in four National Institute of Standards and Technology (NIST) Standard Reference Materials (SRM) (Figure 17) (Reddy et al., 2002b). The results obtained for SRM 1941 (Baltimore Harbor) showed that most of the PAHs analyzed carried a fossil signature (expressed in terms of fraction modern[2] - $f_M$). Perylene was the exception, yielding more modern $^{14}C$ values, suggesting that some portion of this PAH had been produced naturally by *in situ* diagenesis (Figure 17a). PAHs isolated from SRM 1944 (New York Harbor) were also mostly derived from fossil sources (Figure 17b). However, the $^{14}C$ content of BghiP in this sample was slightly more modern than perylene, implying a combustion source for the latter and posing a question on the feasibility of using BghiP as a marker for emissions from automobiles (Currie et al., 1994). Chrysene yielded the least modern $^{14}C$ values in SRMs

[2] Calculated based on pre-bomb values of 1950 being modern ($f_M$=1). Carbon fixed later than this date incorporates bomb-derived $^{14}C$, giving rise to $f_M$>1, while utilization of fossil carbon results in $f_M$=0.

1941 and 1944, while in SRM 1649a (Urban Dust) pyrene had the lowest $^{14}C$ abundance. The fact that all the PAHs extracted from an urban dust sample collected by the NIST in the Washington DC area in 1976-1977 contained low $^{14}C$ abundance implies that combustion of fossil-fuel was the predominant source of these compounds to that region at that time. In all three SRMs, the radiocarbon content of individual PAHs correlated well with values obtained for black carbon and were consistently less modern that the total organic carbon. On a separate contribution, Reddy and collaborators (2003) used radiocarbon measurements in individual PAHs as a way to calculate the relative contribution of two combustion sources to the amount of PAHs found in household soot. It was observed that soot produced by the combustion of creosote-impregnated softwood in household stoves and fireplaces was enriched in PAHs and it was uncertain whether these compounds were derived from the creosote or from the wood. The authors measured the $^{14}C$ of individual PAHs and used a mass balance approach to calculate the relative contribution of each source, knowing that because creosote is a distillation product of coal tar it should have no $^{14}C$ and wood should contain contemporary values ($f_M \geq 1$). It was estimated that 54 to 70% of the PAHs had been generated from the combustion of the wood and the remaining had originated from creosote. If a single marker, such as retene (for the combustion of wood) had been used they would have overlooked the 50-70% contribution from creosote that the molecular-level $^{14}C$ analyses provided. This study also showed that retene had higher $^{14}C$-abundance that any other PAH, which is in agreement with its formation from the pyrolytic convertion of abietic acid (present in the resin of softwood) during combustion of softwood. This finding also confirmed the usefulness of retene as a molecular marker for tracing the combustion of softwood.

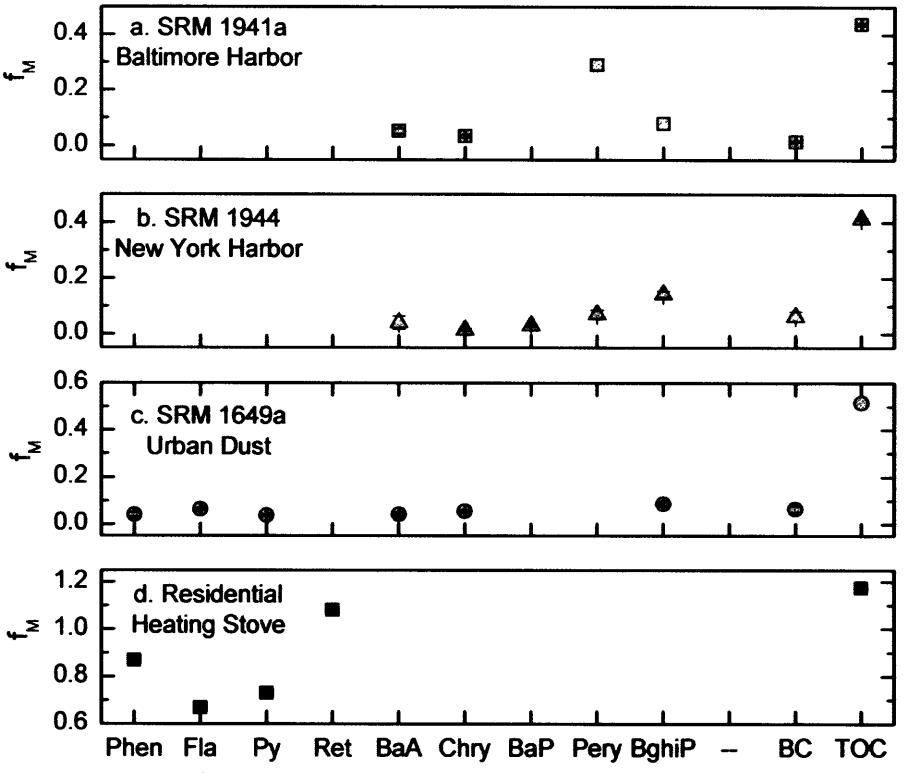


Figure 17. $^{14}C$ abundance of individual PAHs, black carbon and TOC in (a) SRM 1941a, (b) SRM 1944, (c) SRM 1649a (Reddy et al., 2002b), and (d) wood produced in a residential heating stove (Reddy et al., 2003). Ret = retene, Pery = perylene, and BC = black carbon.

Some of the approaches reviewed in this paper are likely to generate biased results when sources specific to a study area are not taken into consideration. For instance, determination of the radiocarbon content of PAHs in Brazil may be biased towards a modern signature due to the unconventional blend of gasoline used in that country. In the city of São Paulo, the largest and most industrialized region of Brazil, approximately 62% of the motor vehicles are fueled with gasohol (gasoline + 22% hydrated alcohol derived from sugar-cane), 8% with diesel and 30% with ethanol (also derived from sugar-cane) (De Martinis et al., 2002).

## 5. CONCLUSIONS

Some of the factors that affect the production, emission and fate of combustion derived PAHs have been outlined in this review, along with a brief discussion of several of the commonly applied methods for apportioning their sources in the environment. The similarity in the assemblage of PAHs produced by different combustion processes makes the apportionment of sources a difficult task. In addition, burning conditions can significantly influence the relative proportion of PAHs from a single source, adding to the complexity of estimating the relative contributions of the major sources of pyrogenic PAHs. Arguably, the combined utilization of $^{14}C$ and $\delta^{13}C$ measurements of individual PAHs, when placed into a historical context such as in sedimentary records, could render the most information on the sources of this group of contaminants to a specific site. However, such approaches require that the study site be chosen carefully, as perturbations to the sediment column (e.g., bioturbation and excessive sediment focusing) can impair reliable chronology. A great deal can be learned about the sources and signatures of combustion derived PAHs by applying a combination of methods to annually laminated sediments. Because the distribution of PAHs is so variable, it is important to examine PAHs on a compound-by-compound basis, paying greatest attention to the most toxic PAHs.

## 6. REFERENCES


Acres G., Harrison B., and Wyatt M. (1982) Catalytic control of motor vehicle exhaust emissions. In *Mobile Source Emissions Including Polycyclic Organic Species* (ed. D. Rondia, M. Cooke, and R. Haroz), pp. 1-12. D. Reidel Publishing Company, Liège, Belgium.

Allen J. O., Dookeran N. M., Smith K. A., Sarofim A. F., Taghizadeh K., and Lafleur A. L. (1996) Measurement of polycyclic aromatic hydrocarbons associated with size-segregated atmospheric aerosols in Massachusetts. *Environ. Sci. Technol.* **30**, 1023 - 1031.

Baek S., Goldstone M., Kirk P., Lester J., and Perry R. (1991a) Phase distribution and particle size dependency of polycyclic aromatic hydrocarbons in the urban atmosphere. *Chemosphere* **22**(5-6), 503-520.

Baek S. O., Field R. A., Goldstone M. E., Kirk P. W., and Lester J. N. (1991b) A review of atmospheric polycyclic aromatic hydrocarbons: sources, fate and behavior. *Water Air Soil Pollut.* **60**, 279-300.

Baker J., Eisenreich S., and Eadie B. (1991) Sediment trap fluxes and benthic recycling of organic carbon, polycyclic aromatic hydrocarbons, and polychlorobiphenyl congeners in Lake Superior. *Environ. Sci. Technol.* **25**, 500-509.

Ballentine D., Macko S., Turekian V., Gilhooly W., and Martincigh B. (1996) Compound specific isotope analysis of fatty acids and polycyclic aromatic hydrocarbons in aerosols: implications for biomass burning. *Org. Geochem.* **25**(1/2), 97-104.

Bauer J. and Capone D. (1988) Effects of co-occuring aromatic hydrocarbons on degradation of individual polycyclic aromatic hydrocarbons in marine sediment slurries. *Appl. Environ. Microbiol.* **54**(7), 1649-1655.

Behymer T. and Hites R. (1988) Photolysis of polycyclic aromatic hydrocarbons adsorbed on fly ash. *Environ. Sci. Technol.* **22**(11), 1311-1319.

Benner B., Bryner N., Wise S., Mulholland G., Lao R., and Fingas M. (1990) Polycyclic aromatic hydrocarbon emissions from the combustion of crude oil on water. *Environ. Sci. Technol.* **24**(9), 1418-1427.

Benner Jr. B. A., Gordon G. E., and Wise S. A. (1989) Mobile sources of atmospheric polycyclic aromatic hydrocarbons: A roadway tunnel study. *Environ. Sci. Technol.* **23**(10), 1269-1278.

Benner Jr. B. A., Wise S. A., Currie L. A., Klouda G. A., Klinedinst D. B., Zweidinger R. B., Stevens R. K., and Lewis C. W. (1995) Distinguishing the contributions of residential wood combustion and mobile source emissions using relative concentrations of dimethylphenanthrene isomers. *Environ. Sci. Technol.* **29**, 2382-2389.

Blumer M. (1976) Polycyclic aromatic compounds in nature. *Scientific American* **234**, 35-45.

Boehm P. and Quinn J. G. (1973) Solubulization of hydrocarbons by the dissolved organic matter in sea water. *Geochim. Cosmochim. Acta* **37**, 2459-2477.

Budzinski H., Raoux C., Baumard P., Bellocq J., and Garrigues P. (1995) Differentiation of contamination sources in recent sediments through PAH distributions: An overview. *Organic Geochemistry developments and applications to energy, climate, environment and human history: selected papers from the 17th International Meeting on Organic Geochemistry*, 616-618.

Budzinski H., Jones I., Bellocq J., Pierard C., and Garrigues P. (1997) Evaluation of sediment contamination by polycyclic aromatic hydrocarbons in the Gironde estuary. *Mar. Chem.* **58**(1-2), 85-97.

Budzinski H., Raymond N., Nadalig T., Gilewicz M., Garrigues P., Bertrand J., and Caumette P. (1998) Aerobic biodegradation of alkylated aromatic hydrocarbons by a bacterial community. *Org. Geochem.* **28**(5), 337-348.

Butler J. and Crossley P. (1981) Reactivity of polycyclic aromatic hydrocarbons adsorbed on soot particles. *Atmos. Environ.* **15**, 91-94.

Cerniglia C. and Heitkamp M. (1989) Microbial degradation of polycyclic aromatic hydrocarbons (PAH) in the aquatic environment. In *Metabolism of polycyclic aromatic hydrocarbons in the aquatic environment* (ed. U. Varanasi), pp. 41-68. CRC Press, Boca Raton, FL.

Christensen E., Rachdawong P., Karls J., and Van Camp R. (1999) PAHs in sediments: unmixing and CMB modeling of sources. *Journal of Environmental Engineering*, 1022-1032.

Coates J., Woodward J., Allen J., Philp P., and Lovley D. (1997) Anaerobic degradation of polycyclic aromatic hydrocarbons and alkanes in petroleum-contaminated marine harbor sediments. *Appl. Environ. Microbiol.* **63**, 3589-3593.

Colmsjö A., Zebühr Y., and Östman C. (1986) Polynuclear aromatic compounds in flue gases and ambient air in the vicinity of a municipal incineration plant. *Atmos. Environ.* **20**(11), 2279-2281.

Colombo J. C., Pelletier E., Brochu C., Khalil M., and Catoggio J. A. (1989) Determination of hydrocarbon sources using n-alkane and polyaromatic hydrocarbon distribution indexes. Case study: Rio de La Plata Estuary, Argentina. *Environ. Sci. Technol.* **23**, 888-894.

Cooper J., Currie L., and Klouda G. (1981) Assessment of contemporary carbon combustion source contributions to urban air particulate levels using carbon-14 measurements. *Environ. Sci. Technol.* **15**(9), 1045-1050.

Currie L. A., klouda G. A., Klinedinst D. B., Sheffield A. E., Jull A. J. T., Donahue D. J., and Connolly M. V. (1994) Fossil- and bio-mass combustion: C-14 for source identification, chemical tracer development, and model validation. *Nucl. Instrum. Methods Phys. Res.* **B92**, 404-409.

Currie L. A., eglinton T. I., Benner B. A. J., and Pearson A. (1997) Radiocarbon "dating" of individual chemical compounds in atmospheric aerosol: First results comparing direct isotopic and multivariate statistical apportionment of specific polycyclic aromatic hydrocarbons. *Nucl. Instrum. Methods Phys. Res. B* **123**, 475-486.

Dasch J. (1982) Particulate and gaseous emissions from wood-burning fireplaces. *Environ. Sci. Technol.* **16**(10), 639-645.

De Martinis B., Okamoto R., Kado N., Gundel L., and Carvalho L. (2002) Polycyclic aromatic hydrocarbons in a bioassay-fractionated extract of $PM_{10}$ in São Paulo, Brazil. *Atmos. Environ.* **36**, 307-314.

Dickhut R., Canuel E., Gustafson K., Liu K., Arzayus K., Walker S., Edgecombe G., Gaylor M., and MacDonald E. (2000) Automotive sources of carcinogenic polycyclic aromatic hydrocarbons associated with particulate matter in the Chesapeake Bay region. *Environ. Sci. Technol.* **34**, 4635-4640.

Eglinton T. I., Aluwihare L. I., Bauer J. E., Druffel E. R. M., and McNichol A. P. (1996a) Gas chromatographic isolation of individual compounds from complex matrices for radiocarbon dating. *Anal. Chem.* **68**(5), 904-912.

Eglinton T. I., Pearson A., McNichol A., Currie L., Benner B. A., and Wise S. (1996b) Compound specific radiocarbon analysis as a tool to quantitatively apportion modern and fossil sources of polycyclic aromatic hydrocarbons in environmental matrices. *212th ACS National Meeting*, 205-207.

Eglinton T. I., Benitez-Nelson B. C., Pearson A., McNichol A. P., Bauer J. E., and Druffel E. R. M. (1997) Variability in radiocarbon ages of individual organic compounds from marine sediments. *Science* **277**, 796-799.

Ehrhardt M., Burns K., and Bicego M. (1992) Sunlight-induced compositional alterations in the seawater-soluble fraction of a crude oil. *Mar. Chem.* **37**, 53-64.

EIA. (2003) Annual Energy Review. Washington, DC, Energy Information Administration. US Department of Energy.

Farrington J., Goldberg E., Risebrough R., Martin J., and Bowen V. (1983) U.S. "Mussel Watch" 1976-1978: an overview of the trace-metal, DDE, PCB, hydrocarbon and artificial radionuclide data. *Environ. Sci. Technol.* **17**, 490-496.

Fernández P., Vilanova R. M., and Grimalt J. O. (1999) Sediment fluxes of polycyclia aromatic hydrocarbons in European high altitude mountain lakes. *Environ. Sci. Technol.* **33**, 3716-3722.

Fine P., Cass G. R., and Simoneit B. R. T. (2001) Chemical characterization of fine particle emissions from fireplace combustion of woods grown in the Northeastern United States. *Environ. Sci. Technol.* **35**, 2665-2675.

Fraser M., Cass G., Simoneit B., and Rasmussen R. (1998) Air quality model evaluation data for organics. 5. C6-C22 nonpolar and semipolar aromatic compounds. *Environ. Sci. Technol.* **32**(12), 1760-1770.

Freeman K., Hayes J., Trendel J.-M., and Albrecht P. (1990) Evidence from carbon isotope measurements fro diverse origins of sedimentary hydrocarbons. *Nature* **343**, 254-256.

Frenklach M., Clary D., Gardiner Jr. W., and Stein S. (1984) Detailed kinetic modelling of soot formation in shock-tube pyrolysis of acetylene. *20th Symposium (International) on Combustion*, 887-901.

Garrett R., Pickering I., Haith C., and Prince R. (1998) Photooxidation of crude oils. *Environ. Sci. Technol.* **32**, 3719-3723.

Garrigues P., Budzinski H., Manitz M. P., and Wise S. A. (1995) Pyrolytic and petrogenic inputs in recent sediments: A definitive signature through phenanthrene and chrysene compound distribution. *Polycyc. Arom. Comp.* **7**, 275-284.

Gevao B., Jones K., and Hamilton-Taylor J. (1998) Polycyclic aromatic hydrocarbon (PAH) deposition to and processing in a small rural lake, Cumbria UK. *Sci. Tot. Environ.* **215**, 231-242.

Golomb D., Ryan D., Underhill J., Wades T., and Zemba S. (1997) Atmospheric deposition of toxics onto Massachussetts Bay - II. Polycyclic aromatic hydrocarbons. *Atmos. Environ.* **31**(9), 1361-1368.

Golomb D., Barry E., Fisher G., Varanusupakul P., Koleda M., and Rooney T. (2001) Atmospheric deposition of polycyclic aromatic hydrocarbons near New England Coastal waters. *Atmos. Environ.* **35**, 6245-6258.

Gordon G. (1988) Receptor models. *Environ. Sci. Technol.* **22**(10), 1132-1142.

Grimmer G. and Böhnke H. (1975) Profile analysis of polycyclic aromatic hydrocarbons and metal content in sediment layers of a lake. *Cancer Lett.* **1**, 75-84.

Gschwend P. M. and Hites R. A. (1981) Fluxes of polycyclic aromatic hydrocarbons to marine and lacustrine sediments in the northeastern United States. *Geochim. Cosmochim. Acta* **45**, 2359-2367.

Gustafsson Ö. and Gschwend P. (1997) Soot as a strong medium for polycyclic aromatic hydrocarbons in aquatic systems. In *Molecular Markers in Environmental Geochemistry* (ed. R. Eganhouse), pp. 365-381. American Chemical Society, Washington, DC.

Hammer B., Kelley C., Coffin R., Cifuentes L., and Mueller J. (1998) $d^{13}C$ values of polycyclic aromatic hydrocarbons collected from two creosote-contaminated sites. *Chem. Geol.* **152**, 43-58.

Harkov R. and Greenberg A. (1985) Benzo(a)pyrene in New Jersey - Results from a twenty-seven-site study. *Journal of the Air Pollution Control Association* **35**, 238-243.

Hawthorne S., Miller D., Langerfeld J., and Krieger M. (1992) PM-10 high-volume collection and quantification of semi-nonvolatile phenols, methoxylated phenols, alkanes, and polycyclic aromatic hydrocarbons from winter urban air and their relationship to wood smoke emissions. *Environ. Sci. Technol.* **26**(11), 2251-2261.

Hayes J., Freeman K., Popp B., and Hoham C. (1989) Compound-specific isotopic analyses: A novel tool for reconstruction of ancient biogeochemical processes. *Org. Geochem.* **16**(4-6), 1115-1128.

Hayes L., Nevin K., and Lovley D. (1999) Role of prior exposure on anaerobic degradation of naphthalene and phenanthrene in marine harbor sediments. *Org. Geochem.* **30**, 937-945.

Heit M., Tan Y., and Miller K. (1988) The origin and deposition history of polycyclic aromatic hydrocarbons in the Finger Lakes region of New York. *Water Air Soil Pollut.* **37**(1-2), 85-110.

Heitkamp M. and Cerniglia C. (1987) Effects of chemical structure and exposure on the microbial degradation of polycyclic aromatic hydrocarbons in freshwater and estuarine ecosystems. *Environ. Toxicol. Chem.* **6**, 535-546.

Hites R. A., Laflamme R. E., Windsor Jr J. G., Farrington J. W., and Deuser W. G. (1980) Polycyclic aromatic hydrocarbons in an anoxic sediment core from the Pettaquamscutt River (Rhode Island, USA). *Geochim. Cosmochim. Acta* **44**, 873-878.

IARC. (1983) *Polynuclear Aromatic Compounds*. International Agency for Research on Cancer, Lyon, France.

Jenkins B. M., Jones A. D., Turn S. Q., and Williams R. B. (1996) Particle concentrations, gas-particle partitioning, and species intercorrelations for polycyclic aromatic hydrocarbons (PAH) emitted during biomass burning. *Atmos. Environ.* **30**(22), 3825-3835.

Jensen T. E. and Hites R. A. (1983) Aromatic diesel emissions as a function of engine conditions. *Anal. Chem.* **55**, 594-599.

Jones D., Rowland S., and Douglas A. (1986) An examination of the fate of Nigerian crude oil in surface sediments of the Humber Estuary by gas chromatography and gas chromatography-mass spectrometry. *Int. J. Environ. Anal. Chem.* **24**, 227-247.

Jones K., Stratford J., Tidridge P., Waterhouse K., and Johnston A. (1989) Polynuclear aromatic hydrocarbons in an agricultural soil:long-term changes in profile distribution. *Environ. Pollut.* **56**, 337-351.

Kamens R., Guo Z., Fulcher J., and Bell D. (1988) Influence of humidity, sunlight, and temperature on the daytime decay of polyaromatic hydrocarbons on atmospheric soot particles. *Environ. Sci. Technol.* **22**(1), 103-108.

Kawamura K. and Suzuki I. (1994) Ice core record of polycyclic aromatic hydrocarbons over the past 400 years. *Naturwissenschaften* **81**, 502-505.

Khalili N., Scheff P., and Holsen T. (1995) PAH source fingerprints for coke ovens, diesel and gasoline engines, highways tunnels, and wood combustion emissions. *Atmos. Environ.* **29**(4), 533-542.

Kim W.-S., Kim S., Lee D., Lee S., Lim C., and Ryu J. (2001) Size analysis of automobile soot particles using field-flow fractionation. *Environ. Sci. Technol.* **35**(6), 1005-1012.

Korfmacher W., Wehry E., Mamantov G., and Natusch D. (1980) Resistance to photochemical decomposition of polycyclic aromatic hydrocarbons vapor-adsorbed on coal fly ash. *Environ. Sci. Technol.* **14**(9), 1094-1099.

Laflamme R. E. and Hites R. A. (1978) The global distribution of polycyclic aromatic hydrocarbons in recent sediments. *Geochim. Cosmochim. Acta* **42**, 289-303.

Latimer J. S. and Quinn J. G. (1996) Historical trends and current inputs of hydrophobic organic compounds in an urban estuary: the sedimentary record. *Environ. Sci. Technol.* **30**(2), 623-633.

Lee M. L., Prado G. P., Howard J. B., and Hites R. A. (1977) Source identification of urban airborne polycyclic aromatic hydrocarbons by gas chromatographic mass spectrometry and high resolution mass spectrometry. *Biomed. Mass Spec.* **4**(3), 182-186.

Li A., Jang J.-K., and Scheff P. (2003) Application of EPA CMB8.2 model for source apportionment of sediment PAHs in Lake Calumet, Chicago. *Environ. Sci. Technol.* **37**, 2958-2965.

Lichtfouse E. and Eglinton T. (1995) $^{13}C$ and $^{14}C$ evidence of pollution of a soil by fossil fuel and reconstruction of the composition of the pollutant. *Org. Geochem.* **23**(10), 969-973.

Lichtfouse E., Budzinski H., Garrigues P., and Eglinton T. (1997) Ancient polycyclic aromatic hydrocarbons in modern soils: $^{13}C$, $^{14}C$ and biomarker evidence. *Org. Geochem.* **26**(5/6), 353-359.

Lima A. L. C., Eglinton T. I., and Reddy C. M. (2003) High-resolution record of pyrogenic polycyclic aromatic hydrocarbon deposition during the 20th century. *Environ. Sci. Technol.* **37**, 53-61.

Lipiatou E., Marty J.-C., and Saliot A. (1993) Sediment trap fluxes of polycyclic aromatic hydrocarbons in the Mediterranean sea. *Mar. Chem.* **44**, 43-54.

Macadam S. (1997) Soot surface growth mechanisms in stationary combustion systems. PhD, Massachusetts Institute of Technology.

MacRae J. and Hall K. (1998) Biodegradation of polycyclic aromatic hydrocarbons (PAH) in marine sediment under denitrifying conditions. *Water Sci. Technol.* **38**(11), 177-185.

Maricq M., Podsiadlik D., and Chase R. (1999) Gasoline vehicle particle size distributions: comparison of steady state, FTP, and US06 measurements. *Environ. Sci. Technol.* **33**, 2007-2015.

Marr L., Kirchstetter T., Harley R., Miguel A., Hering A., and Hammond S. (1999) Characterization of polycyclic aromatic hydrocarbons in motor vehicle fuels and exhaust emissions. *Environ. Sci. Technol.* **33**, 3091-3099.

Masclet P., Bresson M., and Mouvier G. (1987) Polycyclic aromatic hydrocarbons emitted by power stations, and influence of combustion conditions. *Fuel* **66**, 556-562.

Masclet P., Hoyau V., Jaffrezo J. L., and Cachier H. (2000) Polycyclic aromatic hydrocarbon deposition on the ice sheet of Greenland. Part I: Superficial snow. *Atmos. Environ.* **34**, 3195-3207.

Mastral A., Callén M., Murillo R., and García T. (1998) Assessment of PAH emissions as a function of coal combustion variables in fluidized bed. 2. Air excess percentage. *Fuel* **77**(13), 1513-1516.

Mastral A., Callén M., Murillo R., and García T. (1999) Combustion of high calorific value waste material: organic atmospheric pollution. *Environ. Sci. Technol.* **33**, 4155-4158.

Matsuzawa S., Nasser-Ali L., and Garrigues P. (2001) Photolytic behavior of polycyclic aromatic hydrocarbons in diesel particulate matter deposited on the ground. *Environ. Sci. Technol.* **35**, 3139-3143.

Mazeas L., Budzinski H., and Raymond N. (2002) Absence of stable carbon isotope fractionation of saturated and polycyclic aromatic hydrocarbons during aerobic bacterial degradation. *Org. Geochem.* **33**, 1259-1272.

McElroy A., Farrington J., and Teal J. (1989) Bioavailability of polycyclic aromatic hydrocarbons in the aquatic environment. In *Metabolism of polycyclic aromatic hydrocarbons in the aquatic environment* (ed. U. Varanasi), pp. 1-39. CRC Press, Boca Raton, FL.

McGroddy S., Farrington J., and Gschwend P. (1996) Comparison of the in situ and desorption sediment-water partitioning of polycyclic aromatic hydrocarbons and polychlorinated biphenyls. *Environ. Sci. Technol.* **30**, 172-177.

McRae C., Sun C.-G., Snape C., Fallick A., and Taylor D. (1999) $d^{13}C$ values of coal-derived PAHs from different processes and their application to source apportionment. *Org. Geochem.* **30**(8), 881-889.

McVeety B. and Hites R. (1988) Atmospheric deposition of polycyclic aromatic hydrocarbons to water surfaces: a mass balance approach. *Atmos. Environ.* **22**(3), 511-536.

Miguel A., Kirchstetter T., and Harley R. (1998) On-road emissions of particulate polycyclic aromatic hydrocarbons and black carbon from gesoline and diesel vehicles. *Environ. Sci. Technol.* **32**, 450-455.

Müller G., Grimmer G., and Böhnke H. (1977) Sedimentary record of heavy metals and polycyclic aromatic hydrocarbons in Lake Constance. *Naturwissenschaften* **64**, 427-431.

Nishioka M., Chang H.-C., and Lee M. (1986) Structural characteristics of polycyclic aromatic hydrocarbon isomer in coal tars and combustion products. *Environ. Sci. Technol.* **20**, 1023-1027.

Oanh N., Nghiem L., and Phyu Y. (2002) Emission of polycyclic aromatic hydrocarbons, toxicity, and mutagenicity from domestic cooking using sawdust briquettes, wood, and kerosene. *Environ. Sci. Technol.* **36**(5), 833-839.

Offenberg J. and Baker J. (2002) Precipitation scavenging of polychlorinated biphenyls and polycyclic aromatic hydrocarbons along an urban to over-water transect. *Environ. Sci. Technol.* **36**(17), 3763-3771.

Offenberg J. H. and Baker J. E. (1999) Aerosol size distributions of polycyclic aromatic hydrocarbons in urban and over-water atmospheres. *Environ. Sci. Technol.* **33**, 3324-3331.

Ohkouchi N., Kawamura K., and Kawahata H. (1999) Distributions of three- to seven-ring polynuclear aromatic hydrocarbons on the deep sea floor in the Central Pacific. *Environ. Sci. Technol.* **33**, 3086-3090.

Okuda T., Kumata H., Naraoka H., Ishiwatari R., and Takada H. (2002a) Vertical distributions and $d^{13}C$ isotopic compositions of PAHs in Chidorigafuchi Moat sediment, Japan. *Org. Geochem.* **33**, 843-848.

Okuda T., Kumata H., Zakaria M., Naraoka H., Ishiwatari R., and Takada H. (2002b) Source identification of Malaysian atmospheric polycyclic aromatic hydrocarbons nearby forest fires using molecular and isotopic compositions. *Atmos. Environ.* **36**, 611-618.

O'Malley V., Abrajano Jr T., and Hellou J. (1994) Determination of the $^{13}C/^{12}C$ ratios of individual PAH from environmental samples: can PAH sources be apportioned? *Org. Geochem.* **21**(6/7), 809-822.

O'Malley V., Abrajano Jr T., and Hellou J. (1996) Stable carbon isotopic apportionment of individual polycyclic aromatic hydrocarbons in St. John's Harbour, Newfoundland. *Environ. Sci. Technol.* **30**, 634-639.

Palotás A. B., Rainey L. C., Sarofim A. F., Sande J. B. V., and Flagan R. C. (1998) Where did that soot come from? *Chemtech* **7**, 24-30.

Pedersen P., Ingwersen J., Nielsen T., and Larsen E. (1980) Effects of fuel, lubricant, and engine operating parameters on the emission of polycyclic aromatic hydrocarbons. *Environ. Sci. Technol.* **14**(1), 71-79.

Pereira W., Hostettler F., Luoma S., Van Geen A., Fuller C., and Anima R. (1999) Sedimentary record of anthropogenic and biogenic polycyclic aromatic hydrocarbons in San Francisco Bay, California. *Mar. Chem.* **64**, 99-113.

Prado G. and Lahaye J. (1982) Mechanisms of PAH formation and destruction in flames - Relation to organic particulate emissions. In *Mobile Source Emissions Including Polycyclic Organic Species* (ed. D. Rondia, M. Cooke, and R. Haroz), pp. 259-275. D. Reidel Publishing Company, Liège, Belgium.

Prahl F. and Carpenter R. (1983) Polycyclic aromatic hydrocarbon (PAH)-phase associations in Washington coastal sediment. *Geochim. Cosmochim. Acta* **47**, 1013-1023.

Pretsch E., Clerc T., Seibl J., and Simon W. (1989) *Tables of Spectral Data for Structure Determinations of Organic Compounds*. Springer-Verlag, Berlin.

Pruell R. and Quinn J. G. (1988) Accumulation of polycyclic aromatic hydrocarbons in crankcase oil. *Environ. Pollut.* **49**, 89-97.

Ramdahl T., Alfheim I., Rustad S., and Olsen T. (1982) Chemical and biological characterization of emissions from small residential stoves burning wood and charcoal. *Chemosphere* **11**(6), 601-611.

Readman J., Fillmann G., Tolosa I., Bartocci J., Villeneuve J.-P., Catinni C., and Mee L. (2002) Petroleum and PAH contamination of the Black sea. *Mar. Pollut. Bull.* **44**, 48-62.

Reddy C., Eglinton T., Hounshell A., White H. K., Xu L., Gaines R. B., and Frysinger G. S. (2002a) The West Falmouth oil spill after thirty years: The persistence of petroleum hydrocarbons in marsh sediments. *Environ. Sci. Technol.* **36**(22), 4754-4760.

Reddy C., Pearson A., Xu L., McNichol A., Benner Jr. B., Wise S., Klouda G., Currie L., and Eglinton T. (2002b) Radiocarbon as a tool to apportion the sources of polycyclic aromatic hydrocarbons and black carbon in environmental samples. *Environ. Sci. Technol.* **36**, 1774-1782.

Reddy C., Xu L., Eglinton T., Boon J., and Faulkner D. (2002c) Radiocarbon content of synthetic and natural semi-volatile halogenated organic compounds. *Environ. Pollut.* **120**, 163-168.

Reddy C. M. (1997) Studies on the fates of organic contaminants in aquatic environments. PhD, University of Rhode Island.

Reddy C. M., Xu L., and O'Connor R. (2003) Using radiocarbon to apportion sources of polycyclic aromatic hydrocarbons in household soot. *Environ. Forensics* **4**, 191-197.

Rieley G., Collier R., Jones D., Eglinton G., Eakin P., and Fallick A. (1991) Sources of sedimentary lipids deduced from stable carbon-isotope analyses of individual compounds. *Nature* **352**, 425-427.

Ritchter H. and Howard J. (2000) Formation of polycyclic aromatic hydrocarbons and their growth to soot - A review of chemical reaction pathways. *Prog. Energy Combust. Sci.* **26**, 565-608.

Rogge W. F., Hildemann L. M., Mazurek M. A., Cass G. R., and Simoneit B. R. T. (1993) Sources of fine organic aerosol. 2. Noncatalyst and catalyst-equipped automobiles and heavy-duty diesel trucks. *Environ. Sci. Technol.* **27**, 636-651.

Rothermich M., Hayes L., and Lovley D. (2002) Anaerobic, sulfate-dependent degradation of polycyclic aromatic hydrocarbons in petroleum-contaminated harbor sediment. *Environ. Sci. Technol.* **36**(22), 4811-4817.

Sanders G., Jones K. C., and Dorr J. H.-T. H. (1995) PCB and PAH fluxes to a dated UK peat core. *Environ. Pollut.* **89**(1-2), 17-25.

Schauer J., Kleeman M., Cass G. R., and Simoneit B. R. T. (2001) Measurements of emissions from air pollution sources. 3. $C_1$-$C_{29}$ organic compounds from fireplace combustion of wood. *Environ. Sci. Technol.* **35**(9), 1716-1728.

Schauer J., Kleeman M., Cass G., and Simoneit B. (2002) Measurement of emissions from air pollution sources. 5. $C_1$-$C_{32}$ organic compounds from gasoline-powered motor vehicles. *Environ. Sci. Technol.* **36**(6), 1169-1180.

Schauer J. J., Rogge W. F., Hildemann L. M., Mazurek M. A., and Cass G. R. (1996) Source apportionment of airborne particulate matter using organic compounds as tracers. *Atmos. Environ.* **30**, 3837-3855.

Schneider A., Stapleton H., Cornwell J., and Baker J. (2001) Recent declines in PAH, PCB, and toxaphene levels in the northern Great Lakes as determined from high resolution sediment cores. *Environ. Sci. Technol.* **35**(19), 3809-3815.

Schwarzenbach R., Gschwend P., and Imboden D. (2003) *Environmental Organic Chemistry*. John Wiley & Sons, New York.

Seinfeld J. H. and Pandis S. N. (1998) *Atmospheric Chemistry and Physics*. John Wiley & Sons, Inc.

Simcik M., Eisenreich S., and Lioy P. (1999) Source apportionment and source/sink relationships of PAHs in the coastal atmosphere of Chicago and Lake Michigan. *Atmos. Environ.* **33**, 5071-5079.

Simó R., Grimalt J., and Albaigés J. (1997) Loss of urburned-fuel hydrocarbons from combustion aerosols during atmospheric transport. *Environ. Sci. Technol.* **31**(9), 2697-2700.

Simoneit B. R. T. (2002) Biomass burning - a review of organic tracers for smoke from incomplete combustion. *Applied Geochem.* **17**, 129-162.

Talley J. W., Ghosh U., Tucker S. G., Furey J. S., and Luthy R. G. (2002) Particle-scale understanding of the bioavailability of PAHs in sediment. *Environ. Sci. Technol.* **36**(3), 477-483.

Tan Y. L. and Heit M. (1981) Biogenic and abiogenic polynuclear aromatic hydrocarbons in sediments from two remote Adirondack lakes. *Geochim. Cosmochim. Acta* **45**, 2267-2279.

Tolosa I., Bayona J., and Albaigés J. (1996) Aliphatic and polycyclic aromatic hydrocarbons and sulfur/oxygen derivatives in Northwestern Mediterranean sediments: Spatial and temporal variability, fluxes, and budgets. *Environ. Sci. Technol.* **30**(8), 2495-2503.

Van Metre P., Mahler B., and Furlong E. (2000) Urban sprawl leaves its PAH signature. *Environ. Sci. Technol.* **34**, 4064-4070.

Venkataraman C. and Friedlander S. (1994) Size distributions of polycyclic aromatic hydrocarbons and elemental carbon. 2. Ambient measurements and effects of atmospheric processes. *Environ. Sci. Technol.* **28**, 563-572.

Venkataraman C., Lyons J., and Friedlander S. (1994) Size distributions of polycyclic aromatic hydrocarbons and elemental carbon. 1. Sampling, measurement methods, and source Characterization. *Environ. Sci. Technol.* **28**, 555-562.

Wal R. L. V., Jensen K. A., and Choi M. Y. (1997) Simultaneous laser-induced emission of soot and polycyclic aromatic hydrocarbons within a gas-jet diffusion flame. *Combust. Flame* **109**, 399-414.

Wang Z., Fingas M., Landriaukt M., Sigouin L., Feng Y., and Mullin J. (1997) Using systematic and comparative analytical data to identify the source of an unknown oil on contaminated birds. *Journal of Chromatography A* **775**, 251-265.

Wang Z., Fingas M., Shu Y., Sigouin L., Landriault M., Lambert P., Turpin R., Campagna P., and Mullin J. (1999) Quantitative characterization of PAHs in burn residue and soot samples and differentiation of pyrogenic PAHs - The 1994 mobile burn study. *Environ. Sci. Technol.* **33**, 3100-3109.

Westerholm R., Alsberg T., Frommelin A., Strandell M., Rannug U., Winquist L., Grigoriadis V., and Egebaeck K.-E. (1988) Effect of fuel polycyclic aromatic hydrocarbon content on the emissions of polycyclic aromatic hydrocarbons and other mutagenic substances from a gasoline-fueled automobile. *Environ. Sci. Technol.* **22**(8), 925 - 930.

Wild S., Waterhouse K., McGrath S., and Jones K. (1990) Organic contaminants in an agricultural soil with a known history of sewage sludge amendments: polynuclear aromatic hydrocarbons. *Environ. Sci. Technol.* **24**(11), 1706-1711.

Williams P. T., Bartle K. D., and Andrews G. E. (1986) The relation between polycyclic aromatic compounds in diesel fuels and exhaust particulates. *Fuel* **65**, 1150-1158.

Williams P. T., Abbass M. K., Andrews G. E., and Bartle K. D. (1989) Diesel particulate emissions: The role of unburned fuel. *Combust. Flame* **75**(1), 1-24.

Windsor J. and Hites R. (1979) Polycyclic aromatic hydrocarbons in Gulf of Maine sediments and Nova Scotia soil. *Geochim. Cosmochim. Acta* **43**, 27-33.

Yamasaki H., Kuwata K., and Miyamoto H. (1982) Effects of ambient temperature on aspects of airborne polycyclic aromatic hydrocarbons. *Environ. Sci. Technol.* **16**(4), 189-194.

Youngblood W. and Blumer M. (1975) Polycyclic aromatic hydrocarbons in the environment: homologous series in soils and recent marine sediments. *Geochim. Cosmochim. Acta* **39**, 1303-1314.

Yuan S., Chang J., Yen J., and Chang B.-V. (2001) Biodegradation of phenanthrene in river sediment. *Chemosphere* **43**, 273-278.

Yunker M., MacDonald R., Goyette D., Paton D., Fowler B., Sullivan D., and Boyd J. (1999) Natural and anthropogenic inputs of hydrocarbons to the Strait of Georgia. *Sci. Tot. Environ.* **225**, 181-209.

Yunker M., MacDonald R., Vingarzan R., Mitchell R., Goyette D., and Sylvestre S. (2002) PAHs in the Fraser River Basin: a critical appraisal of PAH ratiuos as indicators of PAH source and composition. *Org. Geochem.* **33**, 489-515.

Yunker M. and Mcdonald R. (2003) Alkane and PAH depositionla history, sources and fluxes in sediments from the Fraser River Basin and Strait of Georgia, Canada. *Org. Geochem.* **34**, 1429-1454.

Yunker M. B. and MacDonald R. W. (1995) Composition and origins of polycyclic aromatic hydrocarbons in the Mackenzie River and on the Beaufort Sea Shelf. *Arctic* **48**(2), 118-129.

Yunker M. B., Snowdon L. R., MacDonald R. W., Smith J. N., Fowler M. G., Skibo D. N., McLaughlin F. A., Danyushevskaya A. I., Petrova V. I., and Ivanov G. I. (1996) Polycyclic aromatic hydrocarbon composition and potencial sources for sediment samples from the Beaufort and Barents seas. *Environ. Sci. Technol.* **30**, 1310-1320.

Zheng M., Cass G. R., Schauer J., and Edberton E. (2002) Source apportionment of PM2.5 in the Southeastern United States using solvent-extractable organic compounds as tracers. *Environ. Sci. Technol.* **36**, 2361-2371.

# CHAPTER 3

This manuscript appeared in:
*Environmental Science and Technology* (2003), 37, 53-61
It is re-printed here with permission of the publisher

# A HIGH-RESOLUTION RECORD OF PYROGENIC POLYCYCLIC AROMATIC HYDROCARBON (PAH) DEPOSITION DURING THE 20$^{TH}$ CENTURY

Ana Lúcia C. Lima, Timothy I. Eglinton and Christopher M. Reddy

Department of Marine Chemistry and Geochemistry,
Woods Hole Oceanographic Institution, Woods Hole, MA 02543

## ABSTRACT

A high-resolution record of polycyclic aromatic hydrocarbon (PAH) deposition in Rhode Island over the past ~ 180 yr was constructed using a sediment core from the anoxic Pettaquamscutt River basin. The record showed significantly more structure than has hitherto been reported, and revealed four distinct maxima in PAH fluxes. The characteristic increase in PAH flux at the turn of the 20$^{th}$ century was captured in detail, leading to an initial maximum prior to the Great Depression. The overall peak in PAH flux in the 1950s was followed by a maximum that immediately preceded the 1973 Organization of Petroleum Exporting Countries (OPEC) oil embargo. During the most recent portion of the record, an abrupt increase in PAH flux between 1996 and 1999 has been found to follow a period of near constant fluxes. Since source-diagnostic ratios indicate that petrogenic inputs are minor throughout the record, these trends are interpreted in terms of past variations in the magnitude and type of combustion processes. For the most recent PAH maximum, energy consumption data suggests that diesel fuel combustion, and hence traffic of heavier vehicles, is the most probable cause for the increase in PAH flux. Systematic variations in the relative abundance of individual PAH in conjunction with the above changes in flux are interpreted in relation to the evolution of combustion processes. Coronene, retene, and perylene are notable exceptions, exhibiting unique down-core profiles.

# 1. INTRODUCTION

Sediment cores can provide an excellent means to evaluate and reconstruct historical records of contaminant inputs to the environment (Grimmer and Böhnke, 1975; Goldberg et al., 1977; Hites et al., 1977; Schneider et al., 2001). One important class of organic contaminants that has been the focus of many studies is the polycyclic aromatic hydrocarbons (PAH). These suspected carcinogens and mutagens (IARC, 1983; Denissenko et al., 1996) are released into the environment primarily by the incomplete combustion of fossil fuels (petroleum, natural gas, and coal) and burning of vegetation (Tan and Heit, 1981). Other sources of PAH include petroleum spills, oil seepage, and diagenesis of organic matter in anoxic sediments (Blumer and Youngblood, 1975; Youngblood and Blumer, 1975; Venkatesan, 1988). Although most combustion-derived (pyrogenic) PAH are deposited close to their source, atmospheric transport can carry significant amounts of these compounds to remote locations, such as high altitude lake sediments (Fernández et al., 1999), deep-sea sediments (Laflamme and Hites, 1978), and Arctic ice (Kawamura and Suzuki, 1994) and snow (Masclet et al., 2000), rendering these contaminants ubiquitous in the contemporary environment.

Sedimentary records have shown good correlation between PAH concentration profiles and energy consumption associated with industrialization. Initial studies of PAH in sediment cores collected along the east coast of the United States revealed a gradual increase in PAH concentrations beginning around 1880, coincident with the onset of the Industrial Revolution, to a maximum in the 1950s (Hites et al., 1980; Gschwend and Hites, 1981) when coal usage was still high (EIA, 2000). The substitution of coal with cleaner burning fuels, such as oil and natural gas, is often quoted as an explanation for the steady decrease in PAH concentrations from the 1960s onwards (Gschwend and Hites, 1981). The increasing use of catalytic converters in motor vehicles (Acres et al., 1982) and stricter standards for gas mileage efficiency implemented after the Organization of Petroleum Exporting Countries (OPEC) oil embargo of 1973 (Doniger et al., 2002) most likely also contributed to the decline in PAH deposition in the 1970s and 1980s. While most of the historical records of PAH found in the literature were generated before the

1990s, the trend towards lower concentrations seen in the 1970s and 1980s was assumed to persist.

Contrary to these projections, recent studies reveal that PAH inputs are no longer decreasing. In 2000, Van Metre et al. reported that PAH emissions were increasing again in certain areas of the United States. Based on the analysis of sediment cores from locations experiencing diverse population growth since the 1970s, Van Metre et al. reported that all 10 sites studied exhibited a recent increase in pyrogenic PAH concentrations. The rise in PAH closely parallels the increase in automobile usage in these watersheds, implying a link between PAH inputs and urban sprawl. In contrast, Schneider et al. (2001) did not observe a similar trend in PAH concentrations in cores collected in Lake Michigan. Instead, their results suggest relatively constant PAH inputs since the 1980s. Importantly, neither of these studies indicate a continual decrease in recent PAH inputs in the United States, indicating that the declining trend that began in the 1970s has, at best, stabilized.

As part of a study to develop historical records of combustion, we investigated past changes in PAH deposition in the New England area. We chose to revisit the Pettaquamscutt River, Rhode Island and build upon pioneering studies on sedimentary PAH (Hites et al., 1980; Gschwend and Hites, 1981) to construct a PAH record at quasi-annual resolution spanning the pre-Industrial era to the end of the 20$^{th}$ century. This location is suitable for this type of study for several reasons: (i) it is relatively remote from major point sources, such as power plants, (ii) it receives PAH mostly via atmospheric deposition, (iii) it has a small catchment area, which minimizes the residence time of the PAH, and (iv) it experiences rapid sediment accumulation and minimal post-depositional mixing, allowing for preservation of vertically expanded, high-fidelity historical records. The record generated is used here to closely examine past changes in PAH input and composition and to further evaluate the relationship between urbanization and PAH emission. To this end, we show that (a) the major source of PAH to this area has consistently been combustion processes, (b) several distinct maxima in PAH concentration occur in the record, including the most recent increase in the late 1990s, (c)

the relative abundance of PAH varied over time, and (d) the recent increase in PAH concentrations may be due to a rise in diesel consumption.

## 2. EXPERIMENTAL SECTION

### 2.1 Study Area

The Pettaquamscutt River is located in South Kingston, southern Rhode Island, in close proximity to Narragansett Bay (Figure 1). The Pettaquamscutt "River" is actually a 9.7 km long estuary that has a small drainage area (~ 35 $km^2$) (Orr and Gaines, 1973), which is dominated by oak tree forests, wetlands and open waters (Urish, 1991). In 1991, only 27 % of the watershed was comprised of residential land (Urish, 1991). This percentage has increased in the past decade due to the construction of new developments in the area, but there are no recent estimates of land use for residential purposes.

The bottom waters and surface sediments of the Pettaquamscutt River are highly anoxic and have remained so for the past 1700 ± 300 years, since the marine flooding of this glacial valley (Orr and Gaines, 1973). Two remnant kettle lakes (upper and lower basin) show stable water-column stratification created by the flow of freshwater from the Gilbert Stuart Stream over brackish waters (~ 27 ‰) derived from tidal influx through the Narrows (Gaines and Pilson, 1972). The oxic/anoxic transition zone is presently at 3.5-6 m in the lower basin, below which a sulfide-rich layer (6 to 20 m) is observed (O'Sullivan et al., 1997). The lack of oxygen in the bottom waters prevents macrofaunal bioturbation of the sediments, leading to the preservation of undisturbed sediment sequences that are ideal for the purpose of historical reconstruction.

### 2.2 Sampling

Seven sediment cores were collected in the deepest part (20 m) of the lower basin (Figure 1) in April 1999. A rectangular aluminum freeze corer (30 x 8 x 165 cm) filled with dry ice and methanol was used for sampling, so that each core consisted of two large rectangular sides of frozen sediment. After collection, the sides were wrapped in aluminum foil, kept in dry ice, and transported back to the laboratory where they were

stored in a chest freezer (-18 °C). X-radiographs of the frozen slabs showed varved sediments and confirmed the absence of benthic animal borrows. In the present work, we report results from the slab that showed the highest number and most distinct laminations. The frozen sediment was sectioned at 0.5 cm intervals using a compact tile saw equipped with a diamond wafering blade (0.63 mm thickness). Approximately 90 % of each sample was placed in a pre-combusted glass-jar, air-dried, homogenized with a mortar and pestle, and stored for further PAH and other geochemical analyses. The remaining portion of each sample was set aside for future trace metal measurements.

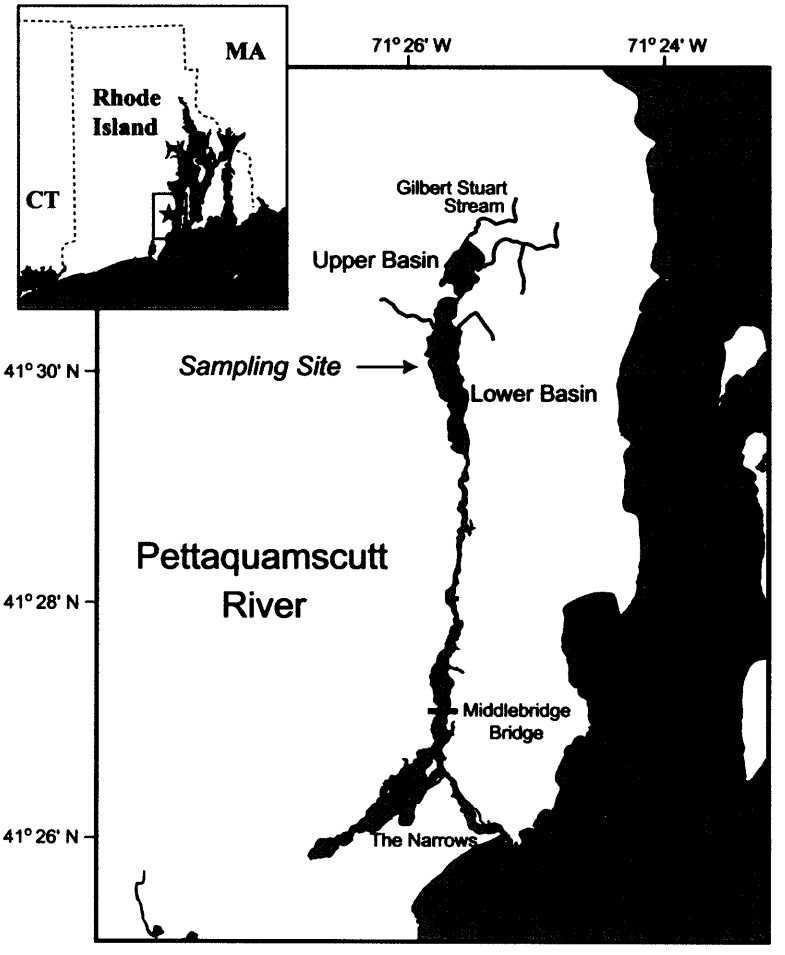


Figure 1. Map showing site of collection of sediment cores.

## 2.3 Sediment Dating

Dry sediment (1-2 g) was gamma counted for $^{210}$Pb (46.5 keV), $^{214}$Pb (351 keV) and $^{137}$Cs (661 keV) using a high purity germanium detector (Canberra model GCW 4023S) with a closed-end coaxial well. The activity of each sample was calculated in disintegrations per minute per gram of salt-free sediment (dpm.g$^{-1}$), with sample masses corrected for salt content (12-30 % dry weight) assuming a pore water salinity of 27 ‰ (O'Sullivan et al., 1997). Counting errors for total $^{210}$Pb and $^{214}$Pb were propagated to unsupported $^{210}$Pb ($^{210}Pb_{unsup} = {}^{210}Pb_{total} - {}^{214}Pb$) and ranged from 4-20 % of the activity ($\pm 1\sigma$), with a mean error of 8.4 %, or 0.97 dpm g$^{-1}$. Counting errors for $^{137}$Cs ranged from 5.8-40 % of the total activity ($\pm 1\sigma$), with a mean error of 18.2 %, or 0.04 dpm.g$^{-1}$.

Sedimentation rates were calculated using the constant rate of supply (CRS) model developed by Appleby and Oldfield (1978). This model assumes constant rate of $^{210}$Pb fallout from the atmosphere ($^{210}Pb_{unsup}$), which results in a rate of supply of $^{210}$Pb to the sediments that is independent of variations in sedimentation rates.

## 2.4 PAH Extraction and Analysis

Dry sediment samples (0.5-1.5 g) were spiked with PAH internal standards (fluorene-$d_{10}$, phenanthrene-$d_{10}$, pyrene-$d_{10}$, chrysene-$d_{12}$ and benzo[*b*]fluoranthene-$d_{12}$) and extracted by pressurized fluid extraction (Dionex ASE 200) using a mixture of acetone and hexane (1:1) at 1000 psi and 100 °C. The extracts were reduced in volume by rotary evaporation, exchanged into hexane, and treated with activated copper to remove elemental sulfur. Each extract was then separated into two fractions by silica column chromatography (6 g of 100-200 mesh fully-activated silica gel topped with 0.5 g of sodium sulfate). The first fraction containing alkanes and PAH was eluted with 30 mL of hexane/dichloromethane (2:1). The second fraction containing the remaining polar material was eluted with 30 mL of dichloromethane/methanol (1:1) and archived for further studies. The first fraction was then concentrated, spiked with 9,10-dihydrophenanthrene, and injected onto an Agilent 6890 Plus GC System interfaced to an Agilent 5973 Network mass selective detector operating at 70 eV in selective ion

monitoring (SIM) mode. Analytes were separated with a DB-XLB capillary column (60 m length; 0.25 mm diameter; 0.25 μm film thickness), and parent PAH were quantified using the mass and area of the corresponding internal standard and the linear term of a 6-point calibration curve generated with standard solutions prepared from the National Institute of Standards and Technology (NIST) Standard Reference Material 2260 (*Aromatic Hydrocarbons in Toluene*). For quantification of the alkylated PAH series, the response factors of the parent PAH were applied (UNEP, 1992). Concentration and fluxes of individual PAH were calculated relative to the salt-free mass of each sample.

To assess the precision and accuracy of our measurements, we analyzed four aliquots of NIST Standard Reference Material 1941a (*Organics in Marine Sediment*), one with each batch of 20 samples. Our results were generally within ± 14 % of certified values (dibenz[*a,h*]anthracene showed the poorest results at ± 40%), and precision was always better than 5 %. Average recovery of the standards spiked into each sample prior to analysis was 84.9 ± 9.9 % (79.1 ± 8.7 % for fluorene-$d_{10}$, 81.4 ± 10.0 % for phenanthrene-$d_{10}$, 98.3 ± 10.5 % for pyrene-$d_{10}$, 83.4 ± 10.2 % for chrysene-$d_{12}$ and 82.6 ± 10.2 % for benzo[*b*]fluoranthene-$d_{12}$). The method detection limit was defined as three times the standard deviation of seven replicate extractions of a background level sample from the core (70-70.5 cm) (Glaser et al., 1981). The detection limit for parent compounds was between 0.7-5.2 ng $g^{-1}$, with an average of 2.5 ng $g^{-1}$. Blanks ($n$ = 4) were run with each batch of 20 samples, and concentrations of individual PAH were always below the method detection limit.

Total PAH (ΣPAH) concentrations were computed as the sum of the following fifteen compounds: fluorene (Flu), phenanthrene (Phen), anthracene (Anth), fluoranthene (Fla), pyrene (Py), benz[*a*]anthracene (B*a*A), chrysene (Chry), benzo[*b*]fluoranthene (BbF), benzo[*k*]fluoranthene (BkF), benzo[*a*]pyrene (BaP), benzo[*e*]pyrene (BeP), dibenz[*ah*]anthracene (DahA), indeno[*123-cd*]pyrene (IP), benzo[*ghi*]perylene (BghiP) and coronene (Cor).

## 3. RESULTS AND DISCUSSION

Concentration values for individual PAH at all depth intervals analyzed are listed in Appendix 1A. In addition, because improvements were made to the sediment chronology since the publication of this paper the data was re-ploted in Appendix 1B.

### 3.1 $^{210}$Pb Dating

Sedimentation rates were calculated from the unsupported $^{210}$Pb activity and used to determine the year of deposition of each sediment layer, shown with an envelope of uncertainty (± 1σ) in Figure 2. The validity of this dating method was checked by comparing the $^{210}$Pb chronology to the profile and historical fallout of $^{137}$Cs.

The activity profile of $^{137}$Cs shows a broad subsurface maximum with highest activity in 1965 ± 1, which closely corresponds to the time of maximum deposition of $^{137}$Cs in the United States (1963-1964) from nuclear weapon testing (Robbins et al., 2000). Increased activity is detected down to 24 cm (1952 ± 1), matching the initial atmospheric occurrence of $^{137}$Cs (1952) (Carter and Moghissi, 1977). The smaller and more surficial (7 cm) $^{137}$Cs peak corresponds to a date of 1987 ± 1, which is consistent with fallout resulting from the accidental release of radioactivity that followed the 1986 Chernobyl reactor fire in the former Soviet Union (Carter and Moghissi, 1977). The presence of the Chernobyl peak was not expected at this location because this peak is not commonly seen in North America, even though it is often observed in European cores (Wieland et al., 1993; Reiser et al., 1997). For example, the $^{137}$Cs derived from the Chernobyl accident was not detected in recent sediment records from Florida (Robbins et al., 2000), Massachusetts (Spliethoff and Hemond, 1996), and other locations in the United States (Van Metre et al., 1997). The presence of this unusual signal, in addition to a good correspondence between the broad $^{137}$Cs peak and penetration depths to maximum

fallout (1964) and onset (1952) dates, testifies to the fidelity of the Pettaquamscutt River sediments, and hence their suitability for high-resolution geochronological investigations. A more rigorous discussion of the chronology at this site, incorporating varve and pollen counting, as well as $^{14}C$ measurements in total organic carbon, will be the subject of a separate contribution.

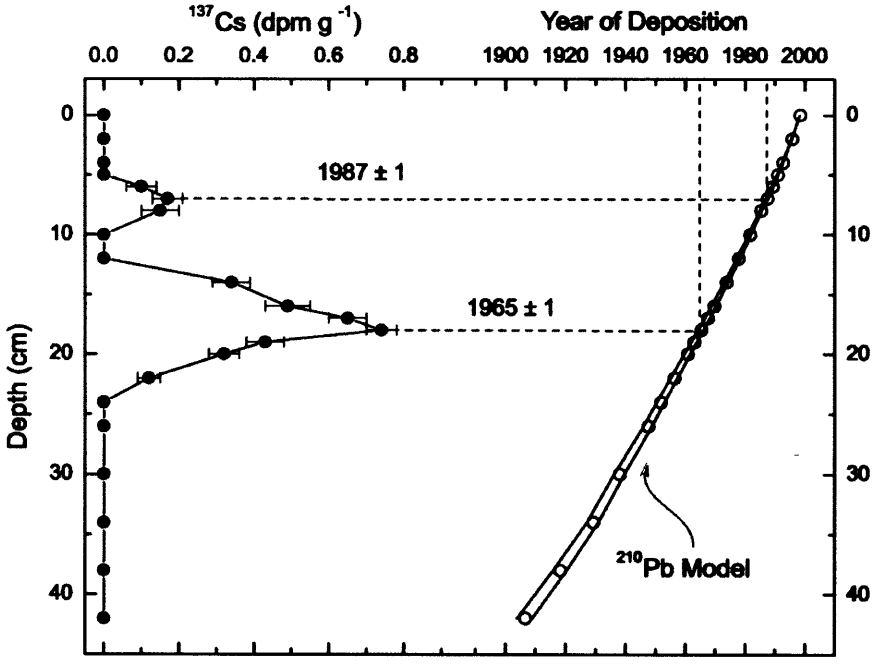


Figure 2. $^{137}Cs$ activity (closed circles) and year of deposition (calculated using unsupported $^{210}Pb$, open circles) plotted versus the sediment depth. Samples correspond to 0.5 cm thick sediment slices. Year of deposition is shown with a $\pm 1\sigma$ envelope of uncertainty.

Sediment resuspension and redistribution can modify the record of atmospheric deposition of allochthonous constituents such as $^{210}Pb$ and PAH. Deep basins tend to exhibit high sediment accumulation rates due to advection from the basin periphery, a process called sediment focusing (Crusius and Anderson, 1995). PAH accumulating at these locations can exceed the vertical flux associated with atmospheric deposition. To account for this overestimation, focusing factors can be calculated by integrating the

unsupported $^{210}$Pb over depth and dividing the result by the expected $^{210}$Pb inventory from regional atmospheric fallout (Kada and Heit, 1992; Crusius and Anderson, 1995). Since the atmospheric deposition of $^{210}$Pb is relatively uniform in the northeastern United States (Graunstein and Turekian, 1986), we used the $^{210}$Pb deposition inventory measured in New Haven, CT (38.6 dpm.cm$^{-2}$) for our calculations (Turekian et al., 1983). Vertically integrated unsupported $^{210}$Pb calculated for the Pettaquamscutt River sediments yield an inventory of 51.6 dpm.cm$^{-2}$, which corresponds to a focusing factor of 1.3. Thus, sedimentary inventories do not greatly exceed the amounts expected from $^{210}$Pb fallout alone.

### 3.2 Variations in Abundance and Flux of PAH

The compound specific high-resolution PAH profiles generated for the Pettaquamscutt River (Figure 3) show more structure than previously reported for this or any other location, probably as a result of the fine sampling scale undertaken in this study. The concentration profiles for most of the PAH analyzed follow the general pattern displayed by phenanthrene, pyrene and benzo[*a*]pyrene (Figure 3). Coronene, retene and perylene, also shown in Figure 3, are the exceptions to this pattern and will be discussed separately. In general, low and constant levels (< 10 ng g$^{-1}$) of phenanthrene, pyrene and benzo[*a*]pyrene are observed for the section of the core that comprises most of the 19$^{th}$ century. Concentrations then start to increase near the turn of the century (~ 1890), and reach a first maximum in the early 1930s before decreasing slightly from that point until 1945. A major rise in PAH is observed from 1945 to a maximum in 1960. During this period the concentration of phenanthrene increased 185 %, with an average rise of 86 % for the total PAH (ΣPAH). The decrease in concentration that followed is also noteworthy. Between 1960 and 1965, the amount of individual PAH diminished by an average of 41 %, returning to values existent in the late 1940s. The profiles show a third peak in PAH concentration that is smaller and less well defined, centered in 1974. This feature was not distinguished in previous studies at the Pettaquamscutt River sediments (Hites et al., 1980), presumably due to coarser sampling. A steady decrease in

concentrations followed the 1974 maximum before stabilizing around 1983 and remaining relatively constant until 1996. The constant concentrations observed on this last portion of the profile resemble that described by Schneider et al. (2001) for the same period. The most recent sediment sections corresponding to deposition between 1996 and 1999 reveal an abrupt and substantial increase in concentrations of phenanthrene, pyrene and benzo[*a*]pyrene (mean increase in ΣPAH = 42 %, Figure 3). This trend is consistent with work of Van Metre et al. (2000) that showed increasing PAH concentrations at several locations in the United States during this time interval.

Since sedimentation rate at the Pettaquamscutt River has changed over time and concentration values vary as a function of sediment dilution, it is more meaningful to assess changes in PAH levels in terms of depositional flux. We combined measured PAH concentrations with in situ densities and sedimentation rates to calculate PAH fluxes ($ng.cm^{-2}.yr^{-1}$), which were also corrected for sediment focusing (Figures 3 and 4, histograms of Figure 4 will be discussed later). The flux profiles still largely resemble the concentration record, but now we can take advantage of the high temporal resolution of our core to calculate the rate at which PAH deposition fluxes changed over several distinct time intervals. ΣPAH flux remained largely constant ($0.23 \pm 0.17$ ng $cm^{-2}$ $yr^{-1}$) during pre-Industrial times (1822-1842), while a small, but statistically significant increase in ΣPAH flux (0.06 ng $cm^{-2}$ $yr^{-2}$, $n = 16$, $r^2 = 0.817$) is observed in the subsequent period (1842-1887). The slope of the ΣPAH flux curve changed abruptly in the following 9 years (1887 to 1906) to a near-linear increase at 2.7 ng $cm^{-2}$ $yr^{-2}$ ($n = 8$, $r^2 = 0.992$). This increase is followed by another distinct change in the flux rate (9.2 ng $cm^{-2}$ $yr^{-2}$, $n = 11$, $r^2 = 0.983$) leading to the 1934 maximum. After a brief subsequent decrease, ΣPAH flux rose again between 1940 and 1959 at a rate of 14.2 ng $cm^{-2}$ $yr^{-2}$ ($n = 9$, $r^2 = 0.973$), and individual PAH fluxes attained values between 1.4 – 98.1 ng $cm^{-2}$ $yr^{-1}$. An extremely abrupt decrease in ΣPAH flux (~ 30 ng $cm^{-2}$ $yr^{-2}$) followed before recovery to a third maximum in 1974 that, to our knowledge, has not been previously reported. In ten years (1965-1974), the flux of ΣPAH increased 20 % at a rate of 5.9 ng $cm^{-2}$ $yr^{-2}$ ($n = 5$, $r^2 = 0.776$). The decline that followed was presumably due to stricter standards for gasoline

mileage efficiency implemented after the OPEC oil embargo (Doniger et al., 2002). Between 1983 and 1996, ΣPAH flux remained relatively constant (206.7 ± 11.9 ng $cm^{-2}$ $yr^{-1}$; R.S.D. = 5.7 %), in agreement with work by Schneider et al. (2001), but in the short period between 1996 and 1999, the flux of ΣPAH rose by 48 % (57 % from the 1983-1996 mean), at a rate of 48.1 ng $cm^{-2}$ $yr^{-2}$ ($n$ = 3, $r^2$ = 0.881). This increase in flux is 3.4 times faster than the rate of change observed between 1943 and 1959 leading to the overall PAH maximum, and the 1999 ΣPAH flux value is only 1.5 times lower than that

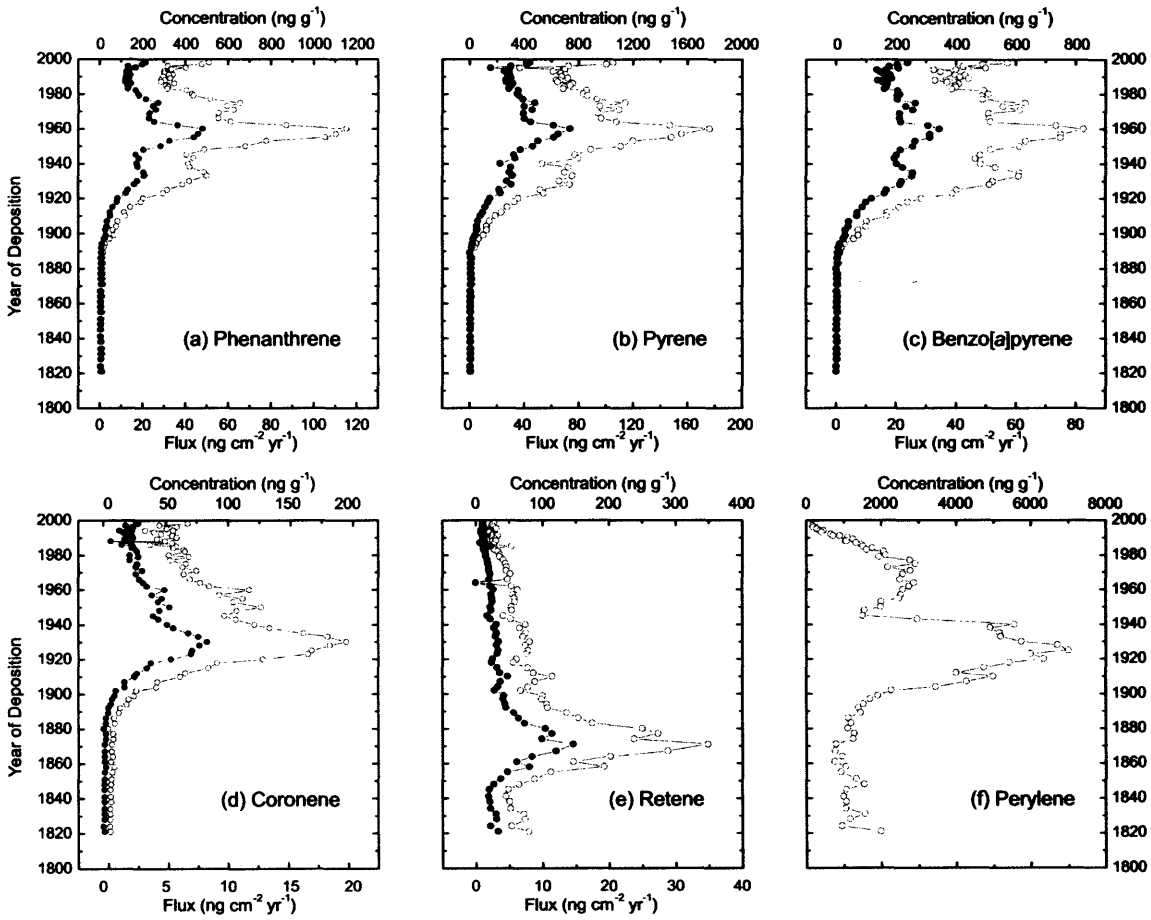


Figure 3. Down-core profiles of selected PAH. Concentration (open circles) and flux (closed circles) values were corrected for the salt content of the sediment. Flux was additionally corrected for sediment focusing.

maximum. To verify if this abrupt increase in flux reflects a new trend in the PAH record, the data obtained for the top portion of the core were analyzed using a two-phase linear regression model incorporating parametric bootstrapping (Efron and Tibshirani, 1993). The statistic results confirmed that the recent increase in ΣPAH delivered to Pettaquamscutt River sediments constitutes a new trend in the PAH historical record.

The most recent increase in sedimentary ΣPAH flux far outpaces the growth in population (13.4 %) and number of vehicles (14 %) in the region around the Pettaquamscutt River during this time interval (Census, 2000; Lovesky, 2001). Even though these increases were roughly the same, the amount of fuel used for residential heating and for transportation did not grow in the same direction. Energy use for home heating decreased (coal by 50 %, wood 39 %, petroleum 11 % and natural gas 11 %), while use of fuel for transportation increased (gasoline by 7 % and diesel by 20 %) in the area (EIA, 1999). Although natural gas consumption for heating of commercial facilities outpaced energy consumption associated with transportation, combustion of natural gas is not considered a major producer of PAH (NAS, 1972). There are three major roads (Routes 138, 1 and 1A) in the watershed of the Pettaquamscutt River. It is reasonable to assume that larger particles produced during fuel combustion, and which tend to accumulate close to the source (Windsor Jr. and Hites, 1979) contribute the majority of the PAH load seen in the sediments. PAH from engine exhaust reach the Pettaquamscutt mainly by atmospheric transport and not by runoff. One indication of the negligible contribution of the latter to our samples is the absence of an unresolved complex mixture (UCM) usually associated with PAH introduced via urban runoff. Long-range atmospheric transport is also a viable mechanism, but it may only contribute minor amounts of PAH since deposition strength decreases with distance from the source (Gardner and Hewitt, 1993). Combustion of gasoline and diesel thus appear to be the most plausible source for the increase in sedimentary PAH in recent years. It is extremely difficult to distinguish PAH contributions from these two sources; nevertheless, the larger rise in diesel consumption between 1996 and 1999 seems probable as the cause of the rise

in pyrogenic PAH contributions. Diesel engines also produce 1 to 2 orders of magnitude more soot (and associated PAH) than a comparable gasoline engine (Mauderly, 1992) and while we are currently lacking standard values for soot emissions by diesel vehicles (Hwang et al., 2001), it seems likely that traffic of heavier vehicles using diesel as fuel, and not passenger automobiles, is responsible for the increased PAH load to this region.

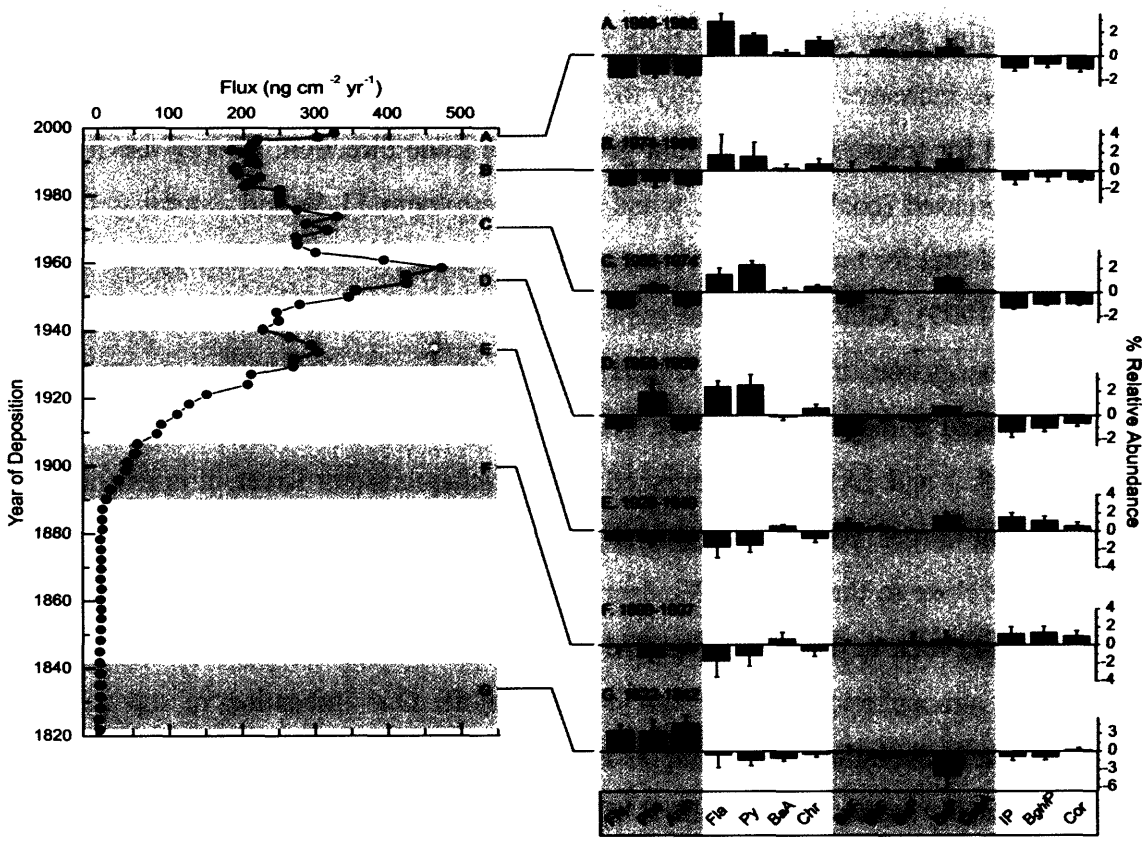


Figure 4. Flux record of total PAH (sum of 15 parent PAH, excluding perylene) in ng $cm^{-2}$ $yr^{-1}$ (left), and variation from the mean relative abundance of individual PAH over selected time intervals (right). Error bars correspond to one standard deviation ($\pm 1\sigma$) from the mean values for each individual PAH at that time interval.

### 3.3 Compositional Variations in Pyrogenic PAH

Assessments of isomer ratios or relative abundances are the classic methods for apportioning sources of PAH to the environment (Youngblood and Blumer, 1975; Lee et al., 1977). Ratios of parent PAH to their alkylated homologues are commonly used to differentiate between pyrogenic and petrogenic contributions, with the former being relatively depleted in alkyl-substituted PAH (Youngblood and Blumer, 1975). We used the compilation of source-diagnostic ratios of the phenanthrene and pyrene series by Gustafsson and Gschwend (1997) to evaluate the relative importance of pyrogenic and petrogenic contamination pathways to the Pettaquamscutt River. Sediments dominated by PAH from combustion processes show the sum of methyl-phenanthrenes and methyl-anthracenes to phenanthrene ratio between 0.5 - 1, and the sum of methyl-pyrenes and methyl-fluoranthenes to pyrene of about 0.4. As can be seen in Figure 5, combustion processes have been the main contributors of PAH to this site since the early 1900s. It is also apparent that the increase in ΣPAH flux observed in recent years was not the result of petrogenic inputs.

While pyrogenic processes dominate PAH inputs and even though the concentration and flux profiles of individual PAH (Figures 3a, 3b and 3c) follow that of the ΣPAH (Figure 4), the relative abundances of individual PAH (compared to ΣPAH) in the Pettaquamscutt River have varied significantly and systematically over time. For example, despite their structural similarities, the abundance profiles of phenanthrene and anthracene have distinct characteristic features (Figure 6). The relative abundance of anthracene decreased from maximum values (~ 10 %) in the early 1800s before leveling off at approximately 2 % in 1900, whereas the percent abundance of phenanthrene decreased only slightly in the 1800s, peaked in the 1950s and stabilized at approximately 6.5 % in the 1980s. Figure 6 shows no evidence of a decline in the abundance of 3-ring PAH relative to higher molecular weight compounds at the top of the core, as would be expected if diagenesis were affecting these samples (MacRae and Hall, 1998). Contrary to the behavior of 3-ring PAH, the relative abundance of 5-ring compounds such as

benzo[*a*]pyrene (Figure 6c) increased after the turn of the century. The mean relative abundance of benzo[*a*]pyrene increased from 3.6 ± 1.6 % between 1822 and 1884 to 7.9 ± 0.5 % between 1895 and 1999. Gevao et al. (1998) also reported historical variations in the relative abundance of individual PAH in sediments collected in the United Kingdom. Although only 3 individual PAH (anthracene, benzo[*a*]pyrene and benzo[*ghi*]perylene – not shown) investigated in this study show similar trends to those presented by Gevao et al., both studies indicate that the relative abundance of individual PAH has changed over

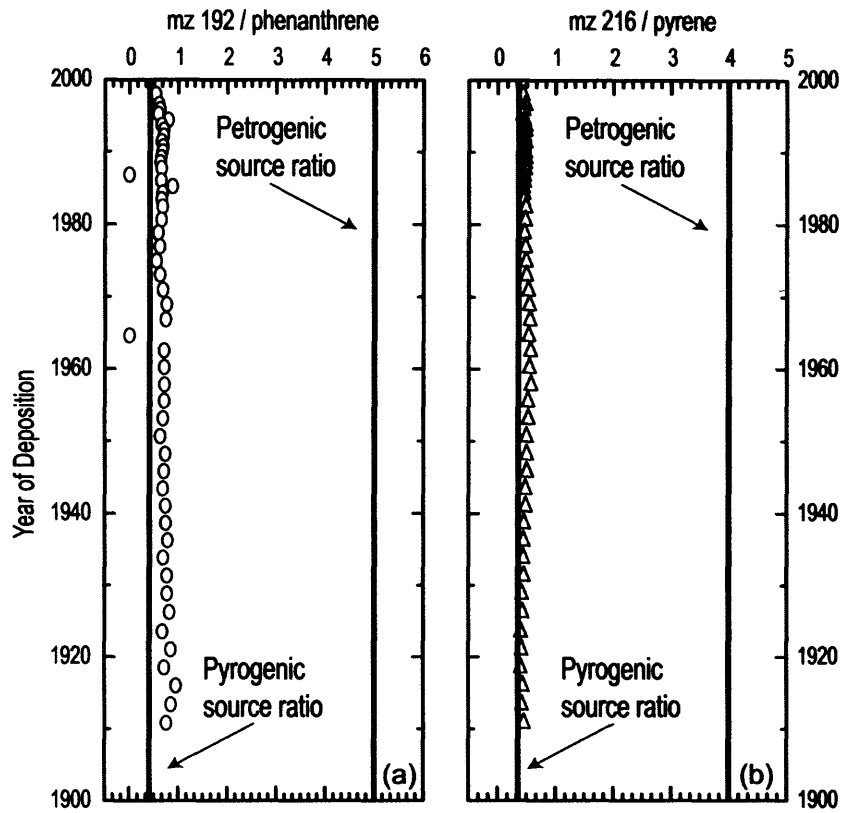


Figure 5. PAH source-diagnostic ratios taken from Gustafsson and Gschwend (1997) (Gustafsson and Gschwend, 1997). (a) sum of methyl-phenanthrenes and methyl-anthracenes to phenanthrene, and (b) sum of methyl-pyrenes and methyl-fluoranthenes to pyrene.

time, which is in contrast with reports of no change in contribution of specific PAH with depth (Pruell and Quinn, 1985). It is also interesting to note that the relative abundance of coronene (Figure 6d) was highest in the 1920s, while its concentration reached a maximum in 1932 (Figure 3d). Coronene is generally associated with emissions from vehicle exhaust (Masclet et al., 1986), but these peaks in relative and absolute abundance significantly precede the time period (1960-1975) when motor vehicle emissions were likely greatest. Our work implies that coronene may not necessarily be a good marker for emissions from vehicle exhaust, as also stated by Freeman and Cattell (Hayes et al., 1989) after finding elevated amounts of this compound in emissions from bush fires. The exact origin of the 1932 maximum in coronene abundance remains unclear.

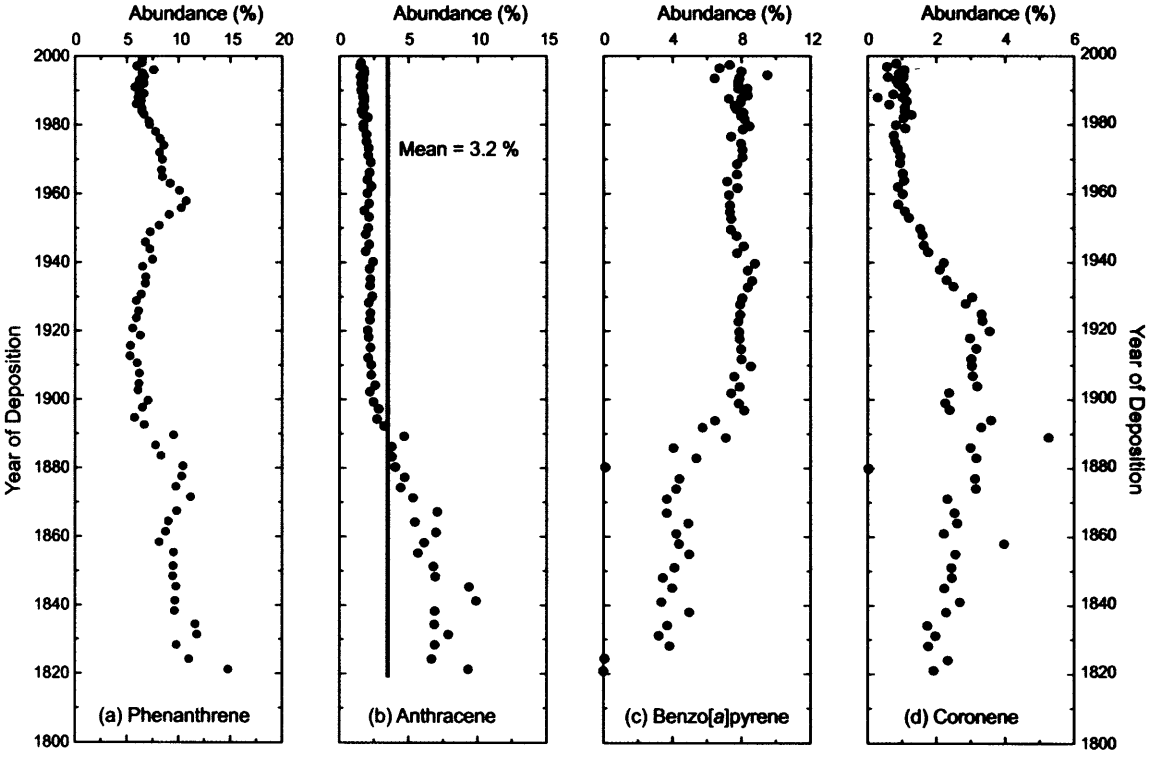


Figure 6. Down-core relative abundance (relative to ΣPAH) of selected individual PAH.

Some interesting features in the PAH profile become apparent when the relative contribution of each compound is averaged over the depth of the profile and the deviations from the mean are then plotted. This is shown in Figure 4 for selected time intervals corresponding to key features of the ΣPAH record. During the early portion of the record, corresponding to pre-Industrial times (1822-1842, Figure 4g), three-ring PAH (fluorene, phenanthrene and anthracene) and coronene were the only compounds above their down-core mean abundances. The fact that 3-ring compounds show higher values in the deeper portion of the core indicates that degradation, which tends to act faster on low molecular weight PAH than on higher-ringed homologues (MacRae and Hall, 1998), has not significantly altered the PAH distribution in these sediments. In the late 1880s, Rhode Island switched from an agrarian and commercial economy to an industrially-based economy (Conley, 1986), and coal usage increased in relation to wood consumption (EIA, 2000). This change in energy sources could arguably have altered the assemblage of emitted PAH at the turn of the century. During this time period, the relative abundance of 3-ring compounds shifted to values below their mean, while 5- and 6-ring PAH values increased (Figure 4f). Benz[*a*]anthracene was the only 4-ring PAH whose relative abundance rose above the mean between 1890-1907. At the first PAH maximum, spanning the Depression years (1929-1940) (Figure 4e), the pattern of relative abundances of individual PAH was comparable to that of the turn of the century (Figure 4f). During both periods, coal was the most important energy source (EIA, 2000) and apparently dominated the PAH loading and assemblage. The interval corresponding to the overall PAH maximum (1950-1959) reveals a marked shift in PAH abundance distribution compared to the prior maximum. Compounds that had abundances below their mean between 1929 and 1940 switched to higher values during 1950-1959, and vice-versa. For example, with the exception of benzo[*a*]pyrene and dibenz[*a,h*]anthracene, the distribution of 4-, 5- and 6-ring PAH completely inverted. Phenanthrene was the only 3-ring PAH whose relative abundance increased above its mean value. The reason for such dramatic and systematic variations in relative abundance

of individual compounds could reside in a change of energy source. During the Depression years, coal was the main fuel used, while between 1950 and 1959 petroleum was the dominant energy source (EIA, 2000). In comparison, the abundance of individual PAH for the periods of 1950 - 1960 (Figure 4d) and the third ΣPAH flux maximum of 1965-1974 (Figure 4c) appears similar, despite distinct historical accounts of shifts in energy usage. In the 1950s, petroleum and natural gas replaced coal as the main energy source. In a period of 10 years coal consumption decreased 20 % in the United States, while petroleum and natural gas increased 63 % and 128 %, respectively (EIA, 2000). The mixture of fuels used in 1950-1960 and 1965-1974 was clearly very different; nonetheless, we see similar trends in PAH abundances in the sediment.

In the 1960s, stricter emission controls came into effect in the United States and after 1975 vehicles started to be fitted with catalytic converters (Acres et al., 1982). These actions most likely resulted in the change in PAH assemblage observed between the time periods 1965-1974 (Figure 4c) and 1974-1996 (Figure 4b), as well as in the trend towards lower PAH fluxes between 1974 and 1996 (Figure 4). Finally, despite the most recent abrupt increase in PAH concentrations (Figure 3), the relative distribution of individual PAH remains the same as the prior interval (Figures 4b and 4a). PAHs with 4- and 5-ring still show relative abundances above their mean, while 3- and 6-ring PAH show the inverse trend.

### 3.4 Retene and Perylene

Retene and perylene were not considered in the calculation of ΣPAH and relative abundances discussed above. These compounds do not follow the general pattern of anthropogenic PAH seen in Figures 3a, 3b and 3c, and their sources remain uncertain. Retene (1-methyl-7-isopropylphenanthrene) has been proposed as a tracer for the combustion of soft wood (Ramdahl, 1983). This compound is also formed by the natural degradation of abietic acid present in coniferous resins (Tan and Heit, 1981; Simoneit and Mazurek, 1982; Tavendale et al., 1997), and is present in extracts of algal and bacterial organic matter (Wen et al., 2000). The most striking feature of the Pettaquamscutt River

sedimentary profile of retene is a maximum in concentration in ca.1870 (Figure 3e), which was also observed by Hites et al. (1980). Shipbuilding was conducted on the margins of the Pettaquamscutt River, but the timing of this activity (1813 to 1847) and the type of wood used for ship building (hardwoods such as oak, chestnut and buttonwood) (Tootell, 1963) are not consistent with such a large increase in retene concentration. The flux of retene increased 7.7 fold between 1842 and 1870 (from 1.9 to 14.6 ng $cm^{-2}$ $yr^{-1}$), and may be due to a period of intense deforestation in that region. The White Pine forests of the northeastern United States were nearly depleted by 1870 (Anonymous, 1999) and wood as an energy source was scarce enough to encourage the transition to coal. Notably, the return in retene flux after 1870 to early $19^{th}$ century values occurred just as the flux of other PAHs began to increase (Figure 3).

The origin of perylene has also been subject of considerable debate. The literature cites emissions from automobiles (Blumer et al., 1977) and municipal incinerators (Davies et al., 1976), as well as in situ diagenesis of marine and terrestrial organic matter (Venkatesan, 1988) as potential sources of perylene. Recent radiocarbon evidence indicates that both fossil-fuel combustion and modern biomass can be important contributors of perylene to sedimentary settings (Reddy et al., 2002). The concentration profile of perylene in the Pettaquamscutt sediments (Figure 3f) differs markedly from that of the pyrogenic PAHs (Tan and Heit, 1981). Concentrations of perylene were relatively constant from 1822 to 1890, increased 5-fold by 1927, and decreased back to 1890s values by 1945. The timing of this abrupt decrease is coincident with the construction of the Middlebridge Bridge (Figure 1) (Gaines, 1975), which could mean that a reduction in saltwater intrusion and possibly smaller influx of marine diatoms that may act as a source of perylene precursors, was responsible for the decrease in perylene (Venkatesan, 1988). The elucidation of the true precursors of perylene is beyond the scope of our present work, but in the Pettaquamscutt River, the concentration profile of perylene seems to be related to the influence of tidal waters from the Narragansett Bay. The most recent portion of the perylene record resembles a profile of a product from in situ diagenesis, with low concentrations at the surface and increasing values at depth. It is worth noting

that, the shape of the profile presented here does not resemble that previously shown by Hites et al. The latter authors show a ten-fold increase in perylene concentrations on the top portion of the core, constant values until 1895 and a dip in concentrations between approximately 1875 and 1855. Our core was taken in the Lower Basin of the Pettaquamscutt while that used by Hites et al. (1980) derived from the Upper Basin. These two basins differ distinctly in sedimentary organic carbon contents and hydrological regimes (Urish, 1991), therefore differences in perylene profile are not surprising.

## 4. SUMMARY

The excellent temporal resolution afforded by the Pettaquamscutt River sediments allowed us to observe structure in the sedimentary PAH record that had been previously overlooked, as well as to more quantitatively define past changes in flux. For example, the timing and rates of change in PAH flux at the turn of the $20^{th}$ century and accompanying subsequent PAH maximum are better constrained, including identification of a new peak in PAH levels immediately preceding the 1973 OPEC oil embargo. Our data reveal relatively constant PAH fluxes between 1978 and 1996, and an abrupt increase trend from 1996 and 1999. This trend is in agreement with the findings of Schneider et al. (2001) and Van Metre et al. (2000), respectively. Energy consumption records suggest that combustion of diesel fuel, and therefore traffic of heavier vehicles, is responsible for this recent increase in PAH fluxes. This finding is contrary to Van Metre et al., who associated the increase in PAH to greater utilization of passenger automobiles linked to urban sprawl. Irrespective of their source, increasing PAH fluxes may also indicate that emissions of other important combustion-related species, such as $NO_X$ and black carbon (soot) have increased. Coronene, retene and perylene exhibit profiles that are distinct from the other PAH. Of particular note, coronene fluxes reach a maximum in 1932, casting doubt on the validity of this PAH as a marker for vehicle exhaust emissions.

The remarkable short-term variability in PAH flux and composition evident in the Pettaquamscutt River record implies that sedimentary records of these compounds serve as a rich source of information on past combustion processes. An immediate question is whether the trends evident in this study reflect local phenomena, or whether they are a manifestation of more regional combustion activity. Unfortunately, detailed historical PAH records are not common in the literature. There is a need to identify and develop historical records from other sites with suitable temporal resolution in order to assess the geographic reproducibility of the present observations.

**Acknowledgments**

We wish to thank Dr. Andrew Solow (Marine Policy Center, WHOI) for his invaluable help with the statistical model; Mr. John Andrews (WHOI) for performing $^{210}Pb$ and $^{137}Cs$ measurements; Dr. John King (GSO-URI) for assistance with core collection; Dr. John Farrington and Dr. Konrad Hughen for helpful discussions; Mr. George Lovesky (South Kingston Town Hall) for the information on number of vehicles registered in South Kingston, and Ms. Jessica Baker for constructing the Pettaquamscutt map. This work was supported by funds from the National Science Foundation (OCE-9708478 and CHE-0089172), and A.L.C. Lima acknowledges a fellowship from the Brazilian Council for Research (CNPq). This is WHOI contribution # 10682.

## 5. REFERENCES

Acres G., Harrison B., and Wyatt M. (1982) Catalytic control of motor vehicle exhaust emissions. In *Mobile Source Emissions Including Polycyclic Organic Species* (ed. D. Rondia, M. Cooke, and R. Haroz), pp. 1-12. D. Reidel Publishing Company, Liège, Belgium.

Anonymous. (1999) Tapping "Green Gold", pp. 2. Forest Resources. (http://www.forestresources.com/novdec99.html).

Appleby P. and Oldfield F. (1978) The calculation of lead-210 dates assuming a constant rate of supply of unsupported $^{210}Pb$ to the sediment. *Catena* 5, 1-8.

Blumer M. and Youngblood W. W. (1975) Polycyclic aromatic hydrocarbons in soils and recent sediments. *Science* 188, 53-55.

Blumer M., Blumer W., and Reich T. (1977) Polycyclic aromatic hydrocarbons in soils of a Mountain Valley: Correlation with highway traffic and cancer incidence. *Environ. Sci. Technol.* 11(12), 1082-1084.

Carter M. and Moghissi A. (1977) Three decades of nuclear testing. *Health Phys. Press* 33, 55-71.

Census. (2000) Population density - Rhode Island cities and towns. US Bureau of the Census. (http://www.planning.state.ri.us/census/).

Conley P. (1986) *An Album of Rhode Island History, 1636-1986*. The Rhode Island Publications Society

Crusius J. and Anderson R. (1995) Sediment focusing in six small lakes inferred from radionuclide profiles. *J. Paleolimnol.* 13, 143-155.

Davies I., Harrison R., Perry R., Ratnayaka D., and Wellings R. (1976) Municipal incinerator as source of polynuclear aromatic hydrocarbons in environment. *Environ. Sci. Technol.* 10(5), 451-453.

Denissenko M., Pao A., Tang M.-S., and Pfeifer G. (1996) Preferential formation of benzo[*a*]pyrene adducts at lung cancer mutational hotspots in P53. *Science* 274, 430-432.

Doniger D., Friedman D., Hwang R., Lashof D., and Mark J. (2002) Dangerous addictions - Ending America's oil dependence, pp. 47Natural Resources Defense Council and Union of Concerned Scientists.

Efron B. and Tibshirani R. (1993) *Introduction to Bootstrapping*. Chapman & Hall, London.

EIA. (1999) State Energy Data Report. http://www.eia.doe.gov/pub/state.data/pdf/ri.pdf, Energy Information Administration. US Department of Energy.

EIA. (2000) Annual Energy Review, pp. 414. http://www.eia.doe.gov/emeu/aer/contents.html, Energy Information Administration. US Department of Energy.

Fernández P., Vilanova R. M., and Grimalt J. O. (1999) Sediment fluxes of polycyclia aromatic hydrocarbons in European high altitude mountain lakes. *Environ. Sci. Technol.* 33, 3716-3722.

Gaines A. (1975) Papers on the geomorphology, hydrography and geochemistry of the Pettaquamscutt River estuary. PhD, University of Rhode Island.

Gaines A. G. J. and Pilson M. E. Q. (1972) Anoxic water in the Pettaquamscutt River. *Limnol. Oceanogr.* 17(1), 42-49.

Gardner B. and Hewitt C. (1993) The design and application of a novel automated sampler for wet and dry deposition to water surfaces. *Sci. Total Environ.* 135, 135-245.

Gevao B., Jones K., and Hamilton-Taylor J. (1998) Polycyclic aromatic hydrocarbon (PAH) deposition to and processing in a small rural lake, Cumbria UK. *Sci. Tot. Environ.* 215, 231-242.

Glaser J., Foerst D., McKee G., Quave S., and Budoe W. (1981) Trace analyses for wastewater. *Environ. Sci. Technol.* 15(12), 1426-1435.

Goldberg E., Gamble E., Griffin J., and Koide M. (1977) Pollution history of Narragansett Bay as recorded in its sediments. *Estuar. Coastal Mar. Sci.* 5, 549-561.

Graunstein W. and Turekian K. (1986) $^{210}$Pb and $^{137}$Cs in air and soils measure the rate and vertical profile of aerosol scavenging. *J. Geophys. Res.* 91, 14355-14366.

Grimmer G. and Böhnke H. (1975) Profile analysis of polycyclic aromatic hydrocarbons and metal content in sediment layers of a lake. *Cancer Lett.* 1, 75-84.

Gschwend P. M. and Hites R. A. (1981) Fluxes of polycyclic aromatic hydrocarbons to marine and lacustrine sediments in the northeastern United States. *Geochim. Cosmochim. Acta* 45, 2359-2367.

Gustafsson Ö. and Gschwend P. (1997) Soot as a strong medium for polycyclic aromatic hydrocarbons in aquatic systems. In *Molecular Markers in Environmental Geochemistry* (ed. R. Eganhouse), pp. 365-381. American Chemical Society, Washington, DC.

Hayes J., Freeman K., Popp B., and Hoham C. (1989) Compound-specific isotopic analyses: A novel tool for reconstruction of ancient biogeochemical processes. *Org. Geochem.* 16(4-6), 1115-1128.

Hites R., Laflamme R., and Farrington J. (1977) Sedimentary polycyclic aromatic hydrocarbons: The historical record. *Science* 198, 829-831.

Hites R. A., Laflamme R. E., Windsor Jr J. G., Farrington J. W., and Deuser W. G. (1980) Polycyclic aromatic hydrocarbons in an anoxic sediment core from the Pettaquamscutt River (Rhode Island, USA). *Geochim. Cosmochim. Acta* 44, 873-878.

Hwang R., Millis B., and Spencer T. (2001) Clean getaway - Toward safe and efficient vehicles, pp. 13Natural Resources Defense Council (NRDC).

IARC. (1983) *Polynuclear Aromatic Compounds.* International Agency for Research on Cancer, Lyon, France.

Kada J. and Heit M. (1992) The inventories of anthropogenic Pb, Zn, As, Cd, and the radionuclides $^{137}Cs$ and excess $^{210}Pb$ in sediments of the Adirondack region, USA. *Hydrobiologia* 246, 231-241.

Kawamura K. and Suzuki I. (1994) Ice core record of polycyclic aromatic hydrocarbons over the past 400 years. *Naturwissenschaften* 81, 502-505.

Laflamme R. E. and Hites R. A. (1978) The global distribution of polycyclic aromatic hydrocarbons in recent sediments. *Geochim. Cosmochim. Acta* 42, 289-303.

Lee M. L., Prado G. P., Howard J. B., and Hites R. A. (1977) Source identification of urban airborne polycyclic aromatic hydrocarbons by gas chromatographic mass spectrometry and high resolution mass spectrometry. *Biomed. Mass Spec.* 4(3), 182-186.

Lovesky G. (2001) South Kingston Town Assessor. Personal Communication.

MacRae J. and Hall K. (1998) Biodegradation of polycyclic aromatic hydrocarbons (PAH) in marine sediment under denitrifying conditions. *Water Sci. Technol.* 38(11), 177-185.

Masclet P., Mouvier G., and Nikolaou K. (1986) Relative decay and sources of polycyclic aromatic hydrocarbons. *Atmos. Environ.* 20(3), 439-446.

Masclet P., Hoyau V., Jaffrezo J. L., and Cachier H. (2000) Polycyclic aromatic hydrocarbon deposition on the ice sheet of Greenland. Part I: Superficial snow. *Atmos. Environ.* 34, 3195-3207.

Mauderly J. (1992) Diesel exhaust. In *Environmental Toxicants: Human Exposures and Their Health Effects* (ed. M. Lippman). Van Nostrand Reinhold, New York.

NAS. (1972) *Particulate Polycyclic Organic Matter.* National Academy of Sciences, Washington.

Orr W. L. and Gaines A. G. J. (1973) Observations on the rate of sulfate reduction and organic matter oxidation in the bottom waters of an estuarine basin: the upper basin of the Pettaquamscutt River (Rhode Island). In *Advances in Organic Geochemistry* (ed. B.Tissot and F. Bienner), pp. 791-812. Technip.

O'Sullivan D., Hanson Jr A., and Kester D. (1997) The distribution and redox chemistry of iron in the Pettaquamscutt Estuary. *Estuar. Coastal Shelf. Sci.* 45, 769-788.

Pruell R. and Quinn J. (1985) Geochemistry of organic contaminants in Narragansett Bay sediments. *Estuar. Coastal Shelf. Sci.* 21, 295-312.

Ramdahl T. (1983) Retene - a molecular marker of wood combustion in ambient air. *Nature* 306, 580-582.

Reddy C., Pearson A., Xu L., McNichol A., Benner Jr. B., Wise S., Klouda G., Currie L., and Eglinton T. (2002) Radiocarbon as a tool to apportion the sources of polycyclic aromatic hydrocarbons and black carbon in environmental samples. *Environ. Sci. Technol.* 36, 1774-1782.

Reiser R., Toljander H., Albrecht A., and Giger W. (1997) Alkylbenzenesulfonates in recent lake sediments as molecular markers for the environmental behavior of detergent-derived chemicals. In *Molecular Markers in Environmental Geochemistry* (ed. R. Eganhouse), pp. 196-212. American Chemical Society.

Robbins J., Holmes C., Halley R., Bothner M., Shinn E., Graney J., Keeler G., tenBrink M., Orlandini K., and Rudnick D. (2000) Time-averaged fluxes of lead and fallout radionuclides to sediments in Florida Bay. *J. Geophys. Res.* 105(C12), 28805-28821.

Schneider A., Stapleton H., Cornwell J., and Baker J. (2001) Recent declines in PAH, PCB, and toxaphene levels in the northern Great Lakes as determined from high resolution sediment cores. *Environ. Sci. Technol.* 35(19), 3809-3815.

Simoneit B. R. T. and Mazurek M. A. (1982) Organic matter in the troposphere. II. Natural background of biogenic lipid matter in aerosols over the rural western United States. *Atmos. Environ.* 16, 2139-2159.

Spliethoff H. and Hemond H. (1996) History of toxic metal discharge to surface waters of the Aberjona watershed. *Environ. Sci. Technol.* 30, 121-128.

Tan Y. L. and Heit M. (1981) Biogenic and abiogenic polynuclear aromatic hydrocarbons in sediments from two remote Adirondack lakes. *Geochim. Cosmochim. Acta* 45, 2267-2279.

Tavendale M., McFarlane P., Mackie K., Wilkins A., and Langdon A. (1997) The fate of resin acids-1: The biotransformation and degradation of deuterium labelled dehydroabietic acid in anaerobic sediments. *Chemosphere* 35(10), 2137-2151.

Tootell L. (1963) Shipwright Saunders shipshape ships. In *Ships, Sailors and Seaports*, pp. 29-39. The Pettaquamscutt Historical Society, Kingston, RI.

Turekian K., Benninger L., and Dion E. (1983) $^{7}$Be and $^{210}$Pb total deposition fluxes at New Haven, Connecticut and at Bermuda. *J. Geophys. Res.* 88(C9), 5411-5415.

UNEP. (1992) Determination of petroleum hydrocarbons in sediments, pp. 75United Nation Environment Programme.

Urish D. (1991) Freshwater inflow to the Narrow River. *Maritimes* 35(2), 12-14.

Van Metre P., Callender E., and Fuller C. (1997) Historical trends in organochlorine compounds in river basins identified using sediment cores from reservoirs. *Environ. Sci. Technol.* 31, 2339-2344.

Van Metre P., Mahler B., and Furlong E. (2000) Urban sprawl leaves its PAH signature. *Environ. Sci. Technol.* 34, 4064-4070.

Venkatesan M. I. (1988) Occurrence and possible sources of perylene in marine sediments - a review. *Mar. Chem.* 25, 1-27.

Wen Z., Ruiyong W., Radke M., Qingyu W., Guoying S., and Zhili L. (2000) Retene in pyrolysates of algal and bacterial organic matter. *Org. Geochem.* 31, 757-762.

Wieland E., Santschi P., Höhener P., and Sturm M. (1993) Scavenging of Chernobyl $^{137}$Cs and natural $^{210}$Pb in Lake Sempach, Switzerland. *Geochim. Cosmochim. Acta* 57, 2959-2979.

Windsor Jr. J. and Hites R. (1979) Polycyclic aromatic hydrocarbons in Gulf of Maine sediments and Nova Scotia soil. *Geochim. Cosmochim. Acta* 43, 27-33.

Youngblood W. and Blumer M. (1975) Polycyclic aromatic hydrocarbons in the environment: homologous series in soils and recent marine sediments. *Geochim. Cosmochim. Acta* 39, 1303-1314.

# CHAPTER 4

# CHRONOLOGY AND RECORD OF $^{137}$CS RELEASED BY THE CHERNOBYL ACCIDENT

**Abstract** – Cesium-137 derived from the explosion of the Chernobyl reactor in 1986 was preserved in anoxic sediments from a coastal environment in southern Rhode Island. Although the radioactive plume was detected in surface air samples at several locations in the US, this is the first known record of a Chernobyl $^{137}$Cs peak in sediments from North America. The inventory of Chernobyl $^{137}$Cs that was preserved in the Pettaquamscutt River is small compared to European counterparts and should only be detectable for the next 15-20 years. However, the presence of two $^{137}$Cs peaks (1963 and 1987) identifies a well-dated segment of the sediment column that could be exploited in understanding the decomposition and preservation of terrestrial and aquatic organic matter. Different methods for calculating the $^{210}$Pb chronology were also evaluated in this study and checked against the independent varve counting. The end result is a detailed chronology of a site well suited for reconstruction of historical records of environmental change.

## 1. INTRODUCTION

On 26 April 1986, during a test to determine how long the turbines would spin after a loss of electrical power supply, a flaw in design and a series of operator actions caused the Chernobyl-4 reactor to explode. The initial release of fission products to the atmosphere was followed by a second explosion, which allowed air to flow into the core and caused the graphite moderator to burst into flames (Hohenemser et al., 1986; Mould, 2000). The nine-day fire that followed was held responsible for the main release of radioactivity into the environment. Roughly all of the xenon gas, 20% of the cesium and iodine, and about 5% of the remaining radioactive material in the reactor was set free by the accident, accounting for a total of more than 8 x $10^{18}$ Bq (1 becquerel = 1 disintegration per second) of fission products released into the atmosphere (Mould, 2000; www.world.nuclear.org). While most of the released material was deposited close to the

site of the accident in northern Ukraine, southern Belarus and Russia's Bryansk region (Stone, 2001), strong winds carried the plume towards Finland and Sweden (ApSimon and Wilson, 1986; Mould, 2000). By May 2, the plume had reached the UK and Japan, and by May 6, Canada and the United States (Ayoama et al., 1986; Smith and Clark, 1986; Mould, 2000). Although $^{137}Cs$ was detected in the atmosphere in several regions of the United States following the accident (Larsen et al., 1986; Feely et al., 1988; Holloway and Liu, 1988), there is no known record of a Chernobyl $^{137}Cs$ peak in recent sediments from Florida (Robbins et al., 2000), Massachusetts (Spliethoff and Hemond, 1996), California (Fuller et al., 1999) or other locations in the country (Van Metre et al., 1997).

Significant levels of $^{137}Cs$ first appeared in the atmosphere in the early 1950s as a result of above ground nuclear weapons testing. The number of nuclear detonations peaked in 1962, resulting in a maximum in $^{137}Cs$ fallout in 1963, when the Test Ban Treaty was instated (Carter and Moghissi, 1977). As a consequence of the treaty, little radioactive fallout was observed in the late 1960s and 1970s in the northern hemisphere. Because $^{137}Cs$ deposition reflects the history of nuclear tests, this artificial radionuclide is commonly used as a chronostratigraphic marker to constrain records (Anderson et al., 1988; Ritchie and McHenry, 1990; Spliethoff and Hemond, 1996; Appleby, 2001). Following the 1986 Chernobyl accident, the atmospheric concentration of $^{137}Cs$ in Europe remained approximately 4-times higher than the 1963 levels for a few months (Cambray et al., 1987) and a number of investigations reported the presence of Chernobyl-derived $^{137}Cs$ in sediment traps (Buesseler et al., 1987; Wieland et al., 1993) and in surficial sediments from Denmark (Ehlers et al., 1993), Netherlands (Zwolsman et al., 1993), Switzerland (Dominik and Span, 1992; Gunten et al., 1997; Albrecht et al., 1998) and UK (Gevao et al., 1997). At these locations, elevated activities of sedimentary $^{137}Cs$ imply that the 1986 peak can serve as a valuable marker for several decades ($^{137}Cs$ half-life = 30 years).

As part of a study to develop historical records of combustion, we collected sediment cores from an estuarine anoxic basin site in southern Rhode Island and generated detailed $^{210}Pb$, $^{137}Cs$, and varve chronologies. The anoxic nature of this

environment inhibits bioturbation, creating undisturbed laminations that are ideal for sediment dating. Here, we revisit the $^{210}Pb$ models used for dating recent sediments, demonstrate a good correlation between radiometric models and varve counting, and show that $^{137}Cs$ derived from the Chernobyl accident was preserved in sediments from a site in the Northeastern USA.

## 2. EXPERIMENTAL

### 2.1 Study Area

The Pettaquamscutt River, also known as the Narrow River, is located in Washington County, southern Rhode Island (Figure 1). This estuary is approximately 9.7 km long, ranges from 100-700 meters in width (Boothroyd, 1991) and has a small (35 $km^2$) drainage area (Orr and Gaines, 1973). The Pettaquamscutt can be morphologically divided into two basins and a channel. The upper basin is 13.5 m deep at its maximum and receives input of freshwater from the Gilbert Stuart Stream. The lower basin is deeper (19.5 m), has a larger area and is confined to the north by a shallow sill (less than 1 m deep) and to the south by a long narrow channel that connects it to its salt-water source, Rhode Island Sound. The bottom waters and sediments of the upper and lower basins are permanently anoxic, mostly due to a stable salinity-dominated stratification of the water column (Gaines and Pilson, 1972). As a result, no bioturbation of the surficial sediments is observed and annually laminated layers are well preserved (Figure 2).

### 2.2 Sampling

Freeze-cores were collected in the deepest part of the lower basin (Figure 1) in April 1999 (Lima et al., 2003). Unlike gravity coring, which can disturb the surficial sediments and lead to compaction of sediment layers, freeze coring allows for recovery of intact sediment-water interfaces (Shapiro, 1958). Consequently, this sampling technique is ideal for high-resolution records of aquatic sediments, and especially those containing high amounts of siliceous tests that render sediments flocculant (Koide et al., 1973). Prior

to lowering into the water, an aluminum corer (30 x 8 x 165 cm) was filled with a slurry of dry ice and methanol. The corer was lowered slowly to approximately two meters above the sediment-water interface, allowed to drop rapidly into the sediment, and left there for about 10-15 minutes so that a thick slab of sediment froze onto the metal surface

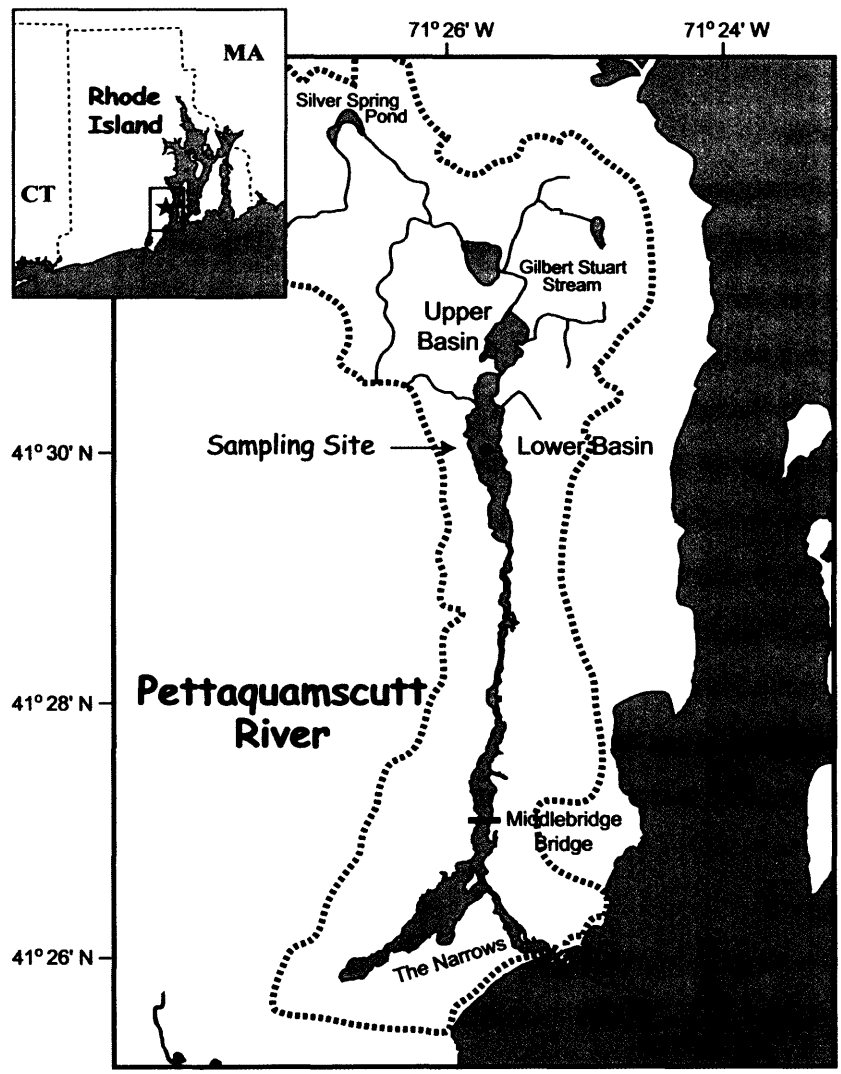


Figure 1. Map showing the boundaries of the watershed of the Pettaquamscutt River (RI) (dotted line) and the location of the site of sediment freeze-core collection. Modified after Lima et al. (2003).

of the corer. After collection, the sediment slabs were separated from the corer, wrapped in aluminum foil, kept in dry ice, and transported back to the laboratory where they were stored in a chest freezer (-18 °C).

X-radiographs of the frozen slabs showed laminated sediments and confirmed the absence of benthic animal burrows (Figure 2). Here, we report results from the slab that showed the most distinct and the highest number of laminations. Prior to sampling the core, a 10-cm wide sub-section of the slab was cut lengthwise to be made into thin sections for subsequent varve counting. The frozen sediment was subsequently sliced at 0.5 cm intervals using a compact tile saw equipped with a diamond wafering blade, while the slab was kept frozen by regular applications of liquid nitrogen. The samples were placed in pre-combusted glass-jars, air-dried, homogenized with a mortar and pestle, and stored until radiometric measurements and geochemical analyses were performed.

### 2.3 Varve Counting

Sediment pieces (6 cm x 4 cm) were taken from the 10-cm wide sub-section saved for varve counting, dehydrated and embedded with Spurr resin (1969), following the procedure of Pike and Kemp (1996). The resulting slabs of sediment/resin were mounted on glass slides and thin-sectioned using standard petrographic techniques. Thin sections were scanned under cross-polarized films using a flat bed scanner with transparency capabilities in order to produce tag image file (TIFF) digital images with resolutions of 1440 dpi (Figure 2) (De Keyser, 1999). The images were imported into Adobe Photoshop®, lamination boundaries were marked with the "path" tool and the exported paths were processed using an algorithm that counts and measures the thickness of each lamination (Francus et al., 2002). The resulting data files for each sediment piece were overlain to produce a continuous record of varve thickness, number, and depth. Because some of the laminae were disturbed during processing, we compiled data from freeze cores taken in 1999, 2002, and 2003 to fill in the gaps and produce a master varve chronology for the lower basin. This multiple-core chronology is superior to that from a single core

because it enables the identification of laminae that may have been disturbed in the original core (Lamoureux, 2001).

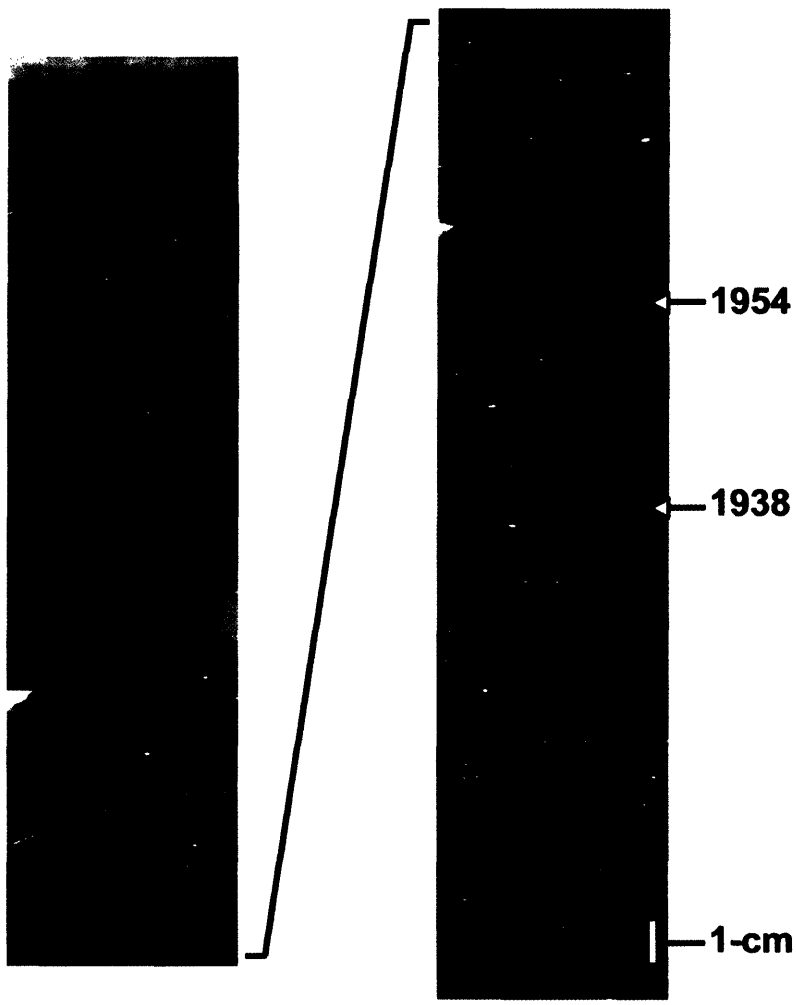


Figure 2. Composite image of 20th century laminations from the lower basin of the Pettaquamscutt River. Laminae deposited by historical hurricanes (1954, 1938) are marked with arrows and help constrain the varve chronology. The width of the composite has been exaggerated 2x; scale bar = 1cm.

## 2.4 Radiometric Dating

Aliquots of dry sediment (1-2 g) were measured for $^{210}Pb$, $^{226}Ra$ and $^{137}Cs$ by direct gamma counting using a high purity germanium detector (Canberra model GCW

4023S) with a closed-end coaxial well. $^{210}Pb$ was measured by its emission at 46.5 keV, and $^{226}Ra$ by the 351 keV emission of its daughter isotope $^{214}Pb$ (with a correction for losses of the intermediary gaseous isotope $^{222}Rn$). $^{137}Cs$ was measured by its emissions at 661 keV. Detector efficiency was determined by counting a National Institute of Standards and Technology (NIST) traceable mixed liquid gamma standard (Isotope Products Labs) and a certified $^{210}Pb$ standard (Physikalisch Technische Bundesanstalt – PTB). The background corrected counts were then analyzed with the GESPECOR software, which uses Monte Carlo simulations to correct for self-absorption and coincidence-summing effects. Excess, or unsupported $^{210}Pb$ was calculated as the difference between the measured total $^{210}Pb$ and the estimate of the supported $^{210}Pb$ activity given by the parent nuclide ($^{210}Pb_{exc} = {}^{210}Pb_{total} - {}^{214}Pb$). Counting errors for $^{137}Cs$ ranged from 5.8 to 40% of the total activity ($\pm 1\sigma$) and those for total $^{210}Pb$ and $^{214}Pb$ were propagated to $^{210}Pb_{exc}$, which ranged between 4-20% ($\pm 1\sigma$). Minimum detectable activity was calculated at 0.004 Bq for $^{137}Cs$ and 0.040 Bq for $^{210}Pb_{exc}$.

## 2.5 Total Organic Carbon Concentration and Radiocarbon Content

A Fisons 1108 elemental analyzer was used to measure the total organic carbon (TOC) content of the samples. To remove inorganic carbon, about 2 mg of dry sample was weighed into a silver capsule and acidified with HCl under vacuum. The samples were then dried in an oven at 50°C, folded, placed inside tin capsules (for better catalysis of the oxidation reaction) and analyzed. Samples were run in triplicate and all reported weight percentages represent the mean ± one standard deviation. Carbon content was determined through a 5-point calibration curve of a sulfanilamide standard (0.05 to 0.50 mgC). Sub-samples of the dry sediment were submitted to the National Ocean Sciences Accelerator Mass Spectrometry (NOSAMS) facility where they were analyzed for radiocarbon ($^{14}C$) and stable carbon isotopic composition ($\delta^{13}C$[1]) according to established procedures (McNichol et al., 1994). $^{14}C$ values are expressed as $\Delta^{14}C$[2], which is the

[1] $\delta^{13}C$ (‰) = $(((^{13}C/^{12}C)_{sample}/(^{13}C/^{12}C)_{PDB})-1)*1000$; where PDB = Pee Dee Belemnite carbonate standard.
[2] $\Delta^{14}C$ (‰) = $(\%modern*e^{\lambda t}-1)*1000$, where $\lambda = {}^{14}C$ decay constant and $t$ = calendar age.

measured $^{14}C$ concentration normalized to pre-industrial atmospheric values reported in permil (‰) (Stuiver and Polach, 1977). Routine precision for $\delta^{13}C$ and $\Delta^{14}C$ measurements at NOSAMS are ~0.1 and 5‰, respectively.

## 3. $^{210}$Pb AGE MODELLING

Since its introduction in the early 1970s, the use of $^{210}Pb$ as a dating technique has become established as the best means of deriving sedimentation rates and ages of recently deposited sediments. $^{210}Pb$ enters aquatic systems by direct precipitation or by run-off from the catchment area. The total amount of $^{210}Pb$ present in lake sediments represents a mixture of that formed within the sediment from the decay of $^{226}Ra$ deposited by soil erosion (supported $^{210}Pb$), and that formed in the atmosphere by the decay of $^{222}Rn$ (unsupported or excess $^{210}Pb$, $^{210}Pb_{exc}$). The activity of supported $^{210}Pb$ is estimated by measuring the activity of either $^{214}Pb$ or $^{226}Ra$, while the activity of $^{210}Pb_{exc}$ is determined by the difference between the total and the supported $^{210}Pb$ ($^{210}Pb_{exc} = {}^{210}Pb_{total} - {}^{214}Pb$). The decay of this atmospherically derived $^{210}Pb$ provides a measure of the rate of deposition of the sediment column. In the absence of sediment mixing, two models are commonly used to derive age-depth correlations in sedimentary profiles. The constant rate of supply (CRS) model (Appleby and Oldfield, 1978) assumes that sedimentation rate and sediment compaction change throughout the core and automatically corrects for these parameters, while the constant initial concentration (CIC) model (Goldberg, 1962; Krishnaswamy et al., 1971) assumes that sedimentation rate is constant in the area under study and requires that the depth of the sediment column be corrected for compaction before the method be applied. Both models assume no post-depositional migration of $^{210}Pb$ and a constant flux of $^{210}Pb_{exc}$ at the sediment-water interface.

Concentration and flux relate to each other by the equation:

$$C = \frac{F}{r} \qquad (1)$$

where $r$ is the mass accumulation rate. By assuming a constant flux of $^{210}Pb_{exc}$ at the sediment-water interface and constant sedimentation rate, the CIC model fixes the concentration of $^{210}Pb_{exc}$ at the surface. If no physical processes alter the amount of

$^{210}Pb_{exc}$ in the surface sediments, the activity of $^{210}Pb_{exc}$ declines down the sedimentary profile according to its natural radioactive decay:

$$C_{(x)} = C_{(0)} * \exp(-\lambda t) \quad (2)$$

where $C$ is the $^{210}Pb_{exc}$ concentration per mass of dry sediment (Bq $kg^{-1}$) at the sediment-water interface ($C_{(0)}$) and at depth $x$ ($C_{(x)}$), $\lambda$ is the decay constant of $^{210}Pb$ (0.03114 $yr^{-1}$), and $t$ is the age of the sediment at depth $x$. Because the age of the sediment is a function of sedimentation rate ($R$) (cm $yr^{-1}$) and depth ($x$) (cm), equation 2 takes the form:

$$C_{(x)} = C_{(0)} * \exp(-\frac{\lambda}{R} * x) \quad (3)$$

From this point, there are at least three different ways of calculating sedimentation rate using the CIC model. Graphically, the semi-logarithmic plot of $^{210}Pb_{exc}$ concentration against depth is predominantly linear and the mean sedimentation rate is taken from the ratio of the decay constant of $^{210}Pb$ to the slope of the line. If compaction plays an important role in the study site, such as in the Pettaquamscutt River sediments, the slope of this line decreases towards the top of the core as a result of reduced compaction at the surface, assuming no physical mixing and no change in accumulation rate has taken place. The effects of compaction can be eliminated from the CIC model by expressing depth in terms of cumulative dry mass of sediment ($m$)(g $cm^{-2}$):

$$Dry\ bulk\ density\ (DBD)_{(x)} = (1-\phi_{(x)}) * \rho_{sed} \quad (4)$$

$$m = \Sigma(DBD_{(x)} * T_{(x)}) \quad (5)$$

where $\phi_{(x)}$ is the porosity at depth $x$; $\rho_{sed}$ is the density of the sediment at depth $x$ and $T$ is the thickness of the sediment layer. Equation 3 now takes the form (Hughen et al., 1996):

$$C_{(x)} = C_{(0)} * \exp(-\frac{\lambda}{r} * m) \quad (6)$$

$r$, the mass accumulation rate (g $cm^{-2}$ $y^{-1}$), is calculated by the ratio of the decay constant of $^{210}Pb$ to the slope of the line of the semi-logarithmic plot of $^{210}Pb_{exc}$ concentration against cumulative dry mass, and sedimentation rate as a function of depth is calculated by (Hughen et al., 1996):

$$R = \frac{r}{(1-\phi) * \rho_{sed}} \tag{7}$$

A third way of calculating sedimentation rate with the CIC model is by simply applying equation 2 to the data. $C_{(0)}$ is the $^{210}Pb_{exc}$ concentration per mass of dry sediment (Bq $kg^{-1}$) at the sediment-water interface and $C_{(x)}$ is the $^{210}Pb_{exc}$ concentration of the layer under investigation, so $t$, the age of the sediment at depth $x$, can be calculated for each depth. Because this method does not fit a regression line through the data, calculated sedimentation rates vary with depth and yield scattered results.

In the CRS model, the initial concentration of $^{210}Pb_{exc}$ and the sediment accumulation rate vary with time, but their product remains constant and equals the flux of $^{210}Pb_{exc}$ that reaches the sediment-water interface. The constant flux assumption implies a constant residue of $^{210}Pb_{exc}$ within the sediment column. Equation 2 then takes the form:

$$A_{(x)} = A_{(0)} * \exp(-\lambda t) \tag{8}$$

where $A_{(x)}$ is the residual $^{210}Pb_{exc}$ in the core below depth $x$ (Bq $m^{-2}$), and $A_{(0)}$ is the entire $^{210}Pb_{exc}$ inventory below the sediment-water interface. The residual $^{210}Pb_{exc}$ for each sediment layer is calculated by multiplying $^{210}Pb_{exc}$ concentration ($C_{(x)}$) by cumulative dry mass ($m$). The age of each sediment layer can be calculated by rearranging equation 8,

$$t = \frac{1}{\lambda} \ln\left(\frac{A_{(0)}}{A_{(x)}}\right) \tag{9}$$

and the mass accumulation rate at time $t$ from (Appleby, 2001):

$$r = \frac{\lambda * A}{C} \tag{10}$$

For a more extensive discussion of applications of CIC and CRS models and derivation of mathematical equations, refer to Appleby (2001), Turner and Delorme (1996) and Eakins (1983).

## 4. RESULTS AND DISCUSSION

### 4.1 Sediment Properties

Water content, density and porosity are some of the basic parameters necessary for dating sediments. Most studies assume a sediment dry density between 2.3 and 2.7 g $cm^{-3}$ throughout a core. However, dry densities measured at 2-cm intervals using a 2-mL specific gravity bottle for the Pettaquamscutt River sediments ranged from 1.58 to 2.29 g $cm^{-3}$ (Figure 3, Table 1), well below the commonly assumed values. These low values reflect the composition of the sediments, which are dominated by diatom frustules (45 to 65%) and organic matter, with small amounts of pyrite and clastic material and no

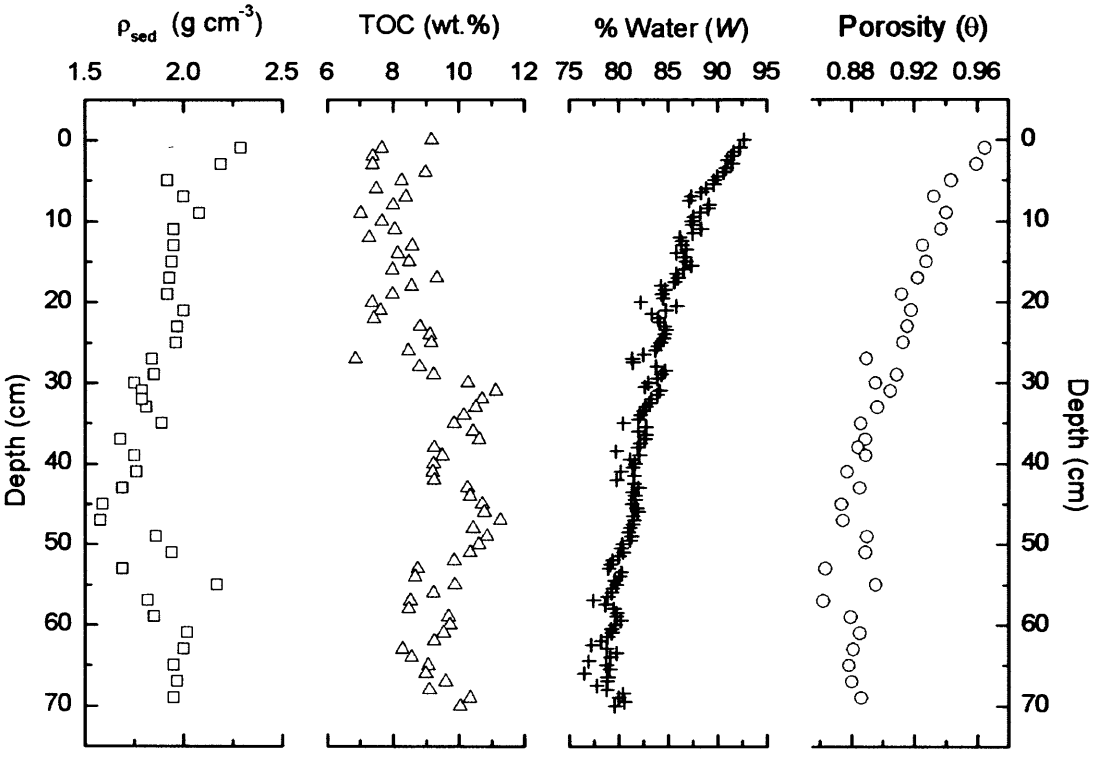


Figure 3. Down-core profile of dry sediment density ($\rho_{sed}$), total organic carbon (TOC), water content ($W$), and porosity ($\theta$) in the Pettaquamscutt River.

carbonates (Orr and Gaines, 1973). The down-core profiles of sediment dry density and organic carbon content (Figure 3) show a slight inverse correlation below 25-cm. The organic carbon content varied from an average of 8.1 ± 0.7% in surface layers to 9.8 ± 0.8% below 30 cm, and increases in organic carbon content were frequently associated with declines in sediment density.

Table 1. Values obtained for selected sediment properties, radiometric determinations and $^{210}$Pb chronology calculation using the CRS model are listed below.

| Mid-point depth (cm) | $\rho_{sed}$ (g cm$^{-3}$) | $W$ (%) | Porosity $\phi$ | $DBD$ (g cm$^{-3}$) | $m$ (g cm$^{-2}$) | $^{210}$Pb$_{exc}$ ± error (Bq kg$^{-1}$) | $^{210}$Pb$_{exc}$ Inventory (Bq m$^{-2}$) | CRS (cm y$^{-1}$) | Model Date | $^{137}$Cs ± error (Bq kg$^{-1}$) |
|---|---|---|---|---|---|---|---|---|---|---|
| 0.5 | 2.3 | 93 | 0.967 | 0.08 | 0.04 | 550 ± 20 | 10287 | 0.76 | 1999 | ≤ DL |
| 2.25 | 2.3 | 92 | 0.961 | 0.09 | 0.18 | 470 ± 29 | 9334 | 0.69 | 1995 | ≤ DL |
| 4.25 | 2.2 | 90 | 0.955 | 0.10 | 0.37 | 370 ± 22 | 8541 | 0.73 | 1992 | ≤ DL |
| 5.25 | 1.9 | 90 | 0.943 | 0.11 | 0.48 | 470 ± 28 | 8104 | 0.49 | 1990 | ≤ DL |
| 6.25 | 1.9 | 90 | 0.939 | 0.12 | 0.59 | 280 ± 13 | 7677 | 0.72 | 1988 | 3 ± 1 |
| 7.25 | 2.0 | 89 | 0.933 | 0.14 | 0.72 | 375 ± 27 | 7261 | 0.45 | 1987 | 6 ± 1 |
| 8.25 | 2.0 | 87 | 0.943 | 0.11 | 0.84 | 310 ± 25 | 6833 | 0.60 | 1985 | 5 ± 2 |
| 10.25 | 2.1 | 88 | 0.935 | 0.14 | 1.09 | 300 ± 30 | 6069 | 0.46 | 1981 | ≤ DL |
| 12.25 | 1.9 | 87 | 0.924 | 0.15 | 1.37 | 217 ± 15 | 5333 | 0.52 | 1977 | ≤ DL |
| 14.25 | 1.9 | 87 | 0.922 | 0.15 | 1.67 | 220 ± 23 | 4678 | 0.44 | 1972 | 11 ± 2 |
| 16.25 | 1.9 | 87 | 0.926 | 0.14 | 1.97 | 179 ± 12 | 4090 | 0.50 | 1968 | 16 ± 2 |
| 17.25 | 1.9 | 86 | 0.922 | 0.15 | 2.11 | 195 ± 11 | 3816 | 0.41 | 1966 | 21 ± 2 |
| 18.25 | 1.9 | 86 | 0.912 | 0.17 | 2.27 | 158 ± 15 | 3535 | 0.41 | 1963 | 25 ± 2 |
| 19.25 | 1.9 | 85 | 0.912 | 0.17 | 2.44 | 135 ± 9 | 3287 | 0.45 | 1961 | 14 ± 2 |
| 20.25 | 1.9 | 84 | 0.898 | 0.19 | 2.63 | 149 ± 11 | 3029 | 0.33 | 1958 | 11 ± 1 |
| 22.25 | 2.0 | 83 | 0.913 | 0.17 | 2.99 | 112 ± 11 | 2549 | 0.41 | 1953 | 4 ± 1 |
| 24.25 | 2.0 | 85 | 0.916 | 0.17 | 3.33 | 125 ± 8 | 2146 | 0.32 | 1947 | ≤ DL |
| 26.25 | 2.0 | 84 | 0.910 | 0.18 | 3.68 | 93 ± 11 | 1772 | 0.34 | 1941 | ≤ DL |
| 30.25 | 1.7 | 84 | 0.895 | 0.18 | 4.40 | 96 ± 16 | 1093 | 0.19 | 1926 | ≤ DL |
| 34.25 | 1.8 | 83 | 0.893 | 0.19 | 5.15 | 47 ± 9 | 555 | 0.19 | 1904 | ≤ DL |
| 38.25 | 1.7 | 82 | 0.884 | 0.19 | 5.93 | 23 ± 7 | 282 | 0.20 | 1882 | ≤ DL |
| 42.25 | 1.8 | 82 | 0.874 | 0.22 | 6.76 | 8 ± 3 | 154 | 0.28 | 1863 | ≤ DL |
| 44.25 | 1.7 | 81 | 0.883 | 0.20 | 7.18 | 7 ± 3 | 123 | 0.26 | 1855 | ≤ DL |
| 46.25 | 1.6 | 82 | 0.879 | 0.19 | 7.58 | -2.7 | | | | ≤ DL |
| 48.25 | 1.6 | 81 | 0.872 | 0.20 | 7.97 | -4.6 | | | | ≤ DL |

DL = detection limit = 0.004Bq

Porosity ($\phi$) was calculated from the weight percent of water in the sediments, following equation by Berner et al. (1971):

$$\phi = \frac{W * \rho_{sed}}{W * \rho_{sed} + (1 - W)\rho_{water}} \quad (11)$$

where $W$ is the weight percent water, $\rho_{sed}$ is the dry density of the sediment, and $\rho_{water}$ is the density of the pore water ($\rho_{water}$ = 0.9997; assuming a salinity of 27 ‰ and temperature of 10°C for the pore water (O'Sullivan et al., 1997). The porosity in the Pettaquamscutt River sediments ranged from 0.965 at the surface to an average of 0.883 below 30 cm (Figure 3, Table 1). Although this is only a 8.5% decrease over 30 cm, the ratio of volume of solids to volume of pore water [$(1-\phi)/\phi$] increases by almost a factor of 3. This variation indicates that the bottom layers of the core are undergoing continuous compaction due to the weight of overlying sediments, so that the thickness of a one-year increment is larger at the surface (8 mm at 6.7-cm) than in deeper layers (2 mm at 54.5-cm) (Figure 2).

### 4.2 Varve Counting and $^{210}$Pb Chronology

A key assumption in varve counting chronologies is that two seasonally controlled laminae are deposited annually and sediment ages can be calculated by counting each couplet. Predominantly biogenic layers form as phytoplankton remains from the spring/summer bloom settle out of the water column. These biogenic layers appear dark under cross-polarized light due to the small amounts of birefringent minerals. During the fall/winter, productivity is much lower and clastic material from the watershed dominates the input to the sediment surface. Such clastic layers appear bright under cross-polarized light. Examination of the thin sections from the upper sediment column of the lower basin of the Pettaquamscutt River showed that this pattern of deposition occurs annually, allowing construction of a precise varve chronology. Additional constraints to the varve chronology come from occasional coarse-grained (fine sand) winter laminae. These layers are deposited as large hurricanes rework the material from the surrounding watershed. The good correlation between coarse-grained layers and

the two largest hurricanes to hit Rhode Island in the twentieth century (1954, 1938, Figure 2) supports the accuracy of this varve chronology.

Radiometric results obtained for the Pettaquamscutt River sediments are shown in Figures 4 to 7 and Table 1. The down-core profile of $^{214}Pb$ activities is nearly uniform with depth, while total $^{210}Pb$ activities decrease exponentially until $^{214}Pb$-supported levels are reached at approximately 42 cm (Figure 4a). The resulting $^{210}Pb_{exc}$ profile (Figure 4b) follows closely the exponential shape of the total $^{210}Pb$, attesting to the good preservation of these sediments. Indeed, if the surficial sediments were physically disturbed (either during recovery of the core or due to rapid bioturbation), the $^{210}Pb_{exc}$ distribution would be uniform within the mixed layer.

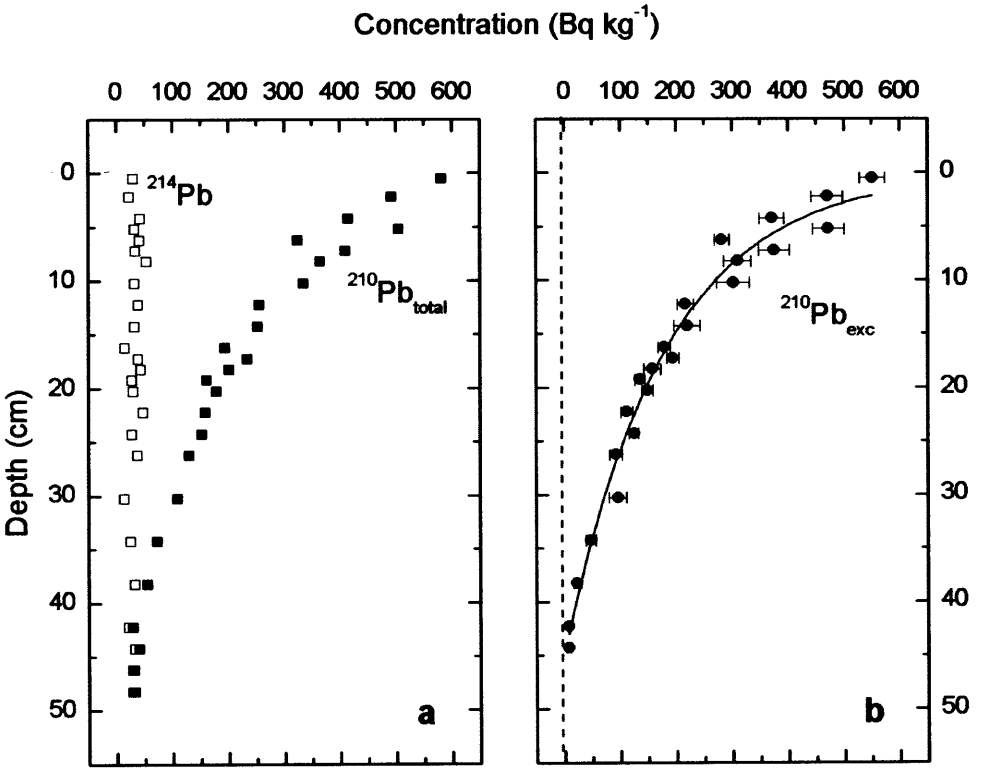


Figure 4. a) Down-core profile of $^{214}Pb$ activities is nearly uniform with depth, while total $^{210}Pb$ activities decrease exponentially until supported levels are reached at 42 cm; b) Resulting $^{210}Pb_{exc}$ profile (exponential fit) is consistent with the lack of rapid bioturbation of the sediments.

Discrepancies among the three different methods for CIC calculation and the CRS model were checked against the independent varve counting (Figure 5). The different ways of determining age-depth correlations using the CIC model yield contrasting results. Compaction is an important process in the sediments of the Pettaquamscutt River, consequently the CIC chronologies generated by neglecting compaction (e.g., calculating age from the slope of the plot of $^{210}Pb_{exc}$ concentration against depth and from equation 2) did not agree well with the varve counts. The former CIC method underestimated sedimentation rates for layers above 30 cm resulting in ages older than the varve chronology, while the latter CIC method resulted in scattered values. The CIC model calculated from the slope of the plot of $^{210}Pb_{exc}$ concentration against cumulative dry mass yield results similar to those generated by the CRS. However, for a given sediment depth, the model ages from the CIC model were slightly older than those from the CRS, probably because this CIC model does not account for the possibility of small changes in mass accumulation rate. For instance, sediments deposited at the peak of $^{137}Cs$ deposition (18.25 cm) were assigned a date of 1958 by the CIC model and 1963 by the CRS model, the latter date being in good agreement with the historical fallout of $^{137}Cs$. If the sedimentation rate at the Pettaquamscutt River were constant, then both $^{210}Pb$ models would have produced identical results. Instead, the results obtained by the CRS model followed the varve chronology more closely than the CIC model, as expected for an environment that has undergone changes in sedimentation rate. Land use changes within a watershed tend to modify the rate of sediment transport to nearby lakes and rivers. In 1995, only 22.7% of the watershed of the Pettaquamscutt River was comprised of residential land (Hubeny and King, 2003). Although there are no recent estimates available for land use for residential purpose, this percentage is likely to have increased in the past decade due to new urban developments in the region.

The good age agreement obtained between the varve counts and $^{210}Pb$ dates calculated by the CRS model (e.g., within 2 years for the sand layer deposited by the 1954 hurricane, 3 years for the 1938 hurricane and 9 years at 1860, Figure 5) allowed the extension of the sediment chronology beyond the limit of the $^{210}Pb$ method (100-150

years). The deposition dates adopted for the Pettaquamscutt River sediments are a composite of these two dating techniques. The CRS model ages were used for the uppermost 34-cm (1904), while the varve chronology was applied for sediments deposited below between 1900 and 1735 (35-70 cm).

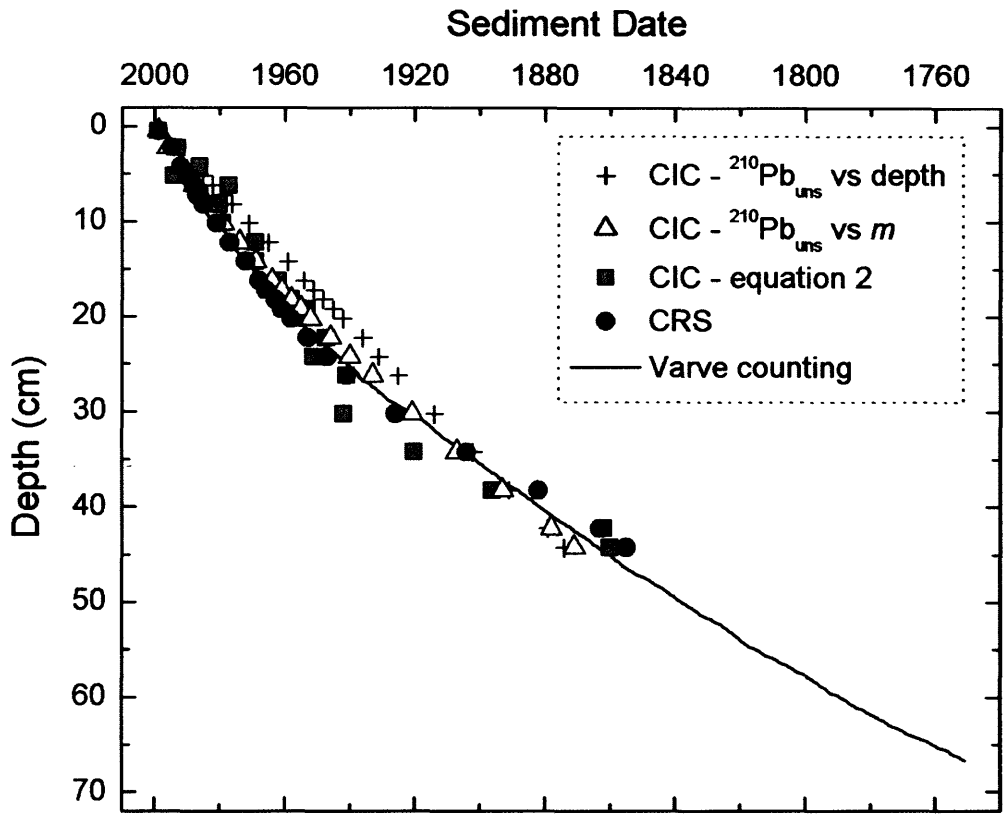


Figure 5. Chronology results obtained by the CRS model and by three different forms of applying the CIC model were checked against the independent varve counting ($m$ = cumulative dry mass in g $cm^{-2}$).

### 4.3 $^{137}Cs$ and $^{14}C$ Profiles

The sedimentary profile of $^{137}Cs$ (Figure 6) in the Pettaquamscutt River shows good correlation with the history of atmospheric deposition of radionuclides derived from

nuclear weapons testing. The first detection of $^{137}Cs$ in the sediment core (22.25 cm) corresponds to 1953, which closely matches the early 1950s increase in total fission yields from the explosions (Carter and Moghissi, 1977). The yield and number of nuclear detonations per year peaked in 1962, resulting in extensive deposition of radionuclides in the Northern Hemisphere in 1963 when the Test Ban Treaty was signed (Carter and Moghissi, 1977; Appleby, 2001). The elevated amount of radioactivity released in the 1960s was preserved in the Pettaquamscutt River sedimentary record in the form of a sharp $^{137}Cs$ subsurface maximum with highest activity in 1963, as well as increased amounts of radiocarbon ($^{14}C$) in the total organic carbon (TOC) (Figure 6). Nuclear weapons tests roughly doubled the levels of $^{14}C$ in the atmosphere (Levin and Kromer, 1997), raising the $\Delta^{14}C$ of $CO_2$ to values greater than +900 permil (‰) (Levin et al., 1985), the so-called "bomb spike". The incorporation of bomb-$^{14}C$ into terrestrial and aquatic plant biomass through photosynthetic carbon fixation is manifested in the sedimentary record as an increase in $\Delta^{14}C$ in the TOC (Figure 6). The relative timing of the $^{137}Cs$ peak and the rapid $\Delta^{14}C$ rise is primarily determined by the pathways by which these radionuclides are incorporated into the sediments. $^{137}Cs$ deposited in aquatic systems by direct dry and wet fallout quickly sorbs onto settling particles, reaching the sediments in a matter of months (depending on the water column depth) (Santschi et al., 1988; Wieland et al., 1993). The rate at which atmospheric $^{14}C$ signals propagate into sedimentary TOC depends on the relative contributions from different organic carbon sources (e.g., terrestrial vs. marine) and the residence times for carbon in each reservoir. The similar timing of the rise in $\Delta^{14}C$ and $^{137}Cs$ (Figure 6), together with the relatively depleted stable carbon isotopic composition ($\delta^{13}C$) of the TOC throughout the core (–24.1 ± 0.5‰, $n$ = 37) suggests that terrestrial OC plays a significant role in the amount of "pre-aged" organic carbon deposited in the Pettaquamscutt River sediments. However, the fact that the $\Delta^{14}C$ profile of TOC does not exceed 0‰, typical of atmospheric "bomb $^{14}C$" (Levin and Hesshaimer, 2000), implies that recent material is being diluted by relict terrestrial OC from sedimentary and fossil sources.

The down-core profile of $^{137}Cs$ also reveals a smaller peak in activity closer to the surface $^{210}Pb$-dated at 1987. The timing of this peak is consistent with fallout resulting from the release of radioactivity that followed the 1986 Chernobyl reactor fire in Ukraine. Elevated surface air concentrations and ground deposition of radionuclides due to the Chernobyl accident were reported throughout the Northern Hemisphere, in locations as far apart as Japan (Ayoama et al., 1986), Switzerland (Santschi et al., 1988), and Sweden (Devell et al., 1986). At some European sites, the deposition of Chernobyl $^{137}Cs$ provided another datable horizon in the sediments, characterized in some cases by an even greater

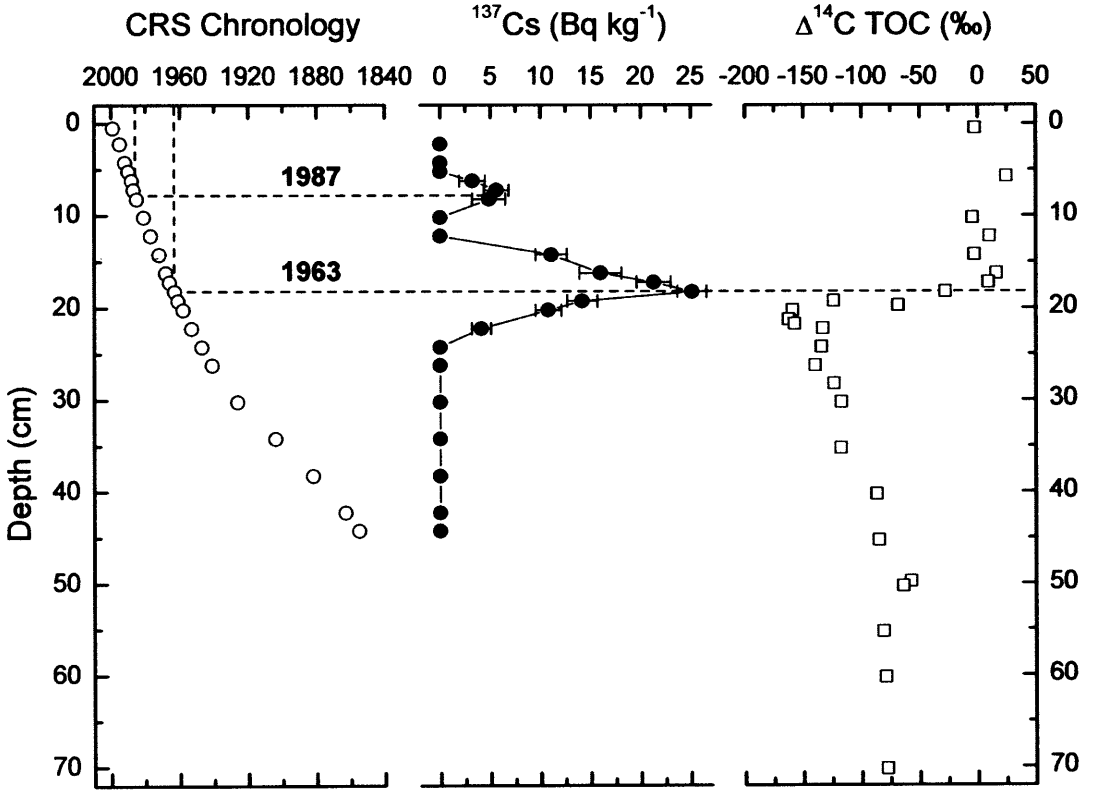


Figure 6. Radioactivity released by nuclear bomb testing in the 1960s was preserved in the Pettaquamscutt River sedimentary record in the form of a sharp $^{137}Cs$ peak and increased amounts of radiocarbon in the total organic carbon ($\Delta^{14}C$ TOC). A smaller and more surficial peak in $^{137}Cs$ activity dated at 1987 is consistent with fallout resulting from the Chernobyl accident.

inventory than that resulting from the bomb tests (Dominik and Span, 1992; Ehlers et al., 1993; Callway et al., 1996; Gevao et al., 1997). Several studies reported the passage of the Chernobyl plume over the United States (Bondietti and Brantley, 1986; Larsen et al., 1986; Dibb and Rice, 1988; Feely et al., 1988). Surface air measurements conducted by the Environmental Measurements Laboratory (EML) following the announcement of the reactor explosion revealed simultaneous appearance of elevated radioactivity in both the eastern and western US (Larsen et al., 1986). Monitoring of $^{137}Cs$ concentrations from 6 May to 29 May showed comparable surface air concentrations at 8 sites (Larsen et al., 1986), suggesting that the portion of the Chernobyl plume that arrived in the US was homogeneous in composition. The closest EML monitoring sites to the Pettaquamscutt River were New York City (NY) and Chester (NJ). The total fallout of $^{137}Cs$ at these locations in May 1986 was ~41 Bq $m^{-2}$ and ~68.5 Bq $m^{-2}$, respectively, and rainfall was responsible for ~90% of the deposition (Larsen et al., 1986). The higher efficiency of rain events in removing $^{137}Cs$ from the atmosphere relative to dry fallout was also demonstrated by $^{137}Cs$ accumulation rate measurements in Switzerland (70-80% efficiency for rain versus 20-25% for dry fallout) (Santschi et al., 1988), where the amount of $^{137}Cs$ deposited varied by at least one order of magnitude depending on the volume of precipitation (Dominik and Span, 1992). Because rain removes $^{137}Cs$ efficiently from the atmosphere, the ratio of $^{137}Cs$ deposited by wet fallout to the amount of precipitation that fell in May 1986 is fairly similar in both New York City (12440 Bq $m^{-3}$) and Chester (13880 Bq $m^{-3}$). To our knowledge there is no data on the surface air concentration or deposition of $^{137}Cs$ available for the state of Rhode Island following the Chernobyl accident. However, it is possible to estimate the total amount of $^{137}Cs$ deposited in the Pettaquamscutt River using the volumetric concentrations of $^{137}Cs$ calculated for New York and Chester and the amount of rain that fell in the Kingston area in May (4.77 cm; (NOAA, 1986)). While this exercise gives a range in $^{137}Cs$ accumulation between 59.4 Bq $m^{-2}$ and 66.2 Bq $m^{-2}$, the decay-corrected Chernobyl $^{137}Cs$ inventory in the Pettaquamscutt River sediments is only 22.5 Bq $m^{-2}$. Therefore, even if

only a third of the Chernobyl $^{137}Cs$ washed out by local rain reached the sediments of the lower basin of the Pettaquamscutt River, the undisturbed nature of this depositional environment was able to record it.

Another line of compelling evidence in support for the Chernobyl origin of the surficial $^{137}Cs$ peak derives from a sediment freeze-core collected in 1987 in the lower basin of the Pettaquamscutt River (Figure 7). After slicing the sediment at 2 cm intervals, $^{137}Cs$ and $^{210}Pb$ were measured by direct gamma assay at the Liverpool University Environmental Radioactivity Research Center. The down core profile of $^{137}Cs$ obtained for the 1987 core shows an increase in activity at 1 cm that correlates well with the Chernobyl $^{137}Cs$ maximum that we observed in this study. Deposition of the Chernobyl $^{137}Cs$ peak was not yet complete when the 1987 core was collected, which is reasonable considering that settling particles can reside in the water column for months before reaching the sediments (Santschi et al., 1988). However, the good agreement between cores collected 11 years apart strengthens our belief that the elevated $^{137}Cs$ activities observed in the Pettaquamscutt River sediments at depths dated ~1987 are the first record of Chernobyl $^{137}Cs$ deposition in North American sediments. This peak in $^{137}Cs$ may not be recognizable in other locations of the United States because the fallout was strongly dependent on local rainfall, among other things. The similarity of profile shapes for the 1987 and 1998 cores also indicates that diffusion and resuspension of $^{137}Cs$ are not significant in this system. If resuspension were a substantial process in the Pettaquamscutt River, higher $^{137}Cs$ activities would be observed at sediment layers younger than the maximum deposition (1963 and 1987). Furthermore, if diffusion were an active process, $^{137}Cs$ deposited in 1963 would have diffused into adjacent layers of lower activity and Figure 6 shows that this is not the case. The presence of two $^{137}Cs$ marker points (1963 and 1987) in the Pettaquamscutt River segregates a portion of the sediment column that could prove valuable in the understanding of processes of decomposition and preservation of terrestrial and aquatic organic matter. This information is often lacking and can be useful in determining long-term diagenetic

processes. Although the 1987 $^{137}Cs$ peak has low activity, it should still be detectable in this environment for the next few decades.

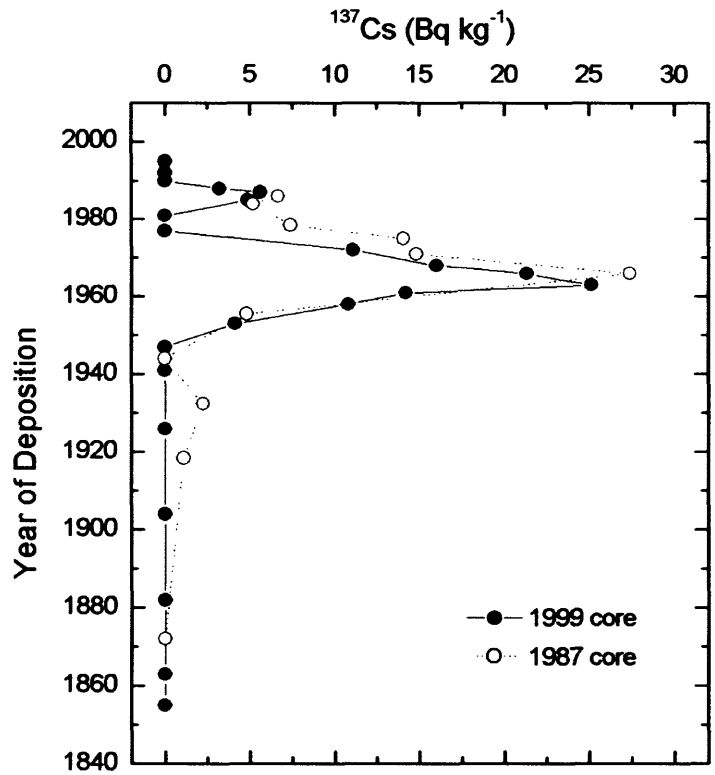


Figure 7. The $^{137}Cs$ profile obtained for a core collected in 1987 in the Pettaquamscutt River (Mecray et al., 1991) showed a rise in activity that correlates extremely well with the Chernobyl $^{137}Cs$ maximum observed in this study.

## 5. CONCLUSIONS

The anoxic and laminated sediments of the Pettaquamscutt River display the first known record of a Chernobyl $^{137}Cs$ peak in sediments from North America. The inventory of activities of this peak is small compared to European counterparts, but reasonable considering the reduced amount of radioactivity that reached the US. The Chernobyl $^{137}Cs$ activities measured in the sediments are three-times lower than the

calculated wet deposition for this area, demonstrating that rainfall alone could have produced the observed peak in $^{137}Cs$. Although this peak may only be detectable for the next few decades, the presence of two $^{137}Cs$ marker points (1963 and 1987) identifies a segment of the sediment column that can potentially be used to evaluate the importance of compaction and decomposition and preservation of organic matter. Different methods for calculating the $^{210}Pb$ chronology were also evaluated in this study and checked against independent varve counting. In the case of the Pettaquamscutt River system, the CRS model provided results that matched the varve counting more closely and was applied for the most recent portion (100 years) of the core. The absence of sediment mixing by benthic organisms was consistent with the exponentially decreasing trend of the $^{210}Pb_{exc}$ profile, making this site well suited for reconstruction of historical records.

## 6. REFERENCES


Albrecht A., Reiser R., Lück A., Stoll J.-M. A., and Giger W. (1998) Radiocesium dating of sediments from lakes and reservoirs of different hydrological regimes. *Environ. Sci. Technol.* **32**, 1882-1887.

Anderson R., Bopp R., Buesseler K., and Biscaye P. (1988) Mixing of particles and organic constituents in sediments from the contiunental shelf and slope off Cape Cod: SEEP-I results. *Cont. Shelf Res.* **8**(5-7), 925-946.

Appleby P. and Oldfield F. (1978) The calculation of lead-210 dates assuming a constant rate of supply of unsupported $^{210}Pb$ to the sediment. *Catena* **5**, 1-8.

Appleby P. G. (2001) Chronostratigraphic techniques in recent sediments. In *Tracking environmental change using lake sediments*, Vol. 1 (ed. W. Last and J. Smol), pp. 171-203. Kluwer Academic Publishers, Dordrecht.

ApSimon H. and Wilson J. (1986) Tracking the cloud from Chernobyl. *New Sci.* **1517**, 42-45.

Ayoama M., Hirose K., Suzuki Y., Inoue H., and Sugimura Y. (1986) High level radioactive nuclides in Japan in May. *Nature* **321**, 819-820.

Berner R. (1971) Diagenetic processes. In *Principles of chemical sedimentology* (ed. F. Press), pp. 86-113. McGraw-Hill Book Company, New York.

Bondietti E. and Brantley J. (1986) Characteristics of Chernobyl radioactivity in Tennessee. *Nature* **322**, 313-314.

Boothroyd J. (1991) The geologic history of Narrow River. *Maritimes* **35**(2), 3-5.

Buesseler K., Livingston H., Honjo S., Hay B., Manganini S., Degens E., Ittekkot V., Izdar E., and Konuk T. (1987) Chernobyl radionuclides in a Black Sea sediment trap. *Nature* **329**, 825-828.

Callway J., DeLaune R., and Patrick W. J. (1996) Chernobyl $^{137}Cs$ used to determine sediment accretion rates at selected northern European coastal wetlands. *Limnol. Oceanogr.* **41**(3), 444-450.

Cambray R., Cawse P., Garland J., Gibson J., Johnson P., Lewis G., Newton D., Salmon L., and Wade B. (1987) Observations on radioactivity from the Chernobyl accident. *Nucl. Energy* **26**, 77-101.

Carter M. and Moghissi A. (1977) Three decades of nuclear testing. *Health Phys. Press* **33**, 55-71.

De Keyser T. L. (1999) Digital scanning of thin sections and peels. *J. Sediment. Res.* **69**, 962-964.

Devell L., Tovedal H., Bergström U., Appelgren A., Chyssler J., and Andersson L. (1986) Initial observations of fallout from the reactor accident at Chernobyl. *Nature* **321**, 192-193.

Dibb J. and Rice D. (1988) Chernobyl fallout in the Chesapeake Bay region. *J. Environ. Radioact.* **7**, 193-196.

Dominik J. and Span D. (1992) The fate of Chernobyl $^{137}Cs$ in Lake Lugano. *Aquat. Sci.* **54**(3/4), 238-254.

Eakins J. (1983) The $^{210}Pb$ technique for dating sediments, and some applications. In *Radioisotopes in sediment studies*, pp. 31-47. IAEA-TecDoc 298, Vienna.

Ehlers J., Nagorny K., Schmidt P., Stieve B., and Zietlow K. (1993) Storm surge deposits in North Sea salt marshes dated by $^{134}Cs$ and $^{137}Cs$ determination. *J. Coastal Res.* **9**(3), 698-701.

Feely H., Helfer I., Juzdan Z., Klusek C., Larsen R. J., Leifer R., and Sanderson C. G. (1988) Fallout in the New York metropolitan area following the Chernobyl accident. *J. Environ. Radioact.* **7**, 177-191.

Francus P., Keimig F., and Besonen M. (2002) An algorithm to aid varve counting and measurement from thin-sections. *J. Paleolimnol.* **28**, 283-286.

Fuller C., Van Geen A., Baskaran M., and Anima R. (1999) Sediment chronology in San Francisco Bay, California, defined by $^{210}Pb$, $^{234}Th$, $^{137}Cs$, and $^{239,240}Pu$. *Mar. Chem.* **64**, 7-27.

Gaines A. G. J. and Pilson M. E. Q. (1972) Anoxic water in the Pettaquamscutt River. *Limnol. Oceanogr.* **17**(1), 42-49.

Gevao B., Hamilton-Taylor J., Murdoch C., Jones K. C., Kelly M., and Tabner B. J. (1997) Depositional time trends and remobilization of PCBs in lake sediments. *Environ. Sci. Technol.* **31**, 3274-3280.

Goldberg E. (1962) Geochronology with $^{210}Pb$. *Symposium on Radioactive Dating*, 121-131.

Gunten H. R. V., Sturm M., and Moser R. N. (1997) 200-year record of metals in lake sediments and natural background concentrations. *Environ. Sci. Technol.* **31**, 2193-2197.

Hohenemser C., Deicher M., Ernst A., Hofsäss H., Lindner G., and Recknagel E. (1986) Chernobyl: An early report. *Environment* **28**, 6-13 and 30-43.

Holloway R. W. and Liu C. K. (1988) Xenon-133 in California, Nevada, and Utah from the Chernobyl accident. *Environ. Sci. Technol.* **22**, 583 - 586.

Hubeny J. B. and King J. W. (2003) Anthropogenic eutrophication as recorded by varved sediments in the Pettaquamscutt River Estuary, Rhode Island, USA. *2003 GSA Annual Meeting. Abstracts with Programs*, 282.

Hughen K., Overpeck J., Anderson R., and Williams K. (1996) The potential for paleoclimate records from varved Arctic lake sediments: Baffin Island, Eastern Canadian Arctic. In *Paleoclimatology and paleoceanography from laminated sediments* (ed. A. Kemp), pp. 57-71. Geological Society Special Publication No.116.

Koide M., Bruland K., and Goldberg E. (1973) $^{228}Th/^{232}Th$ and $^{210}Pb$ geochronologies in marine and lake sediments. *Geochim. Cosmochim. Acta* **37**, 1171-1187.

Krishnaswamy S., Lal D., Martin J., and Meybeck M. (1971) Geochronology of lake sediments. *Earth Planet. Sci. Lett.* **11**, 407-414.

Lamoureux S. (2001) Varve chronology techniques. In *Tracking environmental change using lake sediments*, Vol. 1. Basin analysis, coring, and chronological techniques (ed. W. M. Last and J. P. Smols), pp. 247-260. Kluwer Academic Publishers, Dordrecht, The Netherlands.

Larsen R. J., Sanderson C. G., Rivera W., and Zamichieli M. (1986) The characterization of radionuclides in North American and Hawaiian surface air and deposition following the Chernobyl accident. In *Environmental measurements laboratory: A compendium of the Environmental Measurements Laboratory's research projects related to the Chernobyl nuclear accident*, Vol. October 1, 1986. Report No. EML-460, pp. 1-104. US Department of Energy.

Levin I., Kromer B., Schoch-Fischer H., Bruns M., Münnich M., Berdau D., Vogel J., and Münnich K. (1985) 25 years of tropospheric $^{14}C$ observations in central Europe. *Radiocarbon* **27**(1), 1-19.

Levin I. and Kromer B. (1997) Twenty years of atmospheric $^{14}CO_2$ observations at Schauinsland station, Germany. *Radiocarbon* **39**(2), 205-218.

Levin I. and Hesshaimer V. (2000) Radiocarbon - A unique tracer of global carbon cycle dynamics. *Radiocarbon* **42**, 69-80.

Lima A. L. C., Eglinton T. I., and Reddy C. M. (2003) High-resolution record of pyrogenic polycyclic aromatic hydrocarbon deposition during the 20$^{th}$ century. *Environ. Sci. Technol.* **37**, 53-61.

McNichol A., Osbourne E., Gagnon A., Fry B., and Jones G. (1994) TIC, TOC, DIC, DOC, PIC, POC - Unique aspects in the preparation of oceanographic samples for $^{14}C$-AMS. *Nuclear Instruments & Methods in Physics Research, Section B* **92**, 162-165.

Mecray E., King J., and Corbin J. (1991) Metal pollution recorded in the Pettaquamscutt River sediments. *Maritimes* **35**(2), 10-11.

Mould R. F. (2000) *Chernobyl record: The definite history of the Chernobyl catastrophe.* Institute of Physics Publishing, Philadelphia.

NOAA. (1986) Climatological Data-New England. Daily precipitation, Vol. 98. US Environmental Data Service.

Orr W. L. and Gaines A. G. J. (1973) Observations on the rate of sulfate reduction and organic matter oxidation in the bottom waters of an estuarine basin: the upper basin of the Pettaquamscutt River (Rhode Island). In *Advances in Organic Geochemistry* (ed. B.Tissot and F. Bienner), pp. 791-812. Technip.

O'Sullivan D., Hanson Jr A., and Kester D. (1997) The distribution and redox chemistry of iron in the Pettaquamscutt Estuary. *Estuar. Coastal Shelf. Sci.* **45**, 769-788.

Pike J. and Kemp A. E. S. (1996) Preparation and analysis techniques for studies of laminated sediments. In *Paleoclimatology and Paleoceanography from laminated sediments* (ed. A. E. S. Kemp), pp. 37-48. Geological Society Special Publication No. 116.

Ritchie J. and McHenry J. (1990) Application of radioactive fallout cesium-137 for measuring soil erosion and sediment accumulation rates and patterns: A review. *J. Environ. Qual.* **19**, 215-233.

Robbins J., Holmes C., Halley R., Bothner M., Shinn E., Graney J., Keeler G., tenBrink M., Orlandini K., and Rudnick D. (2000) Time-averaged fluxes of lead and fallout radionuclides to sediments in Florida Bay. *J. Geophys. Res.* **105**(C12), 28805-28821.

Santschi P. H., Bollhalder S., Farrenkothen K., Lueck A., Zingg S., and Sturm M. (1988) Chernobyl radionuclides in the environment: tracers for the tight coupling of atmospheric, terrestrial, and aquatic geochemical processes. *Environ. Sci. Technol.* **22**, 510-516.

Shapiro J. (1958) The freeze-corer - A new sampler for lake sediments. *Ecology* **39**, 748.
Smith F. and Clark M. (1986) Radionuclide deposition from the Chernobyl cloud. *Nature* **322**, 690-691.
Spliethoff H. and Hemond H. (1996) History of toxic metal discharge to surface waters of the Aberjona watershed. *Environ. Sci. Technol.* **30**, 121-128.
Spurr A. R. (1969) A low-viscosity epoxy resin embedding medium for electron microscopy. *J. Ultrastruct. Res.* **26**, 31-43.
Stone R. (2001) Living in the shadow of Chornobyl. *Science* **292**, 420-426.
Stuiver M. and Polach H. A. (1977) Reporting of $^{14}C$ data. *Radiocarbon* **19**(3), 355-363.
Turner L. and Delorme L. (1996) Assessment of $^{210}Pb$ data from Canadian lakes using the CIC and CRS model. *Environ. Geol.* **28**(2), 78-87.
Van Metre P., Callender E., and Fuller C. (1997) Historical trends in organochlorine compounds in river basins identified using sediment cores from reservoirs. *Environ. Sci. Technol.* **31**, 2339-2344.
Wieland E., Santschi P., Höhener P., and Sturm M. (1993) Scavenging of Chernobyl $^{137}Cs$ and natural $^{210}Pb$ in Lake Sempach, Switzerland. *Geochim. Cosmochim. Acta* **57**, 2959-2979.
Zwolsman J. J. G., Berger G. W., and Van Eck G. T. M. (1993) Sediment accumulation rates, historical input, postdepositional mobility and retention of major elements and trace metals in salt marsh sediments of the Scheldt Estuary, SW Netherlands. *Mar. Chem.* **44**, 73-94.

# CHAPTER 5

## Pb-ISOTOPES REVEAL A POTENTIAL NEW STRATIGRAPHIC MARKER

**Abstract** - A high-resolution record of Pb deposition in Rhode Island over the past 250 yr was constructed using a sediment core from the anoxic Pettaquamscutt River basin. The sedimentary Pb concentration record shows the well-described maximum associated with leaded gasoline usage in the United States. Diminished Pb variability during recorded periods of local industrial activity (1735 to 1847) supports the greater importance of regional atmospheric lead transport versus local inputs. The Pb isotopic composition at this site shows a clear maximum in anthropogenic $^{206}Pb/^{207}Pb$ in the mid-1800s. Similar peaks have also been observed in sediments from Chesapeake Bay and the Great Lakes, suggesting a common source. Possible causes for this event include mining and smelting of Pb ores in the Upper Mississippi Valley district, which accounted for almost all Pb production in the United States in that period. The timing of this event can provide an important stratigraphic marker for sediments deposited in the last 100 to 200 years in the Northeastern USA. The down-core profile of anthropogenic $^{206}Pb/^{207}Pb$ provides a classic example of how changes in the mixture of ores for production of tetraethyl lead caused a regional-scale shift in the sedimentary record, and suggests that coal could have played a significant role in Pb emissions post-1920.

## 1. INTRODUCTION

Anthropogenic lead has been introduced into the environment since refinement of lead-bearing sulfide ores and production of silver by cupellation were developed about 5000 yr BP (Settle and Patterson, 1980). Natural processes like volcanic eruptions and rock weathering release Pb to the environment (Nriagu, 1978), but are insignificant compared to high-temperature processes such as utilization of leaded gasoline additives, non-ferrous metal smelting, coal combustion, steel and iron manufacturing, and cement production (Nriagu and Pacyna, 1988). Because the main mechanism of Pb dispersion is atmospheric transport, anthropogenic Pb contamination is widely distributed in the environment and has been detected in polar ice caps (Hong et al., 1994; Rosman et al., 1997), peat bogs (Shotyk et al., 1998; Weiss et al., 1999), remote ponds (Shirahata et al.,

1980), corals (Shen and Boyle, 1987) and aquatic sediments (Graney et al., 1995). Because crustal material is in general more radiogenic than coals and ores, studies commonly rely on the difference in isotopic composition among sources to discern the influence of natural and anthropogenic inputs to a system.

While variations in Pb isotopic ratios are frequently used to apportion sources, the concentration profile of anthropogenic Pb can corroborate sediment chronologies. Determination of accumulation rates and subsequent dating of sediments is vital in reconstructing historical records. Depending on the time scale of interest, the natural radionuclides $^{14}C$ (half-life = 5730 yr), $^{210}Pb$ (22.3 yr), $^{228}Th$ (1.9 yr) or $^{234}Th$ (24 days) can be used in determining sedimentation rates in freshwater and marine environments (Koide et al., 1973; Robbins and Edgington, 1975; Anderson et al., 1988; Spliethoff and Hemond, 1996; Shotyk et al., 1998; Fuller et al., 1999). Even though $^{210}Pb$ chronologies become unreliable after approximately 100 years, this radionuclide is still the most widely used for dating sediments for contamination studies, which usually focus on the last 100-200 years. To validate $^{210}Pb$ dates, independent chronological evidence is used whenever possible. Radionuclides derived from nuclear weapons testing (e.g., $^{137}Cs$, $^{239+240}Pu$) are the most reliable markers since their widespread deposition follows the well-documented history of atmospheric fallout (Anderson et al., 1988; Spliethoff and Hemond, 1996), but other chronological markers can also be employed. For example, the increase in abundance of ragweed (*Ambrosia*) pollen grains is interpreted to define the period when deforestation, agricultural development, or intense urbanization took place (Bruland et al., 1975). However, since this transition occurred at different times in different regions, the depth-age relationship is only valid within a narrow geographic area. In contrast, the appearance of certain organic contaminants (e.g., polychlorinated byphenyls - PCBs) and the peak in Pb utilization occurred simultaneously in most of the United States and both can be used as relative markers in sediments from a variety of regions (Latimer and Quinn, 1996; Van Metre et al., 2000). Unfortunately, as with $^{137}Cs$ (peak in 1963), these chemical markers are only useful for sediments deposited in the last

60 years (Latimer and Quinn, 1996). There is, therefore, a hiatus in chronological markers for records that span between 100 to 200 years.

In this paper, we report a large mid-19$^{th}$ century peak in $^{206}Pb/^{207}Pb$ ratio in anoxic sediments from the Pettaquamscutt River, Rhode Island, and note that a similar feature has been reported for sediments from the Great Lakes (Graney et al., 1995), Chesapeake Bay (Marcantonio et al., 2002), and possibly in corals from Bermuda (Reuer et al., 2003). We argue that the most likely source of radiogenic Pb during that period was mining and smelting of lead ores in the Upper Mississippi Valley district and suggest that this event could be useful as a stratigraphic marker for sedimentary records in the Northeastern United States that span more than 100 years.

## 2. EXPERIMENTAL

### 2.1 Study Area

The Pettaquamscutt River is located in Washington County, southern Rhode Island, in close proximity to Narragansett Bay (Figure 1). This 9.7 km long estuary has a small drainage area (~ 35 $km^2$) (Orr and Gaines, 1973) and is dominated by oak forests, wetlands, and open waters (Urish, 1991). The main perennial freshwater source to this system is the Gilbert Stuart Stream, contributing about 34% of the annual total. Groundwater seepage and smaller brooks account for the remaining 66% of the freshwater inflow (Urish, 1991). The flow of freshwater from the Gilbert Stuart Stream over brackish waters (~ 27 ‰) from tidal influx from Narragansett Bay through The Narrows (Gaines and Pilson, 1972) creates water-column stratification. The stable stratification results in permanent bottom water anoxia in the upper and lower basins. The lack of oxygen in the bottom waters prevents the survival of macrofauna and consequent bioturbation of the sediments. As a result, the surface sediments of the Pettaquamscutt River are well preserved, displaying undisturbed laminations that are ideal for historical reconstruction (Lima et al., 2003).

## 2.2 Sampling

Sediment cores were collected in the deepest portion (20 m) of the lower basin of the Pettaquamscutt River (Figure 1) in April 1999. A rectangular aluminum freeze corer (30 x 8 x 165 cm) filled with dry ice and methanol was used for sampling, so that each core consisted of two large rectangular slabs of sediment as the smaller sides were not preserved during separation from the metal corer. After collection, each side was wrapped in aluminum foil, kept on dry ice, and transported back to the laboratory where they were stored in a chest freezer (-18°C). X-radiographs of the frozen slabs showed varved sediments and confirmed the absence of benthic animal burrows. In the present work, we report results from the slab that showed the highest number and most distinct laminations. The frozen sediment was sectioned at 0.5-cm intervals using a compact tile saw equipped with a diamond wafering blade (0.63-mm thickness). Approximately 10% of each frozen sample was dipped into 10% HCl (trace-metal grade) to remove any outer contamination by the tile saw blade, placed in a previously cleaned polyethylene jar, dried in an oven at 60°C, homogenized, and stored for further lead analysis. The remaining 90% of each sample was used to construct a high-resolution record of polycyclic aromatic hydrocarbon deposition (Lima et al., 2003).

## 2.3 Sediment Dating

Dry sediment samples (1-2 g) were analyzed for $^{210}Pb$ (46.5 keV), $^{214}Pb$ (351 keV), and $^{137}Cs$ (661 keV) by a high purity germanium detector (Canberra model GCW 4023S) with a closed-end coaxial well, following storage in sealed containers for 3 weeks to allow radioactive equilibrium of $^{214}Pb$ with $^{210}Pb$. Sedimentation rates were calculated using the constant rate of supply (CRS) model (Appleby and Oldfield, 1978) and validated using the $^{137}Cs$ fallout peak. Since $^{210}Pb$ chronology becomes unreliable after about five half-lives ($t_{1/2}$ = 22.3 years), sediment layers older than 100 years were dated by varve counting (see Chapter 4). The varve and $^{210}Pb$ time scales agree within 2 years at 1960 and within 9 years at 1860 (Figure 2). The sediment chronology in the Pettaquamscutt River is discussed in detail in Chapter 4.

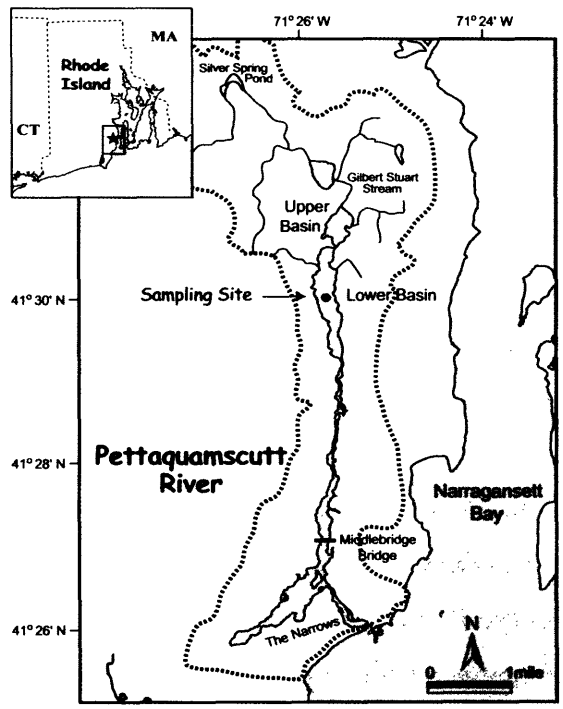


Figure 1. Map showing the site of collection of sediment cores and delineation of the watershed of the Pettaquamscutt River (RI). Modified after Lima et al. (2003).

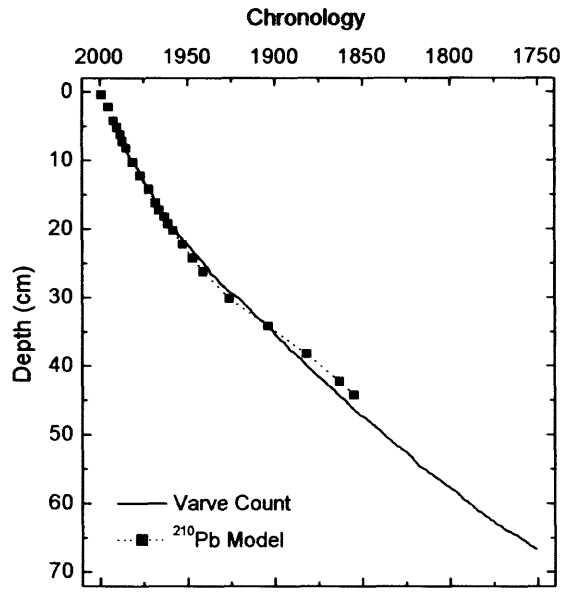


Figure 2. Correlation between the varve counting scale (see Chapter 4) and the $^{210}Pb$ chronology calculated by the CRS Model (Appleby and Oldfield, 1978).

## 2.4 Lead Concentration Analysis

Dilute acid leaches are commonly employed to extract metals from sediment matrices. In the case of Pb, this technique removes only the fraction sorbed onto ferro-manganese oxides, mineral surfaces, and organic debris, leaving behind Pb present in the mineral structure of silicates (Shirahata et al., 1980), which possesses a distinct isotopic composition as determined by HF digestions (Graney et al., 1995). For the Pettaquamscutt River samples, we followed the dilute acid leach procedure described by Graney et al. (1995), which preferentially extracts the exchangeable component of the total Pb. Briefly, dried sediment samples were weighed into 1.5 mL polypropylene vials and 1 mL of 1.75 N HCl - 1 N $HNO_3$ solution was added. The acid-sediment mixtures were homogenized using a vortex mixer, placed in an ultrasonic bath for 90 minutes, and allowed to react overnight to ensure efficient leaching of the samples. Subsequently, the leachates were separated by centrifugation, and an aliquot of each sample was diluted with 5% HCl for Pb concentration measurements. Pb measurements from a previous study on Pettaquamscutt River sediments were used as a baseline for estimating dilutions (Goldberg et al., 1977). Pb content was determined by isotope dilution ICP-MS using a VG Fison Plasmaquad 2+ instrument and the well-characterized Oak Ridge National Laboratory $^{204}Pb$ spike (Wu and Boyle, 1997). Analytical precision for this instrument is reported at better than 2 % (Wu and Boyle, 1997), and replicate analysis of one of the samples (depth = 27 cm) yield a 4 % precision ($2\sigma$, $n$=28). The raw lead data was corrected for background, procedural blank, and $^{204}Hg$ interferences before Pb concentrations were calculated. In general, the procedural blank accounted for less than 0.1% of the Pb concentration of all samples and $^{204}Hg$ for less than 0.8% of the $^{204}Pb$ counts. The resulting total lead concentration in the extract was calculated according to the formula:

$$C_{sample} = \frac{A_{spike}}{A_{natural}} \cdot [C_{spike}] \cdot \frac{V_{spike}}{V_{sample}} \cdot \frac{R_{measured} - R_{spike}}{R_{natural} - R_{measured}} \qquad (1)$$

where $A$ is the abundance of $^{204}Pb$ in the spike ($A_{spike}$) and in nature ($A_{natural}$); $C$ is concentration; $V$ is the volume of the spike ($V_{spike}$) and sample ($V_{sample}$) used in the final dilution; $R$ is the ratio of $^{208}Pb$ to $^{204}Pb$ in the spike ($R_{spike}$), in nature ($R_{natural}$) and measured in the sample ($R_{measured}$).

## 2.5 Lead Isotopic Measurements

Elevated salinity and organic content, such as those present in the Pettaquamscutt River samples (Gaines, 1975), can interfere with the measurement of Pb isotopic ratios. To remove the organic carbon fraction (9 to 10%), between 20 and 150 µl of each HCl-$HNO_3$ leachate was combusted overnight in an acid-cleaned quartz beaker at 450°C. The samples were redissolved in 6N HCl, transferred to a 3 mL Savillex PFTE beaker, reduced to dryness, and redissolved in 1.1 N HBr (Reuer et al., 2003). Pb was separated from the brackish matrix (pore water salinity ~ 27 ‰) using Teflon microcolumns loaded with Eichrom AG-1x8 (chloride form, 200-400 mesh) anion exchange resin (Reuer et al., 2003). Following the column separation with HBr and HCl, the eluted sample lead was dried, redissolved in 0.5N $HNO_3$, and lead isotope ratios were determined on the MIT Micromass IsoProbe multiple collector ICP-MS (MC-ICP-MS). The instrument operating parameters, mass bias corrections, and tailing corrections are provided in Reuer et al. (2003). Briefly, MC-ICP-MS mass discrimination was determined by addition of a lead-free thallium spike to each sample (assuming exponential mass bias), and a secondary correction was calculated by repeated analysis of a 32 nM solution of National Institute of Standards and Technology Standard Reference Material 981 (*Natural Lead*). Two procedural blanks were calculated for each column series ($n$=14), and tailing corrections were determined by daily analysis of the monoisotopic $^{209}Bi$. Most importantly, the uncertainty associated with the MC-ICP-MS isotope ratio analysis is small (250 ppm for $^{206}Pb/^{207}Pb$, $2\sigma$) relative to the isotopic variability observed throughout the Pettaquamscutt River sediment core (73000 ppm for total $^{206}Pb/^{207}Pb$), and this measurement technique provides a consistent and rapid method for stratigraphic analyses.

## 3. RESULTS AND DISCUSSION

Both Pb content and isotopic ratios were evaluated in the Pettaquamscutt River sediments (data is listed in Appendix 2). The record of Pb concentrations shows little evidence of extensive contributions from local sources and excellent agreement with leaded gasoline usage in the US (Figure 3). The evaluation of the Pb isotopic record was divided into 2 periods: pre and post-1920 (Figure 4). The earlier record shows a distinct increase in $^{206}Pb/^{207}Pb$ values with peak in ~1842, which coincides with the highest production of Mississippi Valley ore. In comparison, the post-1920 record follows mostly the consumption of Pb in gasoline, with smaller contributions by combustion of coal.

### 3.1 Lead Concentration

The total leachable Pb record for the Pettaquamscutt River sediments (Figure 3) between 1930 and 1987 correlates ($R^2$=0.64) with the consumption of Pb in gasoline in the United States (Nriagu, 1989). Lead concentrations were constant and low (< 20 μg $g^{-1}$) throughout most of the 18$^{th}$ century. Total leachable lead values began to increase around 1830, reached a maximum in the late 1970s, and decreased continuously in the following decades. To assess the possible sources of Pb input to this system, it is necessary to distinguish the natural contribution from surrounding soils (background) from the anthropogenic fraction on the total Pb leached from the samples. The anthropogenic Pb concentration is obtained by subtracting the leached background lead from the total leachable:

$$[Pb]_{Anthrop} = [Pb]_{Total} - [Pb]_{Background} \quad (2)$$

We assumed that the average Pb concentration in the oldest sediments of the core (58-70cm, 1735-1800, 13.2 ± 1.4 ppm, $n$ = 13) was a reasonable estimate of $[Pb]_{Background}$. It is possible that the bottom layers of the Pettaquamscutt core may not represent the true $[Pb]_{Background}$ as ice layers and peat bogs show that atmospheric deposition of lead to

remote locations dates from Roman times (Hong et al., 1994; Shotyk et al., 1998). Nonetheless, even if the true $[Pb]_{Background}$ were 50% lower than our mean estimate of 13.2 ppm, the calculated $[Pb]_{Anthrop}$ reaching this system after 1800 would change by less than 15%.

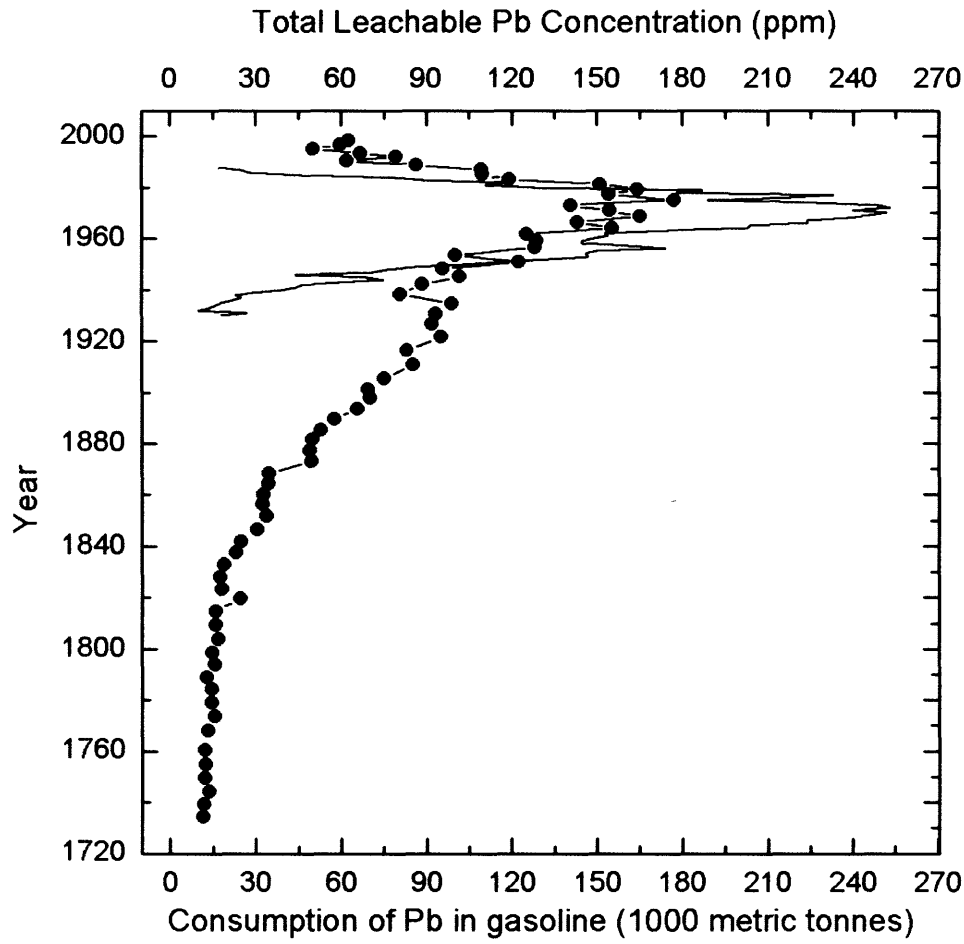


Figure 3. Down-core profile of total leachable Pb concentration (filled circles) in the Pettaquamscutt River, and estimate of consumption of Pb in gasoline (solid line) in the USA (Nriagu, 1989).

To assess the influence of local sources to the Pettaquamscutt River, we evaluated the changes in the flux of Pb to the sediments over time. We combined measured total

leachable Pb content ($\mu g.g^{-1}$) with sediment accumulation rates ($g\ cm^{-2}\ yr^{-1}$) calculated using the CRS model to determine Pb fluxes ($\mu g\ cm^{-2}\ yr^{-1}$), which were also corrected for sediment focusing (Lima et al., 2003). The Pb flux remained largely constant ($0.47 \pm 0.17\ \mu g\ cm^{-2}\ year^{-1}$; $n$ = 23) from 1735 to 1847. During this period, the two economic activities that could have released measurable amounts of Pb to the watershed were shipbuilding and wool spinning and dying. The Saunder's family shipyard was in operation on the west side of the river (Tootell, 1963) between 1813 and 1847, while the Shady Lea Mill, which most likely used lead-based dyes as part of textile manufacturing, operated on the Silver Spring Pond from before 1832 until 1952 (Greenwood, 2002) (Fig. 1). The constancy in Pb flux to sediments deposited prior to 1847 supports the interpretation that direct local sources played a small role in the delivery of Pb to the Pettaquamscutt River. However, between 1852 and 1916 the Pb flux slowly increased (rate=0.02 $\mu g\ cm^{-2}\ year^{-2}$, $n$= 16, $r^2$=0.68), probably associated with increasing US lead ore production (USGS, 1998) and coal utilization (EIA, 1999). The increase in Pb at the turn of the 20$^{th}$ century was followed by another distinct change in the flux rate that culminated in the 1975 maximum. In fifty years (1922 - 1975), the flux of Pb increased 4-fold (rate=0.10 $\mu g\ cm^{-2}\ year^{-2}$, $n$=19, $r^2$=0.91) due to the consumption of leaded gasoline by automobiles. Tetraethyl lead (TEL) was first added to commercial gasoline in 1923 to suppress pre-ignition and to improve its octane rating (Nriagu, 1989). By 1950, most gasoline in the USA contained TEL (Rhue et al., 1992) and consumption continued to increase until a peak was reached in the 1970's (Fig. 3). Studies estimate that between 50 and 75% of all the Pb added to gasoline was subsequently emitted into the atmosphere in the form of fine particles (Facchetti, 1989; Wu and Boyle, 1997; Cadle et al., 1999). The introduction of cars equipped with catalytic converters, which could not use leaded gasoline (TEL poisons the catalyst), and a better understanding of the risks of Pb exposure, initiated the phase-out of leaded gasoline in the mid-1970s. The 3.5-fold decline in Pb flux seen in our record after 1975 can be directly attributed to the reduction in TEL usage in the USA, which in the 1990s had declined to less than 10% of its peak value (Wu and Boyle, 1997).

### 3.2 Lead Isotopic Record

Stable lead isotopic ratios are invaluable tools in distinguishing anthropogenic Pb sources to the environment (Chow et al., 1975). The natural abundance of $^{208}Pb$, $^{206}Pb$ and $^{207}Pb$ are determined by the decay rate of their parents ($^{232}Th$ half life = 13.9 b.y., $^{238}U$ = 4.5 b.y. and $^{235}U$ = 0.7 m.y., respectively), while the non-radiogenic $^{204}Pb$ is found in fixed quantities and is usually used as a reference isotope (Brown, 1962; Faure, 1986). When a lead ore or a coal deposit is formed, the daughter Pb is removed from the parent isotopes and its isotopic composition remains unaltered in time. As a result, lead ores and coals formed at different geological times exhibit contrasting isotopic compositions that can be used to apportion anthropogenic sources. Lead present in crustal material (dust, soil) continues to change isotopic composition over time due to the parent radionuclides still being present and usually shows a more radiogenic signature than Pb ores (Faure, 1986; Chiaradia and Cupelin, 2000). Therefore, the Pb isotopic composition of a sample reflects the concentration of U and Th and the age and geological history of the source material (Brown, 1962). Because of the small fractional mass differences between the isotopes of lead, fractionation during environmental and industrial processes is minimal relative to primary differences in isotopic composition of the sources (Doe, 1970), hence emissions can be traced back to their sources.

Several temporal trends can be distinguished from the isotopic composition of Pb in sediments of the Pettaquamscutt River (Figure 4a). In general, the total leachable $^{206}Pb/^{207}Pb$ ratio remained constant from 1735 to 1815 (1.211±0.001), whereas an isotopic transition began from 1815 to 1820. The total leachable $^{206}Pb/^{207}Pb$ increased toward a maximum in ~1842 ($^{206}Pb/^{207}Pb$=1.263) according to our chronology, after which the ratio decreased towards less radiogenic values. The 30-year interval between the appearance of the more radiogenic $^{206}Pb/^{207}Pb$ ratios (~1815), the well-defined apex (~1842), and the 50-year gradual evolution towards less radiogenic values indicates that the source of this peak may have been short lived. The third major trend observed in this profile is a steady decrease in the $^{206}Pb/^{207}Pb$ ratio from 1922 to 1964. This decrease can be attributed to the introduction and widespread utilization of TEL in gasoline, which had

a non-radiogenic signature during this period. The trend towards lower $^{206}Pb/^{207}Pb$ ratios reversed in the late 1960s and by 1983 the Pb isotopic composition of the Pettaquamscutt sediments was more radiogenic than in the previous 80 years. Elevated total leachable $^{206}Pb/^{207}Pb$ persisted until the late 1980s when values reached a plateau with a subtle downward trend.

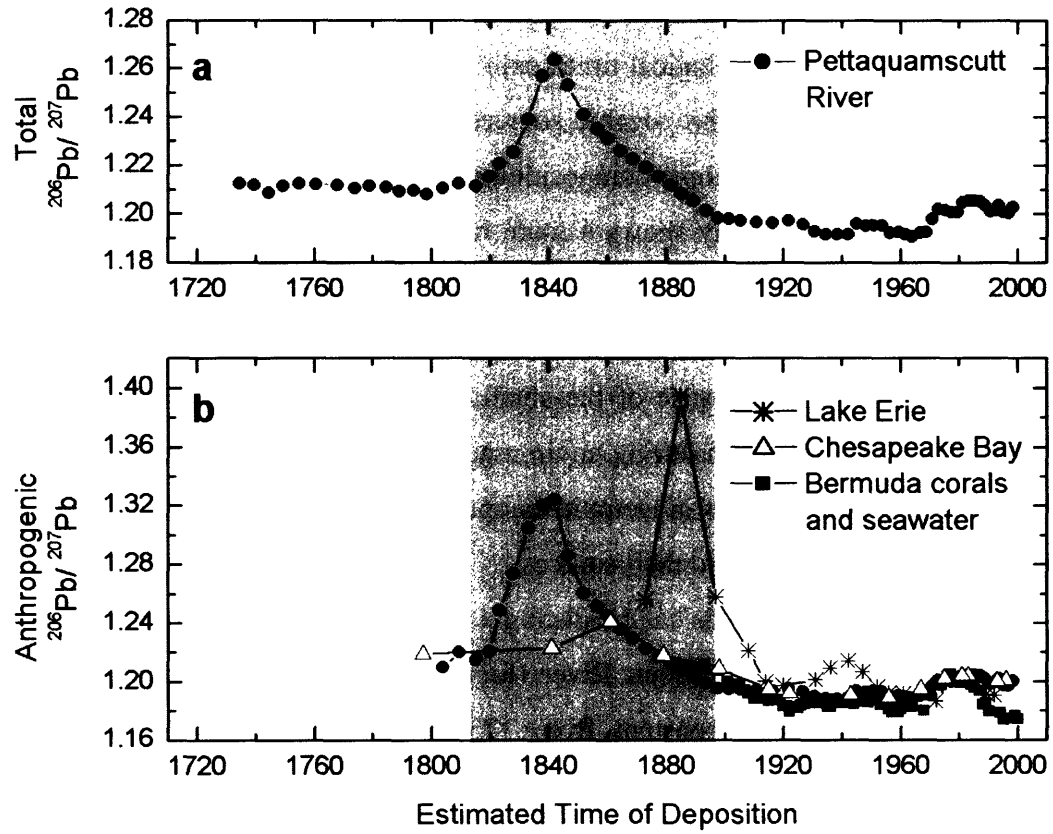


Figure 4. Down-core profiles of (a) total leachable $^{206}Pb/^{207}Pb$ in the Pettaquamscutt River (filled circles); (b) anthropogenic $^{206}Pb/^{207}Pb$ in the Pettaquamscutt River, Chesapeake Bay (open triangles) (Marcantonio et al., 2002), Lake Erie (stars) (Graney et al., 1995), and Bermuda corals and seawater (filled squares) (Véron et al., 1994; Hamelin et al., 1997; Reuer et al., 2003).

As with Pb concentration, the isotopic composition of sediment leachates is a mixture of anthropogenic and natural lead (not present in the mineral lattice), and these components must be differentiated to constrain anthropogenic sources. The isotopic ratios of anthropogenic lead are calculated using the mixing equations proposed by Shirahata (1980):

$$R_{Anthrop} = \frac{(R_{Total} \times [C_{Total}]) - (R_{Background} \times [C_{Background}])}{[C_{Total}] - [C_{Background}]} \quad (3)$$

where $R$ and $C$ denote the isotopic ratio and concentration of total leachable, background, and anthropogenic lead. We assumed that the average Pb isotopic composition in the oldest sediments of the core (58-70cm, 1735-1800, $^{206}Pb/^{207}Pb$ = 1.211 ± 0.001) was representative of the background natural Pb component, $R_{Background}$. Equation 3 shows the dependency of the anthropogenic isotopic ratio of Pb on concentration measurements. This is particularly critical when the total leachable and the background Pb are close in value. Sensitivity tests show that if the $[Pb]_{Background}$ were 50% higher or lower than our 13.2 ppm estimate, the $^{206}Pb/^{207}Pb$ isotopic composition of the anthropogenic Pb would change by only 0.001. An additional line of support for the validity of the assumed $R_{Background}$ is that between 1735 and 1800 the average total $^{206}Pb/^{207}Pb$ remained constant at 1.211 ± 0.001 ($n$ = 13), a value that lies within the range accepted for upper continental crust (Othman et al., 1989). Therefore, the average isotopic composition of sediments deposited prior to 1800 is a reasonable estimate of $[Pb]_{Background}$. It is noteworthy that the anthropogenic $^{206}Pb/^{207}Pb$ profile in the Pettaquamscutt River sediments closely resembles the total $^{206}Pb/^{207}Pb$ (Figures 4a and 4b), confirming that the majority of the Pb present in this system was released by human activities. Appendix 2 lists values for $[Pb]_{Total}$ and $[Pb]_{Anthrop}$ for each sediment layer analyzed.

### *3.2.1 Constraints on the Sources of Pb Prior to 1920*

The large increase in $^{206}Pb/^{207}Pb$ ratio that occurred after 1800 (Figure 4a) is not unique to the Pettaquamscutt River. When the anthropogenic component of the Pb present in Lake Erie (Graney et al., 1995) and the Chesapeake Bay (Marcantonio et al.,

2002) are plotted against time of deposition, a peak in radiogenic $^{206}Pb/^{207}Pb$ is evident (Figure 4b). Graney et al. (1995) also observed a high $^{206}Pb/^{207}Pb$ maximum of 1.34 at approximately 1863 in Lake Michigan and a $^{206}Pb/^{207}Pb$ peak of 1.65 at ~1895 in Lake Ontario, but these peaks are not as well defined as the maximum in Lake Erie. The timing of the radiogenic $^{206}Pb/^{207}Pb$ peak does not coincide amongst all sites and is discussed later in the paper.

The fact that unusually elevated $^{206}Pb/^{207}Pb$ values are observed in five separate locations suggests a common source. It is widely accepted that atmospheric transport is the dominant pathway of anthropogenic Pb to the environment (Schaule and Patterson, 1981; Sturges and Barrie, 1989). The mean residence time of Pb rich aerosols in the atmosphere is about 10 days (Settle and Patterson, 1991), sufficient for Pb to be distributed over long distances by prevailing winds (Sturges and Barrie, 1989). The identification of lead derived from mining and smelting operations in distal repositories is quite common. For example, Rosman et al (1997) observed diminished $^{206}Pb/^{207}Pb$ ratio between 600 B.C. and 300 A.D. in Greenland Ice, suggesting the isotopic reduction resulted from contemporaneous Spanish mining operations. It is therefore possible that atmospheric dispersion mechanisms are responsible for the appearance of the mid-1800s maximum in radiogenic $^{206}Pb/^{207}Pb$ throughout the Northeastern USA.

The Mississippi Valley includes the oldest and most productive lead mines in the US history (Ingalls, 1908). The vast majority of the lead produced in the USA from 1830 to 1870 came from the Upper Mississippi Valley zinc-lead district, with a peak in production around 1845 (Figure 5a) (Ingalls, 1908; Heyl et al., 1959; USGS, 1998). Because ores were abundant in the 19$^{th}$ century, the large amounts of Pb dust emitted due to poor furnace design and smelting procedures were not a concern. It is estimated that 2% of the lead ores smelted between 1750 and 1880 were emitted into the atmosphere as aerosol fumes (Murozumi et al., 1969), and the development of tall stacks during this period expanded the range of the impact of lead emissions (Nriagu, 1998). The release of lead fumes to higher altitudes could have favored the transport of fine, lead-rich particles (Pacyna, 1987) over long distances by prevailing winds. Determining specific back-

trajectories for events that happened over 100 years ago is both difficult and beyond the scope of this study. However, a 50-year composite mean of vector wind generated for the United States through the NOAA-CIRES Climate Diagnostic Center webpage (www.cdc.noaa.gov/cgi-bin/Composites) (Figure 6) shows the Pettaquamscutt River is located downwind from the Great Lakes, which are in turn downwind from the Upper Mississippi Valley mining region. This transport pattern is in good agreement with recent

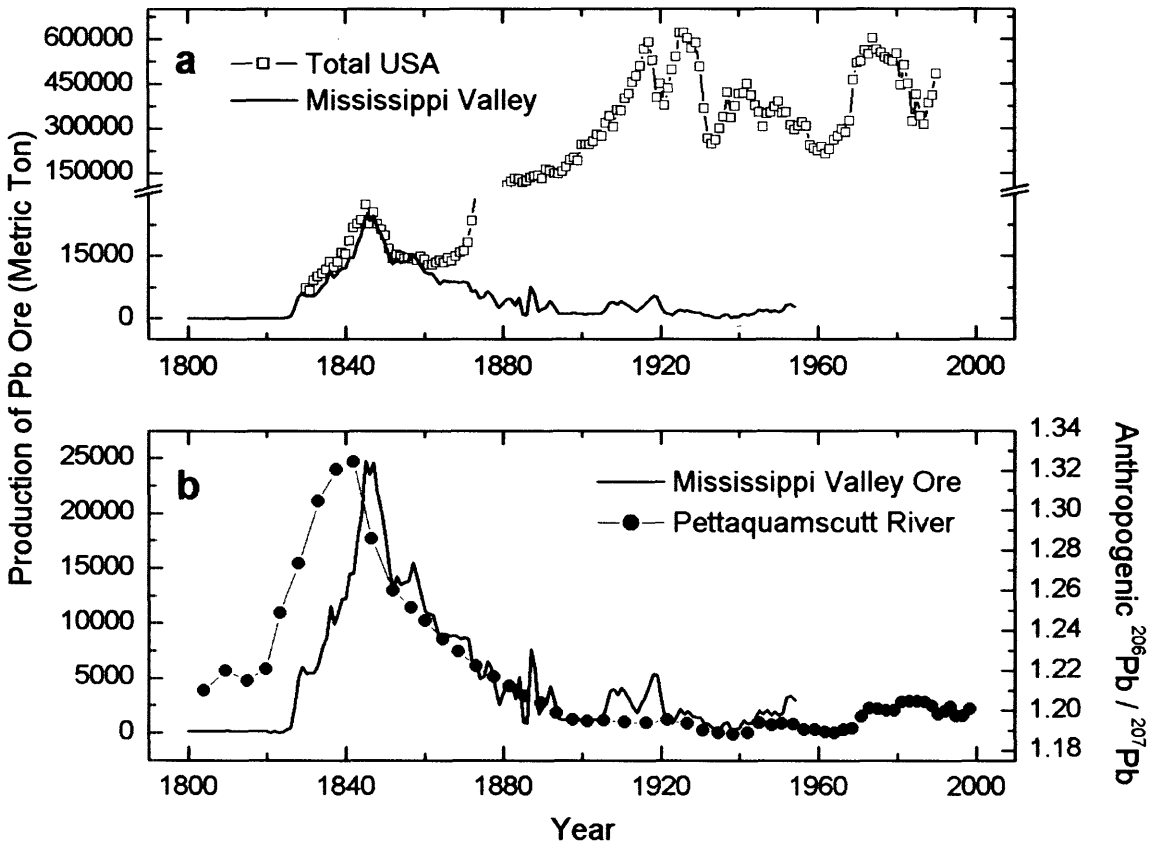


Figure 5. (a) The Mississippi Valley region was the main producer of Pb ore (solid line) in the USA from 1830 to 1870 (Heyl et al., 1959; USGS, 1998); (b) the profile of anthropogenic $^{206}Pb/^{207}Pb$ in the Pettaquamscutt River prior to 1900 correlates well with the production of Mississippi Valley ore.

back-trajectory analysis showing polycyclic aromatic hydrocarbons were transported to Massachussetts by air masses that originated in the Great Lakes region (Golomb et al., 2001). Therefore, it is not surprising that the anthropogenic fraction of the $^{206}Pb/^{207}Pb$ in the Pettaquamscutt River prior to 1900 correlates well with the production of Upper Mississippi Valley ore (Figure 5b). The Chesapeake Bay, however, could have received larger amounts of Pb from the Tri-State and SE Missouri mining regions than from the Upper Mississippi Valley, but production in these districts began after 1848 and 1864, respectively (Brockie et al., 1970; Snyder and Gerdemann, 1970) and did not reach maximum production until the 1900s. Hence, we conclude that the small broad peak in anthropogenic $^{206}Pb/^{207}Pb$ observed in the Chesapeake sediments (Figure 4b) is most likely derived from Upper Mississippi Valley ore particles that reached mid-Atlantic states.

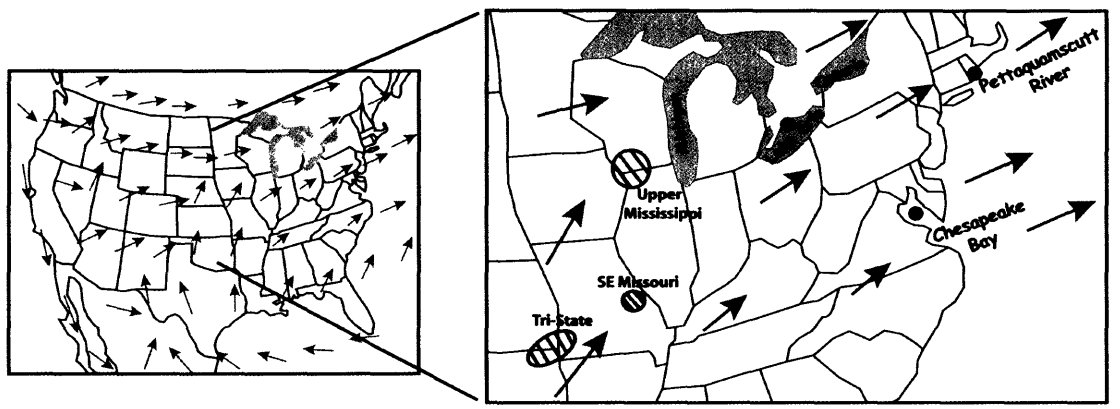


Figure 6. Vector wind composite mean from January to December (1948 to 1998) calculated using the NCEP/NCAR Reanalysis program (see www.cdc.noaa.gov/cgi-bin/Composites/printpage.pl) shows that the Pettaquamscutt River is located downwind from Lake Erie, while the Chesapeake Bay receives a higher contribution of winds from the southwest. Location of Tri-State, SE Missouri and Upper Mississippi mining districts were based on Brockie et al. (1970), Snyder et al. (1970), and Heyl (1970), respectively.

Another potential source of Pb to the atmosphere in the 1800s was coal. The first records of coal used as an energy source in the United States is noted in 1850 (EIA, 2001). Coal contains measurable quantities of Pb and carries distinct isotopic signatures from lead ores, and were therefore considered in the source analysis for the ~1842 peak. $^{206}Pb/^{207}Pb$ values for several coal deposits and Pb ores mined in the United States were gathered from the literature (Figure 7). Any data point whose $^{206}Pb/^{207}Pb$ and $^{208}Pb/^{207}Pb$ ratios were higher than the most radiogenic value encountered in the Chesapeake Bay, Pettaquamscutt River, or Lake Erie sediments was selected as a possible candidate. Assuming the same origin for the anthropogenic $^{206}Pb/^{207}Pb$ peak in all three systems, Upper Mississippi Valley ores are the most probable source. All coals included in the analysis, even those from the Mississippi Valley region (Chow and Earl, 1972), were not radiogenic enough to produce the ~1842 Pb peak. The individual peaks in radiogenic Pb observed in Lake Michigan and Lake Ontario (Graney et al., 1995) are not as well defined as the peak in Lake Erie and were not considered in this analysis.

The relative importance of the Upper Mississippi Valley region and coal combustion as sources of lead to the Pettaquamscutt River in the 19$^{th}$ century can be addressed by means of a ternary mixing model. The following equations were used to calculate the mixing lines shown in Figure 8:

$$R_{Mix} = \frac{(R_1 * C_1 * X_1) + (R_2 * C_2 * X_2)}{C_{Mix}} \tag{4}$$

$$C_{Mix} = (C_1 * X_1) + (C_2 * X_2) \tag{5}$$

$$X_1 + X_2 = 1 \tag{6}$$

where $R_1$, $R_2$ and $R_{mix}$ are respectively the $^{206}Pb/^{207}Pb$ isotopic ratio of end-member 1, end-member 2 and of the mixture of 1 and 2, $C$ is concentration and $X$ is the fractional contribution of each end-member in 10% increments. To calculate proportions we assumed Pennsylvania coal (Chow and Earl, 1972) was representative of the coals combusted in the 1800s. Even though several types of coal may have been combusted

simultaneously, Pennsylvania was the largest producer of US coal at that time (EIA, 2003). The gradual increase in Pb input from smelting of Upper Mississippi Valley ore and subsequent predominance of coal combustion is shown in Figure 8.

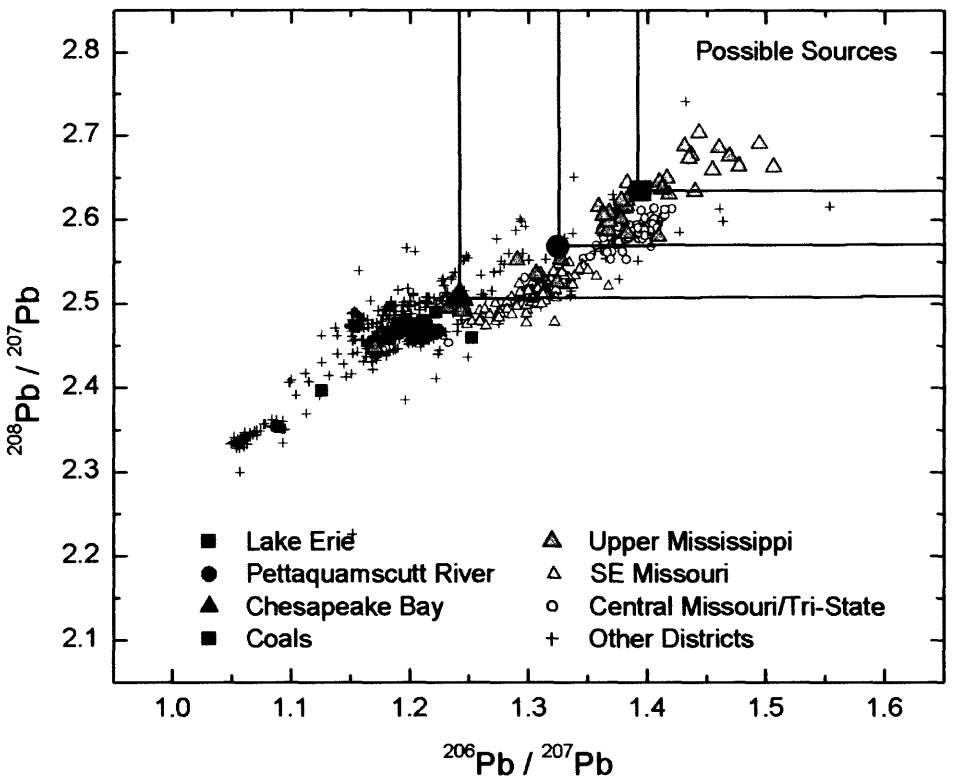


Figure 7. Isotopic composition of different coals (Chow and Earl, 1972) and Pb-producing regions in the USA (Russell and Farquhar, 1960; Cannon et al., 1962; Brown, 1965; Heyl et al., 1966; Brown, 1967; Zartman and Stacey, 1971; Fletcher and Farquhar, 1982; Deloule et al., 1986; Ayuso and Foley, 1987; Thompson and Beaty, 1990; Wilber et al., 1990; Sanford, 1992; Goldhaber et al., 1995; Millen et al., 1995; Leach et al., 1998; Bouse et al., 1999; St. Marie and Kesler, 2000). The areas defined by the highest values obtained for the Chesapeake Bay (closed triangle) (Marcantonio et al., 2002), Pettaquamscutt River (closed circle) and Lake Erie sediments (Graney et al., 1995) (closed squares) delimit the possible sources of the ~1842 maximum to these locations.

Prior to 1815, soil dust delivered over 90% of Pb contributions to the Pettaquamscutt River, but by 1833 this contribution had decreased to 71% and smelting of Pb ores was responsible for over 20%. In 1842, smelting emissions were responsible for 48% of the Pb reaching Rhode Island. The decline in Pb contributions from smelting of ore was accompanied by the rise in coal combustion. At the turn of the 20$^{th}$ century, contribution from smelting had decreased to 5% and coal was responsible for 65% of the Pb input. Before the introduction of leaded gasoline in 1923, most of the Pb reaching the Pettaquamscutt watershed derived from coal combustion (80%), with soil dust contributing most of the remaining portion.

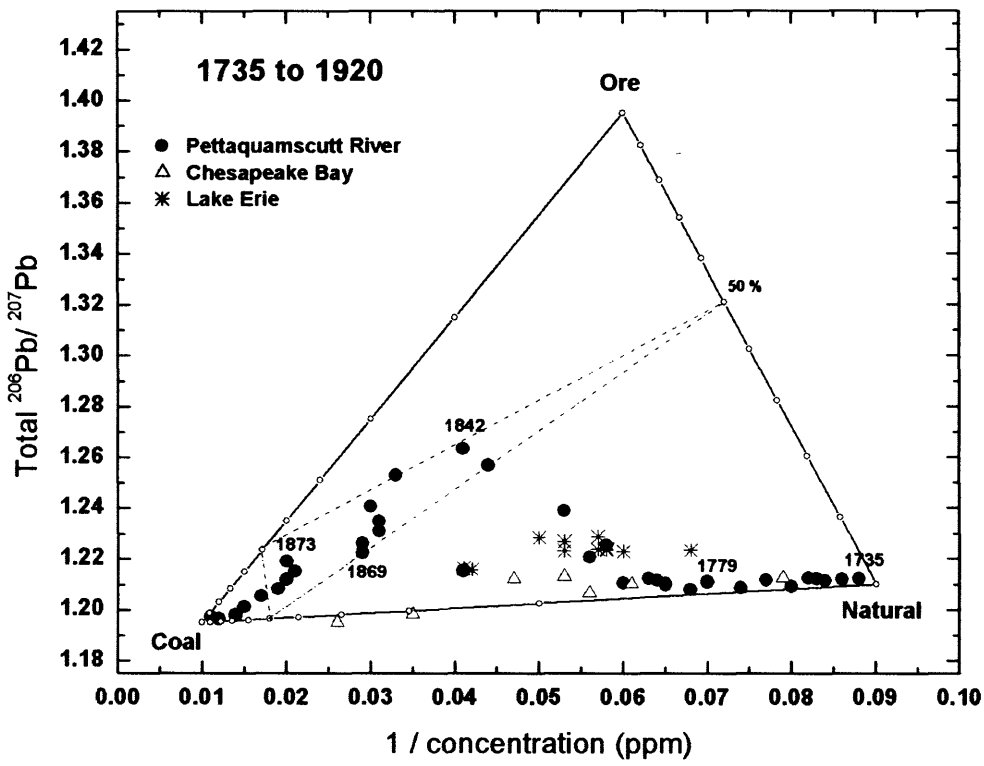


Figure 8. Application of ternary mixing model for Pettaquamscutt River (closed circles), Lake Erie (stars) (Graney et al., 1995) and Chesapeake Bay data (open triangles) (Marcantonio et al., 2002) comprising 1735 to 1920. Marks on mixing lines correspond to 10% increments and dashed lines correspond to 50% mixing.

The end-members chosen for Figure 8 are capable of explaining the trend in isotopic composition observed at Lake Erie and, to a lesser degree, the Chesapeake Bay. Pb isotopic composition changes in Lake Erie sediments have been attributed to inputs from coal combustion and smelting operations in the region (Ritson et al., 1994) and Figure 8 is successful in representing possible end-members. The good correlation between Pb sources to the Pettaquamscutt River and Lake Erie attests to the validity of the atmospheric pathways shown in Figure 6. The mixing diagram on Figure 8 also agrees with the suggestion of Marcantonio (2002) that Pb present in sediments deposited prior to 1923 in the Chesapeake Bay was predominantly derived from a mixture of coal combustion and natural background. However, the isotopic composition of coals (Figure 7) cannot explain the small rise in total $^{206}Pb/^{207}Pb$ observed in ~1861 (Figure 4b), which, we believe, resulted from small contributions of Pb from the Upper Mississippi Valley mining district.

There is compelling evidence that Upper Mississippi Valley ore processing was responsible for the Pb isotopic maximum observed in the mid-1800s in the Pettaquamscutt River, Lake Erie and Chesapeake Bay, although the timing of occurrence at these locations seems different. In this study, the $^{210}Pb$ chronology generated for the laminated anoxic sediments is in excellent agreement with the varve count time scale (Figure 2, Chapter 4). The resulting model age yields a historical record of anthropogenic $^{206}Pb/^{207}Pb$ that mirrors the production of Upper Mississippi Valley ore (Figure 5b), asserting the fidelity of the Pettaquamscutt chronology. In addition, the down-core profile of total leachable Pb concentration correlates extremely well with estimates of consumption of lead in gasoline in the USA (Figure 3). We believe that the Pb isotope peaks in the Great Lake cores and the Pettaquamscutt River sediments all occur at ~1845 and that the seeming disagreement in timing is due to the uncertainty of the $^{210}Pb$ time scales. While the appearance of the $^{206}Pb/^{207}Pb$ maxima in the laminated sediments of the Chesapeake Bay is in moderate agreement with the Upper Mississippi Valley production record, part of the discordance between the time of occurrence of the former and the radiogenic $^{206}Pb/^{207}Pb$ peak in the Great Lakes could be due to the dynamic nature of

these sediments. For example, the region sampled by Graney and collaborators in Lake Erie (East Basin) is heavily influenced by the erosion of shoreline bluffs, which comprise 58% of the natural particulate flux to the lake (Ritson et al., 1994). The difference in timing of the peaks in the different cores highlight the difficulty in obtaining accurate ages estimates in the mid-1800s. Having a chronological marker, such as the peak in $^{206}Pb/^{207}Pb$ would greatly improve correlations amongst cores in the Northeastern US.

*3.2.2 Constraints on the sources of Pb after 1920*

The isotopic composition of the most recent portion of the Pettaquamscutt River sediment record is unlikely to be explained by mixing of natural sources, ore smelting and coal combustion, as was the case for the period between 1735 and 1920. The $^{206}Pb/^{207}Pb$ ratio of lead aerosols decreased from ~1.22 in 1900 to ~1.15 in 1965 in the United States (Lambert et al., 1991), at which point it was strongly influenced by the isotopic composition of lead ores used in gasoline (Chow et al., 1975). Motor vehicle exhaust became an indisputable source of Pb emissions after the introduction of TEL as an anti-knock agent in gasoline in 1923. However, the isotopic composition of TEL varied over time (Hurst, 2002) and the use of a constant value on a mixing diagram would be unreasonable. The anthropogenic lead archaeostratigraphy (ALAS) calibration curve (Hurst, 2002) could potentially be used as a way to estimate the changes in isotopic fingerprint of gasoline additives and separate it from contributions from other sources of Pb. The ALAS method assumes that the major lead additive producers combined Pb ores in making lead alkyls, and thus the average stable isotopic composition of leaded gasoline was uniform on a given year. Figure 9 illustrates the time variation in $^{206}Pb/^{207}Pb$ ratio in leaded-gasoline according to the ALAS model. The Pb isotopic composition of TEL was relatively constant between 1923 and 1965 ($1.165 \pm 0.009$), but started increasing rapidly from the late 1960s to the late 1980s due to the introduction of southeast Missouri Pb ores in the mixture. The high-resolution sampling of the Pettaquamscutt River core is exceptional at recording the rapid temporal increase in $^{206}Pb/^{207}Pb$ ratios post-1970. The sharp increase in anthropogenic ratios observed in both records after 1968 clearly reflects

the introduction of southeast Missouri type Pb into gasoline additives (Figure 8), a phenomena first observed in soils and aerosols of California (Chow et al., 1975; Shirahata et al., 1980).

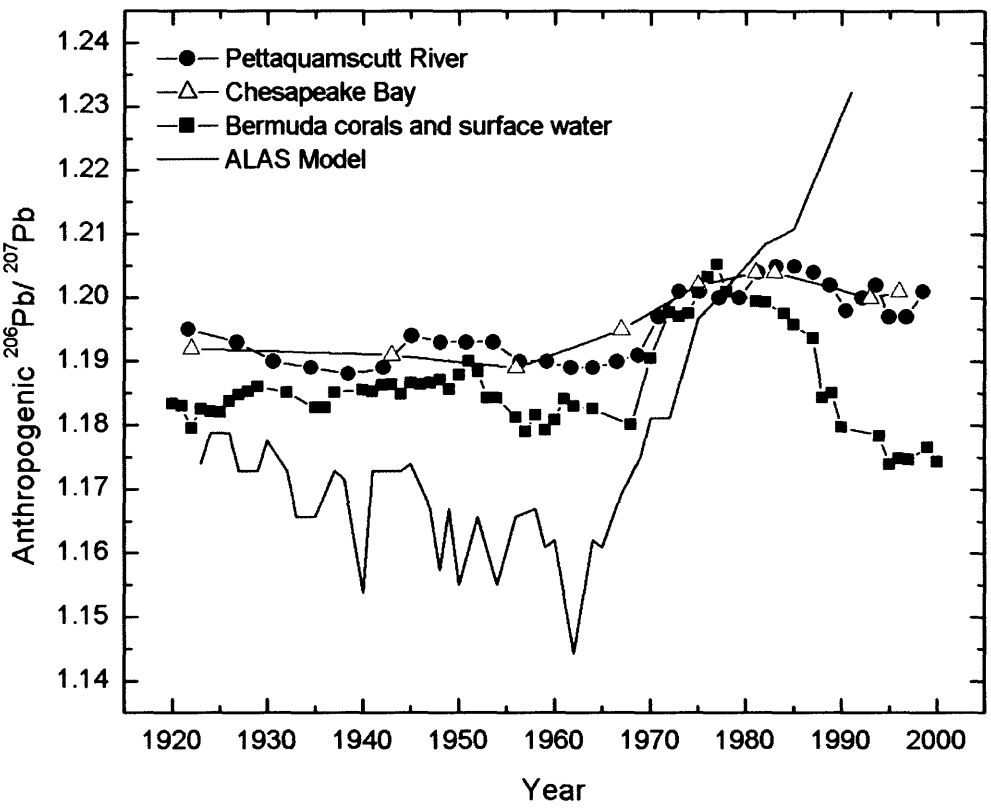


Figure 9. Anthropogenic $^{206}Pb/^{207}Pb$ profile for the Pettaquamscutt River (closed circles), Chesapeake Bay (open triangles) (Marcantonio et al., 2002) and Bermuda corals and surface water (closed squares) (Véron et al., 1994; Hamelin et al., 1997; Reuer et al., 2003). The solid line represents annual average $^{206}Pb/^{207}Pb$ values for industrial US emissions according to the ALAS model (Hurst, 2002).

The systematic variation in isotopic composition of gasoline additives described by the ALAS model can be observed in sediments of the Pettaquamscutt River, Chesapeake Bay, and in corals from Bermuda (Figure 9). However, there is not complete agreement between the records and ALAS. There is growing evidence that the isotopic

values of TEL were not uniform throughout the country (Kaplan, 2003) and, therefore, the ratios reported in the model may not reflect the actual leaded gasoline input signature to all locations. For example, in our record the difference in $^{206}Pb/^{207}Pb$ ratios between the Pettaquamscutt River sediments and the ALAS model suggests the presence of another important supply of Pb. Another logical source of anthropogenic Pb in the 20th century is the combustion of coal, which has remained a major energy resource since its introduction in the mid-1800s (EIA, 2000) and was considered the second largest source of Pb emissions in 1968 (Chow and Earl, 1972). If we assume that TEL and coal emissions constituted the most significant portion of the Pb input to Rhode Island until 1970, the fractional contribution of each source can be quantified by means of the following mixing equations (Gobeil et al., 1995; Weiss et al., 1999):

$$R_{Anthrop} = (R_{gas} * X_{gas}) + (R_{coal} * X_{coal}) \quad (7)$$

$$X_{gas} + X_{coal} = 1 \quad (8)$$

where $R$ is the isotopic ratio for the coal source ($R_{coal}$), the anthropogenic component measured in the sample ($R_{Anthrop}$), and for leaded-gasoline ($R_{gas}$) as given by the ALAS model; and $X$ is the fractional contribution of each source. To use the above mixing equations, we calculated the most likely coal isotopic signature ($R_{coal}$) for each horizon between 1924 and 1970 taking into account the percent contribution of major coal-producing states (EIA, 2003) and $^{206}Pb/^{207}Pb$ ratios published in the literature (Chow and Earl, 1972). Until 1970, practically all of the coal production in the US came from east of the Mississippi (EIA, 2001), with Pennsylvania, West Virginia, Kentucky and Illinois sharing the primary role. The Pb isotopic composition of coals is known to vary from 1.183 (Illinois) to 1.252 (Kentucky), but when the percent contribution from each state is considered (from EIA, 2003) values for coal emissions only vary between 1.202 (1920s) and 1.207 (1970s). If we use this calculated isotopic composition of coal emissions and $R_{gas}$ values from the ALAS model in equations 7 and 8, the result is coal combustion contributing more to the Pb isotopic composition of the Pettaquamscutt River sediments (61.7 ± 8.7% between 1927 and 1969) than Pb from automotive sources. This result contrasts sharply with the notion that leaded gasoline combustion was an overwhelming

source of atmospheric lead aerosols during that period, with coal burning responsible for the second largest emissions (Murozumi et al., 1969; Chow and Earl, 1972; Chow et al., 1975; Nriagu, 1989). In order to reconcile these different scenarios for anthropogenic Pb inputs to the Pettaquamscutt River between the 1920s and the 1970s, the $^{206}Pb/^{207}Pb$ values used in the ALAS model would have to be higher. The same reasoning can be extended to the discrepancy between $^{206}Pb/^{207}Pb$ ratios in US aerosols and the ALAS curve (Hurst, 2003). While the ALAS model is a valuable technique to age-date gasoline spills, it does not seem to function as a reliable end-member to apportion the contribution of leaded gasoline to environmental samples.

Lead isotope ratios have varied significantly since the elimination of alkyl lead from gasoline in the United States (Bollhöfer and Rosman, 2002). The introduction of unleaded gasoline and the enforcement of stricter emission regulations brought about by the Clean Air Act of 1970 generated a decrease in emission of particles and consequent lowering of atmospheric Pb concentrations. As a result, the relative influence of pollutant sources other than the previously overwhelming leaded gasoline increased (Bollhöfer and Rosman, 2002). This change in relative proportions makes it challenging to identify sources and produces greater isotopic unevenness of the signal. The variability existent after 1980 is well illustrated in Figure 9, which shows a good agreement between the anthropogenic $^{206}Pb/^{207}Pb$ profiles of the Pettaquamscutt River and the Chesapeake Bay, but a difference between those and the Bermuda coral record. The isotopic signature of the two continental sites remained invariant from 1982 (1.204) to 1996 (1.201), indicating that industrial sources emitted Pb with a homogeneous signature. The Bermuda corals, on the other hand, show a significant shift in $^{206}Pb/^{207}Pb$ values (1.199 in 1982 to 1.175 in 1996) that may be explained by less radiogenic Pb transported from Europe and/or Africa. Although the island of Bermuda acts as a local source of lead (Shen and Boyle, 1988), the bulk of the contamination observed in the coral sampling site derives from seasonal long-range transport. Over the winter, predominantly North American air masses reach Bermuda, while in the summer and early fall western Mediterranean/African easterlies dominate (Wolff et al., 1986; Véron et al., 1994; Huang

et al., 1996). Prior to the phase-out of leaded gasoline in the USA in the early 1970s, atmospheric Pb concentrations in Bermuda air in the winter were significantly higher than in the summer (5.5 ng $m^{-3}$ and 2.5 ng $m^{-3}$, respectively for 1982-1983) (Wolff et al., 1986), suggesting a link between aerosol concentrations and Pb pollution in North America. Since the drastic decrease of vehicle Pb emissions in the USA, Pb concentrations in Bermuda decreased by an order of magnitude (Huang et al., 1996), and the stable lead isotopic composition of rainwater also changed dramatically. Rainwater samples collected from 1989 to 1990 reflected the less radiogenic isotopic signature (average $^{206}Pb/^{207}Pb = 1.140 \pm 0.028$) of western European industrial lead emissions (Véron et al., 1998), instead of the more radiogenic Mississippi Valley type ores used in the USA. On the whole, the relative importance of inputs by the easterly trade winds to surface waters of the Sargasso Sea seem to have increased from less than 10% in the early 1980s to approximately 50% in the early 1990s (Véron et al., 1998). This change in sources can also be seen in the evolution of $^{206}Pb/^{207}Pb$ profiles at the JGOFS BATS (Joint Global Ocean Flux Study Bermuda Atlantic Time Series) station (Shen and Boyle, 1988; Véron et al., 1993; Véron et al., 1998).

## 4. CONCLUSIONS

A high-resolution record of Pb contamination in the Pettaquamscutt River showed an unusual peak in $^{206}Pb/^{207}Pb$ ratios in sediments deposited in the mid-1800s. Similar radiogenic signals observed for sediments from the Chesapeake Bay and Lake Erie were evaluated for possible sources. Mining and smelting of Pb ores in the Upper Mississippi Valley district dominated the US production during that period, and were most likely responsible for the observed signals. The $^{206}Pb/^{207}Pb$ peak provides three stratigraphic tie points for an age model - onset (~1815), maximum (~1842), and termination (~1898) - and the timing of this event is such that it could become an important marker for sediments deposited in the last 100 to 200 years in the Northeastern US. Also, the Bermuda coral record indicates that the influence of Pb production in the Upper

Mississippi Valley district could potentially have reached the western North Atlantic Ocean (Fig. 4b) (Véron et al., 1994; Hamelin et al., 1997; Reuer et al., 2003). The coral record is not of adequate length to include to the ~1842 radiogenic $^{206}Pb/^{207}Pb$ peak, but the profile of Pb isotopic composition prior to 1900 follows closely the trend observed for the Pettaquamscutt River. The good agreement between these two records could indicate that corals within the North Atlantic subtropical gyre were also affected by Pb contributions from mining in midwest North America, thus extending the estimated range of this anthropogenic source. In addition, the Pb isotopic composition of the Pettaquamscutt River provides a classic example of how the change in mixtures of ores in the production of TEL caused a regional-scale shift in $^{206}Pb/^{207}Pb$ in the sedimentary record, and suggests that coal could have played a significant role in Pb emissions post-1920.

## 5. REFERENCES


Anderson R., Bopp R., Buesseler K., and Biscaye P. (1988) Mixing of particles and organic constituents in sediments from the contiunental shelf and slope off Cape Cod: SEEP-I results. *Cont. Shelf Res.* **8**(5-7), 925-946.

Appleby P. and Oldfield F. (1978) The calculation of lead-210 dates assuming a constant rate of supply of unsupported $^{210}Pb$ to the sediment. *Catena* **5**, 1-8.

Ayuso R. A. and Foley N. K. (1987) Source of lead and mineralizing brines for Rossie-type Pb-Zn veins in the Frontenac Axis area, New York. *Econ. Geol.* **82**, 489-496.

Bollhöfer A. and Rosman K. (2002) The temporal stability in lead isotopic signatures at selected sites in the Southern and Northern hemispheres. *Geochim. Cosmochim. Acta* **66**(8), 1375-1386.

Bouse R. M., Ruiz J., Titley S. R., Tosdal R. M., and Wooden J. L. (1999) Lead isotope compositions of Late Cretaceous and Early Tertiary igneous rocks and sulfide minerals in Arizona: Implications for the sources of plutons and metals in porphyry copper deposits. *Econ. Geol.* **94**, 211-244.

Brockie D., Hare E., Jr., and Dingess P. (1970) The geology and ore deposits of the Tri-State district of Missouri, Kansas, and Oklahoma. In *Ore Depositis of the United States, 1933-1967*, Vol. I (ed. J. Ridge). The American Institute of Mining, Metallurgical, and Petroleum Engineers, Inc., New York.

Brown J. (1962) Ore leads and isotopes. *Econ. Geol.* **57**(5), 673-720.

Brown J. S. (1965) Oceanic lead isotopes and ore genesis. *Econ. Geol.* **60**, 47-68.

Brown J. S. (1967) Isotopic zoning of lead and sulfur in southeast Missouri. *Econ. Geol. Monograph* **3**, 410-426.

Bruland K., Koide M., Bowser C., Maher L., and Goldberg E. (1975) Lead-210 and pollen geochronologies on Lake Superior sediments. *Quat. Res.* **5**, 89-98.

Cadle S. H., Mulawa P. A., Hunsager E. C., Nelson K., Ragazzi R. A., Gallagher G. L., Lawson D. R., Knapp K. T., and Snow R. (1999) Composition of light-duty motor vehicle exhaust particulate matter in the Denver, Colorado area. *Environ. Sci. Technol.* **33**, 2328-2339.

Cannon R. S., Jr., Pierce A. P., Antweiler J. C., and Buck K. L. (1962) Lead isotope studies in the northern Rockies, U.S.A. In *Petrologic Studies: A Volume in Honor of A.F. Buddington* (ed. A. E. J. Engel, H. L. James, and B. F. Leonard), pp. 115-131. Geological Society of America.

Chiaradia M. and Cupelin F. (2000) Behaviour of airborne lead and temporal variations of its source effects in Geneva (Switzerland): comparison of anthropogenic versus natural processes. *Atmos. Environ.* **34**, 959-971.

Chow T. J. and Earl J. L. (1972) Lead isotopes in North American coals. *Science* **176**, 510-511.

Chow T. J., Snyder C., and Earl J. (1975) Isotope ratios of lead as pollutant source indicators. *IAEA-SM*, 95-108.

Deloule E., Allegre C., and Doe B. R. (1986) Lead and sulfur isotope microstratigraphy in galena crystals from Mississippi Valley-type deposits. *Econ. Geol.* **81**, 1307-1321.

Doe B. (1970) *Lead isotopes*. Springer-Verlag, New York.

EIA. (1999) State Energy Data Report. Energy Information Administration. US Department of Energy.

EIA. (2000) Annual Energy Review, pp. 414. Energy Information Administration. US Department of Energy.

EIA. (2001) Annual Energy Review, pp. 432. Energy Information Administration. US Department of Energy.

EIA. (2003) State Coal Profile Index Map, Vol. 2003. Energy Information Administration. US Department of Energy.

Facchetti S. (1989) Lead in petrol. The isotopic lead experiment. *Acc. Chem. Res.* **22**, 370-374.

Faure G. (1986) *Principles of Isotope Geology*. John Wiley & Sons, New York.

Fletcher I. R. and Farquhar R. M. (1982) Lead isotopic compositions of Balmat ores and their genetic implications. *Econ. Geol.* **77**, 464-473.

Fuller C., Van Geen A., Baskaran M., and Anima R. (1999) Sediment chronology in San Francisco Bay, California, defined by $^{210}$Pb, $^{234}$Th, $^{137}$Cs, and $^{239,240}$Pu. *Mar. Chem.* **64**, 7-27.

Gaines A. (1975) Papers on the geomorphology, hydrography and geochemistry of the Pettaquamscutt River estuary. PhD, University of Rhode Island.

Gaines A. G. J. and Pilson M. E. Q. (1972) Anoxic water in the Pettaquamscutt River. *Limnol. Oceanogr.* **17**(1), 42-49.

Gobeil C., Johnson W., MacDonald R., and Wong C. (1995) Sources and burden of lead in St. Lawrence estuary sediments: isotopic evidence. *Environ. Sci. Technol.* **29**, 193-201.

Goldberg E., Gamble E., Griffin J., and Koide M. (1977) Pollution history of Narragansett Bay as recorded in its sediments. *Estuar. Coastal Mar. Sci.* **5**, 549-561.

Goldhaber M. B., Church S. E., Doe B. R., Aleinikoff J. N., Brannon J. C., Podosek F. A., Mosier E. L., Taylor C. D., and Gent C. A. (1995) Lead and sulfur isotope investigation of Paleozoic sedimentary rocks from the southern midcontinent of the United States: Implications for paleohydrology and ore genesis of the southeast Missouri lead belts. *Econ. Geol.* **90**, 1875-1910.

Golomb D., Barry E., Fisher G., Varanusupakul P., Koleda M., and Rooney T. (2001) Atmospheric deposition of polycyclic aromatic hydrocarbons near New England Coastal waters. *Atmos. Environ.* **35**, 6245-6258.

Graney J. R., Halliday A. N., Keeler G. J., Nriagu J. O., Robbins J. A., and Norton S. A. (1995) Isotopic record of lead pollution in lake sediments from the northeastern Unites States. *Geochim. Cosmochim. Acta* **59**(9), 1715-1728.

Greenwood R. (2002) Rhode Island Historical Preservation and Heritage Comission.

Hamelin B., Ferrand J. L., Alleman L., Nicolas E., and Veron A. (1997) Isotopic evidence of pollutant lead transport from North America to the subtropical North Atlantic gyre. *Geochim. Cosmochim. Acta* **61**(20), 4423-4428.

Heyl A. (1970) The Upper Mississippi Valley base-metal district. In *Ore Depositis of the United States, 1933-1967*, Vol. I (ed. J. Ridge). The American Institute of Mining, Metallurgical, and Petroleum Engineers, Inc., New York.

Heyl A., Jr., Agnew A., Lyons E., and Behre C., Jr. (1959) The geology of the Upper Mississippi Valley zinc-lead district. *USGS Prof. Paper* **309**.

Heyl A. V., Delevaux M. H., Zartman R. E., and Brock M. R. (1966) Isotopic study of galenas from the Upper Mississippi Valley, the Illinois-Kentucky, and some Appalachian Valley mineral districts. *Econ. Geol.* **61**, 933-961.

Hong S., Candelone J. P., Patterson C. C., and Boutron C. F. (1994) Greenland ice evidence of hemispheric lead pollution two millenia ago by Greek and Roman Civilizations. *Science* **265**, 1841-1843.

Huang S., Arimoto R., and Rahn K. A. (1996) Changes in atmospheric lead and other pollution elements at Bermuda. *J. Geophys. Res.* **101**(D15), 21033-21040.

Hurst R. (2002) Lead isotopes as age-sensitive genetic markers in hydrocarbons. 3. Leaded gasoline, 1923-1990 (ALAS Model). *Environ. Geosci.* **9**(2), 43-50.

Hurst R. (2003) Invited commentary on Dr. Isaac Kaplan's paper "Age dating of environmental organic residues". *Environ. Forensics* **4**, 145-152.

Ingalls W. (1908) *Lead and Zinc in the United States*. Hill Publishing Company, New york.

Kaplan I. (2003) Age dating of environmental organic residues. *Environ. Forensics* **4**(2), 95-141.

Koide M., Bruland K., and Goldberg E. (1973) $^{228}Th/^{232}Th$ and $^{210}Pb$ geochronologies in marine and lake sediments. *Geochim. Cosmochim. Acta* **37**, 1171-1187.

Lambert C. E., E.Nicolas, Véron A., Buat-Ménard P., Klinkhammer G., Corre P. L. E., and Morin P. (1991) Anthropogenic lead cycle in the northeastern Atlantic. *Oceanol. Acta* **14**(1), 59-66.

Latimer J. S. and Quinn J. G. (1996) Historical trends and current inputs of hydrophobic organic compounds in an urban estuary: The sedimentary record. *Environ. Sci. Technol.* **30**(2), 623-633.

Leach D. L., Hofstra A. H., Church S. E., Snee L. W., Vaughn R. B., and Zartman R. E. (1998) Evidence for Proterozoic and Late Cretaceous-Early Tertiary ore-forming events in the Coeur d'Alene District, Idaho and Montana. *Econ. Geol.* **93**, 347-359.

Lima A. L. C., Eglinton T. I., and Reddy C. M. (2003) High-resolution record of pyrogenic polycyclic aromatic hydrocarbon deposition during the 20$^{th}$ century. *Environ. Sci. Technol.* **37**, 53-61.

Marcantonio F., Zimmerman A., Xu Y., and Canuel E. (2002) A Pb isotope record of mid-Atlantic US atmospheric Pb emissions in Chesapeake Bay sediments. *Mar. Chem.* **77**, 123-132.

Millen T. M., Zartman R. E., and Heyl A. V. (1995) Lead Isotopes from the Upper Mississippi Valley District - A Regional Perspective. *USGS Bull.* **2094-B**, B1-B13.

Murozumi M., Chow T., and Patterson C. (1969) Chemical concentrations of pollutant lead aerosols, terrestrial dusts and sea salts in Greenland and Antarctic snow strata. *Geochim. Cosmochim. Acta* **33**, 1247-1294.

Nriagu J. O. (1978) *Biogeochemistry of Pb in the Environment*. Elsevier, New York.

Nriagu J. O. and Pacyna J. M. (1988) Quantitative assessment of world wide contamination of air, water and soils by trace metals. *Nature* **333**, 134-139.

Nriagu J. (1989) The history of leaded gasoline. In *Heavy Metals in the Environment* (ed. J. Vernet), pp. 361-366. Page Brothers, Norwich.

Nriagu J. O. (1998) Tales told in lead. *Science* **281**, 1622-1623.

Orr W. L. and Gaines A. G. J. (1973) Observations on the rate of sulfate reduction and organic matter oxidation in the bottom waters of an estuarine basin: the upper basin of the Pettaquamscutt River (Rhode Island). In *Advances in Organic Geochemistry* (ed. B.Tissot and F. Bienner), pp. 791-812. Technip.

Othman D., White W., and Patchett J. (1989) The geochemistry of marine sediments, island arc magma genesis, and crust-mantle recycling. *Earth Planet. Sci. Lett.* **94**, 1-21.

Pacyna J. (1987) Atmospheric emissions of arsenic, cadmium, lead and mercury from high temperature processes in power generation and industry. In *Lead, mercury, cadmium and arsenic in the environment* (ed. T. Hutchinson and K. Meema), pp. 69-87. John Wiley and Sons Ltd, New York.

Reuer M. K., Boyle E. A., and Grant B. C. (2003) Lead isotope analysis of marine carbonates and seawater by multiple collector ICP-MS. *Chem. Geol.* **200**(1-2), 137-153.

Rhue R., Mansell R., Ou L., Cox R., Tang S., and Ouyang Y. (1992) The fate and behavior of lead alkyls in the environment - A review. *Crit. Rev. Environ. Control* **22**(3-4), 169-193.

Ritson P., Esser B., Niemeyer S., and Flegal A. (1994) Lead isotopic determination of historical sources of lead to Lake Erie, North America. *Geochim. Cosmochim. Acta* **58**(15), 3297-3305.

Robbins J. and Edgington D. (1975) Determination of recent sedimentation rates in Lake Michigan using $^{210}$Pb and $^{137}$Cs. *Geochim. Cosmochim. Acta* **39**, 285-304.

Rosman K. J. R., W.Chisholm, Hong S., Candelone J. P., and Boutron C. F. (1997) Lead from Carthaginian and Roman Spanish mines isotopically identified in Greenland ice dated from 600 B.C. to 300 A.D. *Environ. Sci. Technol.* **31**, 3413-3416.

Russell R. D. and Farquhar R. M. (1960) *Lead Isotopes in Geology*. Interscience Publishers, New York.

Sanford R. F. (1992) Lead isotopic compositions and paleohydrology of caldera-related epithermal veins, Lake City, Colorado. *GSA Bulletin* **104**, 1236-1245.

Schaule B. K. and Patterson C. C. (1981) Lead concentrations in the northeast Pacific: evidence for global anthropogenic perturbations. *Earth Planet. Sci. Lett.* **54**, 97-116.

Settle D. M. and Patterson C. C. (1980) Lead in Albacore: guide to lead pollution in americans. *Science* **207**(4436), 1167-1176.

Settle D. M. and Patterson C. C. (1991) Eolian inputs of lead to the South Pacific via rain and dry deposition from industrial and natural sources. *Geochim. Cosmochim. Acta*(Special Publication No.3), 285-294.

Shen G. T. and Boyle E. A. (1987) Lead in corals: reconstruction of historical industrial fluxes to the surface ocean. *Earth Planet. Sci. Lett.* **82**, 289-304.

Shen G. T. and Boyle E. A. (1988) Determination of lead, cadmium and other trace metals in annually-banded corals. *Chem. Geol.* **67**(1-2), 47-62.

Shirahata H., Elias R. W., Patterson C. C., and Koide M. (1980) Chronological variations in concenrations and isotopic compositions of anthropogenic atmospheric lead in sediments of a remote subalpine pond. *Geochim. Cosmochim. Acta* **44**, 149-162.

Shotyk W., Weiss D., Appleby P. G., Cheburkin A. K., Frei R., gloor M., Kramers J. D., Reese S., and Knaap W. O. V. D. (1998) History of atmospheric lead deposition since 12,370 $^{14}$C yr BP from a Peat Bog, Jura Mountains, Switzerland. *Science* **281**, 1635-1640.

Snyder F. and Gerdemann P. (1970) Geology of the Southeast Missouri lead district. In *Ore Depositis of the United States, 1933-1967*, Vol. I (ed. J. Ridge). The American Institute of Mining, Metallurgical, and Petroleum Engineers, Inc., New York.

Spliethoff H. and Hemond H. (1996) History of toxic metal discharge to surface waters of the Aberjona watershed. *Environ. Sci. Technol.* **30**, 121-128.

St. Marie J. and Kesler S. E. (2000) Iron-rich and iron-poor Mississippi Valley-type mineralization, Metaline District, Washington. *Econ. Geol.* **95**, 1091-1106.

Sturges W. T. and Barrie L. A. (1989) Stable lead isotope ratios in Arctic aerosols: evidence for the origin of Arctic air pollution. *Atmos. Environ.* **23**(11), 2513-2519.

Thompson T. B. and Beaty D. W. (1990) Geology and origin of ore deposits in the Leadville District, Colorado. Part II: Oxygen, hydrogen, carbon, sulfur and lead isotope data and development of a genetic model. *Econ. Geol. Monograph* **7**, 156-179.

Tootell L. (1963) Shipwright Saunders shipshape ships. In *Ships, Sailors and Seaports*, pp. 29-39. The Pettaquamscutt Historical Society, Kingston, RI.

Urish D. (1991) Freshwater inflow to the Narrow River. *Maritimes* **35**(2), 12-14.

USGS. (1998) Lead statistical compendium, Vol. 2003. U.S. Geological Survey.

Van Metre P., Mahler B., and Furlong E. (2000) Urban sprawl leaves its PAH signature. *Environ. Sci. Technol.* **34**, 4064-4070.

Véron A. J., Church T. M., Flegal A. R., Patterson C. C., and Erel Y. (1993) Response to lead cycling in the surface Sargasso Sea to changes in tropospheric input. *J. Geophys. Res.* **98**, 18269-18276.

Véron A. J., Church T. M., Patterson C. C., and Flegal A. R. (1994) Use of stable lead isotopes to characterize the sources of anthropogenic lead in North Atlantic surface waters. *Geochim. Cosmochim. Acta* **58**(15), 3199-3206.

Véron A. J., Church T. M., and Flegal A. R. (1998) Lead isotopes in the Western North Atlantic: transient tracers of pollutant lead inputs. *Environ. Res. Section A* **78**, 104-111.

Weiss D., Shotyk W., Appleby P. G., Kramers J. D., and Cheburkin A. K. (1999) Atmospheric Pb deposition since the industrial revolution recorded by five Swiss peat profiles: enrichment factors, fluxes, isotopic composition, and sources. *Environ. Sci. Technol.* **33**(9), 1340-1352.

Wilber J. S., Mutschler F. E., Friedman J. D., and Zartman R. E. (1990) New chemical, isotopic, and fluid inclusion data from zinc-lead-copper veins, Shawangunk Mountains, New York. *Econ. Geol.* **85**, 182-196.

Wolff G., Ruthkosky M., Stroup D., Korsog P., Ferman M., Wendel G., and Stedman D. (1986) Measurements of $SO_x$, $NO_x$ and aerosol species on Bermuda. *Atmos. Environ.* **20**(6), 1229-1239.

Wu J. and Boyle E. A. (1997) Lead in the western North Atlantic Ocean: Completed response to leaded gasoline phaseout. *Geochim. Cosmochim. Acta* **61**(15), 3279-3283.

Zartman R. E. and Stacey J. S. (1971) Lead isotopes and mineralization ages in Belt Supergroup rocks, northwestern Montana and northern Idaho. *Econ. Geol.* **66**, 849-860.

# CHAPTER 6

# APPORTIONING SOURCES OF PYROGENIC PAHs USING RADIOCARBON MEASUREMENTS

## 1. INTRODUCTION

Polycyclic aromatic hydrocarbons (PAHs) are a class of environmental contaminants that include suspected carcinogens and mutagens, such as benzo[*a*]pyrene (Denissenko et al., 1996). These compounds are widespread and can be found in measurable concentrations in remote locations such as Arctic ice (Kawamura and Suzuki, 1994) and snow (Masclet et al., 2000), high altitude lakes (Fernández et al., 1999) and deep-sea sediments (Ohkouchi et al., 1999). PAHs can be released directly to the environment by human activities (oil spills) and natural processes (oil seeps), and some can be generated by diagenetic processes from biogenic precursors (e.g. perylene) (Laflamme and Hites, 1978; Tan and Heit, 1981). However, the most prominent source of PAHs to the environment is the incomplete combustion of modern (wood) and fossil (e.g., petroleum and coal) carbon. Recent sediment-based studies from a variety of locations in the United States have shown that the fluxes of PAHs are at least constant or potentially increasing (Van Metre et al., 2000; Schneider et al., 2001; Lima et al., 2003). This is contrary to the case for most other environmental contaminants (such as polychlorinated biphenyls), which show decreasing fluxes to sediments. Because of the potential harm associated with emissions of PAHs to the environment, it is essential to understand and apportion the sources of these compounds for better source control and pollution abatement.

Classic studies on PAH apportionment in coastal and marine sediments have relied on ratios of individual compounds or groups of compounds and molecular fingerprints (e.g., retene for combustion of softwood) to distinguish PAHs derived from

petroleum and derivatives (petrogenic) from those derived from combustion (pyrogenic). For example, Youngblood and Blumer (1975) suggested that the distribution of alkylated versus parent PAHs in sedimentary environments could be used to discriminate between these two modes of formation. Since then, the sum of methyl-phenanthrenes and methyl-anthracenes to phenanthrene (ΣMPhen/Phen) has been widely used in apportioning sources of PAHs in environmental samples (Hites et al., 1980; Gschwend and Hites, 1981; Prahl and Carpenter, 1983; Lipiatou et al., 1993; Ohkouchi et al., 1999; Pereira et al., 1999). However, while ratios can be helpful at discriminating between a fresh oil contamination (higher alkyl/parent ratio) (Wang et al., 1997) and a pyrogenic source, typically they cannot distinguish between combustion of fossil and modern biomass.

Measurements of the radiocarbon ($^{14}C$) content at the bulk, compound class, and molecular level have been successfully applied in separating modern from fossil carbon in a number of studies (Cooper et al., 1981; Dasch, 1982; Hawthorne et al., 1992; Lichtfouse and Eglinton, 1995; Eglinton et al., 1997; Reddy et al., 2002b; Reddy et al., 2003). The basis of this approach relies on the incorporation of modern levels of $^{14}C$ by biota during photosynthesis. Because of its half-life (5730 years), $^{14}C$ can help apportion the sources of pyrogenic PAHs by creating two well-defined end members: combustion of modern biomass ($^{14}C$-rich) and combustion of fossil fuels ($^{14}C$-free due to radioactive decay). Cooper and collaborators (1981) conducted one of the earlier studies to use radiocarbon measurements to discriminate the contribution of specific sources of particles to urban air. This study showed that a large portion of the atmospheric particles collected in Portland, OR during the winter derived from burning of wood (39-70%) for residential heating. The latter results were based solely on bulk basis, not benefiting from the information encoded at the molecular-level. Molecular-level radiocarbon analysis was impaired by analytical capabilities until the late 1990s, when Eglinton and collaborators (1996a) successfully demonstrated the use of a preparative capillary gas chromatograph (PCGC) to isolate highly pure compounds in quantities sufficient for radiocarbon determination by accelerator mass spectrometry (AMS).

The use of compound-specific radiocarbon measurements for discerning sources of PAHs was first demonstrated by Eglinton and collaborators (1996b) and Reddy and collaborators (2002a). These initial studies revealed that PAHs in surface sediments near urban centers were primarily due the combustion of fossil fuels. However, a recent contribution by Reddy and collaborators (2003) that investigated household soot showed that biomass could be a significant source of PAHs. Soot produced by the combustion of creosote-impregnated wood in household stoves was enriched in PAHs and there was some debate whether these compounds were derived from the creosote or from the combustion of the wood. The authors measured the $^{14}C$ content of individual PAHs and used a mass balance approach to calculate the relative contribution of each source based on the premise that because creosote is a distillation product of coal tar it should contain no $^{14}C$ and wood should contain contemporary values ($f_M \geq 1$). By doing so, they estimated that 54 to 70% of the PAHs had been generated from the combustion of the wood and the remaining had originated from the creosote. If a single marker, such as retene (for the combustion of wood) had been used they would have overlooked the 50-70% contribution from creosote that the molecular-level $^{14}C$ analyses revealed.

In this study, we construct molecular $^{14}C$ records of combustion-derived PAH to determine how the proportion of fossil fuel derived PAHs has varied since pre-industrial times. We compare records from a suburban (Pettaquamscutt River) and a remote site (Siskiwit Lake) and evaluate which PAHs serve as the most effective tracers of fossil and modern combustion sources.

## 2. EXPERIMENTAL SECTION

### 2.1 Study Area

#### *2.1.1. Pettaquamscutt River – Suburban Site*

The Pettaquamscutt River is located in South Kingston, southern Rhode Island (Figure 1). This 9.7 km long estuary ranges in width from 100 to 700 meters and has a small drainage area (~ 35 $km^2$) dominated by oak forests, wetlands and open waters (Orr

and Gaines, 1973; Boothroyd, 1991). Glacial outwash sediments overlay bedrock of the Rhode Island Formation type, characterized by sandstones, conglomerate, schist and graphite (Hermes et al., 1994). The Pettaquamscutt River can be geographically divided into two remnant kettle lakes (upper and lower basin) and a channel (Figure 1). The lower basin is delimited to the north by a shallow sill (less than 1 meter deep) and to the south by a 6.4-km long channel that connects it to the main source of salt water to this estuary, the Rhode Island Sound (Gaines, 1975). This basin contains the deepest point of the Pettaquamscutt River system at 19.5 m. In contrast, the upper basin is shallower (13.5 m

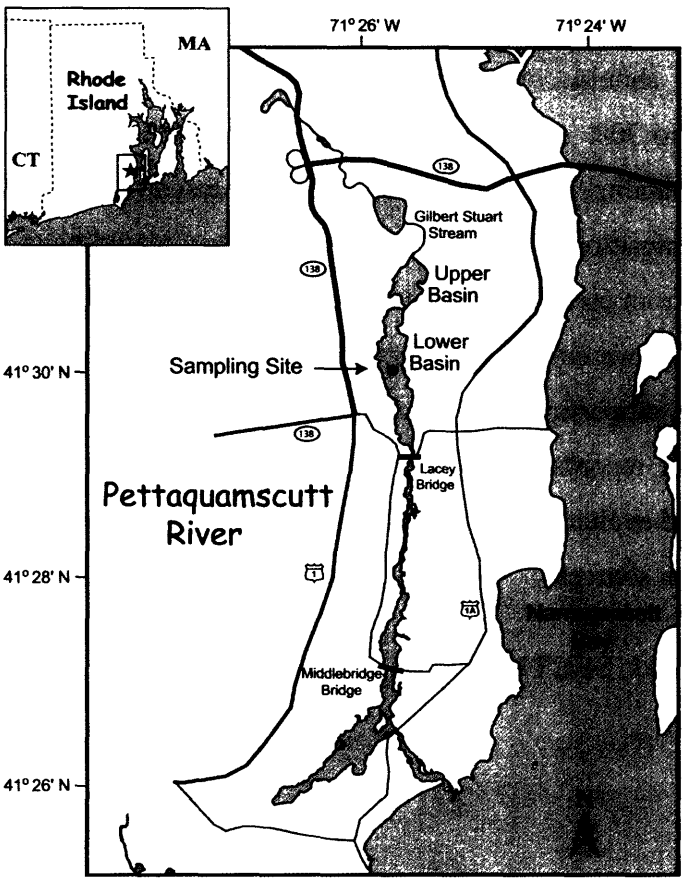


Figure 1. Location of the Pettaquamscutt River and adjacent roads.

at maximum depth) and receives input of freshwater from the Gilbert Stuart Stream (Gaines, 1975), calculated to contribute ~50% of the total freshwater to this system (Kelly and Moran, 2002). The remaining 50% is attributed to small streams and to groundwater input (Kelly and Moran, 2002). The flow of freshwater from the Gilbert Stuart Stream over waters derived from tidal influx creates a strong pycnocline (at 3.5-6 m in the lower basin) that maintains stagnant and anoxic bottom waters in these basins (Gaines and Pilson, 1972; Hodel and Menezes, 2000). The lack of oxygen inhibits the existence of benthic macrofauna that can bioturbate the sediments, leading to the preservation of undisturbed sequences that are ideal for the purpose of historical reconstruction (Lima et al., 2003).

### *2.1.2. Siskiwit Lake – Remote Site*

Siskiwit Lake is a remote lake located on the archipelago of Isle Royale in the northern portion of Lake Superior (Figure 2). Isle Royale became a National Park in 1940 and was designated an International Biosphere Reserve by the United Nations in 1981. Isle Royale is remote from major urban and industrialized centers, over 98% of its land is designated wilderness, it contains few sources of combustion and no roads are present (www.isle.royale.national-park.com; McVeety and Hites, 1988). More than 50 lakes are located on Isle Royale, of which Siskiwit Lake is the largest. Siskiwit Lake has an approximate area of 16.8 $km^2$, is 11.1 km long and has a maximum depth of 46 m. This system is 17 m higher and 0.6 km inland from Lake Superior, which prevents exchange between these two water bodies. Contaminants previously measured in the sediments of Siskiwit Lake include combustion-derived compounds such as dioxins (Czuczwa and Hites, 1986) and PAHs (McVeety, 1986; McVeety and Hites, 1988). Atmospheric deposition is thought to be the only source of contamination to Siskiwit Lake nowadays (McVeety and Hites, 1988). However, Isle Royale was nearly completely cleared and settled by fisherman and miners in the $19^{th}$ century, resulting in the disappearance of more than half of the original plant and animal species. In addition, copper mining was active in the island during the 1800s. Although most of the ventures did not take

significant quantities of ore, the Siskowit Mining Company extracted 95 tons of refined copper ore in a six-year period, starting in 1849 (www.nyx.net/~sjhoward/Isle_Royale). Records of early 19th century forest fires in Isle Royale were found during the 1847 General Land Office Survey (www.usgs.nau.edu/global_change/isroy.html). However, the largest fire in its recent history occurred in 1936, burning roughly 80% of the Siskiwit Lake watershed (McVeety, 1986).

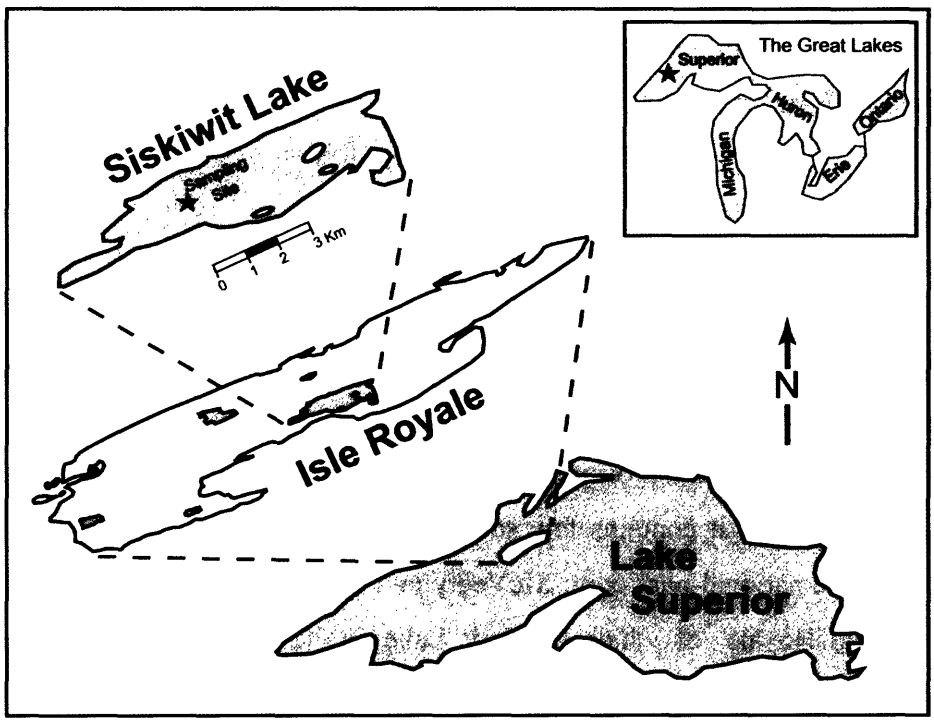


Figure 2. Geographic location of Siskiwit Lake.

## 2.2 Sampling

Seven freeze-cores were collected in the deepest part (20 m) of the lower basin of the Pettaquamscutt River (Figure 1) in April 1999. All the sides were x-rayed and the slab that showed the highest number and most distinct laminations was used to define a high-resolution record of PAHs content and distribution over the past 200 years (Lima et

al., 2003). The high-resolution record helped to determine the amount of sediment needed to build a $^{14}C$ record of individual PAHs. Four sediment slabs were selected for the compound-specific radiocarbon study based on their integrity and number of identifiable features on the x-radiographs. These features were used to align the four cores, which were then sectioned at 0.5-cm intervals using a compact tile saw equipped with a diamond wafering blade (0.63-mm thickness), while maintained frozen by applications of liquid nitrogen. Each 0.5-cm sample ($n$ = 554) was placed in a previously combusted glass-jar, freeze-dried and homogenized with a mortar and pestle. Because the cores were aligned before sectioning, dried samples of equivalent depth could be combined. These samples were then stored for compound-specific $\Delta^{14}C$ and $\delta^{13}C$ and other geochemical analyses.

Due to logistical challenges a simpler sampling procedure was undertaken in Siskiwit Lake. Seven gravity cores (~ 4 inches in diameter) were collected in 1998, sliced at 2-cm intervals, placed into plastic freezer bags, sealed and chilled on ice before transport back to the lab. Sediment samples were later transferred to previously combusted glass jars and freeze-dried.

*2.2.1. Sediment Dating*

Sediment chronology calculations for the Pettaquamscutt River have been detailed elsewhere (Chapter 4). Briefly, $^{210}Pb$, $^{214}Pb$ and $^{137}Cs$ were measured in dry samples by direct $\gamma$-counting using a high purity germanium detector. The constant rate of supply (CRS) (Appleby and Oldfield, 1978) model was applied to the calculated excess $^{210}Pb$ ($^{210}Pb_{Excess} = {}^{210}Pb_{Total} - {}^{214}Pb$) and the results obtained were compared to the independent varve chronology. The good age agreement (e.g., within 2 years at 1960 and within 9 years at 1860) between the CRS model and the varve counts allowed the extension of the sediment chronology beyond the limit of the $^{210}Pb$ method (100-150 years). The resulting chronology is then a composite of these two dating techniques, with $^{210}Pb$ ages used for the uppermost 34-cm (1904-1999), and varve ages applied for sediments deposited prior to that (1900-1735 for 35-70 cm). Because the depth-age

evaluation was performed for a single core, $^{137}Cs$ measurements were conducted on samples from the composite horizons to verify if the stratigraphic resolution had been preserved. The results obtained show a 1-cm shift in the depth of maximum fallout of $^{137}Cs$, from 18.25 cm to 19.25 cm (Figure 3), corresponding to a 2-year difference in chronology between the combined cores and the original high-resolution record of PAHs. This difference is within the range of resolution of $^{210}Pb$-ages, hence no correction was applied to account for this small shift.

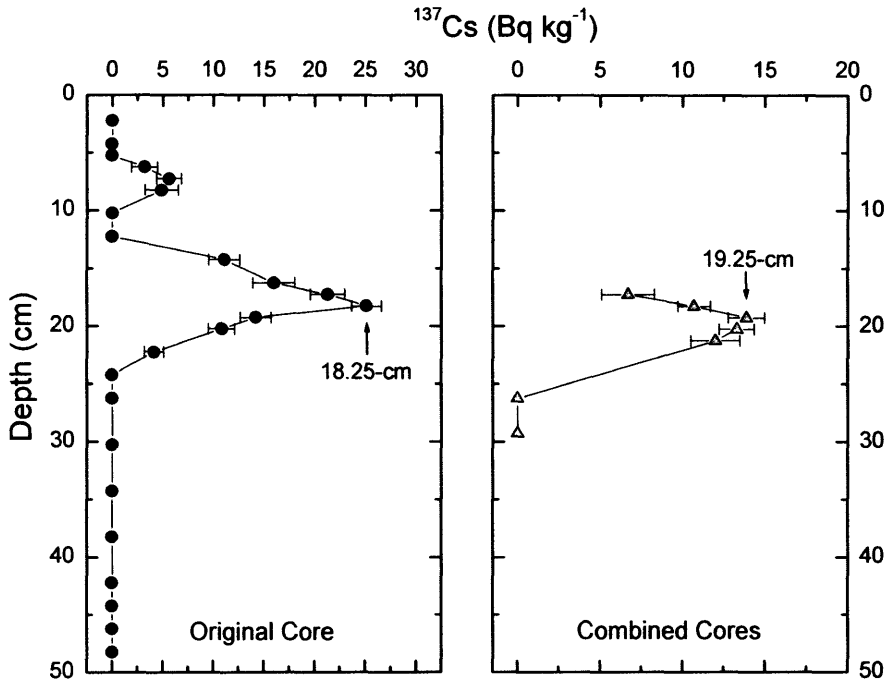


Figure 3. $^{137}Cs$ activity in the combined horizons differs from that of the original core by only 1-cm, or approximately 2 years.

Sediments collected in Siskiwit Lake were also dated by $^{210}Pb$. Excess $^{210}Pb$ was measured at 2-cm intervals and showed that $^{210}Pb$ supported levels were reached at approximately 10 cm for all seven cores (Figure 4). Even though an apparently intact sediment-water interface was observed at the time of collection, $^{210}Pb$ measurements

revealed that the upper portion of the sediment cores had been lost during sampling. A plot of the natural logarithm of the excess $^{210}$Pb against depth (cm) for one of the cores showed no obvious slope inflections characteristic of a change in sedimentation rate or the surficial mixing previously reported by McVeety (1986). Therefore, we used the constant initial concentration (CIC) model (Krishnaswamy et al., 1971) to estimate that the top 8-cm of sediment of that core had been deposited over 43 years. Neither compaction nor sediment focusing were taken into account during these calculations. However, the calculated sedimentation rate (0.18 cm yr$^{-1}$) was in close agreement with values reported by McVeety (1986; 1988) (0.19 cm yr$^{-1}$) for that location. We then

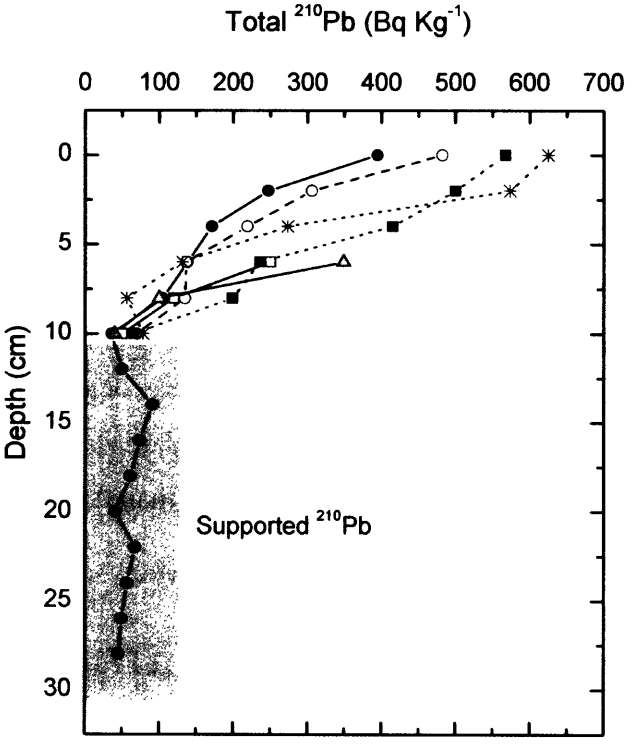


Figure 4. Total $^{210}$Pb activity in seven cores collected in Siskiwit Lake. Supported levels are achieved at 10-cm for all cores.

assumed that $^{210}Pb$ achieved supported levels within 100 years of deposition and reasoned that because these levels were observed 10 cm from the top, the surficial layer of the sediment column was dated at 1954[1]. As a result, we estimated that approximately 44 years (8-cm) of the sediment record were not retrieved by the gravity coring procedure. Because $^{210}Pb$ supported levels were reached at approximately 10 cm for all seven cores, we presumed that a comparable amount of sediment was lost from the upper most portion of all seven cores.

### 2.4 Total Organic Carbon Determinations

A Fisons 1108 elemental analyzer was used to measure the total organic carbon (TOC) content of the samples. To remove the inorganic carbon fraction, about 2 mg of dry sample was weighed into a silver capsule and acidified with 20 μL of HCl 2N. The samples were then dried in an oven at 50°C, wrapped, placed inside tin capsules for better catalysis of the oxidation reaction, and analyzed. TOC concentrations were calculated in relation to the whole sediment and organic carbon/organic nitrogen ($C_{org}/N_{org}$) ratios were calculated on an atomic basis. No significant difference was observed when $C_{org}/N_{org}$ and $C_{org}/N_{total}$ (not acidified) were compared for a couple of samples. Samples were run in triplicate and all reported weight percentages represent the mean ± one standard deviation. Concentration of carbon and nitrogen were determined through a 5-point calibration curve (0.1 to 1 mg) of a sulfanilamide standard. Instrumental blanks were run after sets of 12 analyses, yielding carbon blanks better than 0.004 mg and nitrogen blanks better than 0.005 mg.

### 2.5 Extraction, Purification and Combination of PAH Fractions

Sediment from each 0.5-cm interval was extracted by pressurized fluid extraction (Dionex ASE 200) using a mixture of dichloromethane and methanol (9:1) at 1000 psi and 100 °C. The extracts were concentrated to approximately 10 mL using a Zymark

[1] If 10 cm = 100 years and the core was collected in 1998, then 10cm = 1898. Given that sedimentation rate was calculated at 0.18 cm $yr^{-1}$, then 0 cm = 1954. Because 1998-1954 = 44 years and sedimentation rate = 0.18 cm $yr^{-1}$, we estimate that we lost 8 cm of the top of the core during sampling.

TurboVap evaporator and subsequently treated with activated copper to remove elemental sulfur. Because the Pettaquamscutt River samples were extremely rich in extractable organic compounds, the extracts were air-dried on combusted sand prior to charging on a silica column for separation (as exchanging the original solvent mixture to hexane proved unsuccessful). This step was not necessary for the Siskiwit Lake extracts. Each 0.5-cm interval total lipid extract was separated into four fractions on a column packed with 100-200 mesh fully activated silica gel. The first fraction containing alkanes was eluted with hexane; the second containing PAHs was eluted with toluene/hexane (1:1); the third and fourth fractions were eluted with 2% formic acid in dichlomethane and 2% formic acid in methanol, respectively. All but the second fraction were archived for future studies.

After extraction and purification on a silica column, the PAH fractions were concentrated and further combined into coarser depth intervals to obtain sufficient amounts of individual PAHs for $^{14}C$ analysis. Eight depth-age intervals were defined for the Pettaquamscutt River extracts, taking into account the expected concentrations of each compound and the estimated time of deposition. Because atmospheric weapons testing conducted in the early 1950s and 1960s practically doubled the amount of radiocarbon in the atmosphere (the so-called "bomb spike"), the horizons can be divided into pre- and post-bomb. Three horizons cover the post-bomb portion of the core: H1 (1999-1982), H2 (1981-1962) and H3 (1960-1931). The pre-bomb sections contain horizons deposited after the onset of heavy industrialization, H4 (1929-1898) and H5 (1896-1873), and prior to significant industrial activities, H6 (1871-1842), H7 (1840-1768) and H8 (1764-1735). PAH extracts from these eight horizons were further separated into ring classes by high-pressure liquid-chromatography (HPLC) following procedure described by Wise and collaborators (1986) and modified by Reddy and collaborators (2002a). This HPLC procedure also allowed us to separate pure perylene (98% purity or greater) from four of the eight horizons. That is noteworthy as the concentration of perylene greatly increases with depth, surpassing any other parent PAH (Lima et al., 2003), therefore perylene can limit the amount of extract that can be

separated by preparative capillary gas chromatography (PCGC). The HPLC procedure isolated PAHs into two ring classes: 3+4-ring and 5+6-ring PAHs. The resulting 16 HPLC fractions (8 horizons x 2 ring classes) were subjected to two-dimensional PCGC for isolation of individual PAHs.

Because PAH concentrations were lower in the Siskiwit Lake sediments, the extracts were combined at a coarser resolution. Four horizons were defined: H1 (1954-1926), H2 (1915-1882), H3 (1871-1837) and H4 (1826-1793). These four horizons were also subjected to ring-class separation by HPLC, as described above.

### 2.6 Two-Dimensional Preparative Capillary Gas Chromatography (2D-PCGC)

Automated preparative capillary gas chromatography (PCGC) is a technique that allows the isolation of specific compounds through repetitive injections (~100) of a mixture on a modified capillary gas chromatograph. This method was described and successfully tested by Eglinton and collaborators (1996a) for isolation of individual organic compounds in sufficient quantities for radiocarbon determinations (>50 μg C). PAHs present in the Siskiwit Lake extracts were further isolated using this one-dimensional PCGC system. Because the Pettaquamscutt River extracts were extremely rich in biogenic organic compounds, a sizable number of interfering compounds were still present in the PAH fractions, even after the intensive silica column and HPLC cleanup. This hindered the isolation of pure individual compounds by one-dimensional PCGC.

In order to separate the PAHs from other organic compounds and isolate individual PAH isomers (such as phenanthrene and anthracene) from each other, we utilized a 2D-PCGC system (Figure 5). This instrument works in the same manner as the 1D-PCGC, with the advantage that incompletely separated components can be diverted from the first GC and fully resolved on the second GC equipped with a different stationary phase (Table 1), eliminating undesirable compounds in the process. In the system used in this study, a HP 7683 auto-injector and a multi-column switching system (Gerstel MCS 2) are connected to the first HP 6890 series gas chromatograph, and a

Gerstel preparative fraction collector (PFC) is located at the end of the second GC. Similar to a 1D-PCGC, 1% of the effluent from the GC column is directed to a flame ionization detector (FID), so that compound separation and variations on retention times can be evaluated. The retention time windows corresponding to components of interest are transferred from the first GC to a cryogenic trap system (CTS), where the compounds are retained before introduction into the second GC. After separation on the second column, individual compounds are directed to the PFC for collection in cryogenically-cooled U-tube traps. Of the seven traps present in the PFC, six are used to collect compounds of interest and the 7$^{th}$ trap (waste trap) receives the remainder of the mixture. After isolation, the trapped PAHs were transferred from the U-tubes to 2-mL glass vials by addition of 1 mL of dichloromethane. Approximately 50-100 μL of each extract was transferred to a GC vial for determination of purity, concentration and stable carbon isotopic composition (section 2.7), while the remaining portion was purified (section 2.8) for subsequent radiocarbon determination.

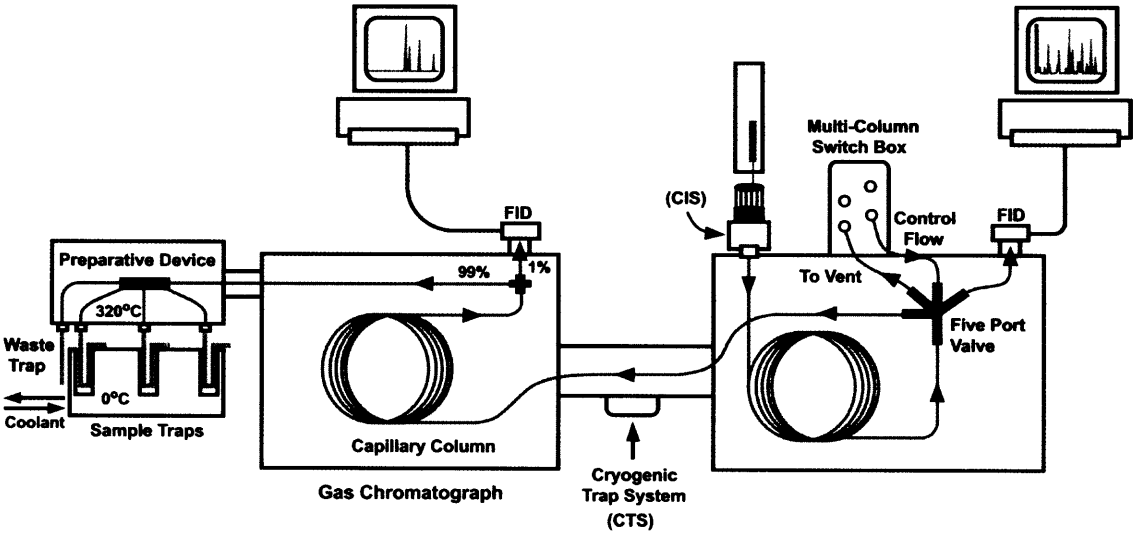


Figure 5. Schematic of a two-dimensional preparative capillary gas chromatograph (2D-PCGC).

Table 1. Chromatographic conditions used in the first and second GC of the 2D-PCGC system for separation of individual PAHs.

| Ring Class | Column GC1 and Temperature Program | Column GC2 and Temperature Program |
|---|---|---|
| 3, 4-Ring PAHs | DB-35ms<br>60 m x 0.53 mm i.d. x 0.50 μm-film<br><br>60°C (15 min hold) to 180°C at 20°C $min^{-1}$, and then from 180°C to 320°C at 5°C $min^{-1}$ (15 min hold) | DB-1<br>60 m x 0.53 mm i.d. x 1 μm-film<br><br>80°C (40 min hold) to 180°C at 20°C $min^{-1}$, and then from 180°C to 320°C at 4.5°C $min^{-1}$ (4 min hold) |
| 5, 6, 7-Ring PAHs | DB-1<br>60 m x 0.53 mm i.d. x 1 μm-film<br><br>80°C (1.5 min hold) to 240°C at 20°C $min^{-1}$, and then from 240°C to 325°C at 5°C $min^{-1}$ (9 min hold) | DB-35ms<br>60 m x 0.53 mm i.d. x 0.50 μm-film<br><br>120°C (38 min hold) to 240°C at 20°C $min^{-1}$, and then from 240°C to 325°C at 4°C $min^{-1}$ (15 min hold) |

### 2.7 Isotope ratio monitoring gas chromatography mass spectrometry (irm-GC/MS)

The $\delta^{13}C$ values of individual PAHs were determined in triplicate on a Finnigan Delta Plus isotope ratio mass spectrometer with attached Finnigan GC combustion III interface and Hewlett-Packard 6890 GC. Compounds were separated on a CP-Sil 5CB capillary column (50 m length, 0.25 mm diameter, 0.25mm film thickness) and isotope ratios for the PAH peaks were calculated relative to $CO_2$ reference gas pulses. The ratio $^{13}C/^{12}C$ for the sample ($R_{Sample}$) is expressed in the delta ($\delta$) notation in permil (‰), which relates it to the internationally employed standard Pee-Dee Belemnite ($R_{PDB}$):

$$\delta^{13}C = (R_{Sample} / R_{PDB} - 1) * 1000 \quad (1)$$

The standard deviation for replicate measurements of individual PAHs was better than 0.6‰ and usually within 0.3‰. Replicate measurement of PAH standards of known $\delta^{13}C$ composition (3 to 6 rings) yielded precision and accuracy better than 0.3‰. The stable carbon isotopic composition of bulk samples (TOC) were determined by automated on-line solid combustion interfaced to the same irm-MS just described.

## 2.8 Radiocarbon Measurements and Data Reporting

Individual PAHs were transferred to pre-combusted quartz tubes (7 mm I.D. x 20 cm) where the solvent was evaporated under a gentle stream of nitrogen and then copper oxide (50 mg) was added. Each tube was then evacuated on a vacuum line, sealed, and combusted at 850°C for 5 hours. The carbon dioxide produced by the combustion of the samples was isolated from water and other gases through a series of cold traps on the vacuum line and quantified with a manometer. The samples were submitted to the National Ocean Sciences Accelerator Mass Spectrometry facility (NOSAMS) where ~95% of the purified carbon dioxide was reduced to graphite, pressed and analyzed for $^{14}C$ according to established procedures (McNichol et al., 2001) (General Statement of $^{14}C$ Procedures at www.nosams.whoi.edu) and the remaining 5% was used for $\delta^{13}C$ measurements. In this chapter, radiocarbon data are reported as the permil deviation from the absolute international standard $^{14}C$ activity ($A_{abs}$) defined as 95% of the $^{14}C$ activity of the original Oxalic Acid standard (HOxI), in the year 1950, corrected for fractionation effects and radioactive decay between 1950 and the year of measurement (Stuiver and Polach, 1977):

$$\Delta^{14}C = (A_{Sample} / A_{abs} - 1) * 1000 \quad (2)$$

Routine precision for $\delta^{13}C$ and $\Delta^{14}C$ measurements at the NOSAMS facility are ~0.1‰ and 5-7‰, respectively. However, AMS performance is more limited for samples smaller than 100 µg C (Pearson et al., 1998) and the uncertainties for such small samples are closer to 20‰. Error associated with measurement of small samples of individual PAHs are listed in Appendix 4 and range from 1-12.8‰. The process of purification of individual compounds requires extensive wet chemical and instrumental laboratory work. NOSAMS corrects the reported data for blanks associated with combustion of samples to $CO_2$ and with graphitisation conducted at the facility, but little is known about possible blanks associated with the entire cleanup procedure. Recent investigations conducted by Mollenhauer (unpublished results) display little variations in $\Delta^{14}C$ values for analysis of alkenone samples of different size (Figure 6). Mollenhauer's algal culture samples covered a large range in mass (> 2 mg to < 50 µg C), showed alkenone $\Delta^{14}C$ values close

to the dissolved inorganic carbon (DIC) of the water and no obvious trend with sample size. The standard deviation of these nine alkenone samples was 17‰, consistent with blank values encountered by NOSAMS for combustion of samples to $CO_2$ and graphitisation. Identical samples processed at the NOSAMS facility and at the Fye laboratory at WHOI showed coincident results (Figure 6), indicating that the cleanup procedure did not introduce a recognizable blank.

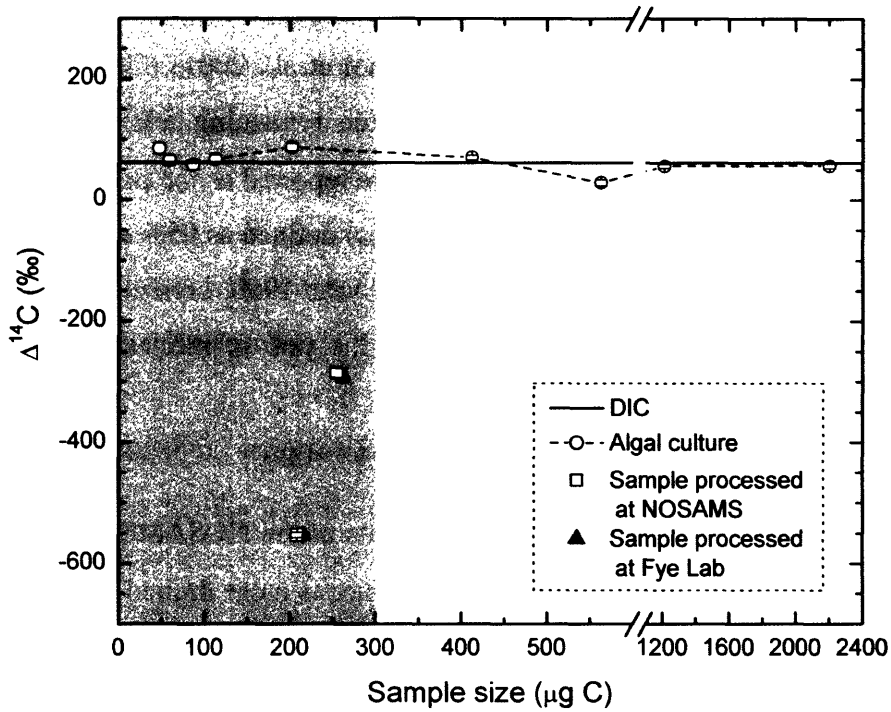


Figure 6. $\Delta^{14}C$ values for analysis of alkenone samples of different mass (> 2 mg to < 50 μg C) show no obvious trend with sample size (Mollenhauer - unpublished results). Samples located in the shaded area are processed as small samples by NOSAMS.

Some of the samples submitted to NOSAMS had just enough carbon for radiocarbon determination, so a $\delta^{13}C$ value was assumed by the facility. Whenever that was the case, the reported $\Delta^{14}C$ values were later corrected for the $\delta^{13}C$ value measured at

the Organic Mass Spectrometry facility at WHOI, using the following formula (see www.nosams.whoi.edu):

$$F_{M(new)} = F_{M(NOSAMS)} * [(1 + 0.001 * \delta^{13}C_{NOSAMS}) / (1 + 0.001 * \delta^{13}C_{new})]^2 \quad (3)$$

where $\delta^{13}C_{NOSAMS}$ is the $\delta^{13}C$ value assumed by NOSAMS; $F_{M(NOSAMS)}$ is the fraction modern value reported by NOSAMS and $\delta^{13}C_{new}$ is the correct $\delta^{13}C$ value for that sample (measured at the Organic Mass Spectrometry facility at WHOI). In addition, because the Pettaquamscutt River samples have a known geochronological age, determined from the $^{210}Pb$ and varve chronologies (Chapter 4), we can further correct the $\Delta^{14}C$ values for any in situ $^{14}C$ decay (half-life = 5730 yr) since the time of deposition, to yield the values that the samples had when first deposited in the sediments. This age correction is done by applying the following formula (Stuiver and Polach, 1977):

$$\Delta^{14}C_{(corrected)} = [(F_{M(new)} * (e^{(1950-x)*\lambda}) - 1] * 1000 \quad (3)$$

$$F_{M(corrected)} = (\Delta^{14}C_{(corrected)} + 1000) / (1000 * e^{-\lambda*(x-1950)}) \quad (4)$$

where x = year of deposition and $\lambda$= $^{14}C$ decay constant (1/8267 $yr^{-1}$).

Perylene was the only compound in high enough concentration at every horizon for $^{14}C$ determination. In certain instances, two or more horizons had to be further combined to obtain sufficient amounts of an individual PAH for $^{14}C$ analysis. That was the case for phenanthrene (H1+H2 and H4+H5), benz[*a*]anthracene (H4+H5) and fluoranthene (H6+H7+H8). In addition, some samples were lost either during pre-treatment (benzo[*b*+*k*]fluoranthene H6+H7+H8) or during $^{14}C$ measurement procedure at NOSAMS (benzo[*b*+*k*]fluoranthene H1, benzo[*b*+*k*]fluoranthene H3, chrysene H1). In general, individual PAH concentrations for samples from the bottom three horizons (H6, H7 and H8) were too low for a reliable $^{14}C$ measurement. The NOSAMS facility is capable of handling samples with as little carbon as 25 μg C. However, because several of our samples contained less than 20 μg C, we investigated the possibility of increasing the amount of carbon in these samples with a standard of known $^{14}C$ and $^{13}C$ content. We conducted three tests by mixing standards in known proportions to verify if a simple mass balance could account for the $^{14}C$ measured in the mixtures. The good agreement between

calculated and measured $\Delta^{14}C$ values for the mixtures (details in Appendix 3), led us to adopt this procedure for 9 samples, namely fluoranthene H1, fluoranthene H6+H7+H8, pyrene H1, chrysene H1, benzo[*a*]pyrene H2, benzo[*e*]pyrene H5, benzo[*ghi*]perylene H1, retene H7 and retene H8. The dilution of samples containing 2-20 μg C to a large enough size to run on the accelerator mass spectrometer (AMS) induces an error that increases with decreasing sample size (details in Appendix 3). The error associated with diluting samples containing initially more than 10 μg C ranged from 10.2-34.7‰, while the dilution of a 2 μg C sample (retene – H8) yielded a much higher error (159‰) (errors are listed in Appendix 4).

## 3. RESULTS AND DISCUSSION

The down-core profiles of the abundance of $^{14}C$ in individual PAHs extracted from the sediments of the Pettaquamscutt River are plotted in Figures 7 and 8 and listed in Appendix 4A. Results obtained for Siskiwit Lake are plotted in Figure 9 and listed in Appendix 4B. Because the Pettaquamscutt River sediments yield a higher resolution record of $^{14}C$ abundance in individual PAHs than Siskiwit Lake, we will focus primarily on the results obtained for the former throughout this discussion. Results obtained for perylene and TOC are detailed in Chapter 7.

The $\Delta^{14}C$ values obtained in this study are an average for the sediment layers that were combined to obtain sufficient sample for compound-specific $^{14}C$ analysis. Because the concentrations of PAHs vary greatly with depth, we used the PAH concentration data to calculate the weighted-average depth at which $\Delta^{14}C$ values for individual PAHs should be plotted. This calculation was particularly important for plotting the $\Delta^{14}C$ values obtained for retene (H7 and H8) and fluoranthene (H6+H7+H8) since horizons 6 to 8 span a large gradient in PAH concentration (10-200 ng $g^{-1}$ for Fla) and sources of contrasting $^{14}C$ content, based on energy consumption data (mainly wood for H7 and H8, and some coal in H6). For example, if the $\Delta^{14}C$ data for fluoranthene (H6+H7+H8) were plotted at the average depth of the combined layers (56.5 cm - 1807) that would give the

impression that combustion of coal was an important source of this compound in 1807. However, the weighted-average depth for fluoranthene (H6+H7+H8) (50.5 cm – 1835) places this $\Delta^{14}C$ data point at a year of deposition coherent with the reported historical consumption of coal and wood in the USA (www.eia.doe.gov/emeu/aer). To calculate the weighted-average depth, the amount (ng) of a given PAH was calculated for each depth interval that comprised the horizon of interested (concentration * mass of sediment extracted). These masses were subsequently summed and the percent contribution of each interval to the horizon of interest was calculated. Each percent contribution was multiplied by its corresponding mid-point depth, and the sum of these results corresponds to the weighted-average depth for the horizon (example in Table 2).

Table 2. Example of calculation of weighted-average depth using data acquired for retene

| Depth (cm) | Mid-Point Depth (cm) | Year | Mass sediment extracted (g) | Concentration (ng $g^{-1}$) | Mass of Compound (ng) | % Contribution to Total in Horizon | Weighted-Average Depth (cm) |
|---|---|---|---|---|---|---|---|
| 65 | 65.25 | 1761 | 1.39 | 50.6 | 70.5 | 13.4 | |
| 66 | 66.25 | 1755 | 1.38 | 51.9 | 71.4 | 13.6 | |
| 67 | 67.25 | 1750 | 1.41 | 71.8 | 101.2 | 19.2 | |
| 68 | 68.25 | 1745 | 1.37 | 73.8 | 101.2 | 19.2 | **67.9**[a] |
| 69 | 69.25 | 1740 | 1.37 | 53.5 | 73.6 | 14.0 | |
| 70 | 70.25 | 1735 | 1.37 | 79.2 | 108.8 | 20.7 | |
| | | | | **Sum** | **526.7** | | |

[a] (0.134*65.25) + (0.136*66.25) + (0.192*67.25) + (0.192*68.25) + (0.140*69.25) + (0.207*70.25)

Some interesting trends can be observed in Figure 7. First, most of the PAHs isolated from sediments deposited after the turn of the 20th century contain little to no $^{14}C$. This result is consistent with combustion of fossil fuels being the dominant source of pyrogenic PAHs in contemporary sediments (Reddy et al., 2002a). Perylene, retene and, to a lesser extent, phenanthrene are exceptions to this generalization. Perylene will be discussed separately in Chapter 7. Excluding retene and perylene, phenanthrene is consistently the most modern PAH analyzed, with $\Delta^{14}C$ values ranging from –650‰ in horizon 3 (~1948) to –800‰ in combined horizons 1 and 2 (~1978). Phenanthrene was

also the most modern PAH determined on a sample of household soot produced by the combustion of creosote-contaminated softwood (Reddy et al., 2003). Although phenanthrene can be produced by virtually any combustion process and is one of the most abundant pyrogenic PAHs found in indoor and outdoor air (Hawthorne et al., 1992; Naumova et al., 2002), its radiocarbon composition seems to be more heavily influenced by combustion of modern biomass than any other pyrogenic PAH analyzed in the top five horizons. Unfortunately, the concentrations of phenanthrene in horizons 6, 7 and 8 were too small to be run by the NOSAMS facility, so we cannot confirm that this compound has consistently retained a mixed $^{14}C$ signature.

The $\Delta^{14}C$ values obtained for retene contrast markedly with results obtained for other pyrogenic PAHs. Retene is derived from the thermal and natural transformation of abietic acid[2] present in resins of coniferous wood and has long been proposed as a marker of combustion of soft wood (Simoneit and Mazurek, 1982; Ramdahl, 1983). Several studies have used retene as a tracer for biomass burning. For example, measurements of retene in extracts of air particulate matter from Albuquerque, NM indicated that residential wood combustion was the dominant source of PAHs to that area (Benner et al., 1995) and the presence of retene in snow samples was used as evidence of boreal forest fire residues in Greenland (Masclet et al., 2000). In addition to combustion of softwood, retene can also be produced *in situ* by the diagenesis of abietic acid (Ramdahl, 1983). For example, Laflamme and Hites (1978) found remarkable amounts of retene and pimanthrene (another component of pine resin) in soils from South Carolina and associated their presence to the pine forest surrounding the sampling site. Analyses of soil samples from a wooded area in Yosemite National Park in California yielded similar results (Laflamme and Hites, 1978). Moreover, anaerobic incubation of sediments spiked

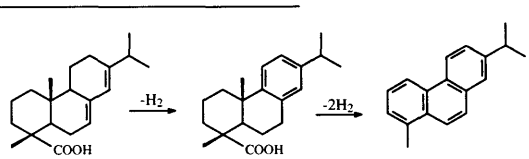


2 Abietic Acid Dehydroabietic Acid Retene

Mechanism of formation of retene (Benner et al., 1995).

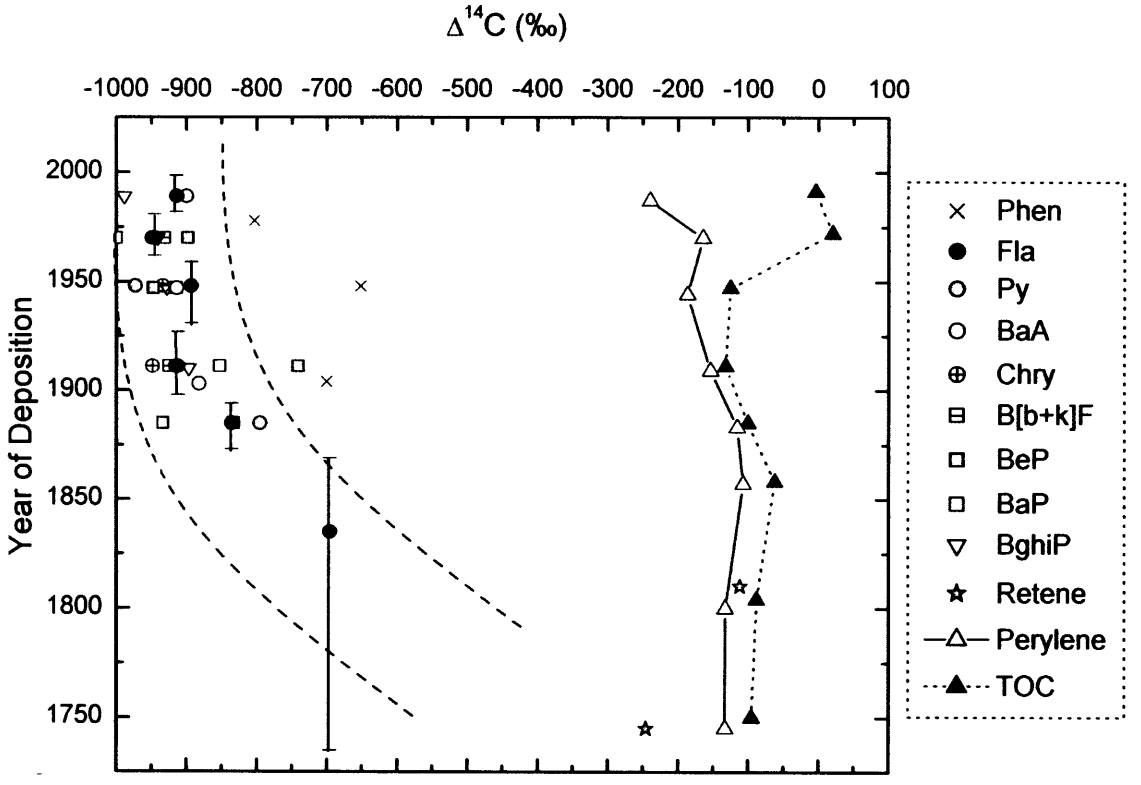


Figure 7. Down-core profile of the radiocarbon abundance of individual PAHs and TOC. Depth-interval of each horizon is shown as error bars on fluoranthene. $\Delta^{14}C$ errors are listed in Appendix 4. The slight differences in year of deposition among compounds of the same horizon are due to the use of weighted-average depth (see text).

with 6-$d_2$-dehydroabietic acid reportedly produced small quantities of *d*-retene (Tavendale et al., 1997). The radiocarbon results obtained for horizons 7 and 8 show good correlation among retene, perylene and TOC (Figure 7). The similar $^{14}C$ values for these components could indicate that retene was produced *in situ* by the diagenesis of abietic acid brought to the sediments as part of the TOC. The sedimentary profile of retene (Appendix 1B, Figure 3) shows a maximum in concentration in the early 1800s, which can be related to a period of intense deforestation in southern Rhode Island. It has been reported that by 1870, the White Pine forests of the northeastern United States were heavily depleted due to land clearing and utilization of wood as energy source

(www.forestresources.com/novdec99.html). If the increase in retene concentration observed in the early 1800s were related to a significant rise in combustion of wood in the region adjacent to the watershed of the Pettaquamscutt River, then a concurrent increase in concentration of other pyrogenic PAHs would be expected. However, while retene concentrations rose 7-fold between 1774 and 1815, pyrene and total PAHs concentrations increased less than 2-fold. The more likely scenarios for the origin of retene in the sediments of the Pettaquamscutt River relate its increase in concentration to intense deforestation of White Pine forests. Either abietic acid (or dehydroabietic acid) was intensively eroded from soils due to land clearing and logging, and transformed into retene in the anoxic sediments, or this transformation occurred in the soils prior to erosion and transport. In either case, the Pettaquamscutt River data indicates that aside from functioning as a marker for combustion of wood in aerosol samples, retene also has the potential to be used as a tracer for land clearing in regions formerly covered by pine forests. It is noteworthy that the radiocarbon results obtained for retene in horizons 7 and 8 of the Pettaquamscutt River sediments are $^{14}C$-poor compared to values reported by Reddy and collaborators (2003) for household soot produced by combustion of softwood in fireplaces. The difference in the $\Delta^{14}C$ content of retene between these two studies probably results from the incorporation of significant amounts of bomb-$^{14}C$ by the wood combusted to produce the soot analyzed by Reddy and collaborators, while our measurements were conducted on retene deposited prior to the onset of nuclear weapons tests.

In general, the $^{14}C$ abundance of individual pyrogenic PAHs vary within 150‰ of each other at a given sediment horizon. This isotopic heterogeneity is clearly apparent in horizon 3 (1940-1963), where compound-specific radiocarbon values vary from -970‰ for pyrene to -650‰ for phenanthrene. In contrast, $\Delta^{14}C$ of TOC and perylene at the same horizon were measured at -130 and -190‰, respectively. $^{14}C$ abundances for structural isomers usually lie within 60‰ (Figure 8), in agreement with results obtained by Reddy and collaborators (2003). In addition, the $\Delta^{14}C$ results obtained for individual PAHs in this study provide a basis to evaluate certain compounds that are currently used as

molecular tracers for specific combustion sources. For example, benzo[*ghi*]perylene has been suggested as a marker for tracing automobile emissions that could compensate for the phase-out of Pb in gasoline (Currie et al., 1994). Benzo[*ghi*]perylene present in the sediments of the Pettaquamscutt River contains little to no $^{14}C$, consistent with its suggested fossil source. Also, while fluoranthene and pyrene reflect a slightly greater contribution of modern $^{14}C$ between 1999-1982 (H1) than in 1982-1963 (H2), benzo[*ghi*]perylene became more $^{14}C$-depleted in the same period. In contrast, benzo[*ghi*]perylene isolated from Standard Reference Material 1944 (New York/New Jersey waterway sediment) was slightly more $^{14}C$-modern than perylene from the same sample (Reddy et al., 2002a). These two studies illustrate the problem associated with relying in one single compound for source apportionment.

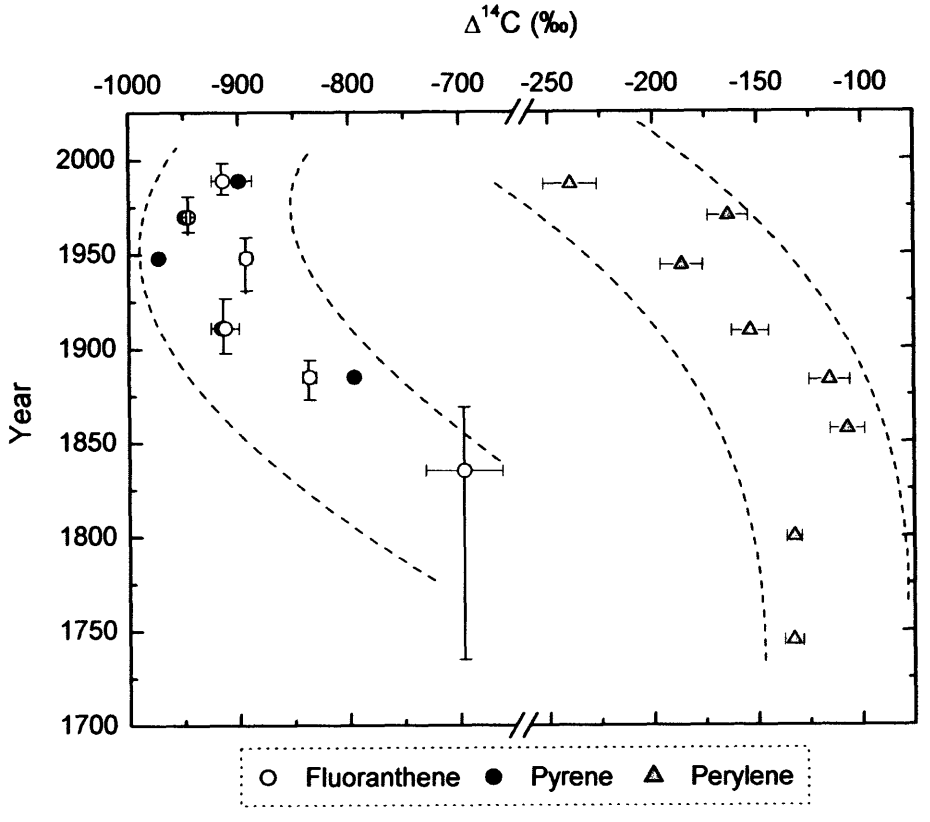


Figure 8. Trends in the radiocarbon content of individual PAHs in the last 250 years.

The $\Delta^{14}C$ profiles of pyrene, fluoranthene and perylene (Figure 8) capture the general trends in $^{14}C$ abundance observed for PAHs present in the sediments of the Pettaquamscutt River. *In situ* production is the dominant source of perylene in sediment intervals deposited prior to 1950. In surficial layers, the concentration of naturally produced perylene is small (Appendix 1B, Figure 3) and perylene derived from the combustion of fossil fuels becomes an important fraction of the total, thus the trend towards $^{14}C$-depleted values with decreasing depth observed in Figure 8. In contrast, the $^{14}C$ contents of pyrene and fluoranthene have decreased significantly since the mid-1800s. Prior to 1850, wood was the main source of energy in the United States, at which point coal became responsible for 10% of the total energy production. By 1900, fossil fuel combustion (coal + petroleum) had drastically increased and accounted for over 75% of the total energy consumption (www.eia.doe.gov/emeu/aer). The accelerated release of $^{14}C$-free $CO_2$ from burning of fossil fuels in the mid to late 1800s was responsible for a dilution of atmospheric $^{14}CO_2$, termed the Suess effect (Stuiver and Quay, 1981). While this term is commonly used in referring to atmospheric $CO_2$, one could argue that the trend towards decreasing $^{14}C$ abundance observed for fluoranthene and pyrene, due to the increased use of fossil fuels, could also be referred to as the Suess effect.

$^{14}C$-depleted values for PAHs deposited prior to 1875 indicate a large fossil component at a time when fossil fuel usage was still low (<35%, www.eia.doe.gov/emeu/aer). By applying a simple mass balance to fluoranthene $^{14}C$ data presented in Figure 8, it is possible to calculate the contribution of combustion of fossil and modern biomass to each horizon (Table 3). We chose fluoranthene for this exercise because it was the only pyrogenic PAH for which we had $^{14}C$ data spanning the largest time interval (1735-1998). The results obtained for the fractional contribution of modern biomass to the fluoranthene $\Delta^{14}C$ signatures are in good agreement with the amount of wood burned for heating purposes in the USA from the 1960s to the present. However, the $^{14}C$ abundance in fluoranthene seems to underestimate the amount of wood burned in the early 1800s. While our calculations point to wood burning contributing 35% of the fluoranthene in the sediment, estimates of the consumption of wood during that time are

much higher (95%) (www.eia.doe.gov/emeu/aer). Unfortunately, we have only been able to acquire one radiocarbon data point for pyrogenic PAHs at the bottom of the Pettaquamscutt River sediment core, where low concentrations prevent isolation of sufficient mass for AMS analysis, so we cannot compare this result to others. It is possible that, instead of underestimating the amount of wood burned in the early 1800s our data may be pointing to a higher contribution of fossil sources to the New England area in those early days, compared to other parts of the country. For example, Levin and collaborators (1989) have shown that highly populated areas can produce localized Suess effects of up to $\Delta^{14}C$ = -100‰, particularly during the winter. More data is needed before we can draw any firm conclusions one way or another. Nevertheless, the $^{14}C$ abundance in isolated PAHs seems to correctly describe the general pattern of energy consumption in the last 100-150 years.

Table 3. Contribution of fossil and modern biomass burning to the PAH inventory over the decades.

| Horizon | Year | $\Delta^{14}C$ Fla (‰) | $\Delta^{14}C$ Wood (‰)[a] | $\Delta^{14}C$ Fossil (‰) | Proportion[b] | | Consumption of Wood as Energy Source[c] (%) | $\Delta^{14}C$ Fla if % Wood = Consumption |
|---|---|---|---|---|---|---|---|---|
| | | | | | Fossil | Wood | | |
| H1 | 1989 | -900 | 500 | -1000 | 0.93 | 0.07 | 0.04 | -940 |
| H2 | 1970 | -950 | 500 | -1000 | 0.97 | 0.03 | 0.04 | -940 |
| H5 | 1885 | -850 | 500 | -1000 | 0.90 | 0.10 | 0.48 | -880 |
| H1 | 1989 | -900 | 225 | -1000 | 0.92 | 0.08 | 0.04 | -951 |
| H2 | 1970 | -950 | 225 | -1000 | 0.96 | 0.04 | 0.04 | -951 |
| H5 | 1885 | -850 | 225 | -1000 | 0.88 | 0.12 | 0.48 | -902 |
| H6+H7+H8 | 1850 | -700 | -150[d] | -1000 | 0.65 | 0.35 | 0.95 | -193 |

[a] Range in modern wood values estimated by (Klinedinst and Currie, 1999) and (Reddy et al., 2003)

[b] $\Delta^{14}C_{Fla} = (f_{Wood} * \Delta^{14}C_{Wood}) + (f_{Fossil} * \Delta^{14}C_{Fossil})$, $f_{Wood} + f_{Fossil} = 1$

[c] Calculated from data obtained at www.eia.doe.gov

[d] Value obtained for retene, a marker of combustion of biomass

It is thought that the range in $\delta^{13}C$ values of PAHs generated during pyrolysis is correlated to the isotopic signature of the source. Therefore, compound-specific carbon isotopic composition could be used to apportion the sources of PAHs. Initial samples analyzed by O'Malley and collaborators (1994) demonstrated that the isotopic composition of PAHs generated by wood burning varied with ring size, with 3- and 5-ring PAHs being more $^{13}C$-depleted than 4-ring compounds. The $\delta^{13}C$ results obtained for individual PAHs from the sediments of the Pettaquamscutt River (Figure 9, Appendix 4 and 5) show no clear trend with ring size. However, pyrogenic PAHs were consistently $^{13}C$-enriched (-26 to -21.5‰) compared to perylene (-28.5 to -27.5‰). The two data points obtained for retene fell within the range of $\delta^{13}C$ of pyrogenic PAHs. The effects of

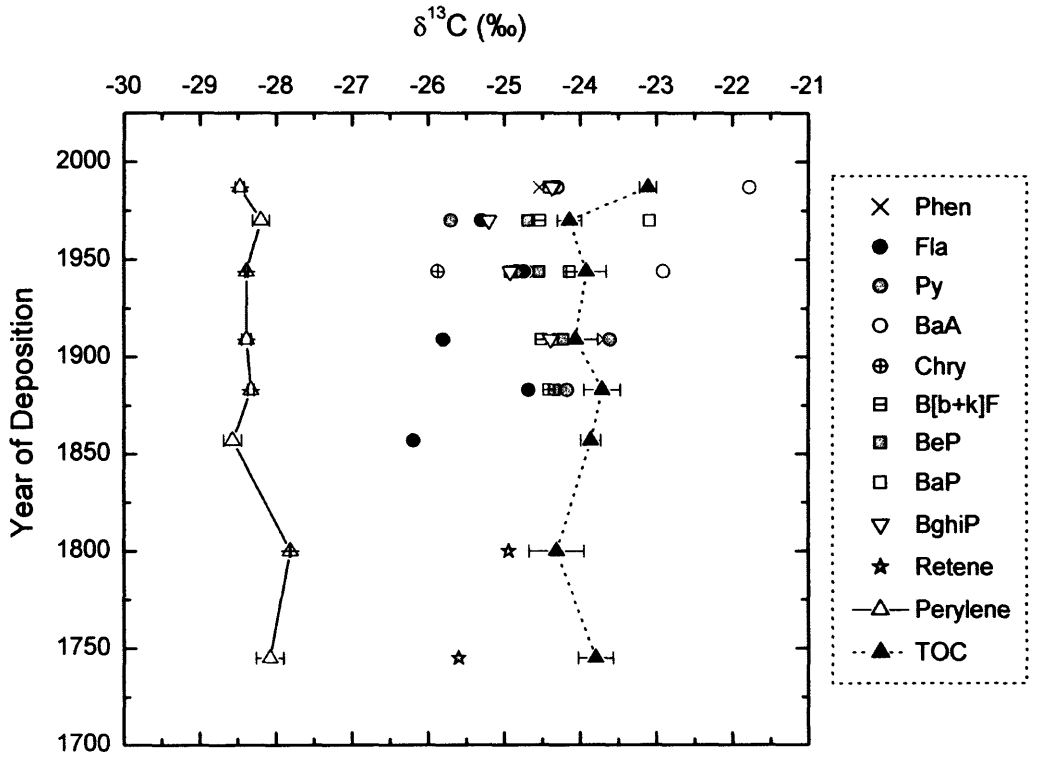


Figure 9. Down-core profile of $\delta^{13}C$ of individual PAHs and TOC from Pettaquamscutt River sediments.

temperature of formation on the $\delta^{13}C$ of PAHs were addressed by McRae and collaborators (1999), who determined the isotopic composition of PAHs derived from coals of different ranks and process conditions. The authors observed that the $\delta^{13}C$ values of individual PAHs became more $^{13}C$-depleted with increasing temperature of formation. PAHs released by low temperature combustion processes showed $\delta^{13}C$ values similar to those of their source, whereas PAHs produced by high temperature pyrolysis were approximately 4‰ more depleted than PAHs produced at low temperature. The idea that the different temperatures achieved during the combustion of coal, wood, gasoline and diesel may allow for a wide enough range in $\delta^{13}C$ that can help further constrain the environmental sources of combustion-derived PAHs is very attractive. However, combustion of different fuels can yield similar mixtures of pyrogenic PAHs and the range in $\delta^{13}C$ of the main energy sources (coal, petroleum and wood) greatly overlaps in the -30 to -20‰ range (Hunt, 1996). Hence, the difficulty in relying solely on $\delta^{13}C$ measurements to separate the contribution of PAHs derived from one combustion process versus another.

The $\Delta^{14}C$ results obtained for the Pettaquamscutt River sediments co-vary with data obtained for Siskiwit Lake (Figure 10). PAH concentrations are low at this location, negating the determination of $^{14}C$ abundance on individual compounds. Instead, 13 PAHs[3] were combined for each horizon before $^{14}C$ determination at the NOSAMS facility. Although measured in coarser resolution, the $\Delta^{14}C$ results obtained for Siskiwit Lake are comparable to those acquired for the Pettaquamscutt River (Figure 10, Appendix 4B). Because this location is approximately 55 km away from the nearest populated area (McVeety and Hites, 1988), it receives a smaller load of PAHs derived from combustion of fossil fuels than the Pettaquamscutt River, much in the way populated areas show a larger and localized Suess effect (Levin et al., 1989). The smaller contribution of fossil-derived PAHs to Siskiwit Lake is clearly illustrated in Figure 10. In

[3] Total PAHs were calculated as the sum of phenanthrene, anthracene, fluoranthene, pyrene, benzo[*a*]anthracene, chrysene, benzo[*b*]fluoranthene, benzo[*j*]fluoranthene, benzo[*k*]fluoranthene, benzo[*a*]pyrene, benzo[*e*]pyrene, indeno[*123-cd*]pyrene and benzo[*ghi*]perylene.

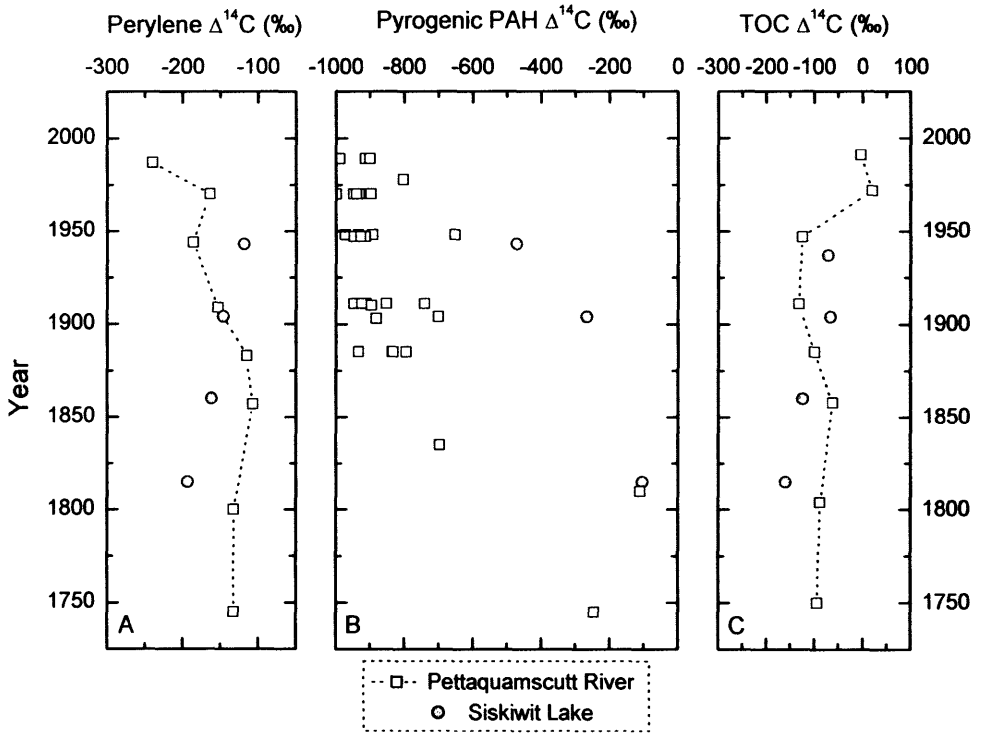


Figure 10. Comparison of the $^{14}C$ abundance in (a) perylene, (b) pyrogenic PAHs and (c) TOC in Siskiwit Lake and in the Pettaquamscutt River. The radiocarbon values presented for pyrogenic PAHs is Siskiwit Lake are a mixture of 13 compounds (Phen, Anth, Fla, Py, BaA, Chry, BbF, BjF, BkF, BaP, BeP, IP and BghiP).

addition, while perylene and TOC $\Delta^{14}C$ values in the Pettaquamscutt River indicate significant fossil fuel contributions beginning in the early 1900s (details in Chapter 7), the radiocarbon abundance of these species increased towards the present in the Siskiwit Lake core and showed no trace of a Suess effect (Figures 10a and c). The higher $^{14}C$ abundance in pyrogenic PAHs from Siskiwit Lake attests to the reduced contribution of fossil-derived compounds to this remote location prior to 1900. This implies that copper mining operations active in Isle Royale from 1849-1855 did not contribute notable amounts of $^{14}C$-poor PAHs to this system. Most likely, 19$^{th}$ century colonization of the island relied solely on combustion of wood, consistent with reports of disappearance of more than half of its original plant species (www.nyx.net/~sjhoward/Isle_Royale). All

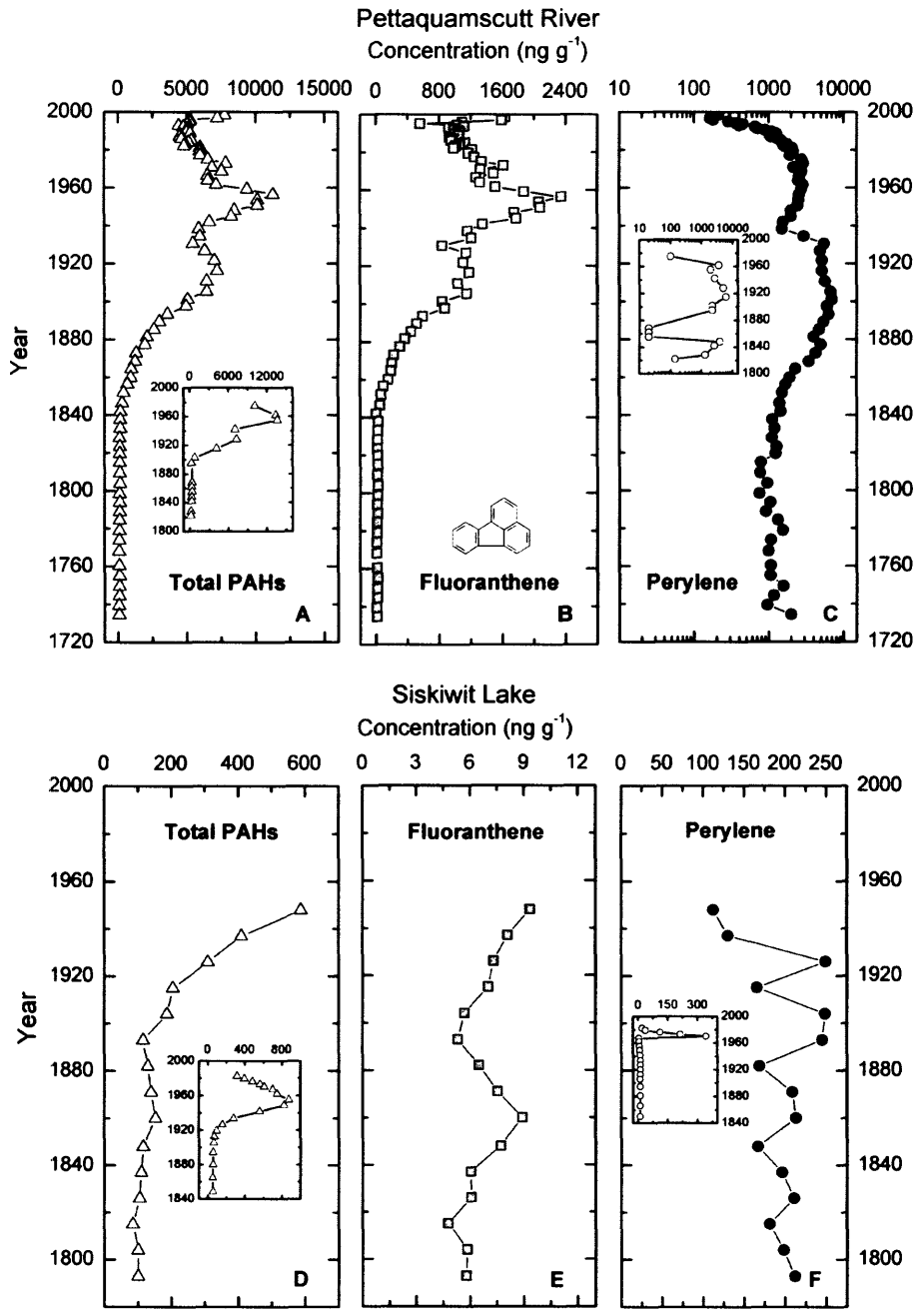


Figure 11. Concentration profile of total PAHs, fluoranthene and perylene in the Pettaquamscutt River (a-c) and Siskiwit Lake (d-f). Total PAHs were calculated as the sum of (Fluo, Phen, Anthr, Fla, Py, BaA, Chry, BbF, BkF, BaP, BeP, DBA, IP, BghiP and Cor – Pettaquamscutt River) and (Phen, Anthr, Fla, Py, BaA, Chry, BbF, BjF, BkF, BaP, BeP, IP and BghiP – Siskiwit Lake). Smaller plots correspond to data obtained by previous work by Hites and collaborators (1980) (Pettaquamscutt River) and McVeety (1986) (Siskiwit Lake).

pyrogenic PAHs deposited in the Pettaquamscutt River during the maximum period of deposition in the 1950s (Figure 11) contained significantly less $^{14}C$ than equivalent compounds reaching Siskiwit Lake (Figure 10). For example, while pyrogenic PAHs deposited in the Pettaquamscutt River sediments in 1900 show $\Delta^{14}C$ values between –700 and –920‰, total PAHs deposited in Siskiwit Lake at that time were significantly more enriched in $^{14}C$ (-270‰). This reinforces our believe that the New England region may have been more heavily affected by the early use of fossil fuels than other parts of the USA.

In summary, radiocarbon measurement of PAHs at the molecular level has given us new insights into the complexity of sources of these compounds. Our increasing reliance on combustion of fossil fuel was clearly illustrated in the trend of individual PAHs towards more negative $\Delta^{14}C$ values, with the well-known Suess effect being easily observed in the $^{14}C$ composition of this class of compounds. The combination of compound-specific radiocarbon measurements and down-core concentration profile revealed the potential of using retene as a tracer for land clearing in regions formerly covered by pine forests. $^{14}C$-poor values for PAHs deposited prior to 1875 indicate a large fossil component at a time when fossil fuel usage was still low. Therefore, the $^{14}C$ content of fluoranthene was used to calculate the fractional contribution of modern biomass to the PAH burden over time. The results obtained showed that either we are underestimating the amount of wood burned in the early 1800s or our data is pointing to a higher contribution of fossil sources to the New England area in those early days, versus other parts of the country. Comparison between the data obtained for the suburban Pettaquamscutt River and the remote Siskiwit Lake highlight that although atmospheric processes transport and widely disperse combustion-derived PAHs, regions closer to point sources receive higher contributions of these compounds. Even at the period of maximum deposition of PAHs (1950), the $^{14}C$ content of the compounds deposited in Siskiwit Lake shows a significant contribution from non-fossil sources.

## 4. REFERENCES


Appleby P. and Oldfield F. (1978) The calculation of lead-210 dates assuming a constant rate of supply of unsupported $^{210}Pb$ to the sediment. *Catena* **5**, 1-8.

Benner B. A., Wise S. A., Currie L. A., Klouda G. A., Klinedinst D. B., Zweidinger R. B., Stevens R. K., and Lewis C. W. (1995) Distinguishing the contributions of residential wood combustion and mobile source emissions using relative concentrations of dimethylphenanthrene isomers. *Environ. Sci. Technol.* **29**, 2382-2389.

Boothroyd J. (1991) The geologic history of Narrow River. *Maritimes* **35**(2), 3-5.

Cooper J., Currie L., and Klouda G. (1981) Assessment of contemporary carbon combustion source contributions to urban air particulate levels using carbon-14 measurements. *Environ. Sci. Technol.* **15**(9), 1045-1050.

Currie L. A., klouda G. A., Klinedinst D. B., Sheffield A. E., Jull A. J. T., Donahue D. J., and Connolly M. V. (1994) Fossil- and bio-mass combustion: C-14 for source identification, chemical tracer development, and model validation. *Nucl. Instrum. Methods Phys. Res.* **B92**, 404-409.

Czuczwa J. and Hites R. (1986) Airborne dioxins and dibenzofurans: sources and fates. *Environ. Sci. Technol.* **20**, 195-200.

Dasch J. (1982) Particulate and gaseous emissions from wood-burning fireplaces. *Environ. Sci. Technol.* **16**(10), 639-645.

Denissenko M., Pao A., Tang M.-S., and Pfeifer G. (1996) Preferential formation of benzo[*a*]pyrene adducts at lung cancer mutational hotspots in P53. *Science* **274**, 430-432.

Eglinton T. I., Aluwihare L. I., Bauer J. E., Druffel E. R. M., and McNichol A. P. (1996a) Gas chromatographic isolation of individual compounds from complex matrices for radiocarbon dating. *Anal. Chem.* **68**(5), 904-912.

Eglinton T. I., Pearson A., McNichol A., Currie L., Benner B. A., and Wise S. (1996b) Compound specific radiocarbon analysis as a tool to quantitatively apportion modern and fossil sources of polycyclic aromatic hydrocarbons in environmental matrices. *212th ACS National Meeting*, 205-207.

Eglinton T. I., Benitez-Nelson B. C., Pearson A., McNichol A. P., Bauer J. E., and Druffel E. R. M. (1997) Variability in radiocarbon ages of individual organic compounds from marine sediments. *Science* **277**, 796-799.

Fernández P., Vilanova R. M., and Grimalt J. O. (1999) Sediment fluxes of polycyclic aromatic hydrocarbons in European high altitude mountain lakes. *Environ. Sci. Technol.* **33**, 3716-3722.

Gaines A. (1975) Papers on the geomorphology, hydrography and geochemistry of the Pettaquamscutt River estuary. PhD, University of Rhode Island.

Gaines A. G. J. and Pilson M. E. Q. (1972) Anoxic water in the Pettaquamscutt River. *Limnol. Oceanogr.* **17**(1), 42-49.

Gschwend P. M. and Hites R. A. (1981) Fluxes of polycyclic aromatic hydrocarbons to marine and lacustrine sediments in the northeastern United States. *Geochim. Cosmochim. Acta* **45**, 2359-2367.

Hawthorne S., Miller D., Langerfeld J., and Krieger M. (1992) PM-10 high-volume collection and quantification of semi-nonvolatile phenols, methoxylated phenols, alkanes, and polycyclic aromatic hydrocarbons from winter urban air and their relationship to wood smoke emissions. *Environ. Sci. Technol.* **26**(11), 2251-2261.

Hermes O., Gromet L., and Murray D. (1994) Bedrock Geologic Map of Rhode Island. In *Rhode Island Map Series No.1.*

Hites R. A., Laflamme R. E., Windsor Jr J. G., Farrington J. W., and Deuser W. G. (1980) Polycyclic aromatic hydrocarbons in an anoxic sediment core from the Pettaquamscutt River (Rhode Island, USA). *Geochim. Cosmochim. Acta* **44**, 873-878.

Hodel E. and Menezes S. (2000) Tidal effects on phytoplankton in the Pettaquamscutt River Estuary. espo.gso.uri.edu/~surfo/pubs/papers/hodel.pdf.

Hunt J. (1996) *Petroleum Geochemistry and Geology*. W.H. Freeman and Company

Kawamura K. and Suzuki I. (1994) Ice core record of polycyclic aromatic hydrocarbons over the past 400 years. *Naturwissenschaften* **81**, 502-505.

Kelly R. and Moran S. (2002) Seasonal changes in groundwater input to a well-mixed estuary estimated using radium isotopes and implications for coastal nutrient budgets. *Limnol. Oceanogr.* **47**(6), 1796-1807.

Klinedinst D. B. and Currie L. A. (1999) Direct quantification of PM2.5 fossil and biomass carbon within the Northern front range air quality study's domain. *Environ. Sci. Technol.* **33**, 4146-4154.

Krishnaswamy S., Lal D., Martin J., and Meybeck M. (1971) Geochronology of lake sediments. *Earth Planet. Sci. Lett.* **11**, 407-414.

Laflamme R. E. and Hites R. A. (1978) The global distribution of polycyclic aromatic hydrocarbons in recent sediments. *Geochim. Cosmochim. Acta* **42**, 289-303.

Levin I., Schuchard J., Kromer B., and Münnich K. (1989) The continental European Suess effect. *Radiocarbon* **31**(3), 431-440.

Lichtfouse E. and Eglinton T. (1995) $^{13}C$ and $^{14}C$ evidence of pollution of a soil by fossil fuel and reconstruction of the composition of the pollutant. *Org. Geochem.* **23**(10), 969-973.

Lima A. L. C., Eglinton T. I., and Reddy C. M. (2003) High-resolution record of pyrogenic polycyclic aromatic hydrocarbon deposition during the 20$^{th}$ century. *Environ. Sci. Technol.* **37**, 53-61.

Lipiatou E., Marty J.-C., and Saliot A. (1993) Sediment trap fluxes of polycyclic aromatic hydrocarbons in the Mediterranean sea. *Mar. Chem.* **44**, 43-54.

Masclet P., Hoyau V., Jaffrezo J. L., and Cachier H. (2000) Polycyclic aromatic hydrocarbon deposition on the ice sheet of Greenland. Part I: Superficial snow. *Atmos. Environ.* **34**, 3195-3207.

McNichol A., Jull A., and Burr G. (2001) Converting AMS data to radiocarbon values: considerations and conventions. *Radiocarbon* **43**(2A), 313-320.

McRae C., Sun C.-G., Snape C., Fallick A., and Taylor D. (1999) $\delta^{13}C$ values of coal-derived PAHs from different processes and their application to source apportionment. *Org. Geochem.* **30**(8), 881-889.

McVeety B. (1986) Atmospheric deposition of polycyclic aromatic hydrocarbons to water surfaces: a mass balance approach. PhD, Indiana University.

McVeety B. and Hites R. (1988) Atmospheric deposition of polycyclic aromatic hydrocarbons to water surfaces: a mass balance approach. *Atmos. Environ.* **22**(3), 511-536.

Naumova Y., Eisenreich S., Turpin B., Weisel C., Morandi M., Colome S., Totten L., Stock T., Winer A., Alimokhtari S., Kwon J., Shendell D., Jones J., Maberti S., and Wall S. (2002) Polycyclic aromatic hydrocarbons in the indoor and outdoor air of three cities in the U.S. *Environ. Sci. Technol.* **36**, 2552-2559.

Ohkouchi N., Kawamura K., and Kawahata H. (1999) Distributions of three- to seven-ring polynuclear aromatic hydrocarbons on the deep sea floor in the Central Pacific. *Environ. Sci. Technol.* **33**, 3086-3090.

O'Malley V., Abrajano Jr T., and Hellou J. (1994) Determination of the $^{13}C/^{12}C$ ratios of individual PAH from environmental samples: can PAH sources be apportioned? *Org. Geochem.* **21**(6/7), 809-822.

Orr W. L. and Gaines A. G. J. (1973) Observations on the rate of sulfate reduction and organic matter oxidation in the bottom waters of an estuarine basin: the upper basin of the Pettaquamscutt River (Rhode Island). In *Advances in Organic Geochemistry* (ed. B.Tissot and F. Bienner), pp. 791-812. Technip.

Pearson A., McNichol A., Schneider R., and von Reden K. (1998) Microscale AMS $^{14}C$ measurement at NOSAMS. *Radiocarbon* **40**(1), 61-75.

Pereira W., Hostettler F., Luoma S., Van Geen A., Fuller C., and Anima R. (1999) Sedimentary record of anthropogenic and biogenic polycyclic aromatic hydrocarbons in San Francisco Bay, California. *Mar. Chem.* **64**, 99-113.

Prahl F. and Carpenter R. (1983) Polycyclic aromatic hydrocarbon (PAH)-phase associations in Washington coastal sediment. *Geochim. Cosmochim. Acta* **47**, 1013-1023.

Ramdahl T. (1983) Retene - a molecular marker of wood combustion in ambient air. *Nature* **306**, 580-582.

Reddy C., Pearson A., Xu L., McNichol A., Benner Jr. B., Wise S., Klouda G., Currie L., and Eglinton T. (2002a) Radiocarbon as a tool to apportion the sources of polycyclic aromatic hydrocarbons and black carbon in environmental samples. *Environ. Sci. Technol.* **36**, 1774-1782.

Reddy C., Xu L., Eglinton T., Boon J., and Faulkner D. (2002b) Radiocarbon content of synthetic and natural semi-volatile halogenated organic compounds. *Environ. Pollut.* **120**, 163-168.

Reddy C. M., Xu L., and O'Connor R. (2003) Using radiocarbon to apportion sources of polycyclic aromatic hydrocarbons in household soot. *Environ. Forensics* **4**, 191-197.

Schneider A., Stapleton H., Cornwell J., and Baker J. (2001) Recent declines in PAH, PCB, and toxaphene levels in the northern Great Lakes as determined from high resolution sediment cores. *Environ. Sci. Technol.* **35**(19), 3809-3815.

Simoneit B. R. T. and Mazurek M. A. (1982) Organic matter in the troposphere. II. Natural background of biogenic lipid matter in aerosols over the rural western United States. *Atmos. Environ.* **16**, 2139-2159.

Stuiver M. and Polach H. A. (1977) Reporting of $^{14}C$ data. *Radiocarbon* **19**(3), 355-363.

Stuiver M. and Quay P. (1981) Atmospheric $^{14}C$ changes resulting from fossil fuel $CO_2$ release and cosmic ray flux variability. *Earth Planet. Sci. Lett.* **53**, 349-362.

Tan Y. L. and Heit M. (1981) Biogenic and abiogenic polynuclear aromatic hydrocarbons in sediments from two remote Adirondack lakes. *Geochim. Cosmochim. Acta* **45**, 2267-2279.

Tavendale M., McFarlane P., Mackie K., Wilkins A., and Langdon A. (1997) The fate of resin acids-1: The biotransformation and degradation of deuterium labelled dehydroabietic acid in anaerobic sediments. *Chemosphere* **35**(10), 2137-2151.

Van Metre P., Mahler B., and Furlong E. (2000) Urban sprawl leaves its PAH signature. *Environ. Sci. Technol.* **34**, 4064-4070.

Wang Z., Fingas M., Landriaukt M., Sigouin L., Feng Y., and Mullin J. (1997) Using systematic and comparative analytical data to identify the source of an unknown oil on contaminated birds. *Journal of Chromatography A* **775**, 251-265.

Wise S. A., Benner B. A., Chesler S. N., Hilpert L. R., Vogt C. R., and May W. E. (1986) Characterization of the polycyclic aromatic hydrocarbons from two standard reference material air particulate samples. *Anal. Chem.* **58**, 3067-3077.

Youngblood W. and Blumer M. (1975) Polycyclic aromatic hydrocarbons in the environment: homologous series in soils and recent marine sediments. *Geochim. Cosmochim. Acta* **39**, 1303-1314.

# CHAPTER 7

# ISOTOPIC CONSTRAINTS ON THE SOURCES OF PERYLENE IN AQUATIC SEDIMENTS

## 1. INTRODUCTION

Perylene is a non-alkylated polycyclic aromatic hydrocarbon (PAH) found widely in marine (Aizenshtat, 1973; Wakeham et al., 1979; Louda and Baker, 1984; Pereira et al., 1999) and lacustrine sediments (Laflamme and Hites, 1978; Wakeham et al., 1980; Gschwend and Hites, 1981; Tan and Heit, 1981; Doskey and Talbot, 2000) and is thought to derive mainly from two processes: *in situ* diagenetic alteration of an unknown precursor and oxidative combustion of carbonaceous materials.

Most studies report that sediment records of perylene differ greatly from those of typical anthropogenic PAHs (Hites et al., 1980; Tan and Heit, 1981; Silliman et al., 2001; Lima et al., 2003). The latter are typically high in sediments deposited in the 1950s and 1960s and low in older sediments, while perylene abundances are low at surface and tend to increase with depth. This increase in perylene concentration with depth reflects its *in situ* production (Aizenshtat, 1973; Wakeham, 1977) by either a first- or second-order reaction requiring anoxic conditions (Gschwend et al., 1983). However, there is still debate as to whether the precursor of perylene is a terrestrial (Aizenshtat, 1973; Laflamme and Hites, 1978) or a marine natural product (Wakeham et al., 1979; Hites et al., 1980). After measuring perylene in marine sediments enriched in hydrocarbons derived from higher plants, Aizenshtat (1973) hypothesized that its precursor was of terrestrial origin. In contrast, Wakeham and collaborators (1979) found elevated amounts of perylene in sediments from the Namibian shelf where land-derived inputs were considered minor and suggested that an aquatic precursor was more likely for that environment.

*In situ* production is not the only source of perylene to environmental settings. Perylene has been previously measured in a number of pyrogenic or combustion products, such as automobile exhaust (Blumer et al., 1977; Rogge et al., 1993), burning of soft and hardwoods (Fine et al., 2001), municipal incineration (Davies et al., 1976) and combustion of waste tires (Mastral et al., 1999). In addition, a few studies have reported good correlation between the down-core profiles of perylene and that of other PAHs (Simcik et al., 1996; Pereira et al., 1999). For example, a study of sediment cores from five sites in Lake Michigan showed that at four locations the profile of perylene paralleled that of other PAHs, suggesting a pyrogenic source for this compound (Simcik et al., 1996). Similar results were obtained for sediments collected in Richardson Bay, CA. At that site, perylene concentration was low prior to 1900 and gradually increased after the turn of the $20^{th}$ century. The authors related the rise in perylene concentrations towards the surface of the sediment core to an increase in anthropogenic activities around the Bay and suggested that combustion was the dominant source of perylene to that environment (Pereira et al., 1999). In addition, recent radiocarbon evidence indicates that both fossil-fuel combustion and modern biomass can be important contributors of perylene to sedimentary settings (Reddy et al., 2002). Measurement of the radiocarbon content of perylene extracted from two National Institute of Standards and Technology (NIST) Standard Reference Materials (SRMs) showed contrasting results. Perylene extracted from SRM 1941a (Organics in Marine Sediment; collected from Chesapeake Bay) yielded a similar $^{14}C$ value to that of bulk TOC and more modern than any other PAH in the sample, suggesting *in situ* production. In comparison, the $^{14}C$ content of perylene extracted from SRM 1944 (New York/New Jersey Waterway Sediment) was similar to the other PAHs of fossil origin, contrasting markedly with the bulk TOC (Reddy et al., 2002). This study demonstrated unambiguously the dual origin of sedimentary perylene.

In this study, we construct historical records of perylene and total organic carbon (TOC) for sediments from a suburban (Pettaquamscutt River) and a remote (Siskiwit Lake) environment. The concentration, radiocarbon and stable carbon isotopic

composition of perylene and TOC present in these basins are evaluated. This exercise underlined the difficulty of unveiling the unknown precursor of perylene. The combination of $\delta^{13}C$ and $\Delta^{14}C$ of perylene and TOC at these two distinct sites helped us discern with some confidence the importance of fossil fuels to the sedimentary profile of this PAH.

## 2. EXPERIMENTAL SECTION

A full description of the sampling sites, collection and depth-age relationship of the sediment cores were given in Chapters 4 and 6. Procedure for extraction and calculation of concentration of perylene was given in Chapter 3. Chapter 6 describes the procedure utilized for combining sediment cores and details the analytical methods employed for stable carbon and radiocarbon isotopic measurements and data reporting. Methods pertinent to TOC determinations are described below.

### 2.1 Total Organic Carbon Determinations

A Fisons 1108 elemental analyzer was used to measure the total organic carbon (TOC) content of the samples. To remove the inorganic carbon fraction, about 2 mg of dry sample was weighed into a silver capsule and acidified with 20 μL of 2N HCl. The samples were then dried in an oven at 50°C, wrapped, placed inside tin capsules for better catalysis of the oxidation reaction, and analyzed. Total organic carbon concentrations were calculated in relation to the whole sediment and organic carbon/organic nitrogen ($C_{org}/N_{org}$) ratios were calculated on an atomic basis. No significant difference was observed when $C_{org}/N_{org}$ and $C_{org}/N_{total}$ (not acidified) were compared for a couple of samples. Samples were run in triplicate and all reported weight percentages represent the mean ± one standard deviation. These values were determined from a 5-point calibration curve (0.09 to 1 mg) of a sulfanilamide standard. Instrumental blanks were run after sets of 12 analyses, yielding carbon blanks smaller than 0.004 mg and nitrogen blanks smaller than 0.005 mg.

### 2.2 Isotope ratio monitoring gas chromatography mass spectrometry (irm-GC/MS)

The stable carbon isotopic composition of bulk samples (TOC) were determined in triplicate by automated on-line solid combustion interfaced to a Finnigan Delta Plus isotope ratio mass spectrometer. Isotope ratios were calculated relative to $CO_2$ reference gas pulses, standard deviation for replicate measurements was always better than 0.6‰ and usually within 0.3‰.

## 3. RESULTS AND DISCUSSION

The concentration, radiocarbon and stable isotopic composition of perylene in the Pettaquamscutt River and Siskiwit Lake are evaluated and contrasted below. In addition, the values obtained in this study are compared to previous work conducted in these basins by Hites and collaborators (1980) and McVeety and Hites (1986; 1988). Diagnostic ratios and isotopic measurements of TOC were also assessed in an attempt at better understanding the possible sources of perylene to these systems.

### 3.1 Perylene

#### *3.1.1 Concentration Constraints*

The concentration profile of perylene in the Pettaquamscutt River and Siskiwit Lake sediments differ markedly from that of other parent PAHs derived from combustion sources (Figure 1, Appendix 1A and 1C). For example, the concentration of total PAHs[1] in the Pettaquamscutt River was low until 1850s, increased steadily to a maximum in the late-1950s, then declined until mid-1990s when this trend again reversed (Figure 1a). In contrast, perylene concentrations were low in surface sediments (210 ng $g^{-1}$), but increase rapidly to an initial maximum in 1973 (2900 ng $g^{-1}$), in a pattern typical of *in situ*

[1] Total PAHs are calculated as the sum of fluorene, phenanthrene, anthracene, fluoranthene, pyrene, benzo[*a*]anthracene, chrysene, benzo[*b*]fluoranthene, benzo[*k*]fluoranthene, benzo[*a*]pyrene, benzo[*e*]pyrene, dibenz[*ah*]anthracene, indeno[*123-cd*]pyrene, benzo[*ghi*]perylene and coronene ($n$ = 15).

production (Figure 1b). Similar trends were observed by Hites and collaborators (1980) in the upper basin of the Pettaquamscutt River (Figure 1a and 1b - detail), and by McVeety (1986) in Siskiwit Lake (Figure 1c and 1d - detail). These finding are consistent with other profiles found in the literature (Tan and Heit, 1981; Silliman et al., 2001) and reflect the differences in major sources of perylene versus other parent PAHs.

Even though the most recent portion (44 years – Chapter 6) of the Siskwit Lake sediment record was lost during sampling, clear differences in PAH concentrations between this remote site and the suburban Pettaquamscutt River are apparent. Anthropogenic PAHs in the sediments of Siskiwit Lake show a steady increase starting in the 1900s (Figure 1a and 1c), 50 years later than in the Pettaquamscutt River region. That is not surprising considering Rhode Island was one of the first states to be industrialized in the United States (Ingalls, 1908). Therefore, the early onset of increased PAH concentrations in the Pettaquamscutt River versus Siskiwit Lake indicates that the former felt the effects of combustion of fossil fuels earlier than other parts of the country due to its proximity to the sources. The fact that the maximum in total PAHs occurs at about the same time in both locations (late-1950s) (McVeety, 1986; McVeety and Hites, 1988) emphasizes the importance of atmospheric processes in the transport and deposition of these compounds.

The concentration profile of perylene seems to vary widely even within one aquatic system. Perylene concentrations in the Pettaquamscutt River sediments increased by an order of magnitude over a 25-year time interval (1973-1999), elevating its proportion in relation to total PAHs from 3% to 37%. A much faster increase in perylene concentrations with depth was observed by Hites and collaborators (1980) in the upper basin of the Pettaquamscutt River (Figure 1b-detail). In that study, perylene was shown to increase from 100 ng $g^{-1}$ in the surficial sediments (1975) to 3600 ng $g^{-1}$ at 4-cm (1962). While the maximum concentration obtained by Hites and collaborators (6000 ng $g^{-1}$ at 18-cm, 1915) resembles our results for the lower basin (6900 ng $g^{-1}$ in 1900), the shape of the two profiles is not similar (Figure 1b). The earlier study found that after

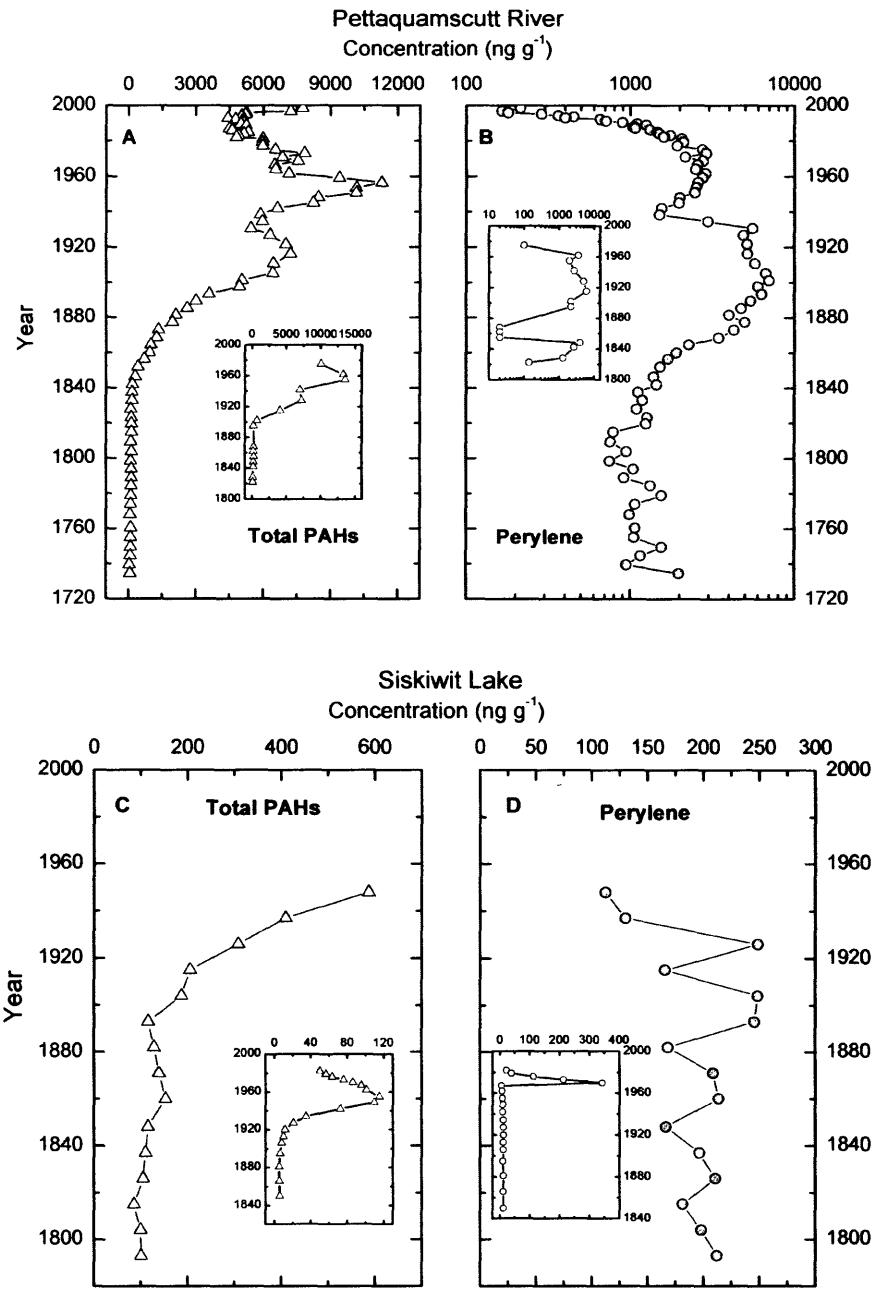


Figure 1. Concentration profile of total PAHs and perylene in the Pettaquamscutt River (a-b) and Siskiwit Lake (c-d). Total PAHs were calculated as the sum of (Fluo, Phen, Anthr, Fla, Py, BaA, Chry, BbF, BkF, BaP, BeP, DBA, IP, BghiP and Cor – Pettaquamscutt River) and (Phen, Anthr, Fla, Py, BaA, Chry, BbF, BjF, BkF, BaP, BeP, IP and BghiP – Siskiwit Lake). Smaller plots correspond to data obtained by previous work at these basins. Hites and collaborators (1980) in the Pettaquamscutt River and McVeety (1986) in Siskiwit Lake.

increasing ten-fold on the top portion of the core, perylene concentrations remained constant until 1895 and then proceeded to dip between 1875-1855. However, this dip in concentrations is not observed in the perylene profile we obtained for the lower basin of the Pettaquamscutt River. Since the upper and lower basin of the Pettaquamscutt River differ in sedimentary organic carbon contents and hydrological regimes (Urish, 1991), differences in the shape of the perylene profile are not surprising. Similar variations in concentration and profile shape were observed between our measurements in Siskiwit Lake and those reported by McVeety (1986). We consistently measured higher perylene concentrations than those reported previously for sediment horizons of the same age. Whereas McVeety reported approximately 10 ng $g^{-1}$ of perylene for sediments deposited in 1950, our data was one order of magnitude higher (110 ng $g^{-1}$). The differences in record are yet more striking when sediments deposited prior to 1900s are considered (250 ng $g^{-1}$ versus 10 ng $g^{-1}$ in 1895). Patchiness in the supply of the unknown precursor of perylene and variations in depositional conditions may account for the differences observed within one aquatic system. Finally, when the perylene record obtained for the Pettaquamscutt River is compared to that from the Siskiwit Lake we observe that perylene concentrations measured in the latter were consistently lower than those found in the former. While perylene was measured at 2500 ng $g^{-1}$ in the Pettaquamscutt River in the early 1950s only 100 ng $g^{-1}$ were found in corresponding layers in Siskiwit Lake. The differences in perylene concentration and profile shape encountered between sampling sites and more specifically in cores collected at the same small enclosed aquatic system (Siskiwit Lake) reveal the complexity of processes and factors that influence perylene formation.

An interesting feature of the perylene record in the Pettaquamscutt River is the abrupt shift in perylene concentrations (1927-1938) that parallels an abrupt change in trend TOC content (Figure 2). As will be discussed in section 3.2, the decrease in TOC concentrations after 1935 is attributed to a dilution of the organic carbon content by higher amounts of clastic material, which yielded the elevated mass accumulation rate (MAR) observed in Figure 2b. Because perylene is a minor constituent of the

sedimentary organic matter, its accumulation in the sediments was not significantly affected by the change in TOC MAR, only its concentration. The > 50% reduction in the maximum concentration of perylene between the 1900s (~6900 ng $g^{-1}$) and the 1970s (2900 ng $g^{-1}$) in the Pettaquamscutt River (Figure 2a) seems to be simply a reflection of variations in sedimentation rate. When MAR is taken into account (Figure 2b), the differences in maximum concentration of perylene are erased.

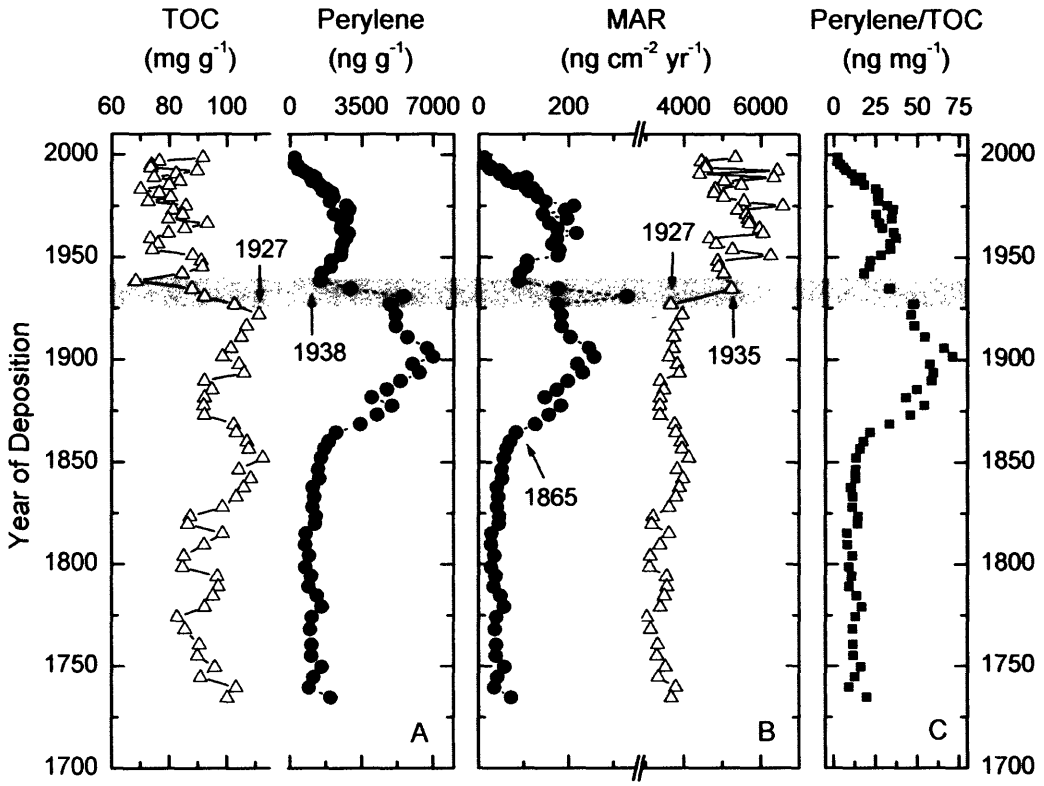


Figure 2. (a) Down core profiles of TOC and perylene show a shift towards lower concentrations between 1927 and 1935; (b) Mass accumulation rate (MAR) of TOC increased after 1927, while the major rise in perylene MAR occurred in 1865; (c) Ratio between perylene and TOC.

A striking feature of the perylene profile in both Pettaquamscutt River and Siskiwit Lake is that concentrations do not remain constant down-core, as would be expected for a compound that is not significantly degraded and is produced *in situ*. This trend towards decreasing concentrations after a peak in perylene concentration is observed in some (Wakeham et al., 1980; Tan and Heit, 1981; McVeety, 1986) (Figure 1b), but not all environments (Gschwend et al., 1983). While Wakeham and collaborators (1980) interpreted the decrease in perylene concentration with depth as a change in the source of the organic material accumulating in the sediments of the Greifensee delta (Germany), Tan and Heit (1981) had no explanation for its occurrence at Sagamore and Woods Lake, NY. Perylene is not known to undergo diagenetic degradation or alteration and has been found in significant amounts in sediments as old as the Lower to Middle Jurassic (~200 Myr) (Jiang et al., 2000). Some of the variables that could control the *in situ* production of perylene are (a) composition of the main source of organic carbon to the sediments; (b) rate of supply of the unknown precursor; (c) constancy of depositional conditions; (d) changes in the microbial community. As will be discussed in section 3.2, the main source of organic carbon to the Pettaquamscutt is thought to be aquatic biomass and that seems to have been the case for at least the past ~200 years. In addition, Orr and Gaines (1973) reported that the bottom waters of the Pettaquamscutt River have been anoxic for about 1700 years, since the marine flooding of this glacial valley. Hence, neither changes in the composition of the main source of organic matter nor changes in depositional conditions seem to be responsible for the lower concentration of perylene at the bottom of the core.

Silliman and collaborators (1998; 2001) have suggested that perylene formation could be controlled by the intensity of microbial degradation rather than the presence of a specific precursor. They hypothesize that perylene production is more efficient in low TOC environments, because perylene-forming microorganisms may not be capable of competing with other microbes when fresh labile TOC is available (Silliman et al., 2001). These authors suggest that environments that favor preservation of TOC are not conducive to perylene formation and give examples of environments where low TOC

(2.2%) gives rise to high perylene/TOC ratio (34.5 ng $mg^{-1}$, (Silliman et al., 1998)) and where high TOC (23%) is associated with low perylene/TOC ratios (Gschwend et al., 1983) to substantiate their hypothesis. A change in the microbial community in the sediments of the Pettaquamscutt River could certainly explain the shift from lower perylene concentrations prior to 1865 to higher values thereafter. However, the TOC content and perylene/TOC ratios obtained for the Pettaquamscutt River core do not agree with Silliman's hypothesis of increased perylene production in low TOC settings. If that were the case, the perylene/TOC ratio in the sediments of the Pettaquamscutt River should vary inversely to the trend in TOC content. That is, a higher perylene/TOC ratio would be expected prior to 1927 when TOC was on average 1.7% lower (Figure 2a and 2c). However, the calculated perylene/TOC ratio for this site is as high in 1868, when TOC content was 10.3%, as in 1954, when it was 7.4%. Moreover, while the TOC content in Siskiwit Lake is invariant at 8.2 ± 0.5%, the perylene/TOC ratio for these sediments varies from 13-30 ng $mg^{-1}$) (Figure 5). While we see no clear correlation between TOC content and perylene concentration, it seems plausible that microbial diversity may exert greater influence on the production of perylene than the source of organic matter. This hypothesis is consistent with the occurrence of perylene in environments dominated by aquatic and by terrestrial organic matter and with the highly variable $\delta^{13}C$ results reported for this compound in the literature (e.g., -23.9 to –23.6‰ (Jiang et al., 2000); -27.7 to –23.6‰ (Silliman et al., 2000); -28.6 to –27.8‰ this study).

*3.1.2 Radiocarbon Constraints*

Down-core compound-specific radiocarbon analysis (CSRA) enabled the decoupling of perylene produced *in situ* in the sediments from that generated during combustion and subsequently deposited in the Pettaquamscutt River. The results obtained show that the $\Delta^{14}C$ profile of perylene closely follows that of TOC in the deeper portions of cores from both locations, suggesting a natural, *in situ* source. However, the radiocarbon content of perylene present in surficial sediments from the Pettaquamscutt

River (H1 and H2, shallower than 19-cm) diverges from that of TOC, indicating an important contribution from fossil fuel combustion. If we assume that the down-core profile of perylene in the Pettaquamscutt River derives from a mixture of combustion of fossil fuel ($\Delta^{14}C$ = -1000 ‰) and *in situ* production ($\Delta^{14}C$ = TOC values), we can calculate the fraction of perylene derived from each end-member using a simple mixing model. The results obtained (Table 1) show that the amount of perylene derived from fossil sources was minor (less than 5%) prior to 1920, but 6.5-fold greater in surficial sediments. This result can either be explained by an increase in recent years of the importance of fossil fuel combustion as a source of perylene and/or by a slow "in-growth" of perylene from diagenetic alteration of a $^{14}C$-modern precursor. One possible scenario is that fossil fuel combustion is a significant source of perylene in surficial sediments, when *in situ* production is at an early stage. As the amount of perylene produced *in situ* increases with time, the $^{14}C$ abundance of perylene can be shifted towards values closer to its precursor and away from the small fossil contribution. While this is a likely scenario, the mass accumulation rate of perylene (Figure 3) (which can also be seen as its production record) indicates that there are uncertainties associated with this model. Using the sediment horizon dated of 1973 as an example, the contribution of perylene from fossil sources is calculated at ~ 18% at a time when the MAR of perylene was already at its maximum (~200 ng $cm^{-2}$ $yr^{-1}$). That would mean that 18% of the concentration of perylene deposited in sediments dated of 1973 (~ 520 ng $g^{-1}$) derived from a fossil source. However, this value is twice as high as the concentration measured for perylene in surface sediments. Irrespective of these scenarios, the $^{14}C$ data implies that in the last 30 years, combustion of fossil fuels has become an increasingly important source of perylene to the sediments of the Pettaquamscutt River. The absence of the most recent portion of the sedimentary record from Siskiwit Lake prevents further discussion on the effects of combustion of fossil fuels on the recorded perylene profile.

Commonly, the contribution of fossil sources to the amount of perylene encountered in sedimentary settings is evaluated by the ratio of a PAH attributed to a pyrogenic source (e.g. pyrene) to perylene (Gschwend et al., 1983; Venkatesan, 1988)

(Lipiatou et al., 1993). Ratios of pyrene to perylene between 0.8-15 have been measured in different combustion sources, while values of 3-54 are encountered in aerosol samples (Venkatesan, 1988). These high pyrene/perylene ratios in pyrogenic sources can be attributed to 4-ring PAHs being consistently produced in higher quantities than 5-ring compounds (Mastral et al., 1998). Our $\Delta^{14}C$ results show that the use of these intervals as diagnostic indicators of the pyrolytic source of perylene in sedimentary settings should be used with caution as *in situ* production can shift the pyrene/perylene ratio towards low values. The $^{14}C$ abundance of perylene in the Pettaquamscutt River reveals that even when ~20% of the perylene concentration is derived from pyrogenic sources the pyrene/perylene ratio can be as low as 0.4 (Table 1).

Table 1. Fraction of the Pettaquamscutt River perylene derived from fossil fuel combustion (considering $\Delta^{14}C$ of TOC as the second end-member).

| Year | Depth (cm) | $\Delta^{14}C$ TOC (‰) | $\Delta^{14}C$ Perylene (‰) | $\Delta^{14}C$ Fossil (‰) | Fraction Fossil (%) | Average Pyrene / Perylene Ratio in Horizon |
|---|---|---|---|---|---|---|
| 1991 | 5 | -3.7 | -239.6 | -1000 | 23.7 | 1.52 |
| 1972 | 14.5 | 20.3 | -164.1 | -1000 | 18.1 | 0.40 |
| 1947 | 24.5 | -125.2 | -186.3 | -1000 | 7.0 | 0.50 |
| 1911 | 33 | -132.2 | -153.5 | -1000 | 2.4 | 0.12 |
| 1885 | 39 | -100.4 | -115.5 | -1000 | 1.7 | 0.05 |
| 1858 | 45.5 | -62.2 | -107.2 | -1000 | 4.8 | 0.03 |
| 1804 | 57 | -88.2 | -132.7 | -1000 | 4.9 | 0.01 |
| 1750 | 67 | -95.2 | -132.9 | -1000 | 4.2 | 0.01 |
| | | | | Average | 3.6 | |

Radiocarbon results obtained for perylene and TOC from Siskiwit Lake contrast greatly with those reported for Pettaquamscutt River. Because Siskiwit Lake is some 55 km away from the nearest populated area (McVeety and Hites, 1988), it receives a smaller load of PAHs derived from combustion of fossil fuels than the Pettaquamscutt River. The smaller contribution of fossil-derived PAHs to Siskiwit Lake is illustrated in Figure 3. While perylene and TOC $\Delta^{14}C$ values in the Pettaquamscutt River indicate a larger fossil contribution beginning in the early 1900s, the radiocarbon abundance of

these species increased towards the present in the Siskiwit Lake core (Figure 3). Perylene and TOC follow basically the same $^{14}C$ trend, but we cannot rule out the influence of fossil sources to the perylene content in recent years, as we have no data for the uppermost portion of core. However, the higher $^{14}C$ abundance in pyrogenic PAHs from Siskiwit Lake relative to the Pettaquamscutt River (Chapter 6) attests to the reduced contribution of fossil fuel derived compounds to this remote location. All pyrogenic PAHs deposited in the Pettaquamscutt River in the 1950s contained significantly less $^{14}C$ than equivalent compounds reaching Siskiwit Lake (Chapter 6).

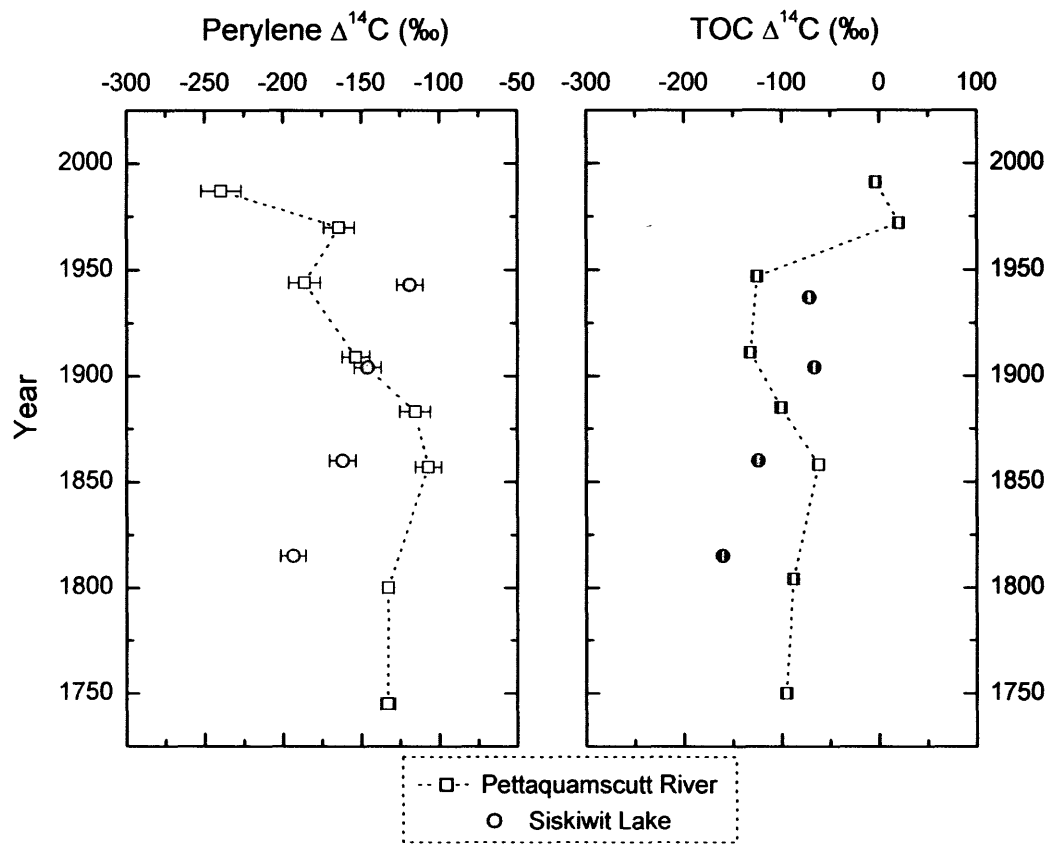


Figure 3. Comparison of the $^{14}C$ abundance in (a) perylene and (b) TOC in Siskiwit Lake and in the Pettaquamscutt River.

### 3.2 TOC

Results for percent of total organic carbon (TOC), percent of organic nitrogen ($N_{org}$), $C_{org}/N_{org}$ ratios, as well as $\delta^{13}C$ and $\Delta^{14}C$ of TOC for the Pettaquamscutt River and Siskiwit Lake sediments are plotted in Figures 2-7 and listed in Appendix 5. Measured values of TOC, $N_{org}$, $C_{org}/N_{org}$, $\delta^{13}C$ and $\Delta^{14}C$ for the combined horizons of the Pettaquamscutt River followed closely the trends set by the high-resolution core, so the following discussion will focus on the more detailed profiles for this system.

TOC and $N_{org}$ contents in the sediments of the Pettaquamscutt River ranged from 6.8-11.2% (average = 9.1 ± 1.1%, *n*= 71) and 0.65-1.35% (average = 0.94 ± 0.12%, *n*= 71) of dry weight, respectively. The lowest TOC content is found at a layer dated 1938 (27-cm) (Figure 2) and is related to a 17.5% shift in the average TOC content from 9.8 ± 0.8 % prior to 1927 to 8.1 ± 0.7 % for sediments deposited after that. The timing of this decrease is coincident with the construction of the Lacey Bridge in 1934 (Figure 1, Chapter 6) (Gaines, 1975), which could have caused a restriction in the seawater intrusion, therefore lowering the influx of marine plankton to the lower basin. The $N_{org}$ content down-core also shows small variations that result in a $C_{org}/N_{org}$ ratio profile (Figure 4d) that can be divided into 3 parts: decreasing $C_{org}/N_{org}$ from 1730s (10.8) to 1850s (9.2), a 50-year reversal towards higher $C_{org}/N_{org}$ ratios (11.2 in 1900), and a century-long $C_{org}/N_{org}$ decline to the present (8.6 in 1999). The fluctuations observed in Figure 4d fall in the transition range between aquatic (C/N = 4 - 10) and terrestrial (C/N > 20) organic matter (Meyers, 1997), yet the $\delta^{13}C$ profile does not show a concomitant shift in one direction or another (Figure 4b). The constancy of $\delta^{13}C$ throughout the core (-25.4 to –23.0 ‰, average = -24.1 ± 0.5, *n*= 37) seems to imply that the mixture of sources of organic matter to this basin has not changed significantly overtime. Similarly, $C_{org}/N_{org}$ ratios and $\delta^{13}C$ values in Siskiwit Lake were invariant at 17.5 ± 0.9 and –25.4 ± 0.2, respectively, throughout the sedimentary record (Figure 5). A plot of $C_{org}/N_{org}$ ratio versus $\delta^{13}C$ of TOC indicates that the majority of organic matter in the Pettaquamscutt River sediments is derived from algal biomass, while that present in Siskiwit Lake contains higher amounts of terrestrial vegetation (Figure 6). Although many freshwater

species are present in the lower basin of the Pettaquamscutt River throughout the year, the vast majority of the cells at this site are brackish and marine species (Menezes, 2003), in agreement with the position of our data in Figure 6. This plot also implies that the decrease in TOC content in the 1930s was not related to a switch of organic matter source to this system. More likely, the lower TOC content in recent years reflects a decrease in

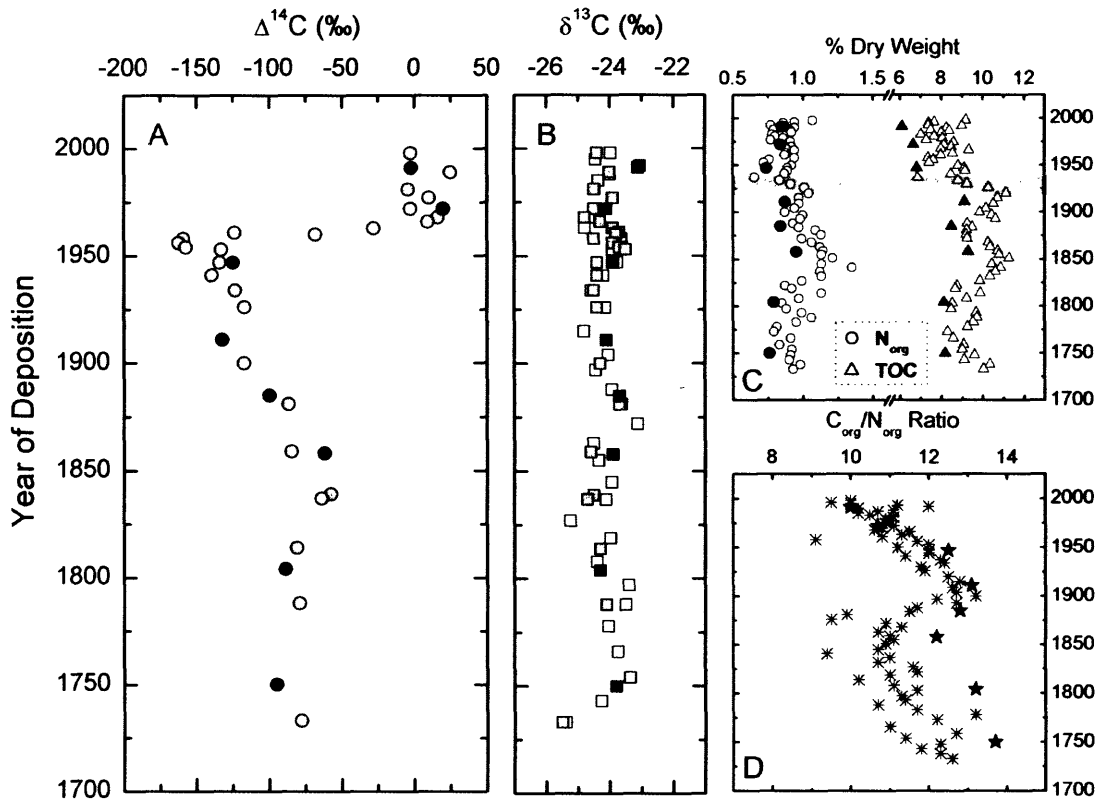


Figure 4. Characterization of the sedimentary TOC in the Pettaquamscutt River. (a) radiocarbon content in per mil ($\Delta^{14}C$ ‰) and (b) stable carbon composition ($\delta^{13}C$ ‰). Gray-filled symbols correspond to samples from the original high-resolution core and solid symbols relate to samples from the combined horizons. These measurements were conducted at the NOSAMS facility. (c) percent of organic nitrogen (○), and TOC (Δ) per dry weight and (d) $C_{org}/N_{org}$ ratio. Open symbols (including $\delta^{13}C$ in panel B) correspond to samples from the original core and solid symbols relate to samples from the combined horizons. These measurements were conducted at the Organic Mass Spectrometry facility at WHOI.

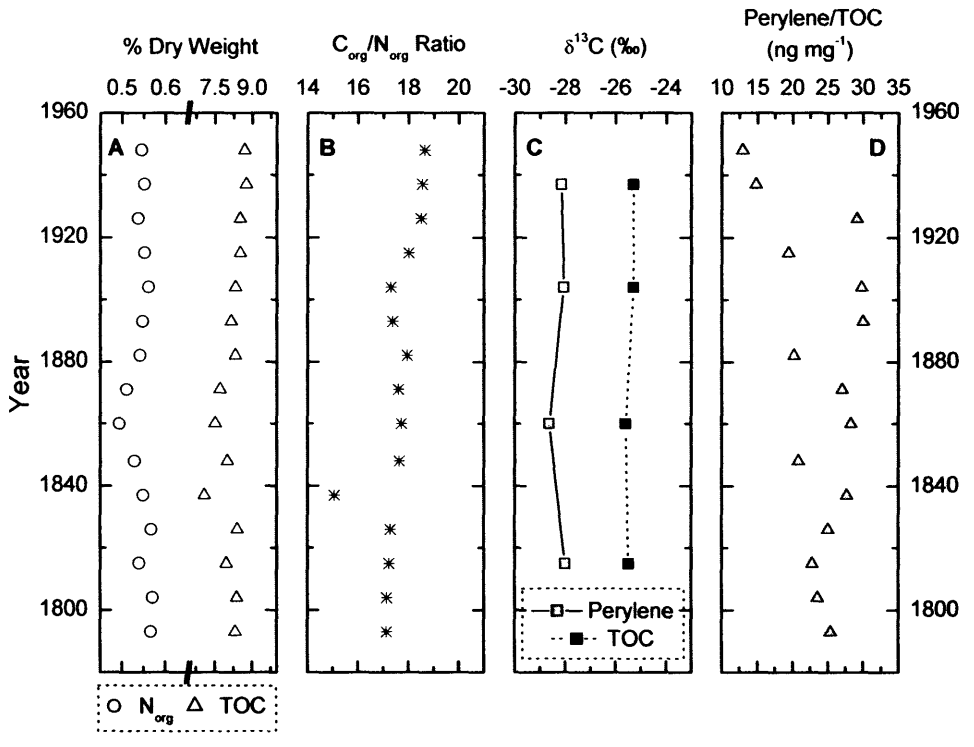


Figure 5. Characterization of the sedimentary TOC in Siskiwit Lake. (a) percent of organic nitrogen (○) and TOC (Δ) per dry weight; (b) $C_{org}/N_{org}$ ratio; (c) stable carbon composition ($\delta^{13}C$ ‰) of perylene and TOC; and (d) perylene/TOC (ng $mg^{-1}$) ratio.

the amount of phytoplankton-derived mass that reaches the lower basin. A comparison between the amount of organic carbon present in the sediment (Figure 2a) versus its mass accumulation rate (MAR) (Figure 2b) shows that the recent reduction in %TOC can be related to a dilution of aquatic biomass with clastic material. Pressures caused by an increase in the local human population could account for the observed increase in sedimentation rate in this region. If dilution rather than change in the main source of organic matter to the sediments is the cause of the decrease in % TOC, then the down-core shifts in $C_{org}/N_{org}$ ratio could be due to differences in preservation of the terrestrial and aquatic components over time. It is known that vascular plant tissues have a tendency to gain N during microbial degradation (lowering the $C_{org}/N_{org}$), while plankton tends to

lose N during the process (elevating the C/N) (Hedges and Oades, 1997). Additional work is required to better understand the organic carbon composition and preservation in this system.

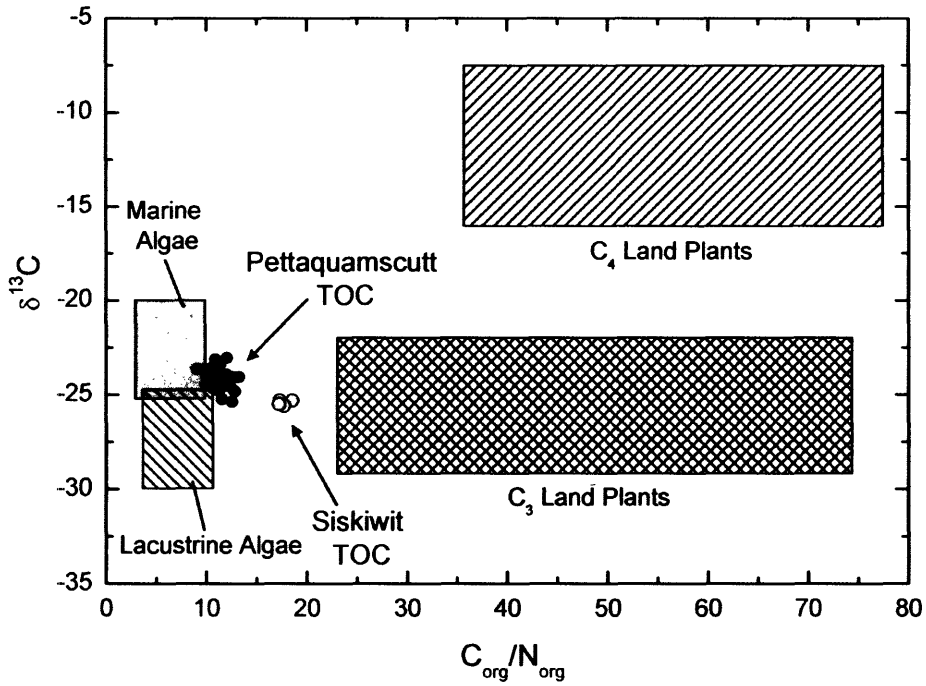


Figure 6. Elemental and isotopic characteristics of organic matter produced by terrestrial ($C_3$ and $C_4$ plants) and aquatic (marine and lacustrine) biomass, based on Meyers (1997). TOC from Siskiwit Lake seems to contain higher amounts of terrestrial organic matter than the Pettaquamscutt River.

Radiocarbon measurements can be valuable in deciphering the origin of the sedimentary TOC. Determination of $^{14}C$ content in tree rings of known age has shown that atmospheric levels of $^{14}CO_2$ were relatively constant prior to the 1800s (Stuiver and Quay, 1981). Similar results were obtained for coral rings from Florida, which showed average $\Delta^{14}C$ values equal to $-51 \pm 2‰$ from 1800 to 1900 (Druffel and Linick, 1978). Significant changes in the radiocarbon content of the atmosphere began at the turn of the

20th century. It is estimated that a 20‰ decrease in $\Delta^{14}C$ of atmospheric $CO_2$ occurred from 1890 to 1950, primarily due to emissions of $^{14}C$-free $CO_2$ from combustion of fossil fuels (the so-called $^{14}C$ Suess effect) (Stuiver and Quay, 1981). However, the major feature in the atmospheric $^{14}CO_2$ content is the almost doubling in $^{14}C$ levels between 1955 and 1963, resulting from radiocarbon production by atmospheric weapons testing (Figure 7). After the Test Ban Treaty was signed in 1963 (Carter and Moghissi, 1977), atmospheric $^{14}CO_2$ levels began to decline at a constant rate due to a combination of uptake by the oceans and biosphere and dilution with $^{14}C$-free fossil fuel emissions. Because atmospheric $CO_2$ and dissolved inorganic carbon contain different amounts of radiocarbon, terrestrial and aquatic organic matter incorporate contrasting amounts of $^{14}C$ that can be used to distinguish them (Pearson and Eglinton, 2000).

To further constrain the sources of TOC to the Pettaquamscutt River sediments, we calculated the relative contribution of possible organic carbon sources to this site using the measured $\Delta^{14}C$ and $\delta^{13}C$ values for the TOC (Figure 4a and 4b, gray-filled symbols). We assumed a simple mixing model among an aquatic, a terrestrial and a fossil end-member:

$$\Delta^{14}C_{TOC} = (f_{Aq}\Delta^{14}C_{Aq}) + (f_{Terr}\Delta^{14}C_{Terr}) + (f_{Fossil}\Delta^{14}C_{Fossil})$$

$$\delta^{13}C_{TOC} = (f_{Aq}\delta^{13}C_{Aq}) + (f_{Terr}\delta^{13}C_{Terr}) + (f_{Fossil}\delta^{13}C_{Fossil})$$

$$f_{Aq} + f_{Terr} + f_{Fossil} = 1$$

where $\Delta^{14}C_{TOC}$ and $\delta^{13}C_{TOC}$ are measured values for each horizon and $f_{Aq}$, $f_{Terr}$ and $f_{Fossil}$ are the unknown fractions of aquatic, terrestrial and fossil organic matter. $\Delta^{14}C$ values for the three end-members were taken from the literature. We used the radiocarbon record of mollusk shells from Georges Bank, North Atlantic (Weidman and Jones, 1993) as the aquatic end-member ($\Delta^{14}C_{Aq}$). The terrestrial end-member was assumed to be a mixture of 20% atmospheric $CO_2$ (Levin et al., 1985; Levin and Kromer, 1997) and 80% soil (Richter et al., 1999) ($\Delta^{14}C_{Terr}$) and a value of −1000‰ was assigned to contributions from combustion of fossil carbon ($\Delta^{14}C_{Fossil}$). For the purpose of this model, $\delta^{13}C$ values for the three end-members were considered invariant through time. An average value for

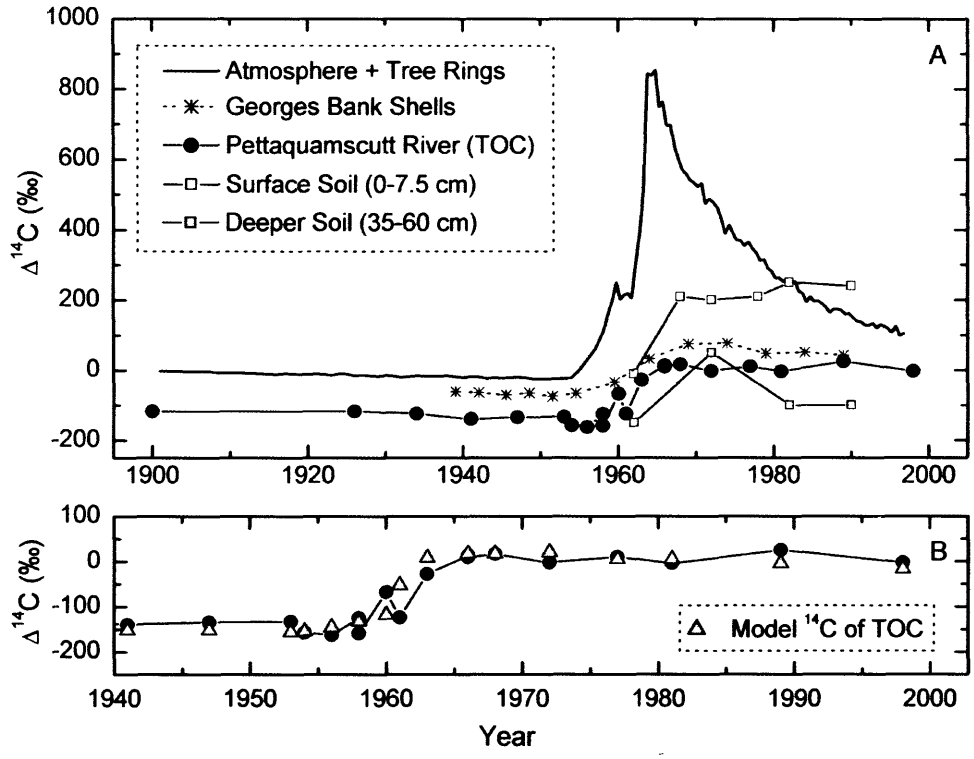


Figure 7. Time trend of (a) $^{14}C$ in atmospheric $CO_2$ (Levin et al., 1985; Levin and Kromer, 1997), tree rings (Stuiver and Quay, 1981), marine shells (Weidman and Jones, 1993), and different soil horizons (Richter et al., 1999) were used to calculate the relative proportion of organic matter sources to the Pettaquamscutt River; (b) results obtained by the mixing model.

$C_3$ plants (-28‰) (O'Leary, 1988) was assigned to the terrestrial component ($\delta^{13}C_{Terr}$), -30‰ was used for fossil fuels ($\delta^{13}C_{Fossil}$) (O'Leary, 1988; Hunt, 1996) and -21‰ was designated as representative of aquatic organic matter ($\delta^{13}C_{Aq}$) (Meyers, 1997). While the carbon isotopic composition of petroleum can vary widely (-30 to –20‰) (Whelan et al., 1993; Hunt, 1996), the $\delta^{13}C$ of the oil standard used by the US National Bureau of Standards is -29.8‰ (Hunt, 1996), thus our choice of value. The relative contribution of the three end-members was calculated for each sediment horizon then averaged down-core. The mean contribution of each end-member was used in the model curve shown in Figure 7b. The use of a mean value for the fractional contribution of the sources implies

that the amount of $\Delta^{14}C$ in each compartment is the only parameter affecting the shape of the $\Delta^{14}C$ profile of TOC. Appendix 6 lists the values used in the model, the results obtained for each depth interval, as well as the calculated values plotted in Figure 7b. This exercise reinforced the notion that aquatic biomass is most likely the dominant source of organic matter to the lower basin of the Pettaquamscutt River sediments (57 ± 4%). Terrestrial organic matter, defined as a mixture of a recently produced $^{14}C$-rich fraction (land plants ~20%) and an older portion (soil ~80%), accounted for 36 ± 5% of the TOC, followed by combustion of fossil fuel (~ 7 ± 2%) (Figure 8).

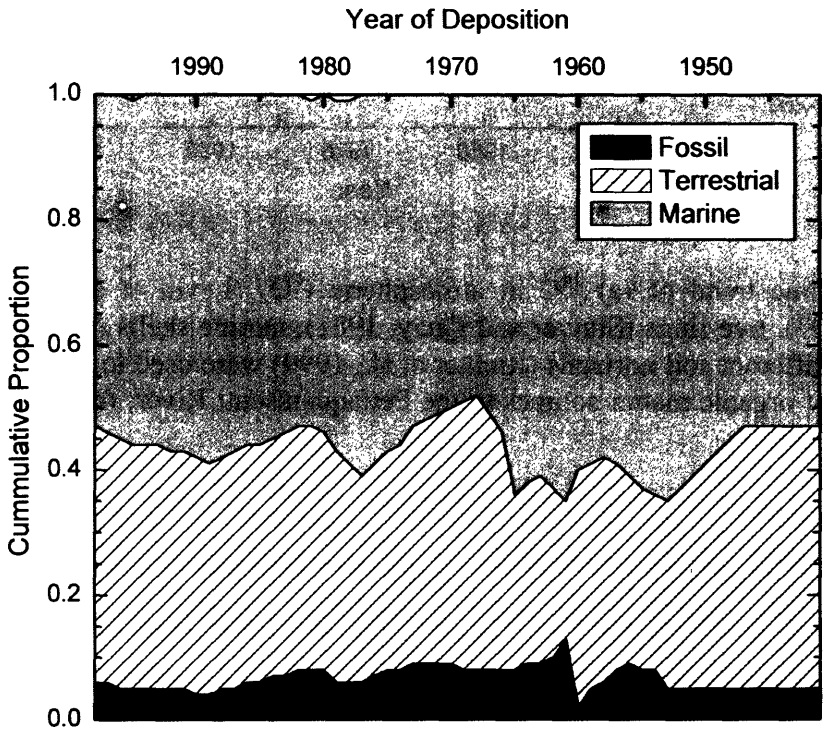


Figure 8. Estimative of the proportion of fossil, terrestrial and marine organic matter present in the TOC of the Pettaquamscutt River sediments.

## 4. CONCLUSIONS

The combination of historical sedimentary record and $\delta^{13}C$ and $\Delta^{14}C$ measurements for perylene and TOC provided some insight into the complexity of sources of these compounds. Perylene seems to be highly sensitive to small variations in depositional conditions, as cores collected in different regions of the same site show contrasting concentrations and down-core profile. The results obtained in this study suggest that variations in the microbial community in the sediments may explain these variations. The combination of $\delta^{13}C$ and $\Delta^{14}C$ of perylene and TOC helped us discern with some confidence the importance of fossil fuels to the sedimentary profile of this PAH. While combustion is a significant source of perylene in the suburban Pettaquamscutt River, that does not seem to be the case for the pristine Siskiwit Lake. Our results also suggest that commonly employed diagnostic ratios such as perylene/TOC (for assessing *in situ* production of perylene) and pyrene/perylene (for assessing the contribution of combustion of fossil fuels to the amount of perylene in the sediments) should be used with caution. While *in situ* production can shift the latter towards low values, no correlation was observed between TOC content and perylene.

## 5. REFERENCES


Aizenshtat Z. (1973) Perylene and its geochemical significance. *Geochim. Cosmochim. Acta* **37**, 559-567.

Blumer M., Blumer W., and Reich T. (1977) Polycyclic aromatic hydrocarbons in soils of a Mountain Valley: Correlation with highway traffic and cancer incidence. *Environ. Sci. Technol.* **11**(12), 1082-1084.

Carter M. and Moghissi A. (1977) Three decades of nuclear testing. *Health Phys. Press* **33**, 55-71.

Davies I., Harrison R., Perry R., Ratnayaka D., and Wellings R. (1976) Municipal incinerator as source of polynuclear aromatic hydrocarbons in environment. *Environ. Sci. Technol.* **10**(5), 451-453.

Doskey P. and Talbot R. (2000) Sediment chronologies of atmospheric deposition in a precipitation-dominated seepage lake. *Limnol. Oceanogr.* **45**(4), 895-904.

Druffel E. and Linick T. (1978) Radiocarbon in annual coral rings of Florida. *Geophys. Res. Lett.* **5**(11), 913-916.

Fine P., Cass G. R., and Simoneit B. R. T. (2001) Chemical characterization of fine particle emissions from fireplace combustion of woods grown in the Northeastern United States. *Environ. Sci. Technol.* **35**, 2665-2675.

Gaines A. (1975) Papers on the geomorphology, hydrography and geochemistry of the Pettaquamscutt River estuary. PhD, University of Rhode Island.

Gschwend P., Chen P., and Hites R. (1983) On the formation of perylene in recent sediments: kinetic models. *Geochim. Cosmochim. Acta* **47**, 2115-2119.

Gschwend P. M. and Hites R. A. (1981) Fluxes of polycyclic aromatic hydrocarbons to marine and lacustrine sediments in the northeastern United States. *Geochim. Cosmochim. Acta* **45**, 2359-2367.

Hedges J. I. and Oades J. M. (1997) Comparative organic geochemistries of soils and marine sediments. *Org. Geochem.* **27**(7-8), 319-361.

Hites R. A., Laflamme R. E., Windsor Jr J. G., Farrington J. W., and Deuser W. G. (1980) Polycyclic aromatic hydrocarbons in an anoxic sediment core from the Pettaquamscutt River (Rhode Island, USA). *Geochim. Cosmochim. Acta* **44**, 873-878.

Hunt J. (1996) *Petroleum Geochemistry and Geology*. W.H. Freeman and Company

Ingalls W. (1908) *Lead and Zinc in the United States*. Hill Publishing Company, New york.

Jiang C., Alexander R., Kagi R., and Murray A. (2000) Origin of perylene in ancient sediments and its geological significance. *Org. Geochem.* **31**, 1545-1559.

Laflamme R. E. and Hites R. A. (1978) The global distribution of polycyclic aromatic hydrocarbons in recent sediments. *Geochim. Cosmochim. Acta* **42**, 289-303.

Levin I., Kromer B., Schoch-Fischer H., Bruns M., Münnich M., Berdau D., Vogel J., and Münnich K. (1985) 25 years of tropospheric $^{14}C$ observations in central Europe. *Radiocarbon* **27**(1), 1-19.

Levin I. and Kromer B. (1997) Twenty years of atmospheric $^{14}CO_2$ observations at Schauinsland station, Germany. *Radiocarbon* **39**(2), 205-218.

Lima A. L. C., Eglinton T. I., and Reddy C. M. (2003) High-resolution record of pyrogenic polycyclic aromatic hydrocarbon deposition during the 20$^{th}$ century. *Environ. Sci. Technol.* **37**, 53-61.

Lipiatou E., Marty J.-C., and Saliot A. (1993) Sediment trap fluxes of polycyclic aromatic hydrocarbons in the Mediterranean sea. *Mar. Chem.* **44**, 43-54.

Louda J. and Baker E. (1984) Perylene occurence, alkylation and possible sources in deep-ocean sediments. *Geochim. Cosmochim. Acta* **48**, 1043-1058.

Mastral A., Callén M., Murillo R., and García T. (1998) Assessment of PAH emissions as a function of coal combustion variables in fluidized bed. 2. Air excess percentage. *Fuel* **77**(13), 1513-1516.

Mastral A., Callén M., Murillo R., and García T. (1999) Combustion of high calorific value waste material: organic atmospheric pollution. *Environ. Sci. Technol.* **33**, 4155-4158.

McVeety B. (1986) Atmospheric deposition of polycyclic aromatic hydrocarbons to water surfaces: a mass balance approach. PhD, Indiana University.

McVeety B. and Hites R. (1988) Atmospheric deposition of polycyclic aromatic hydrocarbons to water surfaces: a mass balance approach. *Atmos. Environ.* **22**(3), 511-536.

Menezes S. (2003).

Meyers P. (1997) Organic geochemical proxies of paleoceanographic, paleolimnologic, and paleoclimatic processes. *Org. Geochem.* **27**(5/6), 213-250.

O'Leary M. (1988) Carbon isotopes in photosynthesis. *BioScience* **38**(5), 328-336.

Orr W. L. and Gaines A. G. J. (1973) Observations on the rate of sulfate reduction and organic matter oxidation in the bottom waters of an estuarine basin: the upper basin of the Pettaquamscutt River (Rhode Island). In *Advances in Organic Geochemistry* (ed. B.Tissot and F. Bienner), pp. 791-812. Technip.

Pearson A. and Eglinton T. (2000) The origin of n-alkanes in Santa Monica basin surface sediment: a model based on compound-specific $\Delta^{14}C$ and $\delta^{13}C$ data. *Org. Geochem.* **31**, 1103-1116.

Pereira W., Hostettler F., Luoma S., Van Geen A., Fuller C., and Anima R. (1999) Sedimentary record of anthropogenic and biogenic polycyclic aromatic hydrocarbons in San Francisco Bay, California. *Mar. Chem.* **64**, 99-113.

Reddy C., Pearson A., Xu L., McNichol A., Benner Jr. B., Wise S., Klouda G., Currie L., and Eglinton T. (2002) Radiocarbon as a tool to apportion the sources of polycyclic aromatic hydrocarbons and black carbon in environmental samples. *Environ. Sci. Technol.* **36**, 1774-1782.

Richter D., Markewitz D., Trumbore S., and Wells C. (1999) Rapid accumulation and turnover of soil carbon is a re-establishing forest. *Nature* **400**, 56-58.

Rogge W. F., Hildemann L. M., Mazurek M. A., Cass G. R., and Simoneit B. R. T. (1993) Sources of fine organic aerosol. 2. Noncatalyst and catalyst-equipped automobiles and heavy-duty diesel trucks. *Environ. Sci. Technol.* **27**, 636-651.

Silliman J., Meyers P., Ostrom P., Ostrom N., and Eadie B. (2000) Insights into the origin of perylene from isotopic analyses of sediments from Saanich inlet, British Columbia. *Org. Geochem.* **31**, 1133-1142.

Silliman J., Meyers P., Eadie B., and Klump J. (2001) A hypothesis for the origin of perylene based on its low abundance in sediments of Green Bay, Wisconsin. *Chem. Geol.* **177**, 309-322.

Silliman J. E., Meyers P. A., and Eadie B. J. (1998) Perylene: an indicator of alteration processes or precursor materials? *Org. Geochem.* **29**(5-7), 1737-1744.

Simcik M., Eisenreich S., Golden K., Liu S.-P., Lipiatou E., Swackhammer D., and Long D. (1996) Atmospheric loading of polycyclic aromatic hydrocarbons to lake Michigan as recorded in the sediments. *Environ. Sci. Technol.* **30**, 3039-3046.

Stuiver M. and Quay P. (1981) Atmospheric $^{14}C$ changes resulting from fossil fuel $CO_2$ release and cosmic ray flux variability. *Earth Planet. Sci. Lett.* **53**, 349-362.

Tan Y. L. and Heit M. (1981) Biogenic and abiogenic polynuclear aromatic hydrocarbons in sediments from two remote Adirondack lakes. *Geochim. Cosmochim. Acta* **45**, 2267-2279.

Urish D. (1991) Freshwater inflow to the Narrow River. *Maritimes* **35**(2), 12-14.

Venkatesan M. I. (1988) Occurrence and possible sources of perylene in marine sediments - a review. *Mar. Chem.* **25**, 1-27.

Wakeham S. (1977) Synchronous fluorescence spectroscopy and its application to indigenous and petroleum-derived hydrocarbons in lacustrine sediments. *Environ. Sci. Technol.* **11**(3), 272-276.

Wakeham S., Schaffner C., Giger W., Boon J., and De Leeuw J. (1979) Perylene in sediments from the Namibian shelf. *Geochim. Cosmochim. Acta* **43**, 1141-1144.

Wakeham S., Schaffner C., and Giger W. (1980) Polycyclic aromatic hydrocarbons in recent lake sediments - II. Compounds derived from biogenic precursors during early diagenesis. *Geochim. Cosmochim. Acta* **44**, 415-429.

Weidman C. and Jones G. (1993) A shell-derived time history of bomb $^{14}C$ on George Bank and its Labrador Sea implications. *J. Geophys. Res.* **98**(C8), 14577-14588.

Whelan J., Kennicutt II M., Brooks J., Schumacher D., and Eglinton L. (1993) Organic geochemical indicators of dynamic fluid flow processes in petroleum basins. *Org. Geochem.* **22**(3-5), 587-615.

# CHAPTER 8

# EVALUATION OF BLACK CARBON ISOLATION METHODS THROUGH COMPARISON WITH WELL-DEFINED COMBUSTION PRODUCTS

## 1. INTRODUCTION

Black carbon (BC) is a generic term used to describe a continuum of reduced carbon species (Figure 1) remaining after incomplete combustion of modern biomass and fossil fuels. In reality, the nomenclature used to define this highly condensed residue depends on the process studied or method of analysis applied and includes soot, elemental carbon, carbon black, char and charcoal. BC particles are ubiquitous in the environment, having been measured in soils, sediments, atmosphere and snow from a variety of locations (Smith et al., 1973; Griffin and Goldberg, 1981; Suman, 1986; Suman et al., 1994; Rose, 1995; Glaser et al., 2000; Schmidt et al., 2001; Eglinton et al., 2002; Masiello et al., 2002). These particles range from submicron in size (<1 μm) to several mm (Figure 1) and their presence in the atmosphere can have hazardous health effects. The EPA began to regulate emission of particles smaller than 2.5 μm ($PM_{2.5}$) (EPA, 1997) after it became apparent that they were too small to be stopped in the upper respiratory tract and could penetrate into the lungs (Pedersen et al., 1980; Samet et al., 2000). In addition to being directly hazardous to human health, recent studies have also shown that BC plays an important role in the absorption of solar radiation (Kirkevåg et al., 1999), biogeochemical cycling of carbon (Gustafsson and Gschwend, 1998; Masiello and Druffel, 1998; Middelburg et al., 1999), and the bioavailability of organic contaminants (McGroddy et al., 1996; Gustafsson et al., 1997; Accardi-Dey, 2003).

Emission inventories generally agree that, at present, volcanic activity and natural vegetation fires are negligible sources of BC compared to the widespread combustion of fossil fuels and anthropogenic burning of biomass (Suman et al., 1994). However, there is

still no agreement on the relative importance of each of these two sources to the total amount of BC emitted yearly. Estimates of annual BC emissions vary from 5.98 to 12 Tg (1 Tg = $10^{12}$g) for biomass burning, and 6 to 7.96 Tg for fossil fuel (Penner, 1995; Cooke and Wilson, 1996). Even though these are good first approximations of the order of magnitude of BC emissions, they yield conflicting information as to the importance of combustion of modern biomass and considerable uncertainty still remains regarding the measurement and source apportionment of this species.

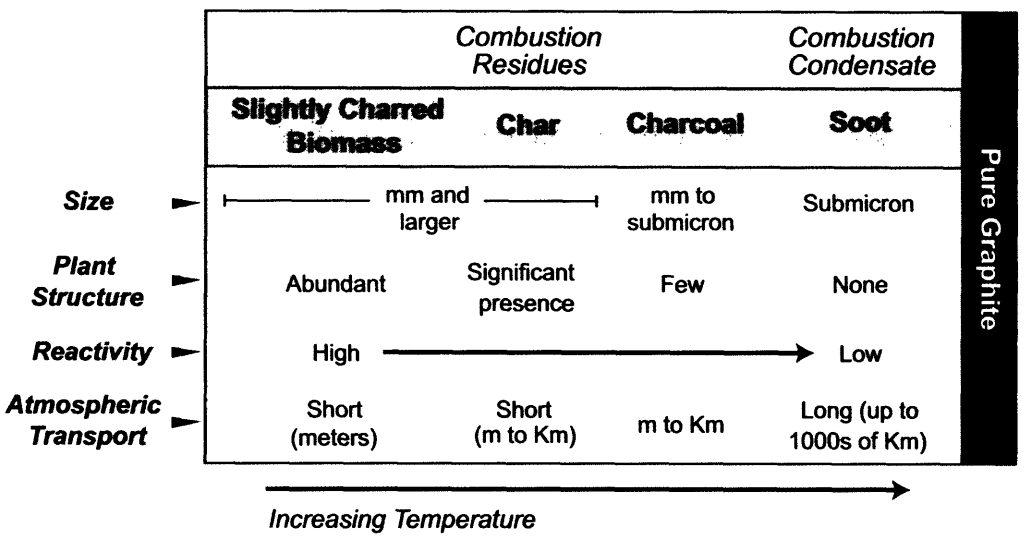


Figure 1. Black carbon is a continuum of combustion products ranging from labile, slightly charred biomass, to highly refractory soot and graphite.

In order to constrain the biogeochemical cycle and global budgets of BC, improvements are needed in its measurement, especially in sedimentary reservoirs, and in the identification and apportionment of BC sources. Several techniques have been explored for quantification and source apportioning of BC, including (a) characterization of surface morphology (Griffin and Goldberg, 1981), (b) measurement of $\delta^{13}C$ (Cachier, 1989) and (c) measurement of $\Delta^{14}C$ (Currie et al., 1983; Masiello and Druffel, 1998;

Klinedinst and Currie, 1999; Reddy et al., 2002). However, BC is an operationally-defined term, and there are still no certified reference materials to intercalibrate results or consensus regarding a standard analytical method. Until a common ground for BC quantification and characterization is achieved, assessment of its implications will remain subject to considerable uncertainty.

In this paper, we evaluate three different methods for the isolation of BC from sediments. We compare the down-core concentration and carbon isotopic trends of BC to that of a well-defined product of incomplete combustion. Polycyclic aromatic hydrocarbons (PAHs) are formed concurrently with BC during combustion, therefore the distribution of these two species are closely related. Assuming BC and PAHs found in sediments derive from a common source, the stable carbon ($\delta^{13}C$) and radiocarbon ($\Delta^{14}C$) content of these fractions should be similar. We evaluate results obtained for PAHs and BC from sediments from the Pettaquamscutt River, RI, a site with well-established chronology and record of total PAHs (Lima et al., 2003). The results obtained illustrate the complex scenario of BC determinations and highlight the benefits of comparing BC results to that of a better-defined combustion product.

## 2. EXPERIMENTAL SECTION

A full description of the sampling site, collection and depth-age relationship of the sediment cores were given in Chapters 4 and 6. Procedures for extracting and calculating the concentrations and fluxes of PAH was given in Chapter 3. Chapter 6 describes the procedure utilized for combining several sediment cores in order to obtain enough carbon mass for radiocarbon measurements, details the analytical methods employed for stable carbon and radiocarbon isotopic measurements and data reporting, and elaborates on $^{14}C$ results obtained for individual PAHs and total organic carbon (TOC). Methods pertinent to BC analysis are described below.

## 2.1 Chemical Oxidation Method

The dichromate/sulfuric acid oxidation method developed by Wolbach and Anders (1989) and modified by Masiello and collaborators (2002) was used to generate an 8-point depth profile of the amount and radiocarbon content of BC ($BC_{Chemical}$). This method separates refractory BC from labile organic carbon and kerogen[1] by slowly oxidizing the organic carbon with a dilute oxidant solution that can be controlled by choice of temperature and duration of the reaction. Mass loss curves showed that elemental C, reactive (marine) kerogen and mature (terrestrial) kerogen have markedly different half-lives (610, 7 and 59 h respectively) (Wolbach and Anders, 1989).

Dried sediment samples (1.5 g) were weighed into Teflon centrifuge tubes (Nalge PFE Oak Ridge Centrifuge tubes, 40 mL) treated with 6 N HCl to remove calcium carbonate, rinsed with Milli-Q water and subsequently demineralized with a 50% HF - 10% HCl solution, by overnight agitation on an orbital shaker table. The samples were then rinsed with Milli-Q water, air-dried and weighed, and repeatedly soaked in excess oxidant (0.25 M $Cr_2O_7^{2-}$ - 2 M $H_2SO_4$ at 23°C) and shaken for a measured length of time. The chemically oxidized samples were centrifuged at 4000 rpm for 10 minutes, rinsed 4 times with Milli-Q water and dried to constant weight under vacuum. A more complete description of this procedure can be found in Masiello and collaborators (2002).

## 2.2 Thermal Method

The thermal oxidation method applied in this study was developed and tested by Gustafsson and collaborators (1997; 2001) for quantifying the amount of BC present in sediment samples. $BC_{Thermal}$ is defined as the reduced carbon content remaining in a sediment sample after a 375°C thermal treatment for 24 hours (g C/g sediment). This method involves the least amount of sample manipulation of all three methods evaluated, and recent radiocarbon measurements conducted on three National Institute of Standards and Technology standard reference material (NIST SRM 1941a – *Organics in Marine Sediment*, NIST SRM 1944 – *New York / New Jersey Waterway Sediment* and 1649a –

[1] Insoluble high molecular weight organic matter formed by condensation of diagenetic products.

*Urban Dust*;) suggested that the 375°C thermal oxidation method could be valuable for determining the BC content in aerosol and sediment samples (Reddy et al., 2002). In this method, dried sediment (~ 200 mg) was spread on a pre-combusted watch glass and heated in a programmable oven (Fisher Scientific IsoTemp) for 24 hours under excess air at 375°C. The oven temperature was ramped at 15°C/min to 300°C (held for 5 min) and then ramped at 5°C/min to 375°C (held at 375°C for 24 hours). The remaining carbon, as measured with an elemental analyzer (section 2.4) is operationally defined as $BC_{Thermal}$. The 375°C-thermal oxidation method was used in two sets of samples from the Pettaquamscutt River. First, a high-resolution profile of $BC_{Thermal}$ content was generated and subsequently a coarser-resolution 8-point depth profile was used to measure the stable carbon isotopic composition and radiocarbon abundance of this fraction.

### 2.3 Chemical Oxidation/Thermal Method

This BC method encompass a demineralization step, the removal of hydrolysable organic matter by chemical treatment using trifluoroacetic acid (TFA) and HCl, and the thermal oxidation of the non-hydrolyzable organic matter by combustion at 375°C for 24 hours, with excess air. Gélinas and collaborators (2001) developed this method as an alternative to the thermal procedure in an attempt at reducing the potential formation of condensation products that could overestimate the amount of BC present in a sample. A more detailed description of each step of the method can be found in Gélinas and collaborators (2001). This method was used to generate a high-resolution profile of $BC_{Chemical}$ using sediment from the original core.

### 2.4 Carbon and Nitrogen Determinations

A Fisons 1108 elemental analyzer was used to measure the total organic carbon, residual carbon (BC) and nitrogen content of the samples. To remove the inorganic carbon fraction, about 2 mg of dry sample was weighed into a silver capsule and acidified with 20 μL of HCl 2N. The samples were then dried in oven at 50°C, placed inside tin capsules for better catalysis of the oxidation reaction, and analyzed. Total organic carbon

concentrations were calculated in relation to the whole sediment and masses are reported as percent weight (% wt.). Organic carbon/organic nitrogen ($C_{org}/N_{org}$) ratios were calculated on an atomic basis. No significant difference was observed when $C_{org}/N_{org}$ was compared to $C_{org}/N_{total}$ (not acidified). Samples were run in triplicate and all reported weight percentages represent the mean. Concentration of carbon and nitrogen were determined through a 5-point calibration curve (0.09 to 1 mg) of a sulfanilamide standard. Instrumental blanks were run after sets of 12 analyses, yielding carbon blanks better than 0.004 mg and nitrogen blanks < 0.005 mg.

## 3. RESULTS AND DISCUSSION

The three analytical procedures employed in this study for quantifying sedimentary BC showed markedly different results (Figure 2-5, Appendix 7). A comparison among the down-core profiles obtained using these methods for the Pettaquamscutt River samples is shown in Figure 2. Stable carbon isotopic composition (as $\delta^{13}C$ values) and radiocarbon content were measured for BC recovered by the chemical and the thermal methods. These results are compared to values obtained for individual PAHs in Figure 5. The amounts for BC recovered by each method, stable carbon and radiocarbon values and residual nitrogen content are listed in Appendix 7.

The three analytical methods evaluated in this study for the quantification of sedimentary BC resulted in noticeably different down-core profiles (Figure 2). When these results are contrasted to the high-resolution record of total PAHs (Lima et al., 2003) and their radiocarbon content, it becomes apparent that the BC particles isolated by the chemical oxidation method better coincide with the well-defined combustion products (PAHs). Because of the intrinsic details inherent to each BC isolation procedure, we will discuss the results obtained by each method separately.

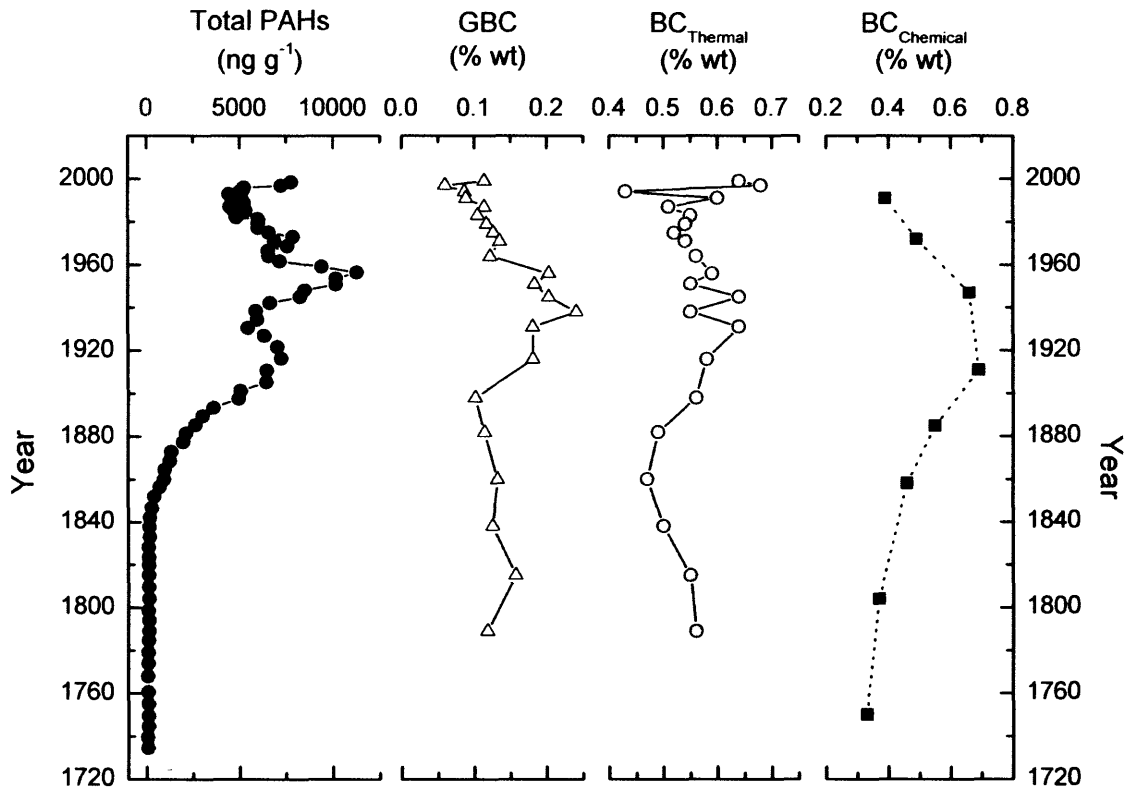


Figure 2. Comparison between the down-core profile of total PAHs and black carbon particles isolated by the chemical/thermal oxidation (GBC) (Gélinas et al., 2001), thermal ($BC_{Thermal}$) (Gustafsson et al., 1997) and chemical oxidation ($BC_{Chemical}$) methods (Masiello et al., 2002).

### 3.1 Thermal Oxidation Method

The sedimentary BC record generated using the 375°C-thermal method did not show any significant down-core trend or coincide with the profile of total PAHs (Figures 2 and 3). This result is in contrast to the remarkable correlation obtained by Gustafsson and collaborators (1997) between the profiles of BC and pyrene for a sediment core from Upper Mystic Lake (MA), which, like the Pettaquamscutt River, contains anoxic bottom waters. Our samples showed no correlation between the high-resolution profile of total PAHs and $BC_{Thermal}$ quantity (Figure 2). $BC_{Thermal}$ weight percent in the Pettaquamscutt

River ranged from 0.43-0.68 %wt. for high-resolution down-core measurements to 0.25-0.95 %wt. when samples were combined into coarser depth-intervals (Figure 3a). The lack of agreement in $BC_{Thermal}$ content for related samples was surprising and led us to investigate some of the possible reasons for this variability.

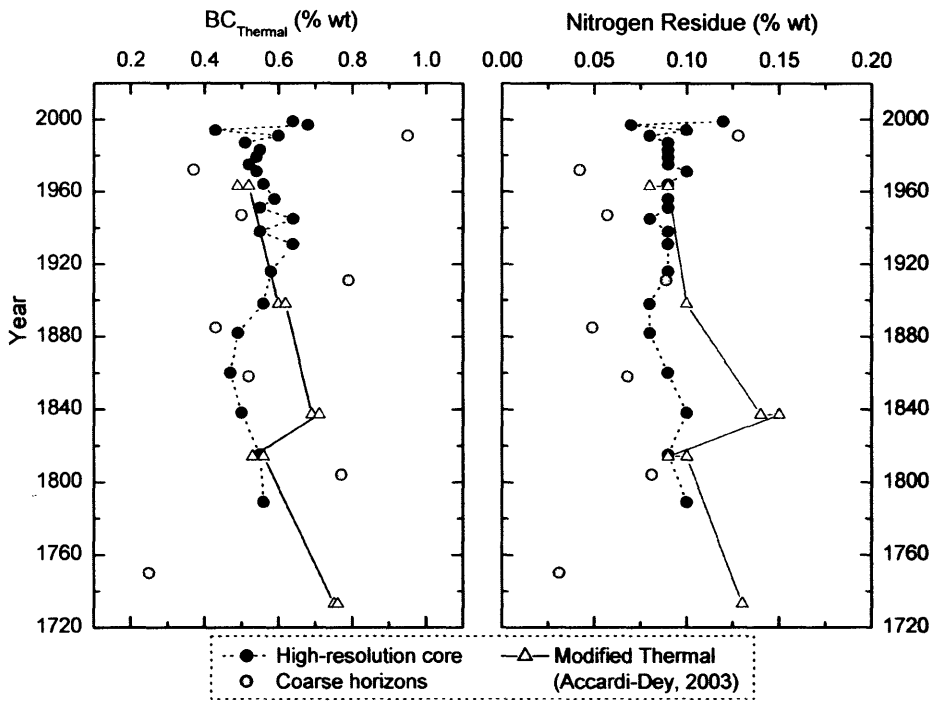


Figure 3. Black carbon content and nitrogen residue in sediment treated with the thermal oxidation method. The modified thermal method utilized sulfurous acid instead of HCl for removal of the inorganic carbon fraction (Accardi-Dey, 2003).

Two common criticisms of the thermal oxidation method are that it can either (a) overestimate the amount of BC present in a sample by inefficiently removing natural OC and promotting "charring"[2] of organic matter (Gélinas et al., 2001) or (b) underestimate the amount of BC by thermally oxidizing some $BC_{Thermal}$ particles (Nguyen et al., 2004).

[2] Charring = includes the incomplete removal of TOC and the condensation of TOC to form a more resistant carbon material.

Accardi-Dey (2003) extensively addressed these concerns and showed that (a) repeated combustion of Boston Harbor sediment (1.3 ±0.1 wt % TOC and 0.10 ±0.01 wt % $N_{total}$) resulted in a Gaussian distribution of $BC_{Thermal}$ content, ranging between 0.08 and 0.17%wt. (average = 0.12 ±0.02 %wt., $n$ = 27), and (b) samples with similar TOC content could yield varying $BC_{Thermal}$ amounts due to incomplete removal of carbon. Accardi-Dey observed that for a given pair of samples with similar TOC content, the one with highest nitrogen amount was more susceptible to charring and suggested that residues of nitrogen in combusted sediments could serve as a signal for the incomplete removal of N-containing macromolecules (e.g., proteins). For example, approximately 20% of the original nitrogen content in the Boston Harbor remained after the sediment was treated with the 375°C-thermal oxidation method (nitrogen residue=0.02±0.01 %wt.). The resulting C/N ratio of these particles was approximately 7, which is extremely low compared to a C/N ratio of 60 ±3 reported for diesel particulate matter (SRM NIST 1650) (Accardi-Dey and Gschwend, 2002). Evaluation of the data acquired for the Pettaquamscutt River shows that the average nitrogen residue was 0.09±0.01%wt $N_{org}$ ($n$ = 22) for the high-resolution core and 0.07±0.03%wt. $N_{org}$ ($n$ = 8) for the coarse resolution samples, suggesting that charring had indeed occurred in these sediments (Figures 3 and 4, Appendix 7). The C/N ratio measured for the $BC_{Thermal}$ particles from the Pettaquamscutt River ranged from 7 to 10. These values are similar to those measured by Accardi-Dey (2003) for sediments from the Boston Harbor and confirm that charring probably occurred in our samples. Selected samples from the Pettaquamscutt River were also measured for $BC_{Thermal}$ and nitrogen residue by Accardi-Dey (2003) using a slightly modified thermal method (using sulfurous acid for elimination of carbonates rather than HCl), and yielded similar concentrations (Figure 3a and 3b). The $^{13}C$-enriched values of $BC_{Thermal}$ compared to TOC (Figure 5b) in conjunction with elevated nitrogen residues in combusted sediment, may imply that proteins present in the Pettaquamscutt River sediments could be resisting thermal oxidation, as proteins are known to be $^{13}C$-enriched compared to bulk TOC.

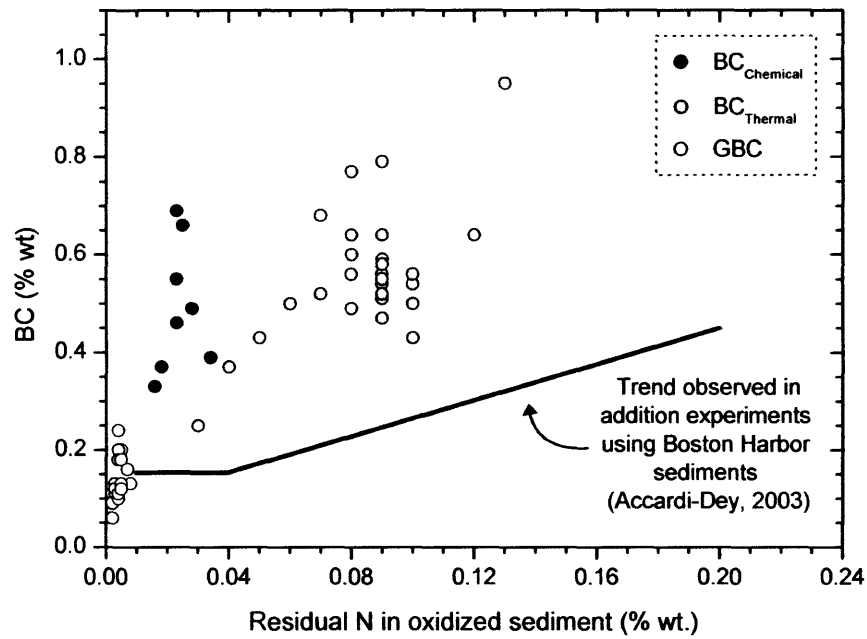


Figure 4. Correlation between the amount of black carbon isolated from the Pettaquamscutt River sediments by three different BC analytical methods and the amount of nitrogen remaining in the treated sample. Solid trend line indicates the results obtained by Accardi-Dey (2003) during addition experiments with Boston Harbor sediment.

Reddy and collaborators (2002) have provided radiocarbon evidence that the 375°C thermal method can isolate BC from marine sediments (NIST SRM 1941a and NIST SRM 1944) without significant interference from organic carbon. In comparison, the radiocarbon and stable carbon results obtained for $BC_{Thermal}$ isolated from the Pettaquamscutt River sediments follows the TOC trends more closely than the combustion-derived PAHs (Figure 5a and 5b), suggesting that a fraction of the original organic carbon was not oxidized. While the $^{14}C$ abundance of the majority of the pyrogenic PAHs analyzed has remained low since the 1950s, $BC_{Thermal}$ shows an increase in $^{14}C$ abundance in the 1960s that correlates with the rise in atmospheric $^{14}C$ due to nuclear weapons tests (bomb-spike) (Levin and Kromer, 1997). This jump in the

$BC_{Thermal}$ $^{14}C$ content is a clear indication that a portion of the TOC initially present in the sediment was not removed by thermal oxidation.

Several factors may contribute to the difference observed between the $BC_{Thermal}$ results for the SRMs and for sediments collected in the environment. Laboratory experiments have shown that the percentage of carbon and nitrogen that survives the thermal method is directly related to the size and morphology of the particulate organic matter in the sediment sample. For example, Accardi-Dey (2003) added known amounts of sodium citrate to pre-combusted sediment samples from the Boston Harbor and observed that the percentage of sodium citrate that remained after the 375°C thermal oxidation method decreased with decreasing crystal size (Figure 4). Accardi-Dey concluded that this resulted from better oxygen access to small OC particles. Therefore, the extensive grinding and sieving that SRMs undergo prior to certification could have reduced the size of OC clumps, favoring oxidation and preventing charring by the thermal method, thus promoting good correlation between $\Delta^{14}C$ of PAHs and $BC_{Thermal}$ in the SRMs. The formation of authigenic minerals in sulfur-rich sediments, such as the Pettaquamscutt River, may also encourage charring of organic matter as the latter can be entrapped in the minerals and not be reached by available oxygen (Accardi-Dey, 2003). However, determination of $BC_{Thermal}$ in sulfur-rich sediments from the Black Sea did not yield elevated $BC_{Thermal}$ values (0.197-0.815 %wt.) (Middelburg et al., 1999).

### 3.2 Chemical Oxidation Method

Accurate results from the chemical oxidation method are dependent on selection of the appropriate length of oxidation for the samples of interest. To determine the response of the organic carbon present in the Pettaquamscutt River sediment samples to dichromate oxidation, we initially combined sediments from all 70 depth horizons into a composite sample and ran triplicate aliquots through the chemical procedure (prior to treating the samples of interest). To follow the oxidation process, eleven oxidation steps were performed on these composite samples (at 0.25, 0.5, 1.5, 3.5, 8, 50, 101.5, 224, 400, 657 and 850 h), following the procedure outlined in section 2.1 and fully described by

Masiello and collaborators (2002). Triplicate determination of the oxidation rate of TOC from the Pettaquamscutt River sediments showed good reproducibility of the method (Figure 6). Approximately 100 h of oxidation were required before sample mass stopped decreasing significantly (Figure 6a). This is two times longer than the 50 h reported by Masiello and collaborators (2002) for coastal marine sediments. Carbon loss, on the other hand, stabilized at approximately 650 h (Figure 6b), similar to the 675 h reported by Masiello and collaborators. The uncertainty for triplicate analyses was ± 0.002 for % OC and ± 0.02 for % wt.. For the 8-point depth profile of $BC_{Chemical}$ shown in Figure 2, about

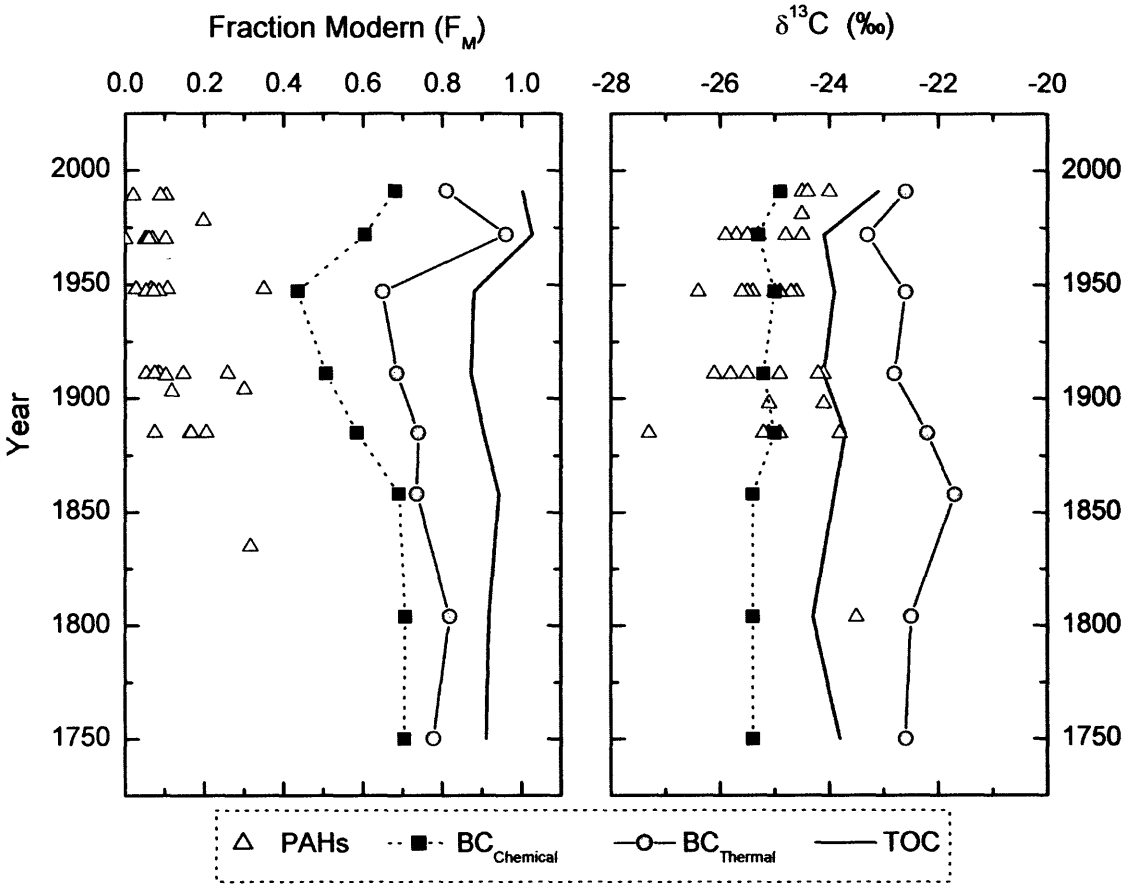


Figure 5. Down-core profiles of the radiocarbon content (expressed as fraction modern) and stable carbon composition of total organic carbon, $BC_{Thermal}$, $BC_{Chemical}$ and individual PAHs isolated from the sediments of the Pettaquamscutt River.

1.5g of dried sample was demineralized and repeatedly treated with 0.25M $Cr_2O_7^{2-}$ - 2M $H_2SO_4$ (23°C) for 650 h. The resulting residue was rinsed 4 times with Milli-Q water, dried to constant weight under vacuum and analyzed for carbon and nitrogen content on the elemental analyzer.

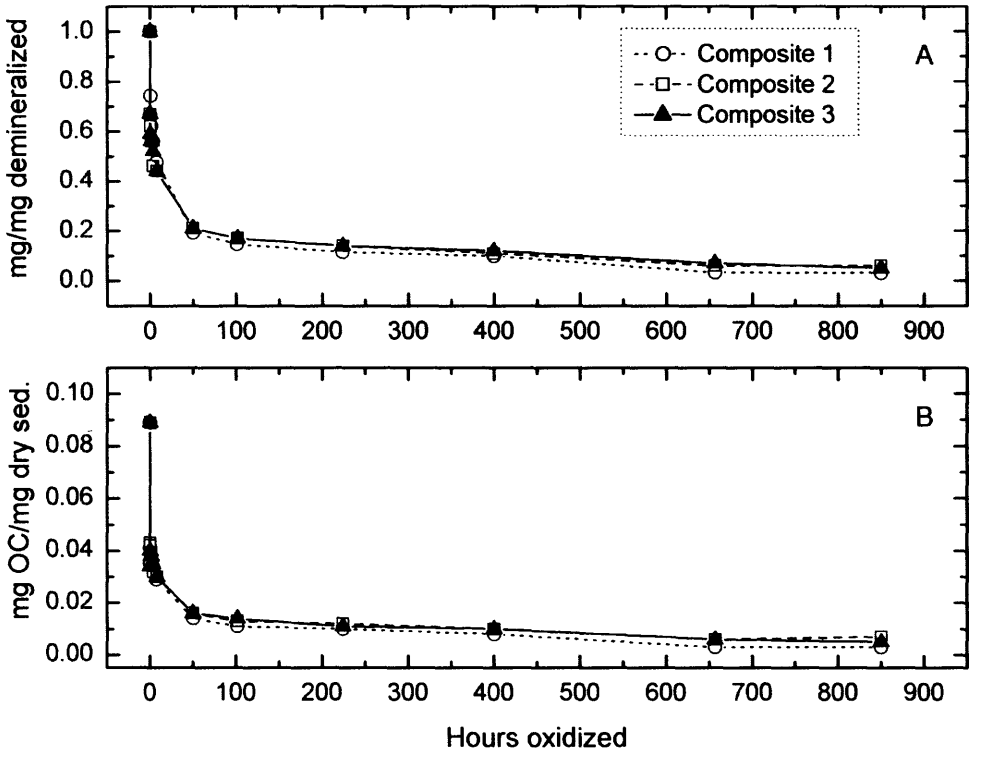


Figure 6. (a) fraction of the demineralized sediment lost versus number of hours of chemical oxidation; (b) fraction of organic carbon (OC) in the dry sediment sample versus number of hours of chemical oxidation.

The down-core profile of $BC_{Chemical}$ generated for the Pettaquamscutt River sediments shows a significant correlation with pyrogenic PAHs (Figure 2). The amount of $BC_{Chemical}$ in these samples is lowest in the late 1700s (0.35 %wt.) and increases steadily to a maximum between 1910 and 1950 (0.70 %wt.), following the classical

profile of sedimentary PAH (Hites et al., 1980; McVeety and Hites, 1988). A typical criticism to this chemical oxidation method is that (a) it may not completely oxidize the OC present in a sample, thus overestimating the BC content of sediments, and that (b) the several steps involved can result in loss of sample. Although care was taken during sample manipulation, losses of BC are possible. Even after centrifuging the samples at 4000 rpm for 10 minutes, it is difficult to determine if micron-sized BC particles are not being pipetted out with the dark/reduced dichromate solution.

The amount of $BC_{Chemical}$ show no correlation ($R^2 = 0.04$) with residual nitrogen content (Figure 4) and show $\delta^{13}C$ values and radiocarbon contents that resemble those of the well-characterized PAHs (Figure 5). Moreover, $\delta^{13}C$ values obtained for the $BC_{Chemical}$ plot within the same range as the pyrogenic PAHs. The low $^{14}C$ abundance in individual PAHs (excluding retene and perylene) from the Pettaquamscutt River sediments is consistent with a dominantly fossil fuel combustion source ($F_M = 0.00\text{-}0.35$). While the $^{14}C$ abundance of $BC_{Chemical}$ isolated from the same sediment horizons were significantly more modern than the PAHs ($F_M = 0.44\text{-}0.71$), $BC_{Chemical}$ particles show a decrease in $^{14}C$ abundance beginning in the 1850s that closely correlate with the onset of widespread fossil fuel burning, in what is usually referred to as the Suess Effect. These observations highlight the agreement encountered in the Pettaquamscutt River sediments for pyrogenic PAHs and chemically isolated BC.

Although good correlation was obtained between the $^{14}C$ abundance of $BC_{Chemical}$ and that of pyrogenic PAHs, if these two species truly derived from a common source their radiocarbon content should be closer in value. Discrepancies in radiocarbon values obtained for $BC_{Chemical}$ and pyrogenic PAHs have been previously observed. Radiocarbon measurements conducted on BC isolated from SRM 1649a by two thermal methods ($F_M$= 0.065 $\pm$0.003 and 0.038 $\pm$0.012) and the chemical oxidation method in question (0.153 $\pm$0.002) yielded contrasting results. In that study, the higher fraction modern measured for $BC_{Chemical}$ versus $BC_{Thermal}$ suggested that the former was not efficient in removing organic carbon, thus raising the fraction modern 3-fold. By applying a simple mass balance to the radiocarbon content of $BC_{Chemical}$ and $BC_{Thermal}$, using $\Delta^{14}C$ of TOC as a

modern end-member and $\Delta^{14}C$ of fluoranthene as the fossil end-member, it is possible to calculate the fraction of organic carbon still present in each operationally defined BC fraction (Table 1). The results obtained show that both BC isolation methods fail to completely remove organic carbon from the samples. However, the chemical oxidation method was on average 25% more efficient for the sediments of the Pettaquamscutt River than the thermal oxidation method.

Table 1. Fraction of organic carbon remaining after oxidation by a thermal and a chemical method.

| Horizon | Year | $\Delta^{14}C$ Fla[a] (‰) | $\Delta^{14}C$ TOC (‰) | $BC_{Thermal}$ | | $BC_{Chemical}$ | |
|---|---|---|---|---|---|---|---|
| | | | | $\Delta^{14}C$ (‰) | OC Remaining (%)[b] | $\Delta^{14}C$ (‰) | OC Remaining (%)[b] |
| H1 | 1991 | -912.2 | -3.7 | -195.1 | 79 | -323.2 | 65 |
| H2 | 1972 | -945.6 | 20.3 | -45.5 | 93 | -398.9 | 57 |
| H3 | 1947 | -893.3 | -125.2 | -354.3 | 70 | -567.0 | 42 |
| H4 | 1911 | -912.4 | -132.2 | -318.3 | 76 | -496.0 | 53 |
| H5 | 1885 | -836.0 | -100.4 | -264.9 | 78 | -418.1 | 57 |

[a] Appendix 4; discussion on significance of fluoranthene in Chapter 6

[b] $\Delta^{14}C_{BC} = (f_{OC}*\Delta^{14}C_{OC}) + (f_{PAHl}*\Delta^{14}C_{PAH})$, $f_{OC} + f_{PAH} = 1$

### 3.3 Chemical / Thermal Method

BC isolated by this method is usually referred to as graphitic black carbon (GBC) (Gélinas et al., 2001; Dickens et al., 2004), so we will keep to this convention when discussing BC isolated by this method. The chemical/thermal method yielded consistently the lowest down-core BC values in the Pettaquamscutt River sediments (Figure 2). GBC values ranged from 0.06 %wt. to 0.24 %wt. throughout the core, with an average C/N ratio of 36±10 ($n$=22). Similar low GBC results were obtained when this method was used in a soil intercomparison exercise involving six different BC methods and five international laboratories (Schmidt et al., 2001). It has been suggested that one reason for the significantly lower BC amounts isolated by the GBC-method may be due to the numerous manipulation steps inherent to the analytical procedure (Accardi-Dey, 2003). However, a different explanation may be that this method isolates only the most

refractory portion of the BC spectrum – fossil graphitic black carbon derived from the weathering of thermally metamorphosed rocks (Figure 1). In fact, Dickens and collaborators (2004) isolated BC particles from sediments off the Washington coast using the GBC method and found a trend of decreasing GBC flux with increasing distance offshore. GBC recovered from these samples was highly depleted in $^{14}C$ and because they studied samples deposited prior to the onset of the industrial revolution, the authors suggested that this fraction corresponded to graphite weathered from rocks rather than from fossil fuel combustion.

GBC in the Pettaquamscutt River sediments was constant at 0.11±0.01 %wt. between 1789-1898 and 1964-1999. However, these values doubled between 1898-1964 (0.20±0.02 %wt.) around the time of maximum increase in PAH concentrations (Figure 2). If GBC isolated from this system were exclusively derived from the weathering of rocks, it would be expected that the percent weight of this fraction would either (a) have remained high (at 0.2 %wt) since the turn of the century due to increased weathering caused by urban development or (b) have kept constant though time, unaffected by urbanization. The bedrock formation underlying the Pettaquamscutt River is predominantly Rhode Island Formation meta-sedimentary rock, consisting of sandstone, conglomerate, schist and graphite (Hermes et al., 1994). Consequently, it is reasonable that a portion of the BC present in the Pettaquamscutt River sediments is GBC. However, the fact that the GBC profile is skewed towards higher values when PAH concentrations are at their maximum does not fit this scenario and suggests an additional anthropogenic source. Unfortunately, no $\delta^{13}C$ or $\Delta^{14}C$ determinations were conducted of these GBC particles due to the low yield of residual carbon achieved with this method. At present, the doubling in GBC content observed between 1898-1964 remains unexplained.

# 4. CONCLUSIONS

Comparison of the quantity and isotopic composition of BC isolated by three different methods from the sediments of the Pettaquamscutt River sediments illustrated the difficulties involved in evaluating a portion of the carbon pool that is still operationally defined. BC isolated by the dichromate/sulfuric acid oxidation method showed the best down-core correlation with the historical trend of total pyrogenic PAHs. Determination of the $^{14}C$ abundance of $BC_{Chemical}$ and individual PAHs supported the quantification results. Although an unknown portion of the true BC quantity may have been lost due to manipulation of the samples, the chemical oxidation method seems to be a the most promising alternative for quantification of environmental BC in anoxic, organic and sulfur rich sediments where the application of the less manipulative 375°C-thermal method can give biased results.

# 5. REFERENCES


Accardi-Dey A. and Gschwend P. (2002) Assessing the combined roles of natural organic matter and black carbon as sorbents in sediments. *Environ. Sci. Technol.* **36**(1), 21-29.

Accardi-Dey A. (2003) Black carbon in marine sediments: quantification and implications for the sorption of polycyclic aromatic hydrocarbons. PhD, Massachusetts Institute of Technology / Woods Hole Oceanographic Institution.

Cachier H. (1989) Isotopic characterization of carbonaceous aerosols. *Aerosol Sci. Technol.* **10**, 379-385.

Cooke W. F. and Wilson J. J. N. (1996) A global black carbon aerosol model. *J. Geophys. Res.* **101**, 19395-19409.

Currie L. A., Klouda G. A., Continetti R. E., Kaplan I. R., Wong W. W., Dzubay T. G., and Stevens R. K. (1983) On the origins of carbonaceous particles in American cities. Results of radiocarbon dating and chemical characterization. *Radiocarbon* **25**, 603-614.

Dickens A., Gélinas Y., Masiello C., Wakeham S., and Hedges J. (2004) Reburial of fossil organic carbon in marine sediments. *Nature* **427**, 336-339.

Eglinton T. I., Eglinton G., Dupont L., Sholkovitz E., Montluçon D., and Reddy C. M. (2002) Composition, age, and provenance of organic matter in NW African dust over the Atlantic. *Geochemistry Geophysics Geosystems ($G^3$)* **3**(8).

EPA. (1997) National air quality status and trends. Six principal pollutants:Particulate matter (PM). http://www.epa.gov/oar/aqtrnd97/brochure/pm10.html, U.S. Environmental Protection Agency.

Gélinas Y., Orentice K. M., Baldock J. A., and Hedges J. I. (2001) An improved thermal oxidation method for the quantification of soot/graphitic black carbon in sediments and soils. *Environ. Sci. Technol.* **35**(17), 3519-3525.

Glaser B., Balashov E., Haumaier L., Guggenberg G., and Zech W. (2000) Black carbon in density fractions of anthropogenic soils of the Brazilian Amazon region. *Org. Geochem.* **31**, 669-678.

Griffin J. J. and Goldberg E. D. (1981) Sphericity as a characteristic of solids from fossil fuel burning in a Lake Michigan sediment. *Geochim. Cosmochim. Acta* **45**, 763-769.

Gustafsson Ö., Haghseta F., Chan C., Macfarlane J., and Gschwend P. (1997) Quantification of the dilute sedimentary soot phase: Implications for PAH speciation and bioavailability. *Environ. Sci. Technol.* **31**, 203-209.

Gustafsson Ö. and Gschwend P. (1998) The flux of black carbon to surface sediments on the New England continental shelf. *Geochim. Cosmochim. Acta* **62**(3), 465-472.

Gustafsson Ö., Bucheli T., Kukulska Z., Andersson M., Largeau C., Rouzaud J.-N., Reddy C., and Eglinton T. (2001) Evaluation of a protocol for the quantification of black carbon in sediments. *Global Biogeochem. Cycles* **0**(0), 1-10.

Hermes O., Gromet L., and Murray D. (1994) Bedrock Geologic Map of Rhode Island. In *Rhode Island Map Series No.1.*

Hites R. A., Laflamme R. E., Windsor Jr J. G., Farrington J. W., and Deuser W. G. (1980) Polycyclic aromatic hydrocarbons in an anoxic sediment core from the Pettaquamscutt River (Rhode Island, USA). *Geochim. Cosmochim. Acta* **44**, 873-878.

Kirkevåg A., Iversen T., and Dahlback A. (1999) On radiative effects of black carbon and sulphate aerosols. *Atmos. Environ.* **33**, 2621-2635.

Klinedinst D. B. and Currie L. A. (1999) Direct quantification of PM2.5 fossil and biomass carbon within the Northern front range air quality study's domain. *Environ. Sci. Technol.* **33**, 4146-4154.

Levin I. and Kromer B. (1997) Twenty years of atmospheric $^{14}CO_2$ observations at Schauinsland station, Germany. *Radiocarbon* **39**(2), 205-218.

Lima A. L. C., Eglinton T. I., and Reddy C. M. (2003) High-resolution record of pyrogenic polycyclic aromatic hydrocarbon deposition during the 20$^{th}$ century. *Environ. Sci. Technol.* **37**, 53-61.

Masiello C., Druffel E., and Currie L. (2002) Radiocarbon measurements of black carbon in aerosols and ocean sediments. *Geochim. Cosmochim. Acta* **66**(6), 1025-1036.

Masiello C. A. and Druffel E. R. M. (1998) Black carbon in deep-sea sediments. *Science* **280**, 1911-1913.

McGroddy S., Farrington J., and Gschwend P. (1996) Comparison of the in situ and desorption sediment-water partitioning of polycyclic aromatic hydrocarbons and polychlorinated biphenyls. *Environ. Sci. Technol.* **30**, 172-177.

McVeety B. and Hites R. (1988) Atmospheric deposition of polycyclic aromatic hydrocarbons to water surfaces: a mass balance approach. *Atmos. Environ.* **22**(3), 511-536.

Middelburg J. J., Nieuwenhuize J., and Breugel P. v. (1999) Black carbon in marine sediments. *Mar. Chem.* **65**, 245-252.

Nguyen T., Brown R., and Ball W. (2004) An evaluation of thermal resistance as a measure of black carbon content in diesel soot, wood char, and sediment. *Org. Geochem.* **35**, 217-234.

Pedersen P., Ingwersen J., Nielsen T., and Larsen E. (1980) Effects of fuel, lubricant, and engine operating parameters on the emission of polycyclic aromatic hydrocarbons. *Environ. Sci. Technol.* **14**(1), 71-79.

Penner J. E. (1995) Carbonaceous aerosols influencing atmospheric radiation: Black and organic carbon. In *Aerosol Forcing of Climate* (ed. R. J. Charlson and J. Heintzenberg). John Wiley and Sons Ltd.

Reddy C., Pearson A., Xu L., McNichol A., Benner Jr. B., Wise S., Klouda G., Currie L., and Eglinton T. (2002) Radiocarbon as a tool to apportion the sources of polycyclic aromatic hydrocarbons and black carbon in environmental samples. *Environ. Sci. Technol.* **36**, 1774-1782.

Rose N. (1995) Carbonaceous particle record in lake sediments from the Arctic and other remote areas of the Northern Hemisphere. *Sci. Tot. Environ.* **160/161**, 487-496.

Samet J., Dominici F., Curriero F., Coursac I., and Zeger S. (2000) Fine particulate air pollution and mortality in 20 U.S. cities, 1987-1994. *The New England Journal of Medicine* **343**(24), 1742-1749.

Schmidt M. W. I., Skjemstad J. O., Czimczik C. I., Glaser B., Prentice K. M., Gelinas Y., and Kuhlbusch T. A. J. (2001) Comparative analysis of black carbon in soils. *Global Biogeochem. Cycles* **15**(1), 163-167.

Smith D. M., Griffin J. J., and Goldberg E. D. (1973) Elemental carbon in marine sediments: A baseline for burning. *Nature* **241**, 268-270.

Suman D. O. (1986) Charcoal production from agricultural burning in Central Panama and its deposition in the sediments of the Gulf of Panama. *Environ. Conserv.* **13**(1), 51-60.

Suman D. O., Kuhlbusch T. A. J., and Lim B. (1994) Marine sediments: A reservoir of black carbon and their use as spatial and temporal records of combustion. In *Sediment records of biomass burning and global change*, Vol. 51 (ed. J. S. Clark, H. Cachier, J. G. Goldammer, and B. Stocks), pp. 271-293. NATO ASI Series.

Wolbach W. S. and Anders E. (1989) Elemental carbon in sediments: Determination and isotopic analysis in the presence of kerogen. *Geochim. Cosmochim. Acta* **53**, 1637-1647.

# CHAPTER 9

# CONCLUSIONS

The excellent preservation of laminated sediments of the Pettaquamscutt River has allowed for the construction of a high-resolution historical record of pyrogenic PAH emissions from fossil fuel and biomass sources since pre-industrial times. Our data revealed relatively constant PAH fluxes between 1978 and 1996, followed by an abrupt increase from 1996 and 1999. This trend agrees with other recent studies that showed constant (Schneider et al., 2001) and increasing (Van Metre et al., 2000) concentrations of PAHs in selected locations. However, contrary to these investigations we believe that the recent increase in PAH deposition may be due to a rise in combustion of diesel fuel associated with traffic of heavy-duty vehicles as opposed to increase in automobile usage. Our historical reconstruction work also cast doubt on the validity of using coronene as a marker for vehicle exhaust emissions, as this compound reach maximum concentration in the Pettaquamscutt River sediments in 1932, preceding the time interval with highest motor vehicle emissions (1960-1975).

Radiocarbon measurement of PAHs at the molecular level provided new insights into the complexity of sources of these compounds. Results obtained for the Pettaquamscutt River sediments show a clear trend of increasing contribution of fossil fuel derived PAHs since the end of the $19^{th}$ century. While most energy consumption information report wood as the major source of energy at that time, early industrialization and higher contribution of fossil sources to the Northeastern United States compared to other parts of the country may explain these results. Comparison between the suburban Pettaquamscutt River and a pristine remote site (Siskiwit Lake, Isle Royale) showed that although atmospheric transport widely disperses combustion-derived PAHs, regions closer to point sources receive higher contributions of these compounds. While the majority of the PAHs present in the Pettaquamscutt River in 1950 were of fossil origin,

those deposited in the Siskiwit Lake showed a significant contribution from burning of modern biomass. This implies that geographic variability, even within short distances on a global scale, may play a greater role than previously anticipated in dictating the composition of sedimentary PAHs. Our $^{14}C$ results have revealed that in addition to functioning as a marker for combustion of wood in aerosol samples, retene also has the potential to be used as a tracer for land clearing in regions formerly covered by pine forests.

The down-core profile and radiocarbon abundance of pyrogenic PAHs were further used to assess the results obtained for black carbon (BC) particles isolated by a chemical and a thermal oxidation method. Because BC is operationally defined, it is difficult to evaluate what portion of the reduced carbon continuum is isolated by a given method. Since PAHs are produced during incomplete combustion, concurrently with BC, the distribution of these two species should be closely related. We compared the radiocarbon abundance of BC and PAHs in sediments based on the premise that they derive from a common source. Our results indicate that both isolation procedures probably overestimate the amount of black carbon present in the sediments. In general, the chemical oxidation method yielded radiocarbon results that more closely followed the PAH trend. Therefore, this method seems to be a good alternative for quantifying environmental black carbon in anoxic, organic and sulfur rich sediments where the application of the less manipulative 375°C-thermal method can give more biased results.

This study also yielded insight into the sources of perylene. The combination of historical sedimentary records and $\delta^{13}C$ and $\Delta^{14}C$ measurements for perylene and TOC helped us discern, with some confidence, the importance of fossil fuel combustion to the sedimentary profile of this PAH. We were able to verify that while combustion was a significant source of perylene to the suburban Pettaquamscutt River in recent years that was not the case for the remote Siskiwit Lake. Our results also suggest that commonly employed diagnostic ratios such as perylene/TOC (for assessing *in situ* production of perylene) and pyrene/perylene (for assessing the contribution of combustion of fossil fuels to the amount of perylene in the sediments) should be used with caution. While *in*

*situ* production can shift the later towards low values, no correlation was observed between TOC content and perylene.

Finally, construction of a high-resolution record of Pb deposition in the Pettaquamscutt River over the past 250 yr closely recorded the well-described maximum associated with leaded gasoline usage in the United States. Evaluation of the Pb isotopic composition of these sediments showed a clear maximum in anthropogenic $^{206}Pb/^{207}Pb$ in the mid-1800s. We determined that mining and smelting of Pb ores in the Upper Mississippi Valley district (which accounted for almost all Pb production in the United States in that period) was the most likely cause for this isotopic maximum and suggest that this event could be useful as a stratigraphic marker for sedimentary records from the Northeastern United States.

## REFERENCES

Schneider A., Stapleton H., Cornwell J., and Baker J. (2001) Recent declines in PAH, PCB, and toxaphene levels in the northern Great Lakes as determined from high resolution sediment cores. *Environ. Sci. Technol.* **35**(19), 3809-3815.

Van Metre P., Mahler B., and Furlong E. (2000) Urban sprawl leaves its PAH signature. *Environ. Sci. Technol.* **34**, 4064-4070.

# APPENDIX 1

A. Concentration of individual PAHs in the sediments of the Pettaquamscutt River

| Depth (cm) | Year | Concentration (ng $g^{-1}$) | | | | | | | | | | | | | | | | | |
|---|---|---|---|---|---|---|---|---|---|---|---|---|---|---|---|---|---|---|---|
| | | Flu | Phen | Anth | Fla | Py | BaA | Chry | BbF | BkF | BeP | BaP | DBahA | IP | BghiP | Cor | Total | Retene | Perylene |
| 0 | 1999 | 45 | 510 | 120 | 1630 | 1050 | 400 | 515 | 955 | 360 | 505 | 570 | 50 | 525 | 455 | 65 | 7755 | 25 | 215 |
| 1 | 1997 | 40 | 475 | 105 | 1590 | 1000 | 400 | 490 | 900 | 315 | 470 | 490 | 45 | 455 | 405 | 45 | 7226 | 25 | 165 |
| 1.5 | 1996 | 30 | 315 | 90 | 1090 | 725 | 275 | 330 | 630 | 230 | 330 | 420 | 35 | 355 | 320 | 55 | 5230 | 25 | 180 |
| 2 | 1995 | 35 | 400 | 90 | 560 | 365 | 350 | 430 | 850 | 300 | 450 | 500 | 40 | 420 | 370 | 50 | 5210 | 30 | 285 |
| 2.5 | 1994.3 | 50 | 330 | 80 | 1030 | 685 | 265 | 310 | 605 | 230 | 320 | 400 | 40 | 340 | 305 | 55 | 5045 | 25 | 54 |
| 3 | 1993.6 | 30 | 335 | 75 | 1120 | 700 | 245 | 320 | 630 | 245 | 340 | 325 | 30 | 325 | 275 | 30 | 5035 | 20 | 450 |
| 3.5 | 1993 | 40 | 300 | 75 | 925 | 610 | 235 | 280 | 550 | 200 | 285 | 345 | 25 | 270 | 240 | 40 | 4420 | 20 | 400 |
| 4 | 1992 | 30 | 300 | 70 | 990 | 665 | 250 | 310 | 600 | 225 | 325 | 375 | 30 | 290 | 250 | 45 | 4755 | 25 | 655 |
| 4.5 | 1991 | 35 | 340 | 85 | 1050 | 700 | 275 | 315 | 610 | 230 | 315 | 395 | 30 | 325 | 295 | 55 | 5055 | 35 | 710 |
| 5 | 1991 | 35 | 325 | 85 | 1060 | 700 | 270 | 300 | 620 | 240 | 330 | 430 | 30 | 350 | 310 | 55 | 5740 | 25 | 895 |
| 5.5 | 1990 | 30 | 295 | 75 | 990 | 675 | 265 | 305 | 620 | 230 | 325 | 410 | 50 | 350 | 315 | 55 | 4990 | 25 | 1100 |
| 6 | 1989 | 35 | 330 | 85 | 1050 | 720 | 275 | 320 | 650 | 245 | 350 | 440 | 35 | 355 | 310 | 40 | 5240 | 30 | 1250 |
| 6.5 | 1988 | 30 | 285 | 75 | 935 | 635 | 240 | 280 | 565 | 200 | 295 | 365 | 30 | 305 | 265 | 45 | 4550 | 25 | 1040 |
| 7 | 1987 | 35 | 305 | 80 | 975 | 660 | 250 | 290 | 580 | 200 | 315 | 330 | 25 | 235 | 210 | 15 | 4505 | 30 | 1070 |
| 7.5 | 1986 | 30 | 285 | 80 | 950 | 645 | 230 | 270 | 555 | 210 | 300 | 370 | 25 | 315 | 295 | 55 | 4615 | 15 | 1320 |
| 8 | 1985 | 40 | 350 | 90 | 1130 | 755 | 275 | 325 | 660 | 225 | 350 | 410 | 35 | 365 | 310 | 35 | 5355 | 25 | 1470 |
| 8.5 | 1984 | 35 | 310 | 90 | 1060 | 735 | 345 | 290 | 620 | 210 | 320 | 400 | 30 | 340 | 300 | 55 | 5140 | 55 | 1500 |
| 9 | 1983 | 40 | 320 | 75 | 1010 | 695 | 250 | 280 | 585 | 220 | 320 | 400 | 30 | 330 | 300 | 55 | 4910 | 25 | 1760 |
| 9.5 | 1982 | 35 | 315 | 80 | 985 | 685 | 245 | 285 | 565 | 200 | 305 | 385 | 30 | 335 | 300 | 65 | 4815 | 30 | 1600 |
| 10 | 1981 | 50 | 405 | 120 | 1220 | 855 | 320 | 350 | 695 | 255 | 375 | 490 | 40 | 390 | 360 | 65 | 5990 | 30 | 2060 |
| 11 | 1979 | 50 | 430 | 100 | 1170 | 830 | 315 | 355 | 730 | 260 | 390 | 510 | 40 | 410 | 320 | 50 | 5960 | 35 | 2110 |
| 12 | 1977 | 50 | 435 | 100 | 1240 | 865 | 305 | 340 | 685 | 260 | 375 | 485 | 35 | 385 | 350 | 65 | 5975 | 35 | 1930 |

| Depth | Year | Flu | Phen | Anth | Fla | Py | BaA | Chry | BbF | BkF | BeP | BaP | DBahA | IP | BghiP | Cor | Total | Retene | Perylene |
|---|---|---|---|---|---|---|---|---|---|---|---|---|---|---|---|---|---|---|---|
| 13 | 1975 | 60 | 515 | 125 | 1340 | 930 | 350 | 400 | 790 | 270 | 410 | 485 | 40 | 420 | 355 | 50 | 6540 | 40 | 2760 |
| 14 | 1973 | 75 | 655 | 150 | 1610 | 1140 | 430 | 445 | 875 | 305 | 475 | 630 | 50 | 500 | 440 | 65 | 7814 | 45 | 2900 |
| 15 | 1971 | 70 | 595 | 140 | 1325 | 955 | 370 | 400 | 805 | 290 | 430 | 555 | 45 | 440 | 385 | 60 | 6865 | 45 | 2160 |
| 16 | 1969 | 75 | 625 | 155 | 1490 | 1100 | 400 | 430 | 850 | 325 | 470 | 610 | 45 | 480 | 425 | 75 | 7555 | 45 | 2770 |
| 17 | 1966 | 75 | 555 | 145 | 1270 | 940 | 340 | 385 | 760 | 265 | 405 | 510 | 40 | 410 | 360 | 65 | 6525 | 50 | 2570 |
| 18 | 1964 | 75 | 555 | 140 | 1320 | 965 | 325 | 385 | 730 | 260 | 400 | 510 | 40 | 410 | 370 | 70 | 6845 | 50 | 2500 |
| 19 | 1962 | 75 | 610 | 140 | 1510 | 1080 | 345 | 440 | 770 | 280 | 440 | 515 | 65 | 425 | 380 | 756 | 7856 | 0 | 2870 |
| 20 | 1959 | 95 | 870 | 215 | 1870 | 1470 | 455 | 545 | 990 | 370 | 560 | 735 | 50 | 560 | 520 | 85 | 9390 | 55 | 2740 |
| 21 | 1956 | 115 | 1150 | 225 | 2350 | 1760 | 515 | 705 | 1140 | 375 | 645 | 825 | 95 | 660 | 610 | 120 | 11290 | 65 | 2570 |
| 22 | 1954 | 120 | 1100 | 215 | 2060 | 1560 | 490 | 600 | 1050 | 395 | 570 | 750 | 50 | 585 | 520 | 95 | 10160 | 55 | 2520 |
| 23 | 1951 | 120 | 1050 | 175 | 2080 | 1480 | 480 | 635 | 1090 | 395 | 580 | 750 | 50 | 615 | 540 | 110 | 10150 | 60 | 2480 |
| 24 | 1948 | 115 | 780 | 180 | 1750 | 1200 | 450 | 475 | 915 | 340 | 475 | 630 | 50 | 535 | 475 | 105 | 8475 | 60 | 2000 |
| 25 | 1945 | 115 | 680 | 170 | 1770 | 1110 | 430 | 465 | 900 | 325 | 455 | 610 | 45 | 560 | 480 | 130 | 8245 | 55 | 1980 |
| 26 | 1942 | 100 | 490 | 125 | 1350 | 890 | 360 | 350 | 765 | 280 | 385 | 515 | 40 | 470 | 410 | 110 | 6640 | 55 | 1550 |
| 27 | 1938 | 80 | 405 | 125 | 1160 | 770 | 335 | 315 | 670 | 225 | 340 | 480 | 40 | 440 | 390 | 95 | 5870 | 40 | 1500 |
| 28 | 1935 | 80 | 435 | 110 | 1210 | 795 | 315 | 300 | 700 | 245 | 345 | 465 | 35 | 440 | 380 | 105 | 5960 | 55 | 2960 |
| 29 | 1931 | 80 | 415 | 130 | 835 | 530 | 310 | 290 | 725 | 245 | 345 | 480 | 40 | 495 | 405 | 120 | 5445 | 75 | 5550 |
| 30 | 1927 | 90 | 420 | 135 | 1150 | 720 | 345 | 2805 | 815 | 280 | 385 | 530 | 40 | 540 | 455 | 135 | 8845 | 65 | 4910 |
| 31 | 1922 | 95 | 485 | 155 | 1110 | 695 | 405 | 330 | 970 | 335 | 445 | 610 | 45 | 645 | 540 | 165 | 7030 | 75 | 5160 |
| 32 | 1916 | 95 | 500 | 155 | 1180 | 750 | 395 | 315 | 960 | 345 | 450 | 610 | 45 | 665 | 570 | 185 | 7220 | 70 | 5190 |
| 33 | 1911 | 90 | 420 | 150 | 1040 | 660 | 360 | 285 | 850 | 270 | 395 | 525 | 45 | 645 | 540 | 200 | 6475 | 80 | 5740 |
| 34 | 1905 | 85 | 385 | 135 | 1150 | 735 | 355 | 265 | 795 | 295 | 380 | 510 | 35 | 600 | 530 | 185 | 6440 | 75 | 6700 |
| 35 | 1901 | 75 | 315 | 110 | 840 | 515 | 260 | 210 | 635 | 220 | 300 | 400 | 50 | 510 | 435 | 170 | 5045 | 80 | 6990 |
| 36 | 1898 | 70 | 295 | 105 | 870 | 540 | 245 | 180 | 620 | 225 | 290 | 390 | 25 | 485 | 430 | 165 | 4935 | 75 | 5990 |
| 37 | 1894 | 55 | 205 | 75 | 590 | 360 | 190 | 135 | 465 | 150 | 220 | 285 | 25 | 385 | 330 | 130 | 3600 | 60 | 6330 |
| 38 | 1890 | 45 | 195 | 65 | 515 | 325 | 170 | 125 | 375 | 130 | 180 | 240 | 20 | 290 | 255 | 90 | 3020 | 55 | 5410 |
| 39 | 1885 | 35 | 145 | 55 | 440 | 275 | 145 | 110 | 340 | 110 | 160 | 210 | 15 | 265 | 225 | 85 | 2615 | 80 | 4740 |
| 40 | 1882 | 30 | 115 | 45 | 365 | 235 | 110 | 80 | 265 | 95 | 130 | 170 | 10 | 210 | 185 | 65 | 2110 | 85 | 4000 |
| 41 | 1878 | 30 | 120 | 45 | 305 | 190 | 110 | 90 | 250 | 80 | 120 | 170 | 20 | 200 | 175 | 60 | 1965 | 115 | 4990 |
| 42 | 1873 | 25 | 85 | 30 | 225 | 145 | 70 | 50 | 165 | 65 | 80 | 100 | 8 | 125 | 110 | 40 | 1323 | 90 | 4270 |

| Depth | Year | Flu | Phen | Anth | Fla | Py | BaA | Chry | BbF | BkF | BeP | BaP | DBahA | IP | BghiP | Cor | Total | Retene | Perylene |
|---|---|---|---|---|---|---|---|---|---|---|---|---|---|---|---|---|---|---|---|
| 43 | 1869 | 20 | 80 | 30 | 200 | 125 | 65 | 55 | 155 | 50 | 80 | 100 | 13 | 125 | 105 | 40 | 1243 | 80 | 3450 |
| 44 | 1865 | 20 | 60 | 20 | 190 | 125 | 60 | 50 | 115 | 40 | 60 | 75 | 6 | 75 | 70 | 25 | 991 | 70 | 2270 |
| 45 | 1860 | 15 | 65 | 25 | 155 | 100 | 60 | 50 | 110 | 40 | 60 | 75 | 10 | 80 | 70 | 20 | 935 | 100 | 1910 |
| 46 | 1857 | 15 | 45 | 20 | 95 | 65 | 45 | 35 | 90 | 35 | 60 | 60 | 5 | 60 | 60 | 17 | 707 | 100 | 1700 |
| 47 | 1852 | 15 | 25 | 11 | 65 | 45 | 20 | 21 | 55 | 16 | 30 | 30 | 0 | 40 | 35 | 15 | 424 | 105 | 1520 |
| 48 | 1847 | 10 | 20 | 10 | 50 | 35 | 14 | 12 | 35 | 11 | 18 | 17 | 1 | 25 | 25 | 10 | 293 | 110 | 1390 |
| 49 | 1842 | 10 | 15 | 8 | 1 | 1 | 9 | 10 | 30 | 7 | 13 | 12 | 0 | 20 | 20 | 9 | 164 | 135 | 1440 |
| 50 | 1838 | 10 | 10 | 6 | 25 | 17 | 6 | 6 | 20 | 5 | 9 | 6 | 0 | 13 | 11 | 5 | 149 | 155 | 1110 |
| 51 | 1833 | 8 | 14 | 6 | 26 | 15 | 7 | 9 | 20 | 6 | 10 | 9 | 0 | 16 | 14 | 5 | 165 | 175 | 1190 |
| 52 | 1828 | 6 | 11 | 4 | 21 | 14 | 4 | 5 | 15 | 4 | 7 | 0 | 0 | 8 | 6 | 0 | 106 | 250 | 1100 |
| 53 | 1823 | 7 | 13 | 6 | 21 | 13 | 5 | 6 | 15 | 3 | 7 | 6 | 0 | 10 | 8 | 4 | 125 | 275 | 1270 |
| 54 | 1820 | 7 | 13 | 6 | 23 | 16 | 6 | 6 | 15 | 5 | 8 | 6 | 0 | 9 | 9 | 4 | 132 | 235 | 1250 |
| 55 | 1815 | 7 | 15 | 7 | 23 | 15 | 5 | 7 | 15 | 4 | 7 | 5 | 0 | 10 | 7 | 3 | 129 | 350 | 785 |
| 56 | 1810 | 6 | 10 | 7 | 18 | 12 | 4 | 5 | 13 | 3 | 6 | 4 | 0 | 7 | 6 | 3 | 105 | 285 | 755 |
| 57 | 1804 | 6 | 12 | 7 | 25 | 15 | 6 | 7 | 16 | 4 | 8 | 7 | 1 | 11 | 8 | 4 | 136 | 200 | 950 |
| 58 | 1799 | 4 | 9 | 7 | 19 | 11 | 4 | 4 | 12 | 3 | 5 | 4 | 0 | 8 | 6 | 2 | 101 | 145 | 750 |
| 59 | 1794 | 7 | 10 | 8 | 18 | 11 | 5 | 8 | 16 | 5 | 7 | 5 | 0 | 11 | 8 | 5 | 123 | 190 | 1045 |
| 60 | 1789 | 6 | 12 | 7 | 21 | 13 | 5 | 7 | 15 | 4 | 7 | 6 | 1 | 10 | 8 | 3 | 124 | 110 | 920 |
| 61 | 1785 | 6 | 11 | 8 | 18 | 11 | 5 | 5 | 14 | 4 | 6 | 5 | 1 | 8 | 7 | 3 | 110 | 90 | 1320 |
| 62 | 1779 | 5 | 9 | 7 | 17 | 10 | 3 | 4 | 12 | 3 | 6 | 3 | 0 | 7 | 6 | 2 | 96 | 65 | 1550 |
| 63 | 1774 | 5 | 8 | 8 | 15 | 8 | 3 | 4 | 10 | 2 | 5 | 3 | 0 | 6 | 5 | 2 | 85 | 50 | 1070 |
| 64 | 1768 | 5 | 8 | 8 | 13 | 7 | 2 | 3 | 10 | 2 | 5 | 3 | 0 | 6 | 5 | 2 | 78 | 45 | 990 |
| 65 | 1761 | 5 | 10 | 7 | 18 | 11 | 4 | 5 | 13 | 3 | 5 | 5 | 0 | 7 | 6 | 2 | 103 | 50 | 1070 |
| 66 | 1755 | 5 | 11 | 6 | 20 | 10 | 4 | 4 | 10 | 3 | 4 | 3 | 0 | 6 | 5 | 2 | 93 | 504 | 1050 |
| 67 | 1750 | 5 | 11 | 7 | 15 | 9 | 4 | 5 | 12 | 2 | 5 | 3 | 0 | 6 | 5 | 2 | 91 | 70 | 1560 |
| 68 | 1745 | 5 | 9 | 6 | 16 | 10 | 4 | 5 | 11 | 3 | 5 | 4 | 0 | 6 | 5 | 2 | 92 | 75 | 1160 |
| 69 | 1740 | 3 | 6 | 3 | 9 | 6 | 2 | 3 | 6 | 1 | 3 | 0 | 0 | 3 | 3 | 1 | 50 | 55 | 950 |
| 70 | 1735 | 6 | 12 | 8 | 13 | 8 | 3 | 4 | 10 | 2 | 5 | 0 | 0 | 5 | 4 | 2 | 82 | 80 | 1980 |

B. Re-plot of figures from Chapter 3 using revised sediment chronology

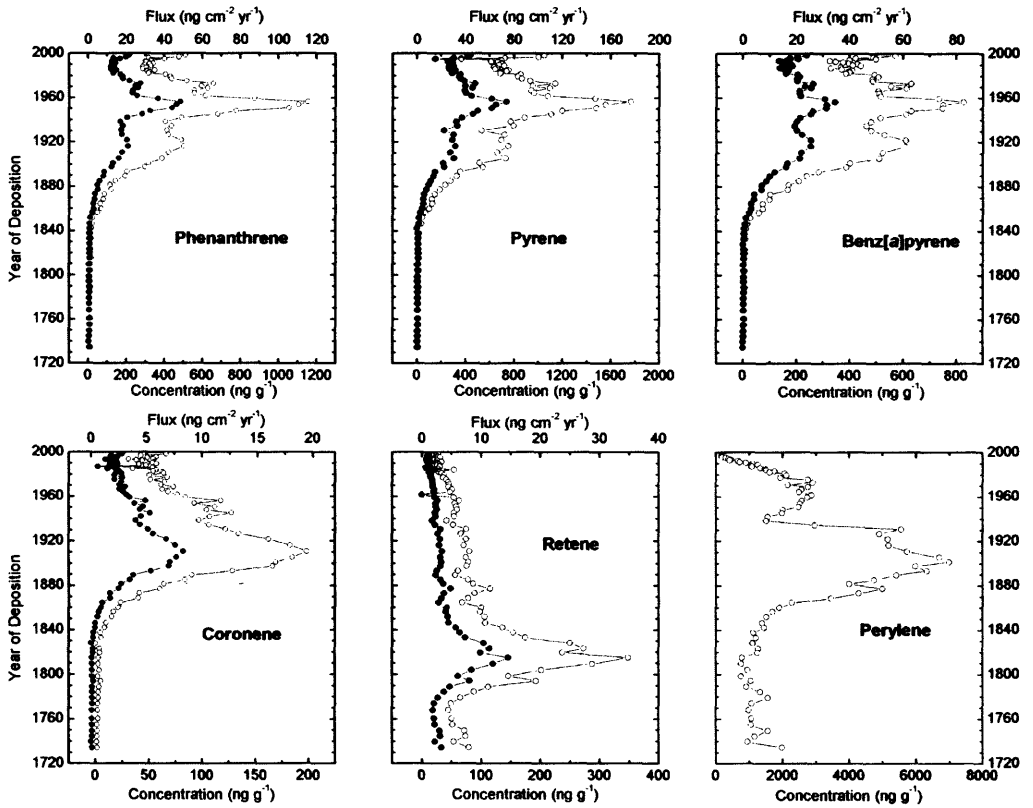


Figure 3. Down-core profiles of selected PAH. Concentration (open circles) and flux (closed circles) values were corrected for the salt content of the sediment. Fluxes were additionally corrected for sediment focusing.

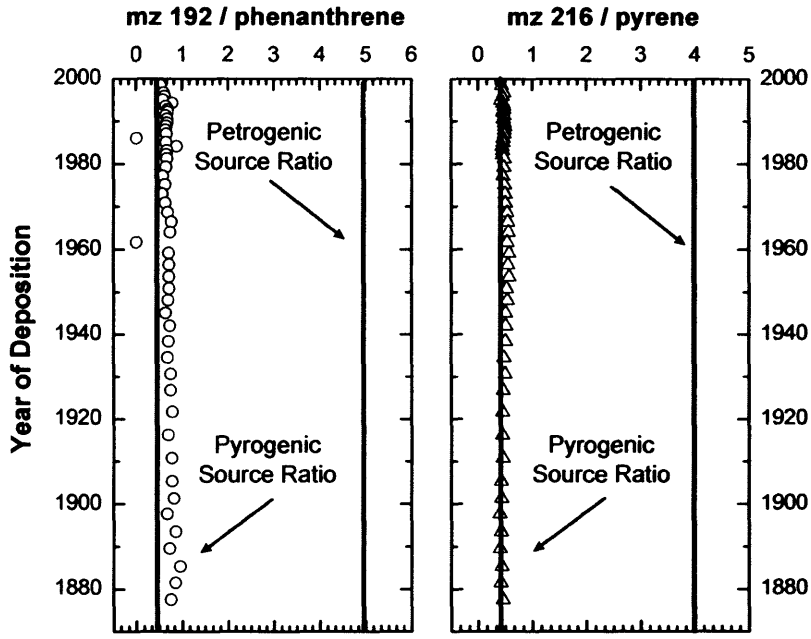


Figure 5. PAH source-diagnostic ratios taken from Gustafsson and Gschwend (1997) (Gustafsson and Gschwend, 1997). (a) sum of methyl-phenanthrenes and methyl-anthracenes to phenanthrene, and (b) sum of methyl-pyrenes and methyl-fluoranthenes to pyrene.

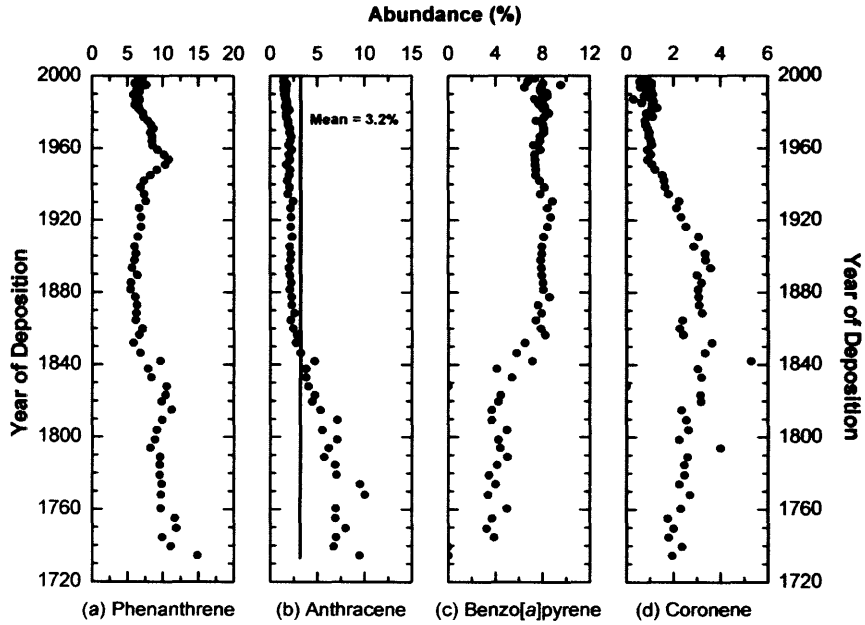


Figure 6. Down-core relative abundance (relative to ΣPAH) of selected individual PAH.

C. Concentration of PAHs in the sediments of Siskiwit Lake.

| Depth (cm) | Year | Concentration (ng $g^{-1}$) | |
|---|---|---|---|
| | | Total[a] | Perylene |
| 0 | 1954 | 590 | 110 |
| 2 | 1943 | 410 | 130 |
| 4 | 1932 | 310 | 250 |
| 6 | 1921 | 200 | 170 |
| 8 | 1910 | 190 | 250 |
| 10 | 1898 | 120 | 240 |
| 12 | 1887 | 130 | 170 |
| 14 | 1876 | 140 | 210 |
| 16 | 1865 | 150 | 210 |
| 18 | 1854 | 120 | 170 |
| 20 | 1843 | 110 | 200 |
| 22 | 1832 | 110 | 210 |
| 24 | 1821 | 85 | 180 |
| 26 | 1810 | 100 | 200 |
| 28 | 1798 | 100 | 210 |

[a] Total PAHs = sum of Phen, Anth, Fla, Py, BaA, Chry, BbF, BjF, BkF, BaP, BeP, IP and BghiP

# APPENDIX 2

Pb concentration, stable Pb isotope data and age model for the Pettaquamscutt River sediments.

| Depth | Age | Total | | | Pb conc. | Anthropogenic | | | Pb conc. |
|---|---|---|---|---|---|---|---|---|---|
| (cm) | Model | $^{208}Pb/^{207}Pb$ | $^{206}Pb/^{207}Pb$ | $^{206}Pb/^{204}Pb$ | (ppm) | $^{208}Pb/^{207}Pb$ | $^{206}Pb/^{207}Pb$ | $^{206}Pb/^{204}Pb$ | (ppm) |
| 0 | 1999 | 2.464 | 1.203 | 21.438 | 62.2 | 2.460 | 1.201 | 21.436 | 48.9 |
| 1 | 1997 | 2.461 | 1.200 | 21.291 | 59.2 | 2.456 | 1.197 | 21.246 | 45.9 |
| 2 | 1995 | 2.461 | 1.201 | 21.237 | 49.8 | 2.454 | 1.197 | 21.161 | 36.5 |
| 3 | 1994 | 2.463 | 1.204 | 21.350 | 66.2 | 2.459 | 1.202 | 21.326 | 53.0 |
| 4 | 1992 | 2.460 | 1.201 | 21.313 | 78.8 | 2.456 | 1.200 | 21.285 | 65.5 |
| 5 | 1991 | 2.460 | 1.201 | 21.303 | 61.5 | 2.455 | 1.198 | 21.264 | 48.2 |
| 6 | 1989 | 2.463 | 1.204 | 21.063 | 85.8 | 2.460 | 1.202 | 20.993 | 72.6 |
| 7 | 1987 | 2.461 | 1.205 | 21.555 | 108.6 | 2.458 | 1.204 | 21.570 | 95.4 |
| 8 | 1985 | 2.458 | 1.205 | 21.339 | 109.0 | 2.455 | 1.205 | 21.324 | 95.8 |
| 9 | 1983 | 2.467 | 1.205 | 21.358 | 118.5 | 2.465 | 1.205 | 21.347 | 105.2 |
| 10 | 1981 | 2.462 | 1.205 | 20.974 | 150.2 | 2.461 | 1.204 | 20.928 | 136.9 |
| 11 | 1979 | 2.459 | 1.201 | 21.298 | 186.8 | 2.457 | 1.200 | 21.287 | 173.6 |
| 12 | 1977 | 2.454 | 1.201 | 21.256 | 153.1 | 2.452 | 1.200 | 21.238 | 139.8 |
| 13 | 1975 | 2.459 | 1.202 | 21.085 | 175.8 | 2.458 | 1.201 | 21.056 | 162.5 |
| 14 | 1973 | 2.459 | 1.202 | 21.257 | 139.7 | 2.457 | 1.201 | 21.237 | 126.5 |
| 15 | 1971 | 2.457 | 1.198 | 21.172 | 153.3 | 2.455 | 1.197 | 21.146 | 140.0 |
| 16 | 1969 | 2.455 | 1.193 | 21.105 | 163.9 | 2.453 | 1.191 | 21.075 | 150.6 |
| 17 | 1966 | 2.456 | 1.192 | 21.152 | 142.0 | 2.454 | 1.190 | 21.122 | 128.7 |
| 18 | 1964 | 2.456 | 1.190 | 21.020 | 154.2 | 2.453 | 1.189 | 20.980 | 141.0 |
| 19 | 1962 | 2.456 | 1.192 | 21.020 | 124.5 | 2.453 | 1.189 | 20.969 | 111.2 |
| 20 | 1959 | 2.457 | 1.192 | 21.041 | 127.8 | 2.455 | 1.190 | 20.994 | 114.6 |
| 21 | 1956 | 2.458 | 1.192 | 21.064 | 127.2 | 2.455 | 1.190 | 21.020 | 114.0 |
| 22 | 1954 | 2.460 | 1.195 | 21.131 | 99.5 | 2.457 | 1.193 | 21.082 | 86.3 |
| 23 | 1951 | 2.460 | 1.195 | 21.038 | 130.4 | 2.458 | 1.193 | 20.991 | 117.1 |
| 24 | 1948 | 2.460 | 1.195 | 21.168 | 95.0 | 2.457 | 1.193 | 21.122 | 81.8 |
| 25 | 1945 | 2.461 | 1.196 | 21.141 | 101.0 | 2.458 | 1.194 | 21.095 | 87.7 |
| 26 | 1942 | 2.459 | 1.192 | 21.142 | 102.5 | 2.456 | 1.189 | 21.097 | 89.2 |
| 27 | 1938 | 2.459 | 1.192 | 21.065 | 80.4 | 2.456 | 1.188 | 20.990 | 67.2 |
| 28 | 1935 | 2.460 | 1.192 | 21.125 | 98.3 | 2.457 | 1.189 | 21.075 | 85.1 |
| 29 | 1931 | 2.461 | 1.193 | 21.062 | 92.7 | 2.458 | 1.190 | 20.998 | 79.5 |
| 30 | 1927 | 2.463 | 1.196 | 21.122 | 91.3 | 2.460 | 1.193 | 21.067 | 78.1 |
| 31 | 1922 | 2.464 | 1.197 | 21.151 | 94.4 | 2.461 | 1.195 | 21.103 | 81.1 |
| 32 | 1916 | 2.464 | 1.196 | 21.131 | 82.5 | 2.461 | 1.194 | 21.071 | 69.2 |
| 33 | 1911 | 2.465 | 1.197 | 21.146 | 84.6 | 2.462 | 1.194 | 21.090 | 71.4 |
| 34 | 1905 | 2.466 | 1.197 | 21.160 | 87.5 | 2.464 | 1.195 | 21.109 | 74.3 |
| 35 | 1901 | 2.467 | 1.198 | 21.153 | 69.2 | 2.464 | 1.195 | 21.084 | 56.0 |

| Depth (cm) | Age Model | Total | | | Pb conc. (ppm) | Anthropogenic | | | Pb conc. (ppm) |
|---|---|---|---|---|---|---|---|---|---|
| | | $^{208}Pb/^{207}Pb$ | $^{206}Pb/^{207}Pb$ | $^{206}Pb/^{204}Pb$ | | $^{208}Pb/^{207}Pb$ | $^{206}Pb/^{207}Pb$ | $^{206}Pb/^{204}Pb$ | |
| 36 | 1898 | 2.467 | 1.198 | 21.185 | 69.7 | 2.464 | 1.195 | 21.124 | 56.5 |
| 37 | 1894 | 2.473 | 1.201 | 21.245 | 65.2 | 2.471 | 1.199 | 21.194 | 51.9 |
| 38 | 1890 | 2.478 | 1.205 | 21.356 | 57.3 | 2.477 | 1.204 | 21.329 | 44.0 |
| 39 | 1885 | 2.480 | 1.208 | 21.377 | 52.6 | 2.480 | 1.207 | 21.353 | 39.3 |
| 40 | 1882 | 2.484 | 1.212 | 21.449 | 49.6 | 2.486 | 1.212 | 21.450 | 36.3 |
| 41 | 1878 | 2.487 | 1.215 | 21.508 | 48.5 | 2.490 | 1.217 | 21.531 | 35.3 |
| 42 | 1873 | 2.489 | 1.219 | 21.602 | 49.1 | 2.493 | 1.222 | 21.660 | 35.9 |
| 43 | 1869 | 2.491 | 1.222 | 21.712 | 34.5 | 2.499 | 1.230 | 21.877 | 21.3 |
| 44 | 1865 | 2.494 | 1.226 | 21.778 | 34.1 | 2.503 | 1.236 | 21.989 | 20.8 |
| 45 | 1860 | 2.498 | 1.231 | 21.885 | 32.3 | 2.510 | 1.245 | 22.189 | 19.1 |
| 46 | 1857 | 2.498 | 1.235 | 22.045 | 32.2 | 2.510 | 1.252 | 22.464 | 18.9 |
| 47 | 1852 | 2.502 | 1.241 | 22.079 | 33.5 | 2.516 | 1.260 | 22.493 | 20.3 |
| 48 | 1847 | 2.513 | 1.253 | 22.291 | 30.2 | 2.539 | 1.286 | 22.950 | 17.0 |
| 49 | 1842 | 2.520 | 1.263 | 22.452 | 24.7 | 2.568 | 1.325 | 23.619 | 11.4 |
| 50 | 1838 | 2.515 | 1.257 | 22.365 | 22.8 | 2.564 | 1.320 | 23.634 | 9.6 |
| 51 | 1833 | 2.502 | 1.239 | 22.014 | 18.9 | 2.554 | 1.305 | 23.338 | 5.7 |
| 52 | 1828 | 2.490 | 1.225 | 21.770 | 17.3 | 2.524 | 1.273 | 22.833 | 4.0 |
| 53 | 1823 | 2.486 | 1.221 | 21.635 | 17.9 | 2.505 | 1.249 | 22.171 | 4.7 |
| 54 | 1820 | 2.481 | 1.215 | 21.544 | 24.3 | 2.481 | 1.215 | 21.544 | 24.3 |
| 55 | 1815 | 2.480 | 1.211 | 21.471 | 15.7 | 2.480 | 1.211 | 21.471 | 15.7 |
| 56 | 1810 | 2.480 | 1.212 | 21.475 | 15.9 | 2.480 | 1.212 | 21.475 | 15.9 |
| 57 | 1804 | 2.479 | 1.211 | 21.443 | 16.6 | 2.479 | 1.211 | 21.443 | 16.6 |
| [redacted] | | | | | | | | | |
| 58 | 1799 | 2.479 | 1.208 | 21.401 | 14.7 | 2.480 | 1.211 | 21.446 | 13.2 |
| 59 | 1794 | 2.479 | 1.210 | 21.416 | 15.5 | | | | |
| 60 | 1789 | 2.478 | 1.209 | 21.391 | 12.5 | | | | |
| 61 | 1785 | 2.480 | 1.211 | 21.428 | 14.3 | | | | |
| 62 | 1779 | 2.480 | 1.211 | 21.447 | 14.4 | | | | |
| 63 | 1774 | 2.479 | 1.211 | 21.429 | 15.4 | | | | |
| 64 | 1768 | 2.480 | 1.212 | 21.450 | 13.0 | | | | |
| 65 | 1761 | 2.480 | 1.212 | 21.488 | 12.0 | | | | |
| 66 | 1755 | 2.480 | 1.212 | 21.504 | 12.2 | | | | |
| 67 | 1750 | 2.480 | 1.211 | 21.460 | 12.0 | | | | |
| 68 | 1745 | 2.478 | 1.209 | 21.432 | 13.5 | | | | |
| 69 | 1740 | 2.481 | 1.212 | 21.461 | 11.6 | | | | |
| 70 | 1735 | 2.480 | 1.212 | 21.496 | 11.3 | | | | |

# APPENDIX 3

Procedure utilized for diluting a small (< 25 μg C) liquid sample with a standard of known $\Delta^{14}C$ and $\delta^{13}C$, prior to combusting to $CO_2$ and making graphite.

Several of our samples contained less than 20 μg C and NOSAMS needs at least 25 μg C for a reliable radiocarbon determination. We investigated the possibility of increasing the amount of carbon of a small sample with a standard of known $\Delta^{14}C$ and $\delta^{13}C$ values by conducting three tests where standards of different $^{14}C$ content were mixed in specified proportions, to verify if a simple mass balance could account for the $^{14}C$ measured in the mixtures. We prepared solutions of a $^{14}C$-modern (squalene), a $^{14}C$-half-modern (heneicosanoic acid) and a $^{14}C$-free (*n*-quinquiphenyl) standard in iso-octane (Table 1) and used a micro-syringe to draw the exact amounts needed for the test mixtures.

Table 1. $\delta^{13}C$ and $\Delta^{14}C$ values for the original standards.

| Compound | $\delta^{13}C$ (‰) | $\Delta^{14}C$ (‰) | $\Delta^{14}C$ (‰) Error | NOSAMS Accession # | Observation |
|---|---|---|---|---|---|
| Heneicosanoic Acid[a] | -27.6 | -385 | 8.2 | OS - 39258 | |
| Heneicosanoic Acid[a] | -27.5 | -397 | 8.7 | OS - 39259 | Half-modern |
| **Average** | **-27.6** | **-391** | | | |
| Squalene[b] | -22.3 | -35.5 | 9.0 | OS - 39260 | |
| Squalene[b] | -22.1 | -35.3 | 8.8 | OS - 39253 | Modern |
| **Average** | **-22.2** | **-35.4** | | | |
| *n*-quinquiphenyl[c] | -26.5 | -977 | 4.2 | OS - 39276 | |
| *n*-quinquiphenyl[c] | -24.4 | -992 | 1.0 | OS - 39532 | Fossil |
| **Average** | **-25.5** | **-985** | | | |

[a] Aldrich lot # 10819JF. Concentration = 130 μg $mL^{-1}$ (in hexane).
[b] Aldrich lot # 05817AN. Concentration = 425 μg $mL^{-1}$ (in hexane).
[c] K&K Lab lot # 24987. Concentration = 175 μg $mL^{-1}$ (in hexane).

The expected $\delta^{13}C$ and $\Delta^{14}C$ values for the test mixtures were calculated using a simple isotopic mass balance:

$$\Delta^{14}C_{Mixture} = (f_{Std1} * \Delta^{14}C_{Std1}) + (f_{Std2} * \Delta^{14}C_{Std2}) \quad (1)$$

$$f_{Std1} + f_{Std2} = 1 \quad (2)$$

where $f_{Std1}$ and $f_{Std2}$ are the proportions of standard 1 and 2 and $\Delta^{14}C_{Std1}$ and $\Delta^{14}C_{Std2}$ are their radiocarbon composition, previously measured at NOSAMS. For the three tests conducted, the $\delta^{13}C$ and $\Delta^{14}C$ calculated and measured match to within 1.2 ‰ and 8 ‰ of each other (Table 2). The good results obtained by the dilution experiment using standards encouraged its application to compound-specific samples that, otherwise, would not contain enough carbon for a $^{14}C$ measurement.

Table 2. Calculated and measured $\delta^{13}C$ and $\Delta^{14}C$ values for the three test mixtures.

| Test # | Mixture | $\delta^{13}C$ (‰) | $\Delta^{14}C$ (‰) | $\Delta^{14}C$ (‰) Error | NOSAMS Accession # |
|---|---|---|---|---|---|
| 1.1 | 95 % fossil + 5 % modern | -24.1 | -941 | 2.9 | OS - 37681 |
| 1.2 | 95 % fossil + 5 % modern | -24.3 | -940 | 2.1 | OS - 37682 |
| | Average | -24.2 | -941 | | |
| | Calculated | -25.3 | -937 | | |
| | **Difference** | **1.1‰** | **3.6‰** | | |
| 2.1 | 95 % modern + 5 % fossil | -21.3 | -76 | 12.8 | OS - 37683 |
| 2.2 | 95 % modern + 5 % fossil | -22.2 | -74 | 10.2 | OS - 37684 |
| | Average | -21.8 | -75 | | |
| | Calculated | -22.3 | -83 | | |
| | **Difference** | **0.6‰** | **7.9‰** | | |
| 3.1 | 30 % modern + 70 % half-modern | -23.3 | -132 | 10.6 | OS - 37685 |
| 3.2 | 30 % modern + 70 % half-modern | -23.4 | -140 | 8.6 | OS - 37686 |
| | Average | -23.3 | -136 | | |
| | Calculated | -23.8 | -142 | | |
| | **Difference** | **0.5‰** | **6.1‰** | | |

Prior to applying this procedure to the samples of interest, we estimated the error associated with diluting samples containing 2-20 μg C to a large enough size to run on

the accelerator mass spectrometer (AMS). Mass balance equations similar to (1) and (2) were used to calculate the expected error:

$$M_{Mix}Fm_{Mix} = M_{Sample}Fm_{Sample} + M_{Std}Fm_{Std} \quad (3)$$

$$M_{Mix} = M_{Sample} + M_{Std} \quad (4)$$

where M= mass and Fm= fraction modern of the mixture, sample and diluent standard. These equations were reformulated to:

$$Fm_{Sample} = R_{Mix}Fm_{Mix} - (R_{Mix} - 1)Fm_{Std} \quad (5)$$

where $R_{Mix} = M_{Mix}/M_{Sample}$ is the dilution factor. The propagation of error then yields (Pearson, 2000):

$$\sigma^2_{Fms} = R_{Mix}^2\,\sigma^2_{Fm(Mix)} + (1 - R_{Mix})^2\,\sigma^2_{Fm(Std)} + (Fm_{Mix} - Fm_{Std})^2(2P^2)R_{Mix}^2 \quad (6)$$

$P = \sigma_m/M$ is the precision with which quantities of carbon are measured using a micro-syringe. Reproducibility of sampling a known volume was 0.8% (P = 0.008)

$Fm_{Std}$ 0.000 ($^{14}$C-dead) or 1.0 ($^{14}$C-modern)

$\sigma_{Fm(Std)}$ error in the diluent; considered to be the smallest error that we can measure on a sample with that Fm. For a dead diluent, $\sigma_{Fm(Std)} = 0.0008$ and for a modern diluent, $\sigma_{Fm(Std)} = 0.003$.

$\sigma_{Fm(Mix)}$ = error in the measured fraction modern; data from NOSAMS' small samples were used to calculate an equation for the $\sigma_{Fm(Mix)}$ as a function of the measured fm, based on a range of sample sizes (McNichol, 2004). The resulting error equations for each size range were:

25-50 µg $\sigma = 0.004 + 0.012*Fm_{Mix}$

75-100 µg $\sigma = 0.0035 + 0.008*Fm_{Mix}$

200-300 µg $\sigma = 0.002 + 0.007*Fm_{Mix}$

Using these parameters and considering the mixture of a $^{14}$C-modern standard to a $^{14}$C-dead sample and vice-versa, $\Delta^{14}$C errors in the final measurement were calculated (Figure 1, Table 3). As shown in Figure 1, dilution of a modern sample with a fossil

standard yields smaller errors if the starting sample mass is <10 μg C than dilution of a $^{14}C$-dead sample with a $^{14}C$-modern standard. In addition, larger $\Delta^{14}C$ errors result from the dilution of a sample to a sizeable final mass (100 μg C) than to a small mass (25 μg C).

Table 3. Calculation of the error associated with diluting a modern sample with a $^{14}C$-dead standard up to a final mass of 25 μg C. Values plotted in Figure 1b, solid line.

| $M_{Mix}$ | $M_{Sample}$ | $M_{Std}$ | $Fm_{Sample}$ | $Fm_{Std}$ | Dilution Factor ($R_{Mix}$) | $Fm_{Mix}$ | P | $\sigma_{fm}$ (Mix) | $\sigma_{fm}$ (Std) | $\sigma_{fm}$ (Sample) | $\Delta^{14}C$ Error (‰) |
|---|---|---|---|---|---|---|---|---|---|---|---|
| 25 | 0 | 25 | 1 | 0 | 25.00 | 0.000 | 0.008 | 0.0040 | 0.003 | 0.1232 | 123.2 |
| 25 | 1 | 24 | 1 | 0 | 25.00 | 0.040 | 0.008 | 0.0045 | 0.003 | 0.1331 | 133.1 |
| 25 | 2 | 23 | 1 | 0 | 12.50 | 0.080 | 0.008 | 0.0050 | 0.003 | 0.0710 | 71.0 |
| 25 | 3 | 22 | 1 | 0 | 8.33 | 0.120 | 0.008 | 0.0054 | 0.003 | 0.0504 | 50.4 |
| 25 | 4 | 21 | 1 | 0 | 6.25 | 0.160 | 0.008 | 0.0059 | 0.003 | 0.0402 | 40.2 |
| 25 | 5 | 20 | 1 | 0 | 5.00 | 0.200 | 0.008 | 0.0064 | 0.003 | 0.0342 | 34.2 |
| 25 | 6 | 19 | 1 | 0 | 4.17 | 0.240 | 0.008 | 0.0069 | 0.003 | 0.0302 | 30.2 |
| 25 | 7 | 18 | 1 | 0 | 3.57 | 0.280 | 0.008 | 0.0074 | 0.003 | 0.0274 | 27.4 |
| 25 | 8 | 17 | 1 | 0 | 3.13 | 0.320 | 0.008 | 0.0078 | 0.003 | 0.0253 | 25.3 |
| 25 | 9 | 16 | 1 | 0 | 2.78 | 0.360 | 0.008 | 0.0083 | 0.003 | 0.0237 | 23.7 |
| 25 | 10 | 15 | 1 | 0 | 2.50 | 0.400 | 0.008 | 0.0088 | 0.003 | 0.0225 | 22.5 |
| 25 | 11 | 14 | 1 | 0 | 2.27 | 0.440 | 0.008 | 0.0093 | 0.003 | 0.0214 | 21.4 |
| 25 | 12 | 13 | 1 | 0 | 2.08 | 0.480 | 0.008 | 0.0098 | 0.003 | 0.0206 | 20.6 |
| 25 | 13 | 12 | 1 | 0 | 1.92 | 0.520 | 0.008 | 0.0102 | 0.003 | 0.0199 | 19.9 |
| 25 | 14 | 11 | 1 | 0 | 1.79 | 0.560 | 0.008 | 0.0107 | 0.003 | 0.0193 | 19.3 |
| 25 | 15 | 10 | 1 | 0 | 1.67 | 0.600 | 0.008 | 0.0112 | 0.003 | 0.0188 | 18.8 |
| 25 | 16 | 9 | 1 | 0 | 1.56 | 0.640 | 0.008 | 0.0117 | 0.003 | 0.0183 | 18.3 |
| 25 | 17 | 8 | 1 | 0 | 1.47 | 0.680 | 0.008 | 0.0122 | 0.003 | 0.0179 | 17.9 |
| 25 | 18 | 7 | 1 | 0 | 1.39 | 0.720 | 0.008 | 0.0126 | 0.003 | 0.0176 | 17.6 |
| 25 | 19 | 6 | 1 | 0 | 1.32 | 0.760 | 0.008 | 0.0131 | 0.003 | 0.0173 | 17.3 |
| 25 | 20 | 5 | 1 | 0 | 1.25 | 0.800 | 0.008 | 0.0136 | 0.003 | 0.0170 | 17.0 |
| 25 | 21 | 4 | 1 | 0 | 1.19 | 0.840 | 0.008 | 0.0141 | 0.003 | 0.0168 | 16.8 |
| 25 | 22 | 3 | 1 | 0 | 1.14 | 0.880 | 0.008 | 0.0146 | 0.003 | 0.0166 | 16.6 |
| 25 | 23 | 2 | 1 | 0 | 1.09 | 0.920 | 0.008 | 0.0150 | 0.003 | 0.0164 | 16.4 |
| 25 | 24 | 1 | 1 | 0 | 1.04 | 0.960 | 0.008 | 0.0155 | 0.003 | 0.0162 | 16.2 |
| 25 | 25 | 0 | 1 | 0 | 1.00 | 1.000 | 0.008 | 0.0160 | 0.003 | 0.0160 | 16.0 |

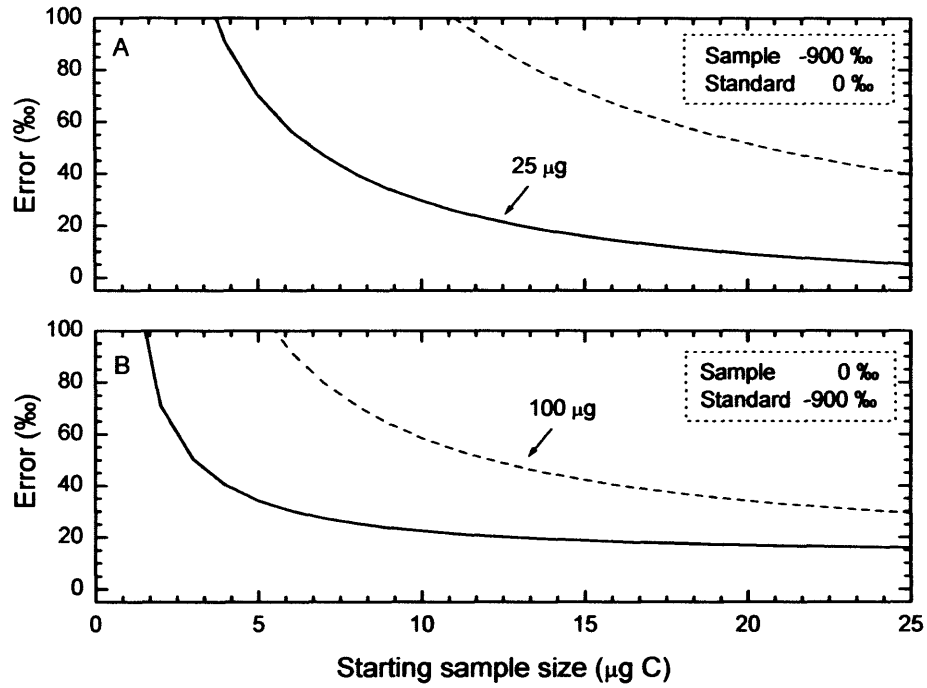


Figure 1. Error associated with diluting a small sample with a standard of known $\Delta^{14}C$. (a) dilution of a $^{14}C$-poor sample with a modern standard; (b) dilution of a modern sample with a $^{14}C$-poor standard. Solid line corresponds to a final sample size of 25 µg C and dashed line corresponds to a final sample size of 100 µg C.

Because of the large errors associated with diluting a $^{14}C$-dead sample to a large enough size to run on the accelerator (25 µg), mostly compound-specific samples between 8-20 µg were selected for the dilution procedure. A list of the nine samples that underwent dilution with a squalene solution is present in Table 4. After adding a known amount of standard to the PAH of interest, the mixtures were analyzed on a GC-FID to double-check the dilution factor. In the case of fluoranthene (H1), pyrene (H1) and chrysene (H4), these GC-FID runs showed higher concentrations than when samples were checked for purity (after being recovered from the PCGC U-tubes), the inverse occurring for retene (H8). The total amount of carbon present in each liquid sample (calculated using the FID trace) was in good agreement with the amount of carbon measured by manometry in the vacuum line (Table 4). $\Delta^{14}C$ values reported by NOSAMS

for the diluted samples (Appendix 4) were corrected for the amount of standard added, using the isotopic mass balance equations (1) and (2). An average $\Delta^{14}C$ value of –38.4‰ ($n$ = 3) was used for the squalene standard used in the dilution. Propagation of errors associated with diluting the samples was conducted using equation 6 and the following parameters: $\sigma_{Fm(Std)}$ = standard deviation of triplicate $\Delta^{14}C$ measurement of diluent (0.0051), $Fm_{Std}$ = average of triplicate measurement of diluent (0.9678) and P = 1%. The resultant values are listed on Appendix 4.

Table 4. Dilution factor, yield of carbon and calculated $\Delta^{14}C$ for samples that underwent dilution with a standard solution.

| Sample | Amount Std. (μg)[a] | FID Area Std. | FID Area PAH | Amount PAH (μg)[b] | Amount in Mix (μg)[c] | % Std in Mix[d] | Amount Vacuum Line (μg)[e] | Line FID (Yield) | PAH $\Delta^{14}C$ (‰)[f] |
|---|---|---|---|---|---|---|---|---|---|
| Fluoranthene - H1 | 11.9 | 396620 | 1234735 | 37.0 | 48.9 | 24.3 | 43.7 | 0.90 | -914.4 |
| Pyrene - H1 | 13.9 | 7799489 | 1823290 | 32.4 | 46.3 | 30.0 | 42.6 | 0.92 | -900.2 |
| Fluoranthene H6+H7+H8 | 19.8 | 1490562 | 897634 | 11.9 | 31.7 | 62.4 | 32.0 | 1.01 | -703.3 |
| Retene - H7 | 17.8 | 471265 | 541333 | 20.5 | 38.3 | 46.5 | 44.2 | 1.15 | -133.1 |
| Retene - H8 | 19.8 | 643785 | 72206 | 2.2 | 22.0 | 89.9 | 24.6 | 1.11 | -269.4 |
| Chrysene - H4 | 11.9 | 1507808 | 4089751 | 32.2 | 44.1 | 26.9 | 42.6 | 0.97 | -949.1 |
| BeP - H5 | 17.8 | 649832.8 | 453624 | 12.4 | 30.3 | 58.9 | 34.7 | 1.15 | -935.0 |
| BaP - H2 | 19.8 | 1064390 | 898456 | 16.7 | 36.5 | 54.2 | 40.7 | 1.12 | -1047.7 |
| BghiP - H1 | 17.8 | 461900 | 341307 | 13.2 | 31.0 | 57.5 | 35.4 | 1.14 | -988.7 |

[a] μL added to mixture times concentration of the stock solution.
[b] (area PAH * amount std)/ (area std), assuming a RF = 1.
[c] Amount std + amount PAH, calculated from FID trace.
[d] Portion of the carbon submitted to $^{14}C$ measurement that corresponds to added standard.
[e] Amount of carbon measured at the vacuum line by manometry.
[f] $\Delta^{14}C$ values calculated for the PAH of interest using the isotopic mass balance equations (1) and (2). Values reported by NOSAMS are listed in Appendix 4.

## REFERENCES

Pearson A. (2000) Biogeochemical applications of compound-specific radiocarbon analysis. PhD, Massachusetts Institute of Technology / Woods Hole Oceanographic Institution.
McNichol AP (2004) Personal communication.

# APPENDIX 4

Compound-specific $\Delta^{14}C$ and $\delta^{13}C$ measurements conducted by the National Ocean Sciences AMS facility (NOSAMS)

A. Pettaquamscutt River

| Sample | Horizon | Depth Interval | Weighed-Average Depth (cm)[a] | Year | Reported by NOSAMS | | | | $\delta^{13}C$ (‰)[b] | Corrected | | | NOSAMS Accession # |
|---|---|---|---|---|---|---|---|---|---|---|---|---|---|
| | | | | | $\delta^{13}C$ (‰) | $F_M$ | $F_M$ Error | $\Delta^{14}C$ (‰) | | $F_M$ | $\Delta^{14}C$ (‰) | $\Delta^{14}C$ Error | |
| Phen | H1+H2 | 0 - 19 | 11.6 | 1978 | -24.5 | 0.1973 | 0.0085 | -804 | - | 0.1978 | -804 | 8.5 | OS - 41639 |
| Phen | H3 | 19.5 - 29 | 23.9 | 1948 | -25.0[c] | 0.3479 | 0.0071 | -654 | -24.6 | 0.3499 | -652 | 7.1 | OS - 39913 |
| Phen | H4+H5 | 29.5 - 42 | 34.4 | 1904 | -25.1 | 0.2975 | 0.0077 | -704 | - | 0.3013 | -701 | 7.7 | OS - 41637 |
| Chry | H3 | 19.5 - 29 | 24.1 | 1948 | -25.4 | 0.0661 | 0.0014 | -934 | - | 0.0665 | -934 | 1.4 | OS - 39900 |
| Chry (Diluted) | H4 | 29.5 - 36 | 32.9 | 1911 | -24.1 | 0.2982[d] | 0.0188 | -704[d] | - | 0.0518 | -948 | 10.5 | OS - 42304 |
| BaA | H3 | 19.5 - 29 | 24.4 | 1947 | -25.0 | 0.0856 | 0.0027 | -915 | - | 0.0862 | -914 | 2.7 | OS - 39905 |
| BaA | H4+H5 | 29.5 - 42 | 34.6 | 1903 | -24.1 | 0.1171 | 0.0035 | -884 | - | 0.1186 | -882 | 3.5 | OS - 41632 |
| Py (Diluted) | H1 | 0 - 9.5 | 5.9 | 1989 | -24.0 | 0.3603[d] | 0.0105 | -642[d] | - | 0.1006 | -900 | 12.1 | OS - 42302 |
| Py | H2 | 10 - 19 | 15.5 | 1970 | -25.7 | 0.0510 | 0.0017 | -949 | - | 0.0511 | -949 | 1.7 | OS - 40307 |
| Py | H3 | 19.5 - 29 | 23.9 | 1948 | -26.4 | 0.0272 | 0.0010 | -973 | - | 0.0274 | -973 | 1.0 | OS - 40297 |
| Py | H4 | 29.5 - 36 | 33 | 1911 | -26.1 | 0.0841 | 0.0037 | -916 | - | 0.0850 | -916 | 3.7 | OS - 41626 |
| Py | H5 | 36.5 - 42 | 39.2 | 1885 | -25.1 | 0.2030 | 0.0040 | -798 | - | 0.2059 | -795 | 4.0 | OS - 41629 |
| Fla (Diluted) | H1 | 0 - 9.5 | 5.9 | 1989 | -24.5 | 0.3006[d] | 0.0131 | -701[d] | - | 0.0863 | -914 | 10.2 | OS - 42300 |
| Fla | H2 | 10 - 19 | 15.5 | 1970 | -25.3 | 0.0545 | 0.0020 | -946 | - | 0.0547 | -946 | 2.0 | OS - 40306 |
| Fla | H3 | 19.5 - 29 | 24.1 | 1948 | -25.0[c] | 0.1066 | 0.0053 | -894 | -24.7 | 0.1074 | -893 | 5.3 | OS - 40315 |
| Fla | H4 | 29.5 - 36 | 33 | 1911 | -25.8 | 0.0872 | 0.0127 | -913 | - | 0.0882 | -912 | 12.7 | OS - 42291 |
| Fla | H5 | 36.5 - 42 | 39.2 | 1885 | -25.2 | 0.1628 | 0.0061 | -838 | - | 0.1651 | -836 | 6.1 | OS - 40904 |
| Fla (Diluted) | H6+H7+H8 | 42.5 - 69.5 | 50.5 | 1835 | -23.5 | 0.7164[d] | 0.0159 | -288[d] | - | 0.3059 | -696 | 34.7 | OS - 42309 |

| Sample | Horizon | Depth Interval | Weighed-Average Depth (cm)[a] | Year | Reported by NOSAMS | | | | $\delta^{13}C$ (‰)[b] | Corrected | | | NOSAMS Accession # |
|---|---|---|---|---|---|---|---|---|---|---|---|---|---|
| | | | | | $\delta^{13}C$ (‰) | $F_M$ | $F_M$ Error | $\Delta^{14}C$ (‰) | | $F_M$ | $\Delta^{14}C$ (‰) | $\Delta^{14}C$ Error | |
| Perylene | H1 | 0 - 9.5 | 7.2 | 1987 | -28.0[c] | 0.7633 | 0.0128 | -242 | -28.5 | 0.7653 | -240 | 12.8 | OS - 40906 |
| Perylene | H2 | 10 - 19 | 15.6 | 1970 | -28.8 | 0.8381 | 0.0097 | -167 | | 0.8413 | -164 | 9.7 | OS - 40891 |
| Perylene | H3 | 19.5 - 29 | 25.4 | 1944 | -28.9 | 0.8134 | 0.0101 | -192 | | 0.8189 | -186 | 10.1 | OS - 40892 |
| Perylene | H4 | 29.5 - 36 | 33.4 | 1909 | -25.0[c] | 0.8367 | 0.0089 | -169 | -28.4 | 0.8520 | -154 | 8.9 | OS - 40888 |
| Perylene | H5 | 36.5 - 42 | 39.5 | 1883 | -28.6 | 0.8776 | 0.0098 | -128 | | 0.8902 | -116 | 9.8 | OS - 41425 |
| Perylene | H6 | 42.5 - 49 | 45.8 | 1857 | -28.7 | 0.8830 | 0.0083 | -123 | | 0.8986 | -107 | 8.3 | OS - 41426 |
| Perylene | H7 | 49.5 - 64 | 57.8 | 1800 | -28.3 | 0.8521 | 0.0036 | -153 | | 0.8729 | -133 | 3.6 | OS - 41481 |
| Perylene | H8 | 64.5 - 69.5 | 68 | 1745 | -28.7 | 0.8463 | 0.0045 | -159 | | 0.8727 | -133 | 4.5 | OS - 41607 |
| B[b+k]F | H2 | 10 - 19 | 15.4 | 1970 | -24.8 | 0.0688 | 0.0094 | -932 | | 0.0690 | -931 | 9.4 | OS - 41447 |
| B[b+k]F | H4 | 29.5 - 36 | 33 | 1911 | -24.9 | 0.0749 | 0.0020 | -926 | | 0.0757 | -925 | 2.0 | OS - 41432 |
| B[b+k]F | H5 | 36.5 - 42 | 39.2 | 1885 | -24.9 | 0.1652 | 0.0055 | -836 | | 0.1676 | -834 | 5.5 | OS - 41450 |
| BeP | H2 | 10 - 19 | 15.4 | 1970 | -25.5 | 0.1022 | 0.0036 | -899 | | 0.1025 | -898 | 3.6 | OS - 41864 |
| BeP | H3 | 19.5 - 29 | 24.3 | 1947 | -25.5 | 0.0527 | 0.0020 | -948 | | 0.0530 | -947 | 2.0 | OS - 41857 |
| BeP | H4 | 29.5 - 36 | 33 | 1911 | -25.5 | 0.2574 | 0.0041 | -744 | | 0.2603 | -741 | 4.1 | OS - 41436 |
| BeP (Diluted) | H5 | 36.5 - 42 | 39.2 | 1885 | -23.8 | 0.5969[d] | 0.0119 | -407[d] | | 0.0664 | -934 | 28.1 | OS - 42307 |
| BaP (Diluted) | H2 | 10 - 19 | 15.4 | 1970 | -24.5 | 0.5029[d] | 0.0125 | -500[d] | | 0.0000 | -1000 | 23.3 | OS - 42303 |
| BaP | H3 | 19.5 - 29 | 24.3 | 1947 | -24.0[c] | 0.0849 | 0.0054 | -916 | -24.9 | 0.0856 | -915 | 5.4 | OS - 42292 |
| BaP | H4 | 29.5 - 36 | 32.9 | 1911 | -27.3 | 0.1458 | 0.0034 | -855 | | 0.1479 | -853 | 3.4 | OS - 41628 |
| BghiP (Diluted) | H1 | 0 - 9.5 | 5.8 | 1989 | -24.0[c] | 0.5615[d] | 0.0132 | -442[d] | -24.4 | 0.0114 | -989 | 26.2 | OS - 42306 |
| BghiP | H2 | 10 - 19 | 15.4 | 1970 | -25.9 | 0.0596 | 0.0048 | -941 | | 0.0598 | -941 | 4.8 | OS - 41635 |
| BghiP | H3 | 19.5 - 29 | 24.5 | 1947 | -25.6 | 0.0721 | 0.0032 | -928 | | 0.0725 | -928 | 3.2 | OS - 41624 |
| BghiP | H4 | 29.5 - 36 | 33.1 | 1910 | -25.5 | 0.1025 | 0.0023 | -898 | | 0.1037 | -897 | 2.3 | OS - 41627 |
| Retene (Diluted) | H7 | 49.5 - 64 | 55.9 | 1810 | -25.7 | 0.9169[d] | 0.0372 | -89[d] | | 0.8937 | -112 | 28.7 | OS - 42299 |
| Retene (Diluted) | H8 | 64.5 - 69.5 | 67.9 | 1745 | -25.0[c] | 0.9445[d] | 0.0205 | -62[d] | -25.6 | 0.7591 | -246 | 159.0 | OS - 42310 |

[a] Depth at which the concentration of the PAH of interest is the average for that horizon.

[b] Values measured by the Organic Mass Spectrometry facility and used to correct $\Delta^{14}C$ for assumed $\delta^{13}C$ .

[c] $\delta^{13}C$ values assumed by NOSAMS

[d] Values as reported by NOSAMS, prior to correction for dilution with standard.

B. Siskiwit Lake

| Sample | Depth Interval | Mid-Point Depth (cm)[a] | Year | Reported by NOSAMS | | | | NOSAMS Accession # |
|---|---|---|---|---|---|---|---|---|
| | | | | $\delta^{13}C$ (‰) | $F_M$ | $F_M$ Error | $\Delta^{14}C$ (‰) | |
| Perylene | 0 - 4 | 2 | 1943 | -28.2 | 0.8868 | 0.0083 | -119 | OS - 27391 |
| Perylene | 6 - 12 | 9 | 1904 | -28.1 | 0.8596 | 0.0086 | -146 | OS - 28135 |
| Perylene | 14 - 20 | 17 | 1860 | -28.6 | 0.8434 | 0.0084 | -162 | OS - 28122 |
| Perylene | 22 - 28 | 25 | 1815 | -28.0 | 0.8116 | 0.0080 | -194 | OS - 28123 |
| Mix PAH[a] | 0 - 4 | 2 | 1943 | -25.4 | 0.5316 | 0.0052 | -472 | OS - 27381 |
| Mix PAH[a] | 6 - 12 | 9 | 1904 | -23.7 | 0.7378 | 0.0077 | -267 | OS - 27388 |
| Mix PAH[a] | 22 - 28 | 25 | 1815 | -22.4 | 0.9010 | 0.0139 | -105 | OS - 28145 |

[a] Mixture of 13 pyrogenic PAHs.

## APPENDIX 5

Characterization of sedimentary TOC ($\delta^{13}C$, % OC, % N, C / N ratio and $\Delta^{14}C$)

A. Measurements of $\delta^{13}C$, % TOC, % $N_{org}$ and $C_{org}/N_{org}$ ratio for Pettaquamscutt River and Siskwit Lake sediments performed at the Organic Mass Spectrometry facility at WHOI

| Sample | Horizon | Depth Interval | Mid-point Depth (cm) | Year | $\delta^{13}C$ (‰) ± 1σ | TOC (%) ± 1σ | $N_{org}$ (%) ± 1σ | $C_{org}$ / $N_{org}$ Ratio |
|---|---|---|---|---|---|---|---|---|
| Petta - TOC | - | 0 - 1 | 0.5 | 1998 | -23.9 ± 0.19 | 9.2 ± 0.38 | 1.07 ± 0.08 | 10.0 |
| Petta - TOC | - | 1 - 1.5 | 1.25 | 1996 | - | 7.7 ± 0.04 | 0.94 ± 0.03 | 9.5 |
| Petta - TOC | - | 2 - 2.5 | 2.25 | 1995 | -24.4 ± 0.12 | 7.4 ± 0.57 | 0.86 ± 0.08 | 10.0 |
| Petta - TOC | - | 3 - 3.5 | 3.25 | 1993 | - | 7.4 ± 0.23 | 0.77 ± 0.01 | 11.2 |
| Petta - TOC | - | 4 - 4.5 | 4.25 | 1992 | -23.0 ± 0.03 | 8.9 ± 1.46 | 0.87 ± 0.16 | 12.0 |
| Petta - TOC | - | 5 - 5.5 | 5.25 | 1990 | - | 8.3 ± 0.27 | 0.94 ± 0.01 | 10.2 |
| Petta - TOC | - | 6 - 6.5 | 6.25 | 1988 | -24.0 ± 0.05 | 7.5 ± 0.37 | 0.79 ± 0.02 | 11.1 |
| Petta - TOC | - | 7 - 7.5 | 7.25 | 1987 | - | 8.4 ± 0.71 | 0.91 ± 0.13 | 10.7 |
| Petta - TOC | - | 8 - 8.5 | 8.25 | 1985 | -24.4 ± 0.06 | 8.0 ± 0.14 | 0.92 ± 0.00 | 10.2 |
| Petta - TOC | - | 9 - 9.5 | 9.25 | 1983 | - | 7.0 ± 0.32 | 0.78 ± 0.06 | 10.5 |
| Petta - TOC | - | 10 - 10.5 | 10.25 | 1981 | -24.5 ± 0.01 | 7.7 ± 0.20 | 0.80 ± 0.05 | 11.1 |
| Petta - TOC | - | 11 - 11.5 | 11.25 | 1979 | - | 8.1 ± 0.11 | 0.86 ± 0.01 | 10.9 |
| Petta - TOC | - | 12 - 12.5 | 12.25 | 1977 | -23.9 ± 0.02 | 7.3 ± 0.17 | 0.77 ± 0.05 | 11.0 |
| Petta - TOC | - | 13 - 13.5 | 13.25 | 1975 | - | 8.6 ± 0.27 | 0.91 ± 0.04 | 10.9 |
| Petta - TOC | - | 14 - 14.5 | 14.25 | 1972 | -24.5 ± 0.03 | 8.1 ± 0.33 | 0.86 ± 0.03 | 11.1 |
| Petta - TOC | - | 15 - 15.5 | 15.25 | 1970 | - | 8.5 ± 0.16 | 0.92 ± 0.01 | 10.8 |
| Petta - TOC | - | 16 - 16.5 | 16.25 | 1968 | -24.7 ± 0.09 | 7.9 ± 0.33 | 0.88 ± 0.09 | 10.6 |
| Petta - TOC | - | 17 - 17.5 | 17.25 | 1966 | - | 9.3 ± 0.01 | 0.94 ± 0.01 | 11.5 |
| Petta - TOC | - | 18 - 18.5 | 18.25 | 1963 | -24.8 ± 0.06 | 8.6 ± 0.30 | 0.88 ± 0.04 | 11.3 |
| Petta - TOC | - | 19 - 19.5 | 19.25 | 1961 | - | 7.9 ± 0.15 | 0.87 ± 0.04 | 10.8 |
| Petta - TOC | - | 20 - 20.5 | 20.25 | 1958 | -23.6 ± 0.05 | 7.4 ± 0.16 | 0.94 ± 0.12 | 9.1 |
| Petta - TOC | - | 21 - 21.5 | 21.25 | 1956 | - | 7.6 ± 0.54 | 0.76 ± 0.01 | 11.7 |
| Petta - TOC | - | 22 - 22.5 | 22.25 | 1953 | -23.9 ± 0.08 | 7.4 ± 0.41 | 0.72 ± 0.04 | 12.0 |
| Petta - TOC | - | 23 - 23.5 | 23.25 | 1950 | - | 8.8 ± 0.23 | 0.92 ± 0.09 | 11.2 |
| Petta - TOC | - | 24 - 24.5 | 24.25 | 1947 | -23.8 ± 0.14 | 9.1 ± 0.09 | 0.89 ± 0.01 | 12.0 |
| Petta - TOC | - | 25 - 25.5 | 25.25 | 1944 | - | 9.2 ± 0.24 | 0.89 ± 0.02 | 12.0 |
| Petta - TOC | - | 26 - 26.5 | 26.25 | 1941 | -24.2 ± 0.10 | 8.5 ± 0.15 | 0.87 ±0.01 | 11.4 |
| Petta - TOC | - | 27 - 27.5 | 27.25 | 1937 | - | 6.9 ± 0.33 | 0.65 ± 0.02 | 12.3 |
| Petta - TOC | - | 28 - 28.5 | 28.25 | 1934 | -24.6 ± 0.35 | 8.8 ± 0.51 | 0.83 ± 0.08 | 12.4 |
| Petta - TOC | - | 29 - 29.5 | 29.25 | 1930 | - | 9.2 ± 0.41 | 0.91 ± 0.06 | 11.8 |

| Sample | Horizon | Interval | Depth | Year | $\delta^{13}C$ (‰) | OC (%) | N (%) | C / N |
|---|---|---|---|---|---|---|---|---|
| Petta - TOC | - | 30 - 30.5 | 30.25 | 1926 | -24.1 ± 0.40 | 10.3 ± 0.11 | 1.01 ± 0.10 | 11.9 |
| Petta - TOC | - | 31 - 31.5 | 31.25 | 1920 | - | 11.1 ± 0.29 | 1.04 ± 0.01 | 12.5 |
| Petta - TOC | - | 32 - 32.5 | 32.25 | 1915 | -24.8 ± 0.09 | 10.7 ± 0.08 | 0.97 ± 0.01 | 12.8 |
| Petta - TOC | - | 33 - 33.5 | 33.25 | 1909 | - | 10.5 ± 0.06 | 0.97 ± 0.03 | 12.6 |
| Petta - TOC | - | 34 - 34.5 | 34.25 | 1904 | -24.1 ± 0.08 | 10.2 ± 0.23 | 0.94 ± 0.01 | 12.7 |
| Petta - TOC | - | 35 - 35.5 | 35.25 | 1900 | - | 9.8 ± 0.08 | 0.87 ± 0.03 | 13.2 |
| Petta - TOC | - | 36 - 36.5 | 36.25 | 1897 | -24.4 ± 0.18 | 10.4 ± 0.28 | 1.00 ± 0.03 | 12.2 |
| Petta - TOC | - | 37 - 37.5 | 37.25 | 1893 | - | 10.6 ± 0.15 | 0.98 ± 0.01 | 12.7 |
| Petta - TOC | - | 38 - 38.5 | 38.25 | 1888 | -23.9 ± 0.21 | 9.2 ± 0.10 | 0.93 ± 0.01 | 11.7 |
| Petta - TOC | - | 39 - 39.5 | 39.25 | 1884 | - | 9.5 ± 0.02 | 0.97 ± 0.01 | 11.5 |
| Petta - TOC | - | 40 - 40.5 | 40.25 | 1881 | -23.6 ± 0.23 | 9.2 ± 0.19 | 1.09 ± 0.10 | 9.9 |
| Petta - TOC | - | 41 - 41.5 | 41.25 | 1876 | - | 9.2 ± 0.69 | 1.13 ± 0.04 | 9.5 |
| Petta - TOC | - | 42 - 42.5 | 42.25 | 1872 | -23.1 ± 0.03 | 9.2 ± 0.11 | 0.99 ± 0.05 | 10.9 |
| Petta - TOC | - | 43 - 43.5 | 43.25 | 1868 | - | 10.3 ± 0.16 | 1.06 ± 0.03 | 11.3 |
| Petta - TOC | - | 44 - 44.5 | 44.25 | 1863 | -24.5 ± 0.12 | 10.3 ± 0.28 | 1.12 ± 0.01 | 10.7 |
| Petta - TOC | - | 45 - 45.5 | 45.25 | 1859 | - | 10.7 ± 0.32 | 1.14 ± 0.02 | 11.0 |
| Petta - TOC | - | 46 - 46.5 | 46.25 | 1855 | -24.4 ± 0.23 | 10.8 ± 0.01 | 1.13 ± 0.01 | 11.1 |
| Petta - TOC | - | 47 - 47.5 | 47.25 | 1851 | - | 11.3 ± 0.67 | 1.21 ± 0.04 | 10.9 |
| Petta - TOC | - | 48 - 48.5 | 48.25 | 1845 | -23.9 ± 0.48 | 10.4 ± 0.05 | 1.13 ± 0.03 | 10.7 |
| Petta - TOC | - | 49 - 49.5 | 49.25 | 1841 | - | 10.9 ± 0.21 | 1.35 ± 0.15 | 9.4 |
| Petta - TOC | - | 50 - 50.5 | 50.25 | 1837 | -24.1 ± 0.17 | 10.6 ± 0.01 | 1.12 ± 0.03 | 11.0 |
| Petta - TOC | - | 51 - 51.5 | 51.25 | 1832 | - | 10.3 ± 0.45 | 1.13 ± 0.16 | 10.7 |
| Petta - TOC | - | 52 - 52.5 | 52.25 | 1827 | -25.2 ± 0.11 | 9.9 ± 0.17 | 0.99 ± 0.01 | 11.6 |
| Petta - TOC | - | 53 - 53.5 | 53.25 | 1822 | - | 8.7 ± 0.07 | 0.87 ± 0.03 | 11.7 |
| Petta - TOC | - | 54 - 54.5 | 54.25 | 1819 | -23.9 ± 0.15 | 8.7 ± 0.39 | 0.92 ± 0.07 | 11.0 |
| Petta - TOC | - | 55 - 55.5 | 55.25 | 1814 | - | 9.9 ± 0.28 | 1.13 ± 0.06 | 10.2 |
| Petta - TOC | - | 56 - 56.5 | 56.25 | 1808 | -24.4 ± 0.12 | 9.2 ± 0.22 | 0.97 ± 0.07 | 11.1 |
| Petta - TOC | - | 57 - 57.5 | 57.25 | 1803 | - | 8.5 ± 0.16 | 0.85 ± 0.05 | 11.7 |
| Petta - TOC | - | 58 - 58.5 | 58.25 | 1797 | -23.4 ± 0.20 | 8.5 ± 0.18 | 0.88 ± 0.06 | 11.3 |
| Petta - TOC | - | 59 - 59.5 | 59.25 | 1793 | - | 9.7 ± 0.06 | 0.99 ± 0.04 | 11.4 |
| Petta - TOC | - | 60 - 60.5 | 60.25 | 1788 | -23.5 ± 0.05 | 9.7 ± 0.17 | 1.06 ± 0.07 | 10.7 |
| Petta - TOC | - | 61 - 61.5 | 61.25 | 1783 | - | 9.5 ± 0.21 | 0.95 ± 0.02 | 11.7 |
| Petta - TOC | - | 62 - 62.5 | 62.25 | 1778 | -24.1 ± 0.21 | 9.2 ± 0.44 | 0.81 ± 0.02 | 13.2 |
| Petta - TOC | - | 63 - 63.5 | 63.25 | 1773 | - | 8.3 ± 0.08 | 0.79 ± 0.03 | 12.2 |
| Petta - TOC | - | 64 - 64.5 | 64.25 | 1766 | -23.7 ± 0.08 | 8.6 ± 0.19 | 0.91 ± 0.04 | 11.0 |
| Petta - TOC | - | 65 - 65.5 | 65.25 | 1759 | - | 9.1 ± 0.02 | 0.83 ± 0.02 | 12.7 |
| Petta - TOC | - | 66 - 66.5 | 66.25 | 1754 | -23.4 ± 0.18 | 8.9 ± 0.32 | 0.92 ± 0.01 | 11.4 |
| Petta - TOC | - | 67 - 67.5 | 67.25 | 1748 | - | 9.6 ± 0.08 | 0.91 ± 0.05 | 12.3 |
| Petta - TOC | - | 68 - 68.5 | 68.25 | 1743 | -24.3 ± 0.10 | 9.1 ± 1.30 | 0.90 ± 0.12 | 11.8 |
| Petta - TOC | - | 69 - 69.5 | 69.25 | 1738 | - | 10.3 ± 0.40 | 0.98 ± 0.05 | 12.3 |
| Petta - TOC | - | 70 - 70.5 | 70.25 | 1733 | -25.4 ± 0.44 | 10.0 ± 0.11 | 0.93 ± 0.04 | 12.6 |

| Sample | Horizon | Interval | Depth | Year | $\delta^{13}C$ (‰) | OC (%) | N (%) | C / N |
|---|---|---|---|---|---|---|---|---|
| Petta - TOC | H1 | 0 - 9.5 | 5 | 1991 | -23.1 ± 0.1 | 7.3 ± 0.20 | 0.85 ± 0.02 | 10.0 |
| Petta - TOC | H2 | 10 - 19 | 14.5 | 1972 | -24.1 ± 0.2 | 7.7 ± 0.42 | 0.84 ± 0.02 | 10.7 |
| Petta - TOC | H3 | 19.5 - 29 | 24.5 | 1947 | -23.9 ± 0.3 | 7.9 ± 0.15 | 0.74 ± 0.01 | 12.5 |
| Petta - TOC | H4 | 29.5 - 36 | 33 | 1911 | -24.1 ± 0.3 | 9.8 ± 0.05 | 0.87 ± 0.02 | 13.1 |
| Petta - TOC | H5 | 36.5 - 42 | 39 | 1885 | -23.7 ± 0.2 | 9.2 ± 0.01 | 0.84 ± 0.01 | 12.8 |
| Petta - TOC | H6 | 42.5 - 49 | 45.5 | 1858 | -23.9 ± 0.1 | 9.9 ± 0.25 | 0.95 ± 0.04 | 12.2 |
| Petta - TOC | H7 | 49.5 - 64 | 57 | 1804 | -24.3 ± 0.4 | 8.9 ± 0.07 | 0.79 ± 0.01 | 13.2 |
| Petta - TOC | H8 | 64.5 - 69.5 | 67 | 1750 | -23.8 ± 0.2 | 8.9 ± 0.06 | 0.76 ± 0.01 | 13.7 |
| | | | | | | | | |
| Siskwit - TOC | - | 0 - 2 | 1 | 1948 | - | 8.7 ± 0.01 | 0.54 ± 0.00 | 18.6 |
| Siskwit - TOC | - | 2 - 4 | 3 | 1937 | - | 8.8 ± 0.01 | 0.55 ± 0.02 | 18.5 |
| Siskwit - TOC | - | 4 - 6 | 5 | 1926 | - | 8.5 ± 0.09 | 0.54 ± 0.01 | 18.5 |
| Siskwit - TOC | - | 6 - 8 | 7 | 1915 | - | 8.5 ± 0.05 | 0.55 ± 0.00 | 18.0 |
| Siskwit - TOC | - | 8 - 10 | 9 | 1904 | - | 8.3 ± 0.02 | 0.56 ± 0.01 | 17.3 |
| Siskwit - TOC | - | 10 - 12 | 11 | 1893 | - | 8.2 ± 0.06 | 0.55 ± 0.00 | 17.4 |
| Siskwit - TOC | - | 12 - 14 | 13 | 1882 | - | 8.3 ± 0.07 | 0.54 ± 0.01 | 17.9 |
| Siskwit - TOC | - | 14 - 16 | 15 | 1871 | - | 7.7 ± 0.08 | 0.51 ± 0.01 | 17.6 |
| Siskwit - TOC | - | 16 - 18 | 17 | 1860 | - | 7.5 ± 0.30 | 0.49 ± 0.02 | 17.7 |
| Siskwit - TOC | - | 18 - 20 | 19 | 1848 | - | 8.0 ± 0.10 | 0.53 ± 0.00 | 17.6 |
| Siskwit - TOC | - | 20 - 22 | 21 | 1837 | - | 7.1 ± 0.13 | 0.55 ± 0.02 | 15.1 |
| Siskwit - TOC | - | 22 - 24 | 23 | 1826 | - | 8.4 ± 0.21 | 0.57 ± 0.01 | 17.3 |
| Siskwit - TOC | - | 24 - 26 | 25 | 1815 | - | 7.9 ± 0.09 | 0.54 ± 0.01 | 17.2 |
| Siskwit - TOC | - | 26 - 28 | 27 | 1804 | - | 8.4 ± 0.10 | 0.57 ± 0.01 | 17.1 |
| Siskwit - TOC | - | 28 - 30 | 29 | 1793 | - | 8.3 ± 0.09 | 0.57 ± 0.01 | 17.1 |

B. Radiocarbon measurements conducted by the National Ocean Sciences AMS facility (NOSAMS)

| Sample | Horizon | Depth Interval | Mid-Point Depth (cm) | Year | Reported by NOSAMS | | | | $\delta^{13}C$ (‰)[a] | Corrected | | NOSAMS Accession # |
|---|---|---|---|---|---|---|---|---|---|---|---|---|
| | | | | | $\delta^{13}C$ (‰) | $F_M$ | $F_M$ Error | $\Delta^{14}C$ (‰) | | $F_M$ | $\Delta^{14}C$ (‰) | |
| Petta TOC | - | 0 - 1 | 0.5 | 1998 | -24.4 | 1.0032 | 0.0048 | -3 | - | 1.0032 | -3 | OS - 30974 |
| Petta TOC | - | 5.5 - 6 | 5.75 | 1989 | -24.0 | 1.0298 | 0.0034 | 23 | - | 1.0298 | 25 | OS - 39287 |
| Petta TOC | - | 10 - 10.5 | 10.25 | 1981 | -24.5 | 0.9994 | 0.0033 | -7 | - | 0.9994 | -4 | OS - 31254 |
| Petta TOC | - | 12 - 12.5 | 12.25 | 1977 | -23.9 | 1.0134 | 0.0039 | 7 | - | 1.0134 | 10 | OS - 31363 |
| Petta TOC | - | 14 - 14.5 | 14.25 | 1972 | -24.5 | 1.0001 | 0.0048 | -6 | - | 1.0001 | -3 | OS - 31364 |
| Petta TOC | - | 16 - 16.5 | 16.26 | 1968 | -24.8 | 1.0185 | 0.0047 | 12 | - | 1.0185 | 16 | OS - 31365 |
| Petta TOC | - | 17 - 17.5 | 17.25 | 1966 | -24.3 | 1.0111 | 0.0038 | 5 | - | 1.0111 | 9 | OS - 33519 |
| Replicate | - | 17 - 17.5 | 17.25 | 1966 | -24.4 | 1.0156 | 0.0042 | 9 | - | 1.0156 | 14 | OS - 33521 |
| Petta TOC | - | 18 - 18.5 | 18.25 | 1963 | -23.9 | 0.9737 | 0.0035 | -32 | - | 0.9737 | -28 | OS - 31366 |
| Petta TOC | - | 19 - 19.5 | 19.25 | 1961 | -23.7 | 0.8775 | 0.0032 | -128 | - | 0.8775 | -124 | OS - 33528 |
| Petta TOC | - | 19.5 - 20 | 19.75 | 1960 | -23.8 | 0.9329 | 0.0036 | -73 | - | 0.9329 | -68 | OS - 39288 |
| Petta TOC | - | 20 - 20.5 | 20.25 | 1958 | -24.5 | 0.8419 | 0.0032 | -163 | - | 0.8419 | -159 | OS - 33725 |
| Replicate | - | 20 - 20.5 | 20.25 | 1958 | -17.9 | 0.8975 | 0.0037 | -108 | - | 0.8975 | -103 | OS - 31367 |
| Replicate | - | 20 - 20.5 | 20.25 | 1958 | -24.1 | 0.8758 | 0.0035 | -130 | - | 0.8758 | -125 | OS - 31568 |
| Petta TOC | - | 21 - 21.5 | 21.25 | 1956 | -23.9 | 0.8382 | 0.0043 | -167 | - | 0.8382 | -162 | OS - 33529 |
| Petta TOC | - | 21.5 - 22 | 21.75 | 1954 | -23.7 | 0.8432 | 0.0030 | -162 | - | 0.8432 | -157 | OS - 39289 |
| Petta TOC | - | 22 - 22.5 | 22.25 | 1953 | -23.5 | 0.8673 | 0.0037 | -138 | - | 0.8673 | -133 | OS - 31368 |
| Petta TOC | - | 24 - 24.5 | 24.25 | 1947 | -24.4 | 0.8656 | 0.0036 | -140 | - | 0.8656 | -134 | OS - 31369 |
| Petta TOC | - | 26 - 26.5 | 26.25 | 1941 | -24.4 | 0.8596 | 0.0036 | -146 | - | 0.8596 | -140 | OS - 31370 |
| Petta TOC | - | 28 - 28.5 | 28.25 | 1934 | -24.5 | 0.8747 | 0.0037 | -131 | - | 0.8747 | -124 | OS - 31371 |
| Petta TOC | - | 30 - 30.5 | 30.25 | 1926 | -24.4 | 0.8804 | 0.0047 | -125 | - | 0.8804 | -117 | OS - 31372 |
| Petta TOC | - | 35 - 35.5 | 35.25 | 1900 | -24.3 | 0.8774 | 0.0029 | -128 | - | 0.8774 | -117 | OS - 39290 |
| Replicate | - | 35 - 35.5 | 35.25 | 1900 | -24.4 | 0.8612 | 0.0029 | -144 | - | 0.8612 | -134 | OS - 33520 |
| Petta TOC | - | 40 - 40.5 | 40.25 | 1881 | -23.7 | 0.9056 | 0.0038 | -100 | - | 0.9056 | -87 | OS - 31488 |
| Petta TOC | - | 45 - 45.5 | 45.25 | 1859 | -24.6 | 0.9053 | 0.0040 | -100 | - | 0.9053 | -85 | OS - 33522 |

| Sample | Horizon | Depth Interval | Mid-Point Depth (cm) | Year | Reported by NOSAMS | | | | $\delta^{13}C$ (‰)[a] | Corrected | | NOSAMS Accession # |
|---|---|---|---|---|---|---|---|---|---|---|---|---|
| | | | | | $\delta^{13}C$ | $F_M$ | $F_M$ Error | $\Delta^{14}C$ | | $F_M$ | $\Delta^{14}C$ | |
| Petta TOC | - | 49.5 - 50 | 49.75 | 1839 | -24.5 | 0.9300 | 0.0036 | -76 | - | 0.9300 | -57 | OS - 39291 |
| Petta TOC | - | 50 - 50.5 | 50.25 | 1837 | -24.7 | 0.9233 | 0.0042 | -82 | - | 0.9233 | -64 | OS - 31489 |
| Replicate | - | 50 - 50.5 | 50.25 | 1837 | -24.5 | 0.9239 | 0.0036 | -82 | - | 0.9240 | -63 | OS - 31492 |
| Petta TOC | - | 55 - 55.5 | 55.75 | 1814 | -24.3 | 0.9038 | 0.0052 | -102 | - | 0.9038 | -81 | OS - 33516 |
| Petta TOC | - | 60 - 60.5 | 60.25 | 1788 | -24.1 | 0.9029 | 0.0037 | -103 | - | 0.9029 | -79 | OS - 31490 |
| Petta TOC | - | 70 - 70.5 | 70.25 | 1733 | -25.5 | 0.8982 | 0.0039 | -107 | - | 0.8982 | -78 | OS - 31491 |
| Petta TOC | H1 | 0 - 9.5 | 5 | 1991 | -24 [b] | 1.0030 | 0.0037 | -3 | -23.1 | 1.0027 | -4 | OS - 40062 |
| Petta TOC | H2 | 10 - 19 | 14.5 | 1972 | -24 [b] | 1.0227 | 0.0039 | 16 | -24.1 | 1.0268 | 20 | OS - 40063 |
| Petta TOC | H3 | 19.5 - 29 | 24.5 | 1947 | -24 [b] | 0.8746 | 0.0033 | -131 | -23.9 | 0.8804 | -125 | OS - 40064 |
| Petta TOC | H4 | 29.5 - 36 | 33 | 1911 | -24 [b] | 0.8636 | 0.0037 | -142 | -24.1 | 0.8733 | -132 | OS - 40419 |
| Petta TOC | H5 | 36.5 - 42 | 39 | 1885 | -24 [b] | 0.8932 | 0.0034 | -113 | -23.7 | 0.9054 | -100 | OS - 40065 |
| Petta TOC | H6 | 42.5 - 49 | 45.5 | 1858 | -24 [b] | 0.9277 | 0.0050 | -78 | -23.9 | 0.9438 | -62 | OS - 40226 |
| Petta TOC | H7 | 49.5 - 64 | 57 | 1804 | -24 [b] | 0.8952 | 0.0033 | -111 | -24.3 | 0.9176 | -88 | OS - 40227 |
| Petta TOC | H8 | 64.5 - 69.5 | 67 | 1750 | -24 [b] | 0.8835 | 0.0039 | -122 | -23.8 | 0.9106 | -95 | OS - 40228 |
| Siskwit - TOC | - | 2 - 4 | 3 | 1937 | -25.3 | 0.9270 | 0.0035 | -79 | - | 0.9344 | -72 | OS - 42436 |
| Siskwit - TOC | - | 8 - 10 | 9 | 1904 | -25.3 | 0.9282 | 0.0030 | -78 | - | 0.9394 | -67 | OS - 42437 |
| Siskwit - TOC | - | 16 - 18 | 17 | 1860 | -25.6 | 0.8664 | 0.0034 | -139 | - | 0.8815 | -124 | OS - 42438 |
| Siskwit - TOC | - | 24 - 26 | 25 | 1815 | -25.5 | 0.8259 | 0.0027 | -180 | - | 0.8449 | -161 | OS - 42439 |

[a] Values measured by the Organic Mass Spectrometry facility and used to correct $\Delta^{14}C$ for assumed $\delta^{13}C$.
[b] $\delta^{13}C$ values assumed by NOSAMS.

# APPENDIX 6

$\Delta^{14}C$ and $\delta^{13}C$ values used for calculation of the relative importance of combustion of fossil fuel, aquatic and terrestrial biomass to the sedimentary TOC in the Pettaquamscutt River sediments.

| Year | Petta TOC | | Aquatic | | Terrestrial | | | | Fossil | | Proportions (%) | | | Model |
|---|---|---|---|---|---|---|---|---|---|---|---|---|---|---|
| | | | Shells | | Atm | Soil | | 0.2 Atm + 0.8 Soil | | | Fossil | Land | Aquatic | |
| | $\Delta^{14}C$ | $\delta^{13}C$ | $\Delta^{14}C^a$ | $\delta^{13}C^b$ | $\Delta^{14}C^c$ | $\Delta^{14}C^d$ | $\delta^{13}C^e$ | | $\Delta^{14}C$ | $\delta^{13}C^f$ | | | | |
| 1941 | -139.5 | -24.4 | -64.4 | -21 | 19.2 | -150 | -28 | -123.8 | -1000 | -30 | 0.05 | 0.42 | 0.53 | -151.3 |
| 1947 | -134.1 | -24.4 | -65.3 | -21 | 20.9 | -150 | -28 | -124.2 | -1000 | -30 | 0.05 | 0.42 | 0.53 | -151.9 |
| 1950 | -133.5 | -24.0 | -68.4 | -21 | 24.8 | -150 | -28 | -124.9 | -1000 | -30 | 0.05 | 0.36 | 0.59 | -153.9 |
| 1951 | -133.4 | -23.8 | -71.5 | -21 | 24.8 | -150 | -28 | -124.9 | -1000 | -30 | 0.05 | 0.34 | 0.61 | -155.7 |
| 1952 | -133.2 | -23.7 | -74.6 | -21 | 25.1 | -150 | -28 | -125.0 | -1000 | -30 | 0.05 | 0.32 | 0.63 | -157.5 |
| 1953 | -133.0 | -23.5 | -71.7 | -21 | 24.0 | -150 | -28 | -124.8 | -1000 | -30 | 0.05 | 0.30 | 0.65 | -155.8 |
| 1954 | -157.3 | -23.7 | -68.9 | -21 | 22.2 | -150 | -28 | -124.4 | -1000 | -30 | 0.08 | 0.28 | 0.64 | -154.0 |
| 1955 | -159.8 | -23.8 | -66.0 | -21 | 0 | -150 | -28 | -120.0 | -1000 | -30 | 0.08 | 0.29 | 0.63 | -150.8 |
| 1956 | -162.4 | -23.9 | -59.7 | -21 | 30 | -150 | -28 | -114.0 | -1000 | -30 | 0.09 | 0.30 | 0.61 | -145.0 |
| 1957 | -143.7 | -24.0 | -53.4 | -21 | 60 | -150 | -28 | -108.0 | -1000 | -30 | 0.08 | 0.33 | 0.59 | -139.3 |
| 1958 | -125.1 | -24.1 | -47.0 | -21 | 110 | -150 | -28 | -98.0 | -1000 | -30 | 0.06 | 0.36 | 0.58 | -132.1 |
| 1959 | -96.7 | -24.0 | -40.7 | -21 | 250 | -150 | -28 | -70.0 | -1000 | -30 | 0.05 | 0.36 | 0.59 | -118.4 |
| 1960 | -68.2 | -23.8 | -34.4 | -21 | 215 | -150 | -28 | -77.0 | -1000 | -30 | 0.02 | 0.38 | 0.60 | -117.3 |
| 1961 | -123.6 | -23.7 | -21.1 | -21 | 205 | 50 | -28 | 81.0 | -1000 | -30 | 0.13 | 0.22 | 0.66 | -52.8 |
| 1962 | -75.7 | -23.8 | -7.7 | -21 | 304 | 50 | -28 | 100.8 | -1000 | -30 | 0.10 | 0.27 | 0.63 | -38.1 |
| 1963 | -27.9 | -23.9 | 5.6 | -21 | 844 | 50 | -28 | 208.8 | -1000 | -30 | 0.09 | 0.30 | 0.61 | 8.4 |
| 1964 | -14.0 | -23.8 | 19.0 | -21 | 854 | 50 | -28 | 210.8 | -1000 | -30 | 0.09 | 0.29 | 0.63 | 16.7 |
| 1965 | -0.2 | -23.6 | 32.3 | -21 | 763 | 50 | -28 | 192.6 | -1000 | -30 | 0.08 | 0.28 | 0.64 | 17.7 |
| 1966 | 13.6 | -24.4 | 40.8 | -21 | 697 | 50 | -28 | 179.4 | -1000 | -30 | 0.08 | 0.38 | 0.54 | 17.8 |
| 1967 | 14.9 | -24.6 | 49.3 | -21 | 600 | 50 | -28 | 160.0 | -1000 | -30 | 0.08 | 0.41 | 0.51 | 15.7 |
| 1968 | 16.3 | -24.8 | 57.8 | -21 | 558 | 50 | -28 | 151.6 | -1000 | -30 | 0.08 | 0.44 | 0.48 | 17.5 |
| 1969 | 11.5 | -24.8 | 66.3 | -21 | 533 | 50 | -28 | 146.6 | -1000 | -30 | 0.08 | 0.43 | 0.49 | 20.6 |
| 1970 | 6.8 | -24.7 | 74.8 | -21 | 532 | 50 | -28 | 146.4 | -1000 | -30 | 0.09 | 0.41 | 0.50 | 25.3 |
| 1971 | 2.1 | -24.6 | 75.2 | -21 | 488 | 50 | -28 | 137.6 | -1000 | -30 | 0.09 | 0.40 | 0.51 | 22.4 |
| 1972 | -2.7 | -24.5 | 75.7 | -21 | 461 | 50 | -28 | 132.2 | -1000 | -30 | 0.09 | 0.39 | 0.52 | 20.7 |
| 1973 | -0.1 | -24.4 | 76.1 | -21 | 389 | 50 | -28 | 117.8 | -1000 | -30 | 0.09 | 0.38 | 0.54 | 15.8 |
| 1974 | 2.5 | -24.3 | 76.6 | -21 | 389 | 50 | -28 | 117.8 | -1000 | -30 | 0.08 | 0.36 | 0.56 | 16.0 |
| 1975 | 5.0 | -24.2 | 77.0 | -21 | 369 | 50 | -28 | 113.8 | -1000 | -30 | 0.08 | 0.35 | 0.57 | 14.8 |
| 1976 | 7.6 | -24.0 | 71.1 | -21 | 365 | 50 | -28 | 113.0 | -1000 | -30 | 0.07 | 0.34 | 0.59 | 11.2 |
| 1977 | 10.1 | -23.9 | 65.3 | -21 | 335 | 50 | -28 | 107.0 | -1000 | -30 | 0.06 | 0.33 | 0.61 | 5.7 |
| 1978 | 6.5 | -24.0 | 59.4 | -21 | 315 | 50 | -28 | 103.0 | -1000 | -30 | 0.06 | 0.35 | 0.58 | 0.9 |
| 1979 | 2.9 | -24.2 | 53.6 | -21 | 282 | 50 | -28 | 96.4 | -1000 | -30 | 0.06 | 0.37 | 0.56 | -4.7 |

| Year | Petta TOC | | Shells | | Atm | Soil | | 0.2 Atm + 0.8 Soil | Fossil | | Proportions (%) | | | Model |
|---|---|---|---|---|---|---|---|---|---|---|---|---|---|---|
| | $\Delta^{14}C$ | $\delta^{13}C$ | $\Delta^{14}C$[a] | $\delta^{13}C$[b] | $\Delta^{14}C$[c] | $\Delta^{14}C$[d] | $\delta^{13}C$[e] | | $\Delta^{14}C$ | $\delta^{13}C$[f] | Fossil | Land | Aquatic | |
| 1980 | -0.7 | -24.3 | 47.7 | -21 | 263 | 100 | -28 | 132.6 | -1000 | -30 | 0.08 | 0.38 | 0.54 | 4.9 |
| 1981 | -4.3 | -24.5 | 48.4 | -21 | 261 | 100 | -28 | 132.2 | -1000 | -30 | 0.08 | 0.39 | 0.52 | 5.2 |
| 1982 | -0.7 | -24.4 | 49.1 | -21 | 254 | 100 | -28 | 130.8 | -1000 | -30 | 0.08 | 0.39 | 0.53 | 5.0 |
| 1983 | 3.0 | -24.4 | 49.7 | -21 | 218 | 100 | -28 | 123.6 | -1000 | -30 | 0.07 | 0.39 | 0.54 | 2.8 |
| 1984 | 6.6 | -24.3 | 50.4 | -21 | 210 | 100 | -28 | 122.0 | -1000 | -30 | 0.07 | 0.38 | 0.55 | 2.6 |
| 1985 | 10.3 | -24.2 | 51.1 | -21 | 197 | 100 | -28 | 119.4 | -1000 | -30 | 0.06 | 0.38 | 0.56 | 2.1 |
| 1986 | 13.9 | -24.2 | 49.4 | -21 | 180 | 100 | -28 | 116.0 | -1000 | -30 | 0.06 | 0.38 | 0.56 | -0.05 |
| 1987 | 17.6 | -24.1 | 47.8 | -21 | 174 | 100 | -28 | 114.8 | -1000 | -30 | 0.05 | 0.38 | 0.57 | -1.4 |
| 1988 | 21.2 | -24.1 | 46.1 | -21 | 171 | 100 | -28 | 114.2 | -1000 | -30 | 0.05 | 0.37 | 0.58 | -2.6 |
| 1989 | 24.9 | -24.0 | 44.5 | -21 | 162 | 100 | -28 | 112.4 | -1000 | -30 | 0.04 | 0.37 | 0.59 | -4.2 |
| 1990 | 21.8 | -24.0 | 42.8 | -21 | 139 | 100 | -28 | 107.8 | -1000 | -30 | 0.04 | 0.38 | 0.58 | -6.7 |
| 1991 | 18.8 | -24.1 | 41.1 | -21 | 128 | 100 | -28 | 105.6 | -1000 | -30 | 0.05 | 0.38 | 0.57 | -8.5 |
| 1992 | 15.8 | -24.1 | 39.5 | -21 | 134 | 100 | -28 | 103.0 | -1000 | -30 | 0.05 | 0.38 | 0.57 | -9.0 |
| 1993 | 12.7 | -24.2 | 37.8 | -21 | 130 | 100 | -28 | 96.4 | -1000 | -30 | 0.05 | 0.39 | 0.56 | -10.3 |
| 1994 | 9.7 | -24.2 | 36.2 | -21 | 118 | 100 | -28 | 132.6 | -1000 | -30 | 0.05 | 0.39 | 0.56 | -12.1 |
| 1995 | 6.6 | -24.2 | 34.5 | -21 | 125 | 100 | -28 | 132.2 | -1000 | -30 | 0.05 | 0.39 | 0.55 | -12.5 |
| 1996 | 3.6 | -24.3 | 32.8 | -21 | 105 | 100 | -28 | 130.8 | -1000 | -30 | 0.05 | 0.40 | 0.55 | -14.9 |
| 1997 | 0.5 | -24.3 | 31.2 | -21 | 108.6 | 100 | -28 | 123.6 | -1000 | -30 | 0.06 | 0.40 | 0.54 | -15.6 |
| 1998 | -2.5 | -24.4 | 29.5 | -21 | 103.5 | 100 | -28 | 122.0 | -1000 | -30 | 0.06 | 0.41 | 0.54 | -16.9 |
| | | | | | | | | **Average** | | | | | | |
| | | | | | | | | **Stdev** | | | | | | |

[a] [Weidman, 1993 #753].
[b] Average value for aquatic biomass [Meyers, 1997 #760].
[c] Values in shaded area were measured in tree rings [Stuiver, 1981 #768]. Other data were determined in atmospheric $^{14}CO_2$ [Levin, 1997 #508;Levin, 1985 #509].
[d] Soil data from [Richter, 1999 #765].
[e] Average value for $C_3$ terrestrial plants [O'Leary, 1988 #356].
[f] Average value for petroleum [O'Leary, 1988 #356]

# APPENDIX 7

A. Amount of black carbon isolated from the sediments of the Pettaquamscutt River and associated nitrogen residues. Total organic carbon present in untreated sample is also listed for comparison.

A.1 Coarser-resolution 8-point depth profile

| Horizon | Mid-Point Depth (cm) | Year | TOC (% wt.) | | $BC_{Thermal}$ (% wt.) | | $BC_{Chemical}$ (% wt.) | |
|---|---|---|---|---|---|---|---|---|
| | | | $C_{Org}$ | $N_{Org}$ | BC | N-Residue | BC | N-Residue |
| H1 | 5 | 1991 | 7.27 ± 0.20 | 0.85 ± 0.02 | 0.95 ± 0.05 | 0.128 ± 0.012 | 0.39 ± 0.07 | 0.034 ± 0.011 |
| H2 | 14.5 | 1972 | 7.72 ± 0.42 | 0.84 ± 0.02 | 0.37 ± 0.01 | 0.042 ± 0.002 | 0.49 ± 0.06 | 0.027 ± 0.004 |
| H3 | 24.5 | 1947 | 7.87 ± 0.15 | 0.74 ± 0.01 | 0.50 ± 0.01 | 0.057 ± 0.001 | 0.66 ± 0.05 | 0.025 ± 0.001 |
| H4 | 33 | 1911 | 9.77 ± 0.05 | 0.87 ± 0.02 | 0.79 ± 0.40 | 0.089 ± 0.044 | 0.69 ± 0.03 | 0.023 ± 0.002 |
| H5 | 39 | 1885 | 9.25 ± 0.01 | 0.84 ± 0.01 | 0.43 ± 0.19 | 0.049 ± 0.02 | 0.55 ± 0.02 | 0.023 ± 0.002 |
| H6 | 45.5 | 1858 | 9.91 ± 0.25 | 0.95 ± 0.04 | 0.52 ± 0.11 | 0.068 ± 0.016 | 0.46 ± 0.01 | 0.023 ± 0.002 |
| H7 | 57 | 1804 | 8.95 ± 0.07 | 0.79 ± 0.01 | 0.77 ± 0.01 | 0.081 ± 0.028 | 0.37 ± 0.04 | 0.018 ± 0.003 |
| H8 | 67 | 1750 | 8.99 ± 0.06 | 0.76 ± 0.01 | 0.25 ± 0.07 | 0.031 ± 0.008 | 0.33 ± 0.03 | 0.016 ± 0.003 |

A.2 High-resolution profile

| Horizon | Year | TOC (% wt.) | | $BC_{Thermal}$ (% wt.) | | GBC (% wt.) | |
|---|---|---|---|---|---|---|---|
| | | $C_{Org}$ | $N_{Org}$ | BC | N-Residue | GBC | N-Residue |
| 0 | 1999 | 9.17 | 1.07 | 0.64 | 0.12 | 0.11 | 0.002 |
| 1 | 1997 | 7.65 | 0.94 | 0.68 | 0.07 | 0.06 | 0.002 |
| 3 | 1994 | 7.37 | 0.77 | 0.43 | 0.10 | 0.09 | 0.002 |
| 5 | 1991 | 8.25 | 0.94 | 0.60 | 0.08 | 0.09 | 0.002 |
| 7 | 1987 | 8.38 | 0.91 | 0.51 | 0.09 | 0.11 | 0.004 |
| 9 | 1983 | 7.01 | 0.78 | 0.55 | 0.09 | 0.11 | 0.003 |
| 11 | 1979 | 8.05 | 0.86 | 0.54 | 0.09 | 0.12 | 0.003 |
| 13 | 1975 | 8.58 | 0.91 | 0.52 | 0.09 | 0.13 | 0.003 |
| 15 | 1971 | 8.48 | 0.92 | 0.54 | 0.10 | 0.13 | 0.005 |
| 18 | 1964 | 8.55 | 0.88 | 0.56 | 0.09 | 0.12 | 0.003 |
| 21 | 1956 | 7.61 | 0.76 | 0.59 | 0.09 | 0.20 | 0.005 |
| 23 | 1951 | 8.81 | 0.92 | 0.55 | 0.09 | 0.18 | 0.004 |
| 25 | 1945 | 9.16 | 0.89 | 0.64 | 0.08 | 0.20 | 0.004 |
| 27 | 1938 | 6.85 | 0.65 | 0.55 | 0.09 | 0.24 | 0.004 |
| 29 | 1931 | 9.23 | 0.91 | 0.64 | 0.09 | 0.18 | 0.004 |
| 32 | 1916 | 10.70 | 0.97 | 0.58 | 0.09 | 0.18 | 0.005 |
| 36 | 1898 | 10.43 | 1.00 | 0.56 | 0.08 | 0.10 | 0.004 |
| 40 | 1882 | 9.23 | 1.09 | 0.49 | 0.08 | 0.11 | 0.004 |
| 45 | 1860 | 10.71 | 1.14 | 0.47 | 0.09 | 0.13 | 0.008 |
| 50 | 1838 | 10.60 | 1.12 | 0.50 | 0.10 | 0.13 | 0.005 |
| 55 | 1815 | 9.87 | 1.13 | 0.55 | 0.09 | 0.16 | 0.007 |
| 60 | 1789 | 9.72 | 1.06 | 0.56 | 0.10 | 0.12 | 0.005 |

B. Radiocarbon measurements conducted on black carbon by the National Ocean Sciences AMS facility (NOSAMS)

| Sample | Horizon | Depth Interval | Weighed-Average Depth (cm)[a] | Year | Reported by NOSAMS | | | | Corrected | | NOSAMS Accession # |
|---|---|---|---|---|---|---|---|---|---|---|---|
| | | | | | $\delta^{13}C$ (‰) | $F_M$ | $F_M$ Error | $\Delta^{14}C$ (‰) | $F_M$ | $\Delta^{14}C$ (‰) | |
| $BC_{Thermal}$ | H1 | 0 - 9.5 | 5 | 1991 | -22.6 | 0.809 | 0.0026 | -196 | 0.8100 | -195 | OS - 39326 |
| | H2 | 10 - 19 | 14.5 | 1972 | -23.3 | 0.957 | 0.0034 | -49 | 0.9606 | -46 | OS - 39850 |
| | H3 | 19.5 - 29 | 24.5 | 1947 | -22.6 | 0.645 | 0.0031 | -359 | 0.6499 | -354 | OS - 39327 |
| | H4 | 29.5 - 36 | 33 | 1911 | -22.8 | 0.679 | 0.0026 | -326 | 0.6861 | -318 | OS - 39328 |
| | H5 | 36.5 - 42 | 39 | 1885 | -22.2 | 0.729 | 0.0028 | -275 | 0.7399 | -265 | OS - 39329 |
| | H6 | 42.5 - 49 | 45.5 | 1858 | -21.7 | 0.724 | 0.0028 | -281 | 0.7368 | -268 | OS - 39330 |
| | H7 | 49.5 - 64 | 57 | 1804 | -22.5 | 0.799 | 0.0031 | -206 | 0.8188 | -186 | OS - 39331 |
| | H8 | 64.5 - 69.5 | 67 | 1750 | -22.6 | 0.754 | 0.0024 | -251 | 0.7772 | -228 | OS - 39332 |
| $BC_{Chemical}$ | H1 | 0 - 9.5 | 5 | 1991 | -24.8 | 0.680 | 0.0023 | -324 | 0.6811 | -323 | OS - 42252 |
| | H2 | 10 - 19 | 14.5 | 1972 | -25.3 | 0.603 | 0.0025 | -401 | 0.6050 | -399 | OS - 42253 |
| | H3 | 19.5 - 29 | 24.5 | 1947 | -25.0 | 0.433 | 0.0024 | -570 | 0.4358 | -567 | OS - 42254 |
| | H4 | 29.5 - 36 | 33 | 1911 | -25.2 | 0.502 | 0.0023 | -502 | 0.5073 | -496 | OS - 42255 |
| | H5 | 36.5 - 42 | 39 | 1885 | -25.0 | 0.577 | 0.0027 | -426 | 0.5857 | -418 | OS - 42256 |
| | H6 | 42.5 - 49 | 45.5 | 1858 | -25.4 | 0.680 | 0.0023 | -325 | 0.6918 | -313 | OS - 42257 |
| | H7 | 49.5 - 64 | 57 | 1804 | -25.4 | 0.690 | 0.0027 | -314 | 0.7071 | -297 | OS - 42258 |
| | H8 | 64.5 - 69.5 | 67 | 1750 | -25.4 | 0.683 | 0.0032 | -322 | 0.7040 | -301 | OS - 42259 |